CONTRIBUTION OF VARIABLE RENEWABLE ENERGY TO INCREASE ENERGY SECURITY IN LATIN AMERICA

Juan Roberto Paredes

IDB

CONTRIBUTION OF VARIABLE RENEWABLE ENERGY TO INCREASE ENERGY SECURITY IN LATIN AMERICA

—

EDITOR:
Juan Roberto Paredes

AUTHORS:
Roberto Schaeffer
Alexandre Szklo
André F. P. Lucena
Cindy Viviescas
Lucas Lima
Gabriela Nascimento
Camila Ludovique
Fabio Amendola
Leticia Magalar
Vanessa Huback
Eveline Vasquez
Francisco Emenson
Carpegiane

December 2017

Cataloging-in-Publication data provided by the Inter-American Development Bank
Felipe Herrera Library

Contribution of variable renewable energy to increase energy security in Latin America / Juan Roberto Paredes, Roberto Schaeffer, Alexandre Szklo, André F.P. Lucena, Cindy Viviescas, Lucas Lima, Gabriela Nascimento, Camila Ludovique, Fabio Amendola, Leticia Magalar, Vanessa Huback; editor, Ricardo López Aparicio.
p. cm. — (IDB Monograph ; 562)

Includes bibliographic references.
1. Renewable energy sources- Environmental aspects-Latin America. 2. Energy security-Latin America. 3. Climatic changes-Latin America. I. Paredes, Juan Roberto. II. Schaeffer, Roberto, 1960-. III. Szklo, Alexandre Salem. IV. F.P. Lucena, André. V. Viviescas, Cindy. VI. Lima, Lucas. VII. Nascimento, Gabriela. VIII. Ludovique, Camila. IX. Amendola, Fabio. X. Magalar, Leticia. XI. Huback, Vanessa. XII. López Aparicio, Ricardo, editor. XIII. Inter-American Development Bank. Energy Division. XIV. Series.

IDB-MG-562
Keywords: Renewable Energy, Energy security, climate change, solar power, wind power, complementarity.
JEL Codes: O13, Q40, Q42, Q51, Q54

Layout:
PH3 estudio

Photo pg 58:
© Bruno Cunha

EXECUTIVE SUMMARY

The emergence of variable renewable energy in the global energy landscape has generated major challenges in both the long-term planning and the day-to-day operation of electrical systems. Although many Latin American (LA) countries have successfully used renewable resources such as water for electricity generation for many decades, there is much less detailed knowledge about the solar and wind resource behavior as they depend on local climate variables and on global atmospheric patterns that had not been studied in the context of electricity generation.

Additionally, the direct interaction between these three resources, sun, wind and water, becomes much more relevant now that many countries are seeking to diversify their energy matrices, either to reduce their dependence on fossil fuels or to reduce pollution and greenhouse gas emissions associated with their use. Governments see in these resources a very attractive option to expand their generation capacity by the advantages they currently offer in terms of long-term electricity price stability and very low carbon footprint. However, climate change has introduced an additional uncertainty in their long-term management since the global increase in temperatures can have direct effects on the availability of these resources and therefore on the electricity generation from them.

These aspects have been scarcely studied in Latin America. Therefore, the analysis presented here aims to shed some light on a successful integration of variable renewable energies to electricity networks and how, despite depending on the fluctuations of the climate itself, they can also contribute to the energy security of the region.

The study is divided in two sections. The first part of this report presents a review of the latest state-of-the-art variability indices for wind and solar energy, as well as a survey of existing studies addressing complementarities between renewable resources. One of the most relevant indexes for the financing and operation of variable renewable energy plants is the Interannual Variability. The study calculates this parameter for the regions with the highest solar and wind potential in Latin America (called throughout the report hotspots) and then performs a statistical analysis to evaluate the complementarity between hotspots using linear correlations.

The data used for the analysis come from the IDB's Grid of the Future project, which evaluated for the first time in the region with a detailed and homogeneous methodology the characteristics of the solar and wind resource in 21 countries in Central and South America. The database generated from satellite data and validated with more than 70 surface measurement stations was used in the Grid of the Future as an input to optimally determine the share of variable renewable energies in the electrical matrix of these countries by 2030.

Results show a higher variability for wind power than for solar power generation. They also show that Brazil plays a significant role regarding renewable energy integration in LA, since it has the strongest capacity to complement and be complemented by several LA countries.

The second part of the study evaluates the possible impacts of climate change on future wind and solar resources in Latin America and how these impacts can affect the complementarities between these two sources of electricity.

Initially, this report presents the background on the Representative Concentration Pathways and Global Circulation Models as well as a survey of existing studies addressing Global Climate Change on renewable energies.

This study considers MIROC-ESM-CHEM and HadGEM2-ES General Circulation Models (GCMs) and two Representative Concentration Pathways: ii) the RCP 4.5 scenario that represents a stabilization scenario in which total radiative forcing[1] is stabilized before 2100 and ii) the RCP 8.5 scenario that represents increasing greenhouse gas emissions over time.

The climate projections for the IDB database were made based on HadGEM2-ES – GCM since this model was the one that best replicates the historical database of wind speed and solar irradiation. Based on these climate projections, the complementarity between hotspots was re-evaluated.

RCP 4.5 is a scenario of intermediate mitigation, with a lower concentration of greenhouse gases in the atmosphere than the RCP 8.5 scenario; therefore, as expected, the impact of climate change in the historical complementarities of the analysed regions was lower. The RCP4.5 scenario presents favourable results for the complementarities of most pairs of regions; in only five pairs of hotspots (26%) the complementarities were lower than the historical values.

In the RCP8.5 scenario the complementarity is maintained or improved between 2010-2070 in most of the complementarities analyzed. However, this trend is highly reduced in the last period of the projection (2070-2100). Regarding the long-term planning in the power sector this result could encourage the expansion of solar and wind power plants since no strong variation in the energy generation profile is expected due to climate change effects in Latin America.

[1] Radiative forcing is a measure of the Earth's energy budget and its equilibrium. If the subtraction of the energy flowing out of the planet from the energy flowing in, is different from zero and positive, there has been some warming (or cooling, if the number is negative).

CONTENTS

SECTION I

Analysis of the value of **wind and solar energy**

SECTION II

Assessment of **Climate Change Impacts on Solar and Wind Energy Resources** in Latin America

SECTION I

Analysis of the value of **wind and solar energy**

01.
Introduction

Renewable energy or, more specifically, wind and solar, are commonly known as variable energy sources, given the fact that the energy they produce varies over time and is highly dependent on geographic location. This variability is a consequence of the dependence on weather and climatic conditions [Anjos et al., 2015]. At the same time, the variations of solar and wind energy output generally do not match the time distribution of the energy load demand [Anjos et al., 2015]. Integrating renewable energy into existing networks poses significant challenges. Addressing them will require not only regulatory changes to existing frameworks, but also detailed knowledge of the physical resources, their variability and possible complementarities.

There are several issues related to integrating large-scale power supplies from renewable energy sources into electrical power systems, such as short-term balancing, the need to back-up power plants and overproduction [Buttler et al., 2016]. The variability of these resources, on the timescale of minutes to hours, impacts load following requirements, while day-to-day variability and longer variations influence day-ahead requirements and long-term regional infrastructure planning, especially at higher penetration levels [Mills & Wiser, 2010].

Uncertainties involved in the prediction of energy production makes it difficult to dispatch the electricity at the exact time consumers need it, in contrast to conventional fossil fuel power plants, where the fuel is stored and can be processed almost immediately, providing firm capacity. Integration of higher shares of renewable energy calls for technologies and techniques to manage load demand fluctuations and optimal operation of reserve capacities [Kougias et al., 2016].

This leads to the question of whether an increasing share of variable renewable energies in an energy system based on conventional generation could contribute to providing firm capacity. What is the inter-annual variability of the solar and wind resources in Latin America (LA) and how does this variability behave across the region? Are the solar and wind resources complementary to hydro resources, i.e., do the seasonal patterns of these resources complement each other?

Due to the abovementioned constraints to solar and wind energy, innovative solutions that lessen the variability of energy production is a key point in ensuring the reliability of future energy systems. According to Kougias et al. [2016], as the currently applied techniques (storage capacity, curtailment and reserves in responsive power) imply either additional costs or partial losses of the energy output, other solutions are worth investigating.

This problem may be partially overcome with hybrid solar-wind (also with other renewable sources, such as hydro) power generation systems that integrate two or more energy resources using their complementary characteristics [Anjos et al., 2015]. For such integration, an optimal trade-off between the overall amount of energy produced and its time stability is the objective. This is equal to smoothing out power production, decreasing the instances of high and low values of electricity production. Such approaches will result in energy systems that support safer energy production, involving variable renewable energy in a significant share. Reducing the variability of energy production and increasing its predictability improves the stability of the grid and reduces dependence on high-cost energy storage systems [Kougias et al., 2016].

This report analyses the seasonality and variability of renewable energy resources, as well as possible complementarities between PV solar, wind and hydraulic energy in Latin American countries. The results of this study are an important input to regional energy planning and policy design authorities regarding the contribution of VRE, such as wind or solar energy, to cover future energy demand in LA.

02.
Background

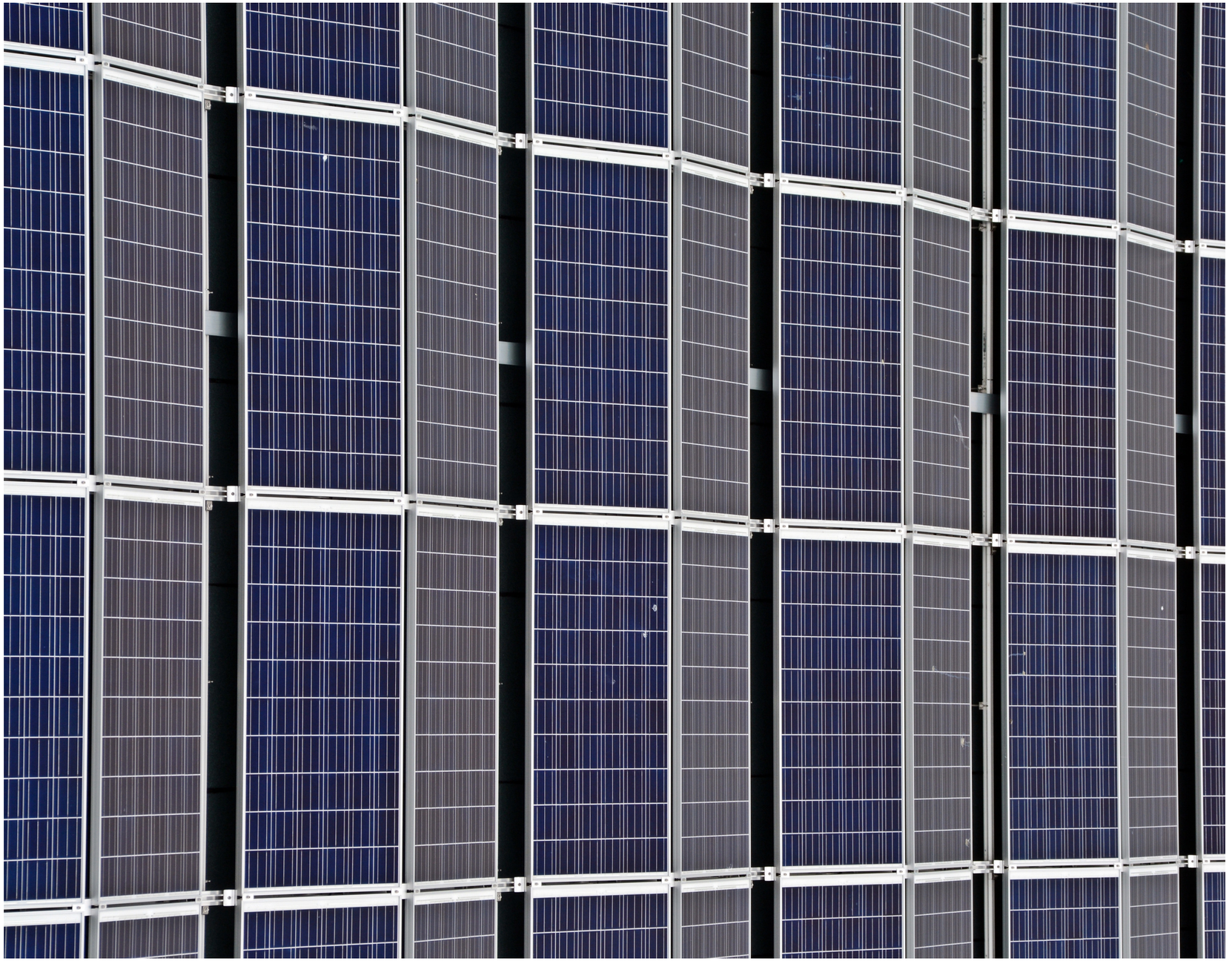

2.1. Review of the state-of-the-art of indices for variability of wind and solar energy

Among the challenges that the unpredictable behavior of renewable sources represents, one is to define a suitable place that will ensure a profitable project. This often requires a detailed, and sometimes costly, analysis of the local meteorological conditions [Ritter et al., 2014].

Since the variability of large scale wind or solar power generation depends on several factors – which include geographic dispersion and weather regimes, the characteristics of the power plants, the size of the area covered by the wind turbines or solar panels of the renewable power plant, etc. [Kiviluoma et al., 2014] –, the use of location-only measurements, such as the local average wind speed or the average local solar irradiation, is not enough to establish an accurate foresight of the production of energy from these resources. As a result, some studies have tried to establish new approaches to assess the local wind and solar potential and its variability [Hammer et al., 2003; Hodge et al., 2012; Kiviluoma et al., 2014; Skartveit et al., 2016]. Among these approaches, the definition and application of indices has been commonly used as a way to estimate long-term values for the variables in question.

The indices used in this kind of analysis describe the fluctuations of the resource or of the energy generated from a power plant (e.g. a wind farm or solar plant) throughout its life span [Ramírez, 2015]. The literature presents several types of indices. Among them, there are simple ones like the long-term variability index (Merra-based wind and Solar index) used by Ramírez [2015], in which the annual energy production (AEP) per year is compared against the 100% value (or long-term value). The 100% value represents the calculated mean of the annual wind production for each site within the time horizon. Therefore, this index represents how variable is the yearly energy production when compared to the long-term value.

Another commonly-used index is the IAV (Inter-annual Variability). The IAV quantifies how much a yearly value differs from the long-term average value. It is a key input to the assessment of wind and PV projects, as it can influence the debt-ratio and the return on investment (ROI) of a project [Darez et al., 2014].

The definition of the IAV is given by (Eq. 1)

$$IAV=(\sigma(x))/(E(x)) \quad \text{(Eq. 1)}$$

where x is the yearly mean value of the chosen variable (GHI, Wind Speed, River flow, etc.), $\sigma(x)$ is the standard deviation of x, and $E(x)$ is the mean value of x. If we consider, for example, the annual mean GHI at a site, the IAV will quantify statistically the likelihood of the mean value of one year deviating from the long-term mean at that site. Mathematically, three years of data is enough to calculate the IAV. However, a three year period is unlikely to be representative of the long term value [Darez et al., 2014]. According to The Crown State [2014], a true estimation of inter-annual variation ideally requires 30 or more years of local measurements.

An alternative to the IAV index is the Inter-monthly Variability (IMV). Its definition is similar to the IAV definition of (Eq. 1), with the difference that in this case the variable x refers to a monthly mean value. This index, as expected, can be much higher than the IAV for the same spot due to several reasons, such as annual weather patterns that do not always fall in the same month, lower time window or random events over the course of the year.

The IMV index, however, is not usually considered during the financial analysis, but as a metric for utilities to understand grid stability issues [The Crown State, 2014]. In Darez et al. [2014] this index is used to evaluate seasonal variability, since it is important to understand the magnitude of the expected fluctuation from season to season.

The above indices can be applied to the resources themselves (wind speed, GHI etc.) or to the energy generated from these resources. In the following sections specific variability indices for wind and solar energy will be presented.

2.1.1. Variability Indices for Wind Energy

The literature presents indices that are more sophisticated and specific to wind energy. The combination of a wind index and production data for existing wind farms can supplement or replace site-specific wind measurements [Rimpl et al., 2013]. The indices associated with wind energy can be classified based on the parameter to which the variability analysis will be applied.

- **Wind Energy Production Index**

The Wind Energy Production Index (WEPI), also known as Energy Yield Production Index, which is the most commonly used index. It is based on many years of operation. As mentioned, an index can be used to calculate the long-term value and, in this case, the long-term average energy yield is calculated by scaling the energy yields of already installed wind turbines; in other words, the monthly or yearly measurements of wind data are extrapolated to long-term periods. The yearly or monthly energy yields are presented as relative values compared to the long-term reference [Winkler et al., 2003]. Wind indices are also used to monitor existing wind farms in order to establish whether any variations in energy productivity are due to deficiencies in wind turbine performance or wind speeds below the expected levels. In this sense, indices help operators by giving them long-term or even short-term data that would allow them to affirm that their machines were operating according to the expectations [Rimpl et al., 2013]. The scaling of the wind energy generation through WEPIs is also used to compare the energy yield predicted before commissioning the power plant, to the energy yield actually achieved, and to carry out plausibility checks on the meteorological data input of energy yield assessments [Winkler et al., 2003].

In this category of Energy Yield Production Indices there is also the German IWET (also called BDB index) [Betreiber-Datenbasis, 2011], that is one of the most well-known wind indices, the IWR index [IWR] and the Danish Wind index, among others. These indices are based on production and in situ wind data from long-term sources like Reanalysis data [Ramírez, 2015].

The IWR uses an average time window of ten years and two regions. On the other hand, the German IWET (also known as Keiler-Häuser index) has 25 regional indices that are determined from selected monthly mean values of wind turbine energy yields for the region. Currently, the IWET takes approximately 4500 monthly production data sets into account [Rimpl et al., 2013; Winkler et al., 2003]. Those two indices, IWET and IWR, are based on monthly mean values of energy yields and therefore do not allow a detailed analysis of wind speed time series and wind direction. These indices have to update the long-term value on a regular basis in order to avoid non-realistic results, as was the case of the IWET index before its update in 2004 [Winkler et al., 2003].

It is worth mentioning that the Energy Yield Production Indices are susceptible to changes in the characteristics of the wind turbines/farms (local distribution, hub height, capacity, etc.), which leads to changes in the representation of all wind data.

- **Wind Speed Index**

The Wind Speed Index is sometimes presented as an alternative to work with operational data. This index considers wind conditions without accounting for energy aspects, which can be useful for comparing wind variations in a specific region [Rimpl et al., 2013]. This index represents the relative wind speed value in comparison to long-term values. Nonetheless, this index has to be managed carefully, since the long duration wind speed data available are from weather stations, which often measures at 10m above ground, much below hub height. An alternative is to use Re-analysis data, such as MERRA [NASA] or ANEMOS [ANEMOS] that can be used without external data for long term correction [Rimpl et al., 2013]. Often a Wind Speed Index is published along with a complementary index, like an Energy Yield Production Index.

- **Wind Power Density Index**

The wind power density can be an alternative parameter for a wind index. The wind power density can be defined as (Eq. 2).

$$P/A=1/2\ \rho v^3 \quad \text{(Eq. 2)}$$

A wind index based on this parameter expresses only the energy from free wind. Rimpl et al. [2013] indicates that this type of index should be used carefully, since it can present higher variations in comparison to harvestable energy due to the difference between the wind energy potential and technically usable potential. Also, although it is true that the power output of a wind turbine follows a cubic function, this only applies to low wind speeds. For high wind speeds, limitations due to the turbine's specifications are more relevant. For example, at high wind speeds, wind turbines could undergo nominal power out and cut-out, after which increases in wind speeds do not increment electricity production [Johnson, 2006].

- **Wind Energy Production Index from Wind Data**

Another kind of index is the Wind Energy Production Index from Wind Data. This index is calculated from the application of a power curve that can be either a standard curve or a project-specific power to wind data curve. Some examples of these indices are:

i) The ISET [ISET -WIND- INDEX], which is based on 60 measured wind data sets at 50 m height that are compared to the long-term average. In this case, the connection between power production and wind speed was determined empirically, by using the annual power production of 1,500 wind turbines of the WMEP database [Bard et al., 2011];

ii) The EuroWind [EUROWIND INDEX], which takes wind measured data exclusively from the international weather services into account; and

iii) The GL-GH Wind Index of the United Kingdom from the UK Met Office, which considers 50 mainland stations. The meteorological stations measure the wind conditions at 10 m above ground level [Rimpl et al., 2013; UK Met office, 2010].

Wind indices can be created for a specific site and they are often used for the operational verification of wind turbines. The site-specific sensitivity is calculated using monthly operational and wind speed data. Alternatively, a site-specific index can be based on site-related wind data and power curves.

Additionally, there are stand-alone production data sets that, having a large database, can be used to create a wind index for verification, such as the Swedish database vindstat, the German database WMEP, among others [Branner et al., 2014; Rimpl et al., 2013].

- **Ramping Index**

The above indices are based on yearly or monthly values. Nonetheless, the inherent variability of power generation clearly distinguishes the variable renewable energy sources from conventional sources. From one minute to another, wind gusts passing through the plane of the rotor or a sudden increase in cloudiness can be translated into large ramp rates. These ramp rates can become an important concern for grid operators [Castro et al., 2014]. The ramping events associated with areas that have large

penetrations of variable generation are one of the most pressing concerns for system operators and planners [Mazumdar et al., 2014]. These energy fluctuations need to be balanced, most likely with conventional power plants or with demand side measures (demand management), requiring more flexibility from controllable and dispatchable power generating units, in order to keep the system stable [Moarefdoost et al., 2016, Kiviluoma et al., 2012].

The increase in the ramping periods on the conventional generators incur in ramping costs, which can degrade the value of the renewable energy sources. In other words, higher ramping costs can have a significant effect on the dispatch policies of renewable energy sources [Moarefdoost et al., 2016].

Frequent ramping up and/or ramping down of fossil-fueled power plants beyond the elastic range causes thermal and pressure stresses, which are the main reasons for thermal creep, fatigue and creep–fatigue interaction damages [Moarefdoost et al., 2016]. There are three main sources of extra costs for conventional generators when they work in a non-optimal way: 1) increased heat rates and losses in efficiency; 2) increased operation and maintenance costs; and 3) increased probability of forced outages [Hamal et al., 2006]. These types of damages and costs could reduce the lifetime of components and increase capital and maintenance costs. Additionally, ramping up and/or ramping down increases fuel inefficiency and, thus, fuel consumption [Moarefdoost et al., 2016].

An index that considers the variability of the sources on hourly or sub-hourly time scales should be considered to understand the impacts on power system operation. The ramp index is essentially the speed at which a generator can increase (ramp up) or decrease (ramp down) its generation [NREL, 2011]. For analyzing wind energy variability, ramp rate can be defined as the change in generator output of a wind power plant over two consecutive periods of Δt duration [Ma et al., 2013]. It can be considered that a ramp event occurred at time t if the generation from a wind power plant increases or decreases above a fixed threshold in a time interval -Δt [Mazumdar et al., 2014]. The ramping index is defined by (Eq. 3).

$$ramping\ index\ (\%) = x_t - x_{t-1} / x_{t-1} * 100 \qquad \text{(Eq. 3)}$$

Where x is the generation of the power plant.

2.1.2. Variability Indices for Solar Energy

Solar irradiance varies on time scales from seconds to years. The radiation passing through the atmosphere during clear conditions is called clear-sky radiation [Widén et al., 2015]. The output power of PV plants depends on the incident solar irradiance, which can fluctuate as clouds pass overhead. There are additional time-varying factors that affect the power output: the conversion efficiency is dependent on the cell temperature which, in turn, is determined by absorbed radiation, ambient temperature, wind speed and mounting. Depending on the site, nearby or distant obstacles may shade the view of the system and cause the power ramp up or down [Widén et al., 2015].

Quantifying and characterizing the solar variability at a given site can help the decision-making process regarding site specificity and implications for grid impacts [Gagné et al., 2016]. The interest in the variability of solar radiation depends on the time scale when solar radiation is analyzed from a time series. Thus, long-term variability studies are performed frequently based on the Typical Meteorological Year (TMY) approach, which is useful for extrapolating the response of solar energy systems. TMY refers to a specific year of meteorological data that represents the average expected values for the long-term and is frequently used for designing and simulating solar energy facilities [Vindel et al., 2014]. The knowledge of this variability at different time scales is important for improving the design of a solar energy system and operational strategies. For instance, a predicted high variability may suggest an adaptation of the operational planning with the ready deployment of standby generation capability.

The theme of solar energy variability has generated a considerable amount of research during recent years. Especial attention has been paid to the study of the short-term variability of the PV power output of a single plant due to cloud fluctuations [Marcos et al., 2011; Mills et al., 2010; Perpinán et al., 2013; Van Haaren et al., 2014].

- **Clear Sky Irradiance**

The daily clear-sky irradiance is a metric used to quantify the amount of available solar radiation that reaches the ground. Taken from Stein et al. [2012], it is defined as the ratio of the area under the Global Horizontal Irradiance curve divided by the area under the clear-sky Global Horizontal Irradiance curve. Figure 1 shows examples of days with different values for Variability Index, which will be presented below and the clear sky irradiance.

- **Clearness Index**

In solar variability studies, the clearness index, which removes seasonal and diurnal variability, showing directly the impact of cloud movements, is commonly cited [Widén et al., 2015]. The daily clearness index is defined as the ratio of the daily sum of global irradiance on horizontal surface to the daily irradiance at the top of atmosphere [Muneer, 2004].

- **Variability Index**

The variability index (VI), introduced by Stein et al. [2012], is defined as the ratio of irradiance time-series curve length over the clear-sky irradiance curve length on a daily basis. The VI has no physical interpretation. It is intended for comparison between days and sites. For a given day, more irradiance fluctuations will result in a higher Variability Index. A clear-sky day should have a VI close to unity [Gagné et al., 2016]. Figure 1 represents examples of days with increasing VI values and the clear sky irradiance.

- **Solar Ramping Indices**

Metrics describing and quantifying variability at different time scales are key to this characterization [Lauret et al., 2016]. In this context, the ramp index presented in section 2.1.1 can also be applied to assess solar energy production. Additionally, Van Haaren et al. [2014] proposed a quantitative metric called the Daily Aggregate Ramp Rate (DARR), which sums 1-min single Plane of Array (POA) irradiance sensor data over each day to characterize daily variability in a utility scale plant. In Lave et al. [2015], the variability score (VS) is introduced as another metric to quantify the variability based on the cumulative distribution of ramp rates. The calculation is based on the cumulative distribution function of ramp rates using a given timescale. Unlike the VI, it does not require a clear-sky model. This index is calculated on a daily basis. Quantifying variability using such indices could help to estimate the necessary mitigation efforts required to adequately support PV integration at a specific site. For example, sites with high values of Variability Score (VS, a variability index that will be defined later) for an interval of 30s are expected to have a larger impact on voltage fluctuations and could require more transformer tap changes [Lave et al., 2015].

Irradiance variability from three sites in the United-States was compared in Stein et al. [2012], where the irradiance was characterized on a daily basis. The Variability Index (VI), in this case, was introduced as a metric to quantify the fluctuations at a 1 min timescale, allowing comparisons between sites and days. The daily clear-sky index was also used in combination with the VI to group the days into categories, accordingly with the site variability [Gagné et al., 2016].

In a similar manner, Kang et al. [2013] proposed a new characterization and classification method (the K-POP method) for daily sky conditions by using the daily clearness index and a new metric called the daily probability of persistence (POPD). POPD observes differences between neighboring instantaneous clearness indices and calculates a probability that the differences are equal to zero [Kang et al., 2013].

Badosa et al. [2013] showed that solar irradiance variability at the diurnal scale can be classified in regimes based on three parameters: daily clear-sky index; solar irradiance morning–afternoon asymmetry; and random variability of the solar irradiance [Lauret et al., 2016].

Gagné et al. [2016] characterized the solar variability over one year at two sites that are approximately 400 km apart in South-Eastern Canada. The quantification and distribution of the variability were developed using the Variability Index (VI), the daily clear-sky index and the Variability Score (VS). To characterize variability based on time-series data, two main metrics have been used: the Variability Index and the Variability Score. In addition, the daily clear-sky index is used to quantify the cloud-free sky fraction for the day. The Global Horizontal Irradiance variability was characterized at recording periods ranging from 1s to 30s. The Variability Score was shown to be nearly proportional to the Variability Index. Gagné et al. [2016] also found that, when averaging irradiance time-series for a given surface, the aggregated variability decreases with increasing area. The variability reduction also depends on the cloud speed: the faster the clouds move, the smaller the reduction [Gagné et al., 2016].

Vindel et al. [2014] studied the intermittency of daily global horizontal and direct normal irradiation using fractal analysis. According to them, the range of relative variability is higher in the case of the global irradiation than in the case of the direct. Regarding the multifractality of the irradiation, the intermittency is similar for both components at each station. However, this phenomenon is more intense in stations where local effects have a greater role in the atmospheric motions [Vindel et al., 2014].

Lauret et al. [2016] presented a site characterization based on two parameters: the daily clear sky index and the intraday variability given by a commonly accepted metric: the standard deviation of the changes in the clear sky index. Lauret et al. [2016] showed that the relationship between these two quantities had little dependence on location – suggesting that intraday variability could be inferred from the day's mean clear sky index. However, the authors noted some influences on the relationship that could be traced to the mountainous landscape of the site and its influence on cloud formation. Sites where the mountainous landscape induces cloud formation tend to exhibit more variability for a given mean daily clear index than sites where cloud regimes are driven by weather.

2.1.3. Summary

Variability studies are often hard to compare because different indicators for variability are used and they give little theoretical foundation for analyzing and predicting vari-

Figure 1. Example of days with increasing VI values from Las Vegas, NV showing how apparent variability increase with VI. Clear sky irradiance is shown in red.

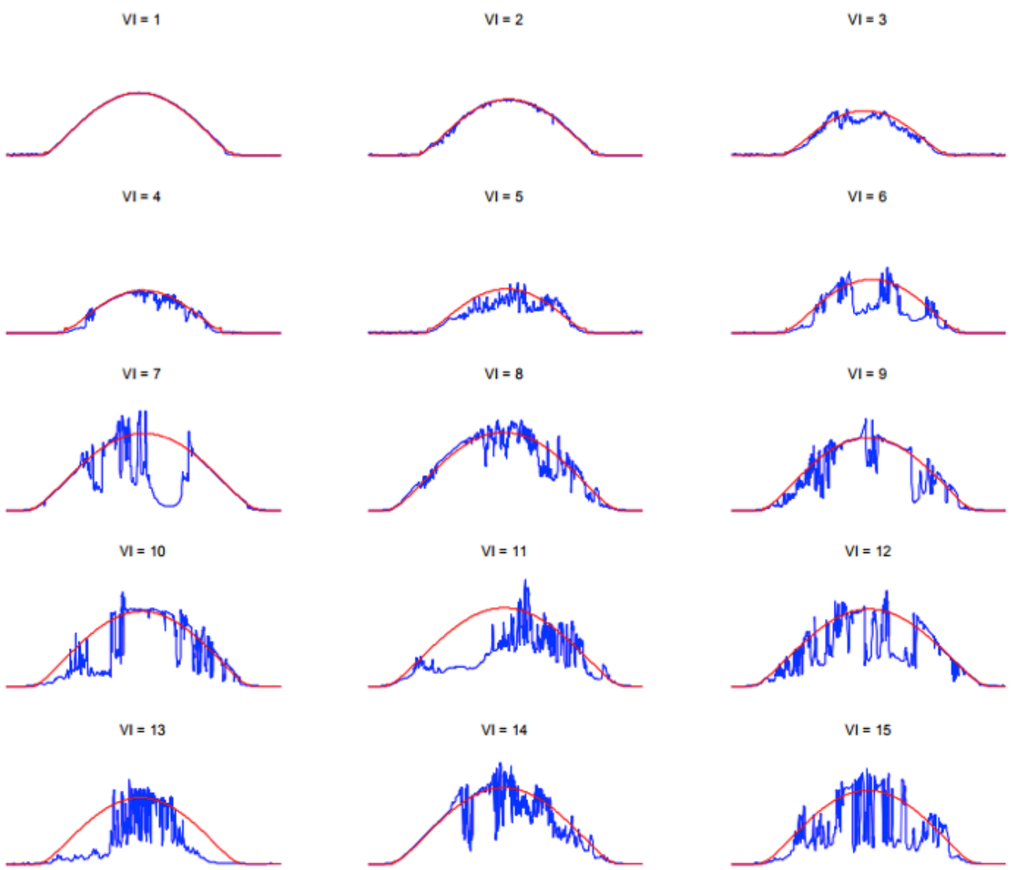

Fuente: Stein et al., 2012.

ability. The indices mentioned in this section for solar and wind resources are listed in Table 1.

2.2. Review of existing studies addressing complementarities between renewable sources

Recent studies estimated the complementarity between renewable resources, such as wind, solar and hydropower [Perez & Fthenakis, 2015; Buttler et al., 2016; Anjos et al., 2015; Beluco et al., 2012; Kougias et al., 2016; Silva et al., 2016]. The majority of these studies used measured climatic data series or, when there is a lack of data from meteorological stations, statistical models to calculate the clearness index for different locations over time [Perez & Fthenakis, 2015; Beluco et al., 2012; Kougias et al., 2016; Silva et al., 2016]. Other studies, such as Buttler et al. [2016], used energy output data in complementarity studies, paying more attention to the residual load challenges.

Kougias et al. [2016] defined the term complementarity as the extent to which energy output from different renewable energy sources is not positively correlated over time. Such complementarity aims to reduce the intermittency of energy production by combining systems that have their min/max energy output at different time periods [Kougias et al., 2016].

Table 1. Indices for solar and wind resources and their description

Indices	Resource	Description
Long-term Variability Index	Wind, Solar	The Long-term Variability Index compares the annual energy production for year to the 100% value. The 100% value represents the calculated mean of the annual wind production for each site within the temporal spam. This index represents how variable is the yearly energy production when compared to the long-term value [Ramírez, 2015].
Inter-Annual Variability (IAV)	Wind, Solar	The IAV is defined as the standard deviation of the annual means divided by the overall mean. The IAV quantifies how much a yearly value differs from the long-term average value. It is a key input to the assessment of wind and PV projects, since it can influence the debt-ratio and the return on investment (ROI) of a project [Darez et al., 2014].
Inter-Monthly Variability (IMV).	Wind	The IMV definition is similar to the IAV, but using a monthly mean value. This index is used to evaluate seasonal variability [The Crown State, 2014].
The Wind Energy Production Index (WEPI)	Wind	The WEPI calculates the long-term average energy yield by extrapolating the monthly or yearly measurements of wind generation data to long-term periods. The yearly or monthly energy yields are presented as relative values compared to the long-term reference [Winkler et al., 2003]. This index is used to monitor the existing wind farms in order to establish whether the variations in energy productivity are due to deficiencies in wind turbine performance or due to wind speeds below the expected levels.
Wind Speed Index	Wind	This index considers wind conditions without a consideration for energy aspects, which can be useful to compare the wind variations in a specific region [Rimpl et al., 2013]. This index represents the relative wind speed value in comparison to long-term values.
Wind Power Density Index	Wind	This index expresses the energy from free wind. This type of index should be used carefully, since it can present high variations in comparison to harvestable energy due to the difference between the wind energy potential and technically usable potential [Rimpl et al., 2013].
Wind Energy Production Index from Wind Data	Wind	This index is calculated from the application of a power curve to wind speed data. Either a standard power curve or that of a specific project can be used. The mean monthly value is calculated in relation to the long-term average.
Ramping Index	Wind, Solar	Ramping index can be defined as the change in the energy production of a wind or solar PV power plant over two consecutive periods of Δt. It can be considered that a ramp event occurred at time t if the generation from a power plant increases or decreases above a fixed threshold in a time interval -Δt [Mazumdar et al., 2014]. This index can be applied in an hourly or sub-hourly time scale and will help understanding the impacts on power system operation.
Clearness index (or cloudiness index)	Solar	The daily clearness index is defined as the ratio of the daily sum of global irradiance on a horizontal surface to the daily irradiance at the top of the atmosphere [Muneer, 2004]. It removes the seasonal and diurnal variability, showing directly the impact of cloud movements.

Índices	Resource	Description
Daily Aggregate Ramp Rate (DARR)	Solar	DARR is a quantitative metric which sums 1-min single Plane Of Array (POA) irradiance sensor over each day to characterize daily variability in a utility scale plant [Van Haaren et al., 2014].
Variability Index (VI)	Solar	The VI is defined as the ratio of irradiance time-series curve length over the clear-sky irradiance curve length on a daily basis. It is intended for comparison between days and sites [Gagné et al., 2016].
Variability Score (VS)	Solar	VS calculation is based on the cumulative distribution function of ramp rates using a given timescale, on a daily basis. The use of this index could help to estimate the necessary mitigation efforts required to support PV integration at a specific site [Lave et al., 2015].
Intraday Variability	Solar	The Intraday Variability is given by the standard deviation of the changes in the clear sky index [Lauret et al., 2016].

There is a consensus in energy complementarity studies that the most suitable way to estimate complementarity is to calculate the correlation between different energy resources of a region. In this sense, the Pearson coefficient is a widely used index to represent correlation and investigate the complementarity between renewable resources in the literature [Silva et al., 2015; Kougias et al., 2015; Perez & Fthenakis, 2015]. The Pearson coefficient is calculated as shown in (Eq. 4) In this case, it compares the data series of wind speed, irradiation or energy output from two specific energy production systems (or from potential locations) over time [Kougias et al., 2016].

$$r=1/(n-1)\ \sum((x_i-\bar{X})/\sigma_x)((y_i-\bar{Y})/\sigma_y) \qquad \text{(Eq. 4)}$$

In this equation, x_i represents the observed value, $\bar{X}$ represents the average and σ_x is the standard deviation. The same applies to Y variables. This index is a measure of the linear association between two variables and its value ranges between 1 and -1, where negative values indicate anti-correlation between the two variables [Kougias et al., 2016] and the magnitude suggests the strength of the relation between them [Silva et al., 2015]. It is clear that the correlation number states that the more negatively correlated are the regions, the more they complement each other, since one tends to increase as the other decreases. Perez & Fthenakis [2015] studied the complementarity of solar (PV) resources in various sites across the American continent (South America, Central America and North America). They calculated the Pearson correlation coefficient between variations in the clearness index in pairs of unique geographic locations and determined how the sites' correlations change as a function of the geographic distance. Kougias et al. [2015] have also used the Pearson correlation coefficient to evaluate the combination of such asynchronous energy production systems.

Anjos et al. [2015] used Detrended Fluctuation Analysis (DFA) method to quantify and compare correlations between wind speed and solar irradiation time series for the Fernando de Noronha Island, Brazil. The DFA method is suitable for quantifying long-term correlations between non-stationary series signals [Anjos et al., 2015]. Anjos et al. [2015] also applied Detrended Cross-Correlation Analysis (DCCA) on wind speed and solar irradiation time series to study long-term correlations. The results indicated the existence of a certain level of complementarity between persistence properties of the two stochastic processes: when the scaling exponent for wind speed increases, the scaling exponent[2] of solar irradiation decreases, and vice versa. It demonstrates the existence of complementarity between long-term correlation properties (measured by the value of DFA exponent), which can be useful in the long-term planning of hybrid generation systems at a site.

[2] The scaling exponent a is obtained as the slope of the regression (least square line fitting) of log[FDFA(n)] versus log n (see more in Anjos et al., 2015). The value of a= 0.5 indicates an uncorrelated signal, a > 0.5 indicates persistent long-term correlations, a < 0.5 indicates anti persistent long-term correlations. The values a=1 and a=1.5 correspond to 1/f noise and Brownian noise (integration of white noise) respectively.

In order to estimate the distance from which the variability of the interconnected system would begin to decrease significantly, Perez & Fthenakis [2015] defined the decorrelation distance as the distance, between a pair of geographic locations, from which the bulk of coordinate pairs exhibit zero correlation between their respective clearness index variations. Beyond this distance, complementarity begins, due to the fact that the correlation becomes negative for longer geographic distances than the decorrelation distance. Therefore, they estimated the size and shape of the region across which solar PV must be spread in order to reduce its unpredictable variability. Expected decorrelation distances between two locations in the Americas (South America, Central America and North America) vary from 1,123 km for day-to-day variations in the clearness index to 3,117 km for month-to-month variations. Perez & Fthenakis [2015] also calculated how much the system variability would decrease with the PV spread. For example: if N PV generation sites are spread across a region where the average separation between sites is 1,123 km, the magnitude of aggregate variations in outputs from day-to-day across the region are reduced by 1/√N. For month-to-month variations in aggregate output, this distance would be different, of 3,117 km, as they found that correlations decrease more slowly (with respect to pair separation) as timescale is increased [Perez & Fthenakis, 2015].

Perez & Fthenakis [2015] examined over 1.4 million unique pairs of sites in the Americas to quantify the influence of each pair's geographic separation and bearing on the correlation between the clearness indices at different timescales. In addition, they examined the trends in decorrelation when the distance between the locations changes, showing that the correlation coefficients between pairs of locations appeared to decrease exponentially with respect to their distance. Regarding the distance, concerning North – South separations, the correlation coefficient appears to decrease faster. It means that pairs of sites require considerably shorter distances to decorrelate when they are oriented North to South versus when they are oriented East to West by the same distance. The reason why this happens is because the meteorological phenomena that drive these variations propagate predominantly from East to West. Therefore, when we talk about PV systems in the Americas, a pair of sites separated North to South by the same distance that sites separated East to West is more likely to experience uncorrelated changes in cloud cover [Perez & Fthenakis, 2015].

Another way to evaluate the complementarity is proposed by Kougias et al. [2015]. In their research about complementarity between PV systems and small hydropower plants, they developed an algorithm that examines the degree of complementarity between different systems in any geographic location. First, the algorithm calculates the correlation between the monthly energy production from small hydropower plants and PV systems. Then, an iterative optimization algorithm analyzes possible changes in the installation characteristics of the solar – PV system (azimuth, tilt), in order to increase the complementarity. This iterative optimization process is repeated several times, changing the values of the threshold of solar PV energy output in order to explore possible gains in complementarity. These variations in solar PV plant characteristics result in minor energy compromises, which mean decreases in energy production by solar PV, associated to the modifications made in the optimization process. The optimization technique has been developed in MATLAB environment and performs an exhaustive search. Consequently, it can be used in cases where solutions' search space is confined, so the optimal solution can be detected with a short computation time.

The Kougias et al. [2015] results showed that small energy compromises result in noticeable increases of the anti-correlation (consequently, the complementarity). Figure 2 shows the relation between gains in complementarity and compromises in solar PV energy output: the curve is initially steep, gradually becomes smoother and then becomes horizontal at the convergence point. For example, a first compromise of 1% on the total production (from 100% to 99%) has a significant impact in the complementarity. However, to have further increases of the complementarity, it is necessary even larger sacrifices of energy compromises. Eventually, a threshold of 85% of the maximum energy production is a convergence point, where further compromise benefits the complementarity only by 2.2%. The curve shown in Figure 2 represents the trade-off between complementarity and solar PV energy output for the specific location and can be a valuable tool for developers, since it helps them estimating the price of different levels of increase in the complementarity while setting the threshold level in the planning phase of renewable energy projects [Kougias et al, 2015].

In a load following context, Buttler et al. [2016] analyzed time series of wind power, solar PV power and load for the year 2014 on a 15min to 8h time scale. The goal of the study was to quantify the variability of wind and solar PV power and the resulting challenges for the residual load in the European countries, in order to support the discussion about the integration of renewable systems. The main aspect analyzed was: the correlation between wind, solar PV power and electricity demand – to have an indicator of the load coverage through these energy sources and the smoothing effect based on geographical spreading in European countries and to have an indication of the benefits of an extension of the European energy grid through system integration of wind and solar PV power.

Figure 2. Trade-off between energy output and complementarity

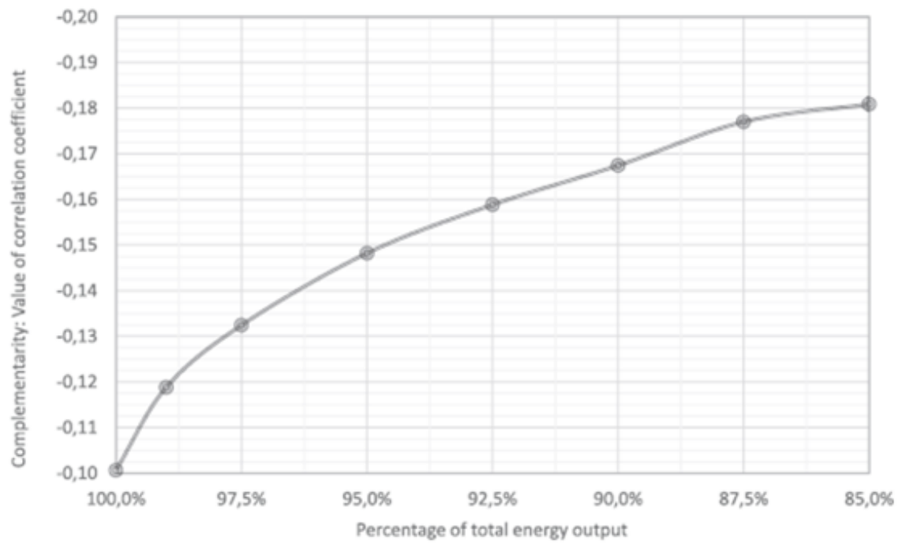

Source : Kougias et al., 2015.

Buttler et al. [2016] showed a high smoothing effect in wind power systems by geographic spreading, which indicates a strong decrease in the correlation coefficient as distance between sites increases. On the other hand, the results showed a high correlation of solar PV power production in Europe, between different regions, thus, they conclude that the smoothing effect of solar PV power is limited. Figure 3 shows the difference between the trend in wind and solar PV correlation coefficients with geographic spreading. The main reason for the limitation in the smoothing effect of solar PV power lies in the east-west extension of Europe, different from the Americas, which has a north-south extension. According to Perez & Fthenakis [2015], the east-west extension is not good for the region to have PV systems spread, due to the stochastic variability of solar power, that spreads faster in a north-south direction, so an east-west spread of solar PV would not result in significant gains in complementarity.

From the point of view of the load, Buttler et al. [2016] found a low positive correlation between wind power and electricity demand, with a correlation coefficient of 0.25 for Europe. The correlation coefficient between solar PV and the load is also positive, although it has a reduced significance due to night hours (there is no sun but there is a significant energy demand), and a high correlation

Figure 3. Correlation coefficients of wind and solar power production between the Europe countries as function of the distance of the respective centers

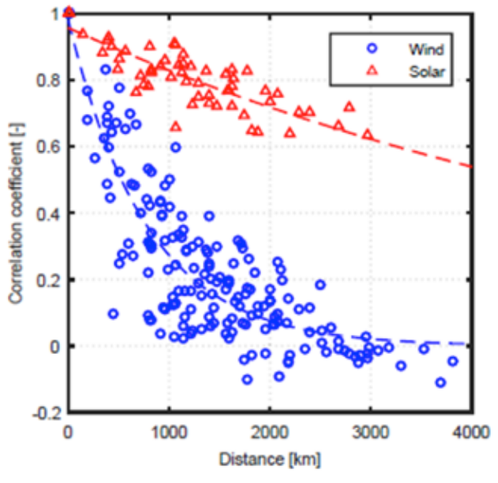

Source: Buttler et al., 2016.

during daytime. There was a negative correlation between wind and solar PV power production, in the range of -0.04 to -0.26 for all available national data and -0.24 for the whole of Europe. The main difference between Buttler et al. [2016] and other above-mentioned studies is that the analysis of Buttler et al. was made only for existing systems and did not take into account the potential resources (using climatic data). Regarding climatic data series, not only existing systems should be analyzed, but also the potential for renewable sources, assessing if the complementarity between wind and solar could be higher. Another particular approach made by Buttler et al. [2016] was to analyze the load and its relation to wind and solar energy. It would be ideal if the load would correlate with available renewable resources. However, as this is unlikely to happen, it is important to analyze how renewable energy sources would better correlate to each other in order to meet load demand. With the goal of producing energy to meet the required energy for end-use consumers, there is no need for a perfect anti-correlation between solar and wind, but an anti-correlation that allows these energy resources to follow, and meet, the load.

The Table 2 shows some aspects of the complementarity studies mentioned in this section.

Table 2. Aspects of the studies of complementarity

Authors	Study Overview	Complementarity analyzed	Location
Perez & Fthenakis (2015)	This research examined over 1.4 million unique pairs of sites in the Americas to quantify the influence of each pair's geographic separation and bearing on the correlation between the clearness indices at different timescales. In addition, This study examined the trends in decorrelation when the distance between the locations changes. Therefore, they estimated the size and shape of the region across which solar PV must be spread in order to reduce its unpredictable variability.	Solar FV - Solar FV	Americas
Kougias et al. (2015)	This research into complementarity between PV systems and small hydropower plants developed an algorithm that examines the degree of complementarity between different systems in any geographic location. The algorithm also analyzes what can be changed in the installation characteristics of the solar PV systems, in order to increase the complementarity. This iterative optimization process is repeated several times, changing the threshold values of the solar PV energy output in order to explore possible gains in complementarity.	Solar PV - Small Hydropower Plants	Any location
Anjos et al. (2015)	Used Detrended Fluctuation Analysis (DFA) method to quantify and compare correlations between wind speed and solar irradiation time series for the Fernando de Noronha Island, Brazil.	Wind - Solar PV	Fernando de Noronha Island, Brazil
Buttler et al. (2016)	The goal of this study was to quantify the variability of wind and solar PV power and the resulting challenges for the residual load in European countries in order to support the discussion about the integration of renewable systems. The main difference between Buttler et al. (2016) and other complementarity studies is that their analysis was made only for existing systems and did not consider potential resources (using climatic data). Another particular approach made by Buttler et al. (2016) was to analyze the load and its relation to wind and solar energy.	Wind - Solar PV - Load	Europe

03.
Methodology

3.1. Data Processing of the wind and solar PV potential power generation database for representative locations of Latin America

This study analyzes the potential integration between renewable energy sources in LA and helps to understand how complementarity can smooth out the resource variability.

The flowchart below shows the steps taken to achieve the goal of the study. The assumptions and procedures of each step are described hereafter:

Figur 4. : Flowchart of the steps taken to achieve the goal of the study

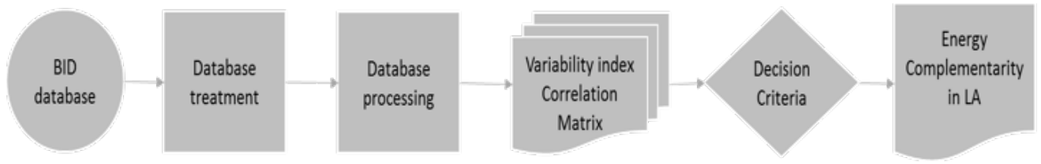

a) IDB Database

The Inter-American Development Bank (IDB) provided a database of fifteen years of wind speed and solar irradiation profiles for LA under an hourly scale, as well as the potential power generation from these resources. The resource data is a byproduct of the IDB´s Grid of the Future study that looked into an optimal long term integration of solar and wind energy in Latin America´s energy matrix.

The fifteen years (2000-2015)[3] of hourly values for each area's capacity factor were computed by simulated historical meteorological data with the Weather Research and Forecasting (WRF) model, which was run at a 27-km resolution.

This study considered the potential power generation data series instead of the series of wind speed and solar irradiance, since renewable energy integration is the prime goal.

The potential was estimated based on a gross capacity potential for solar and wind energy for determined areas that were considered according to some land use criteria[4] that tries to limit the capacity to a realistic upper threshold.

The potential of solar generation for each area was computed by a constant energy density of 29.77 MW/km2 (representative for a single-axis PV tracking system) and a minimum global horizontal irradiance (GHI) threshold of 175W/m2 (in order to be considered economically feasible).

For the wind resource, this study re-evaluated the potential power generation based on a 3.3 MW turbine at 100m hub height, with a cut in/out speeds of 3 m/s and 25 m/s, respectively, a rated speed of 13 m/s, a rotor radius of 112 m (r), a maximum Cp[5] of 0.45 and an efficiency of 95% (η). Other values considered were an air density of 1.225kg/m³ (ρ) and the wind speed (v). The power curve is shown in (Eq. 5) [Bianchi et al., 2007].

$$P=\eta*Cp*\rho*((\pi*r^2)/2)*v^3 \qquad \text{(Eq. 5)}$$

b) Database Treatment

This study analyzed 50 hotspots for wind energy and 36 hotspots for PV solar energy. The power generation data for each hotspot in the hour h were built by the sum of the multiplication of the potential power generation in the hour h by the gross installed capacity. Both terms of the equation consider the respective area and capacity factors (CF). According to the equation (Eq. 6)

$$Power\ Generation\ Hotspot_h = \sum_i^n P_{i,h} * C_i \qquad \text{(Eq. 6)}$$

Where $P_{(i,h)}$ is the potential power generation (in the hour h) for a specified area and capacity factor and C_i is the gross installed capacity for each area and CF.

Hence, a unique capacity potential and generation profile were built for each area.

c) Database Processing

This study used two software packages to analyze the wind and solar data: RStudio and Microsoft Excel.

The first analysis aimed to calculate the monthly $(\bar{G_m})$ and yearly $(\bar{G_y})$ generation values for each region, as (Eq. 7) and (Eq. 8), respectively

$$G_{m,y,a} = \sum_{h=1}^{m_h} G_{h,m,y,a} \qquad \text{(Eq. 7)}$$

$$G_{y,a} = \sum_{h=1}^{yh} G_{h,y,a} \qquad \text{(Eq. 8)}$$

Where

h = the considered hour

Y = the year of analysis

m = the month to be analyzed

a = the area of the database to be analyzed

m_h = is the number of hours in the month m

y_h = is the number of hours in a year

In order to understand the variability behavior of the hotspots, the following variability indices were calculated: Inter-Hourly Variability (IHV), Inter-Monthly Variability (IMV) and Inter-Annual Variability (IAV).

The long-term index and the hourly ramping rates[6] were also determined; for the ramping rates, this study built the histogram curve to evaluate the frequency distribution of this index for each area.

The potential complementarity between areas and resources was evaluated by linear correlation method, Pearson method. Regions that present negative correlation are defined as candidate regions for integration, because the negative correlation leads to a variability smoothing effect in the final energy output. This allows identifying the complementarity between the resources to reduce the intermittency of energy production [Kougias et al, 2016].

The correlation value was calculated for each year of the series (15 years) on hourly and monthly basis. The result is fifteen arrays correlations [86 x 86].

d) Decision Criteria

This study defined two decision criteria to determine areas with potential complementarity considering the computed correlations: i) if the frequency of negative correlation is equal or higher than 12 years, in other words equal or higher than 80% of the cases. This condition aims to guarantee the existence of a consistent correlation between the areas and ii) if the intensity of area-resource correlation is higher than the median of all correlations, then the area-resource is considered as a good candidate to complementarity.

e) Energy Complementarity in LA

To understand how hourly ramping can be reduced by complementarity and how integration can play an important role in energy systems, this study compared the mean hourly generation of some areas. This comparison was made for the five areas that presented the strongest negative correlation coefficient.

With the intention of giving the reader an idea of how the best correlations are geographically distributed, this study also created some maps to represent the best complementarity regions. Hence, fourteen maps were created: two showing hourly correlation for wind and solar power generation, nine for monthly correlation of wind and solar power, and three for monthly correlation considering the standard year for hydro-solar-wind generation, to be explained in the next section.

3.2. Selection and data gathering of representative hydrological basins of representative locations

Unlike wind and solar data that were provided by the Inter-American Development Bank (IDB), the information of hydropower was acquired from the electric power sector of the countries studied in this report. This can cause some inconsistencies in the analysis of complementarities with other sources or even in the typical year trajectory of the hydropower hotspots.

The analysis of hydraulic sources sought to form clusters of hydraulic energy resources for a same country according to its hydrological patterns in order to form hotspots. These were used as parameters to determine the complementarity to wind and solar hotspots.

The methodological procedure consisted firstly in creating a database composed of a time series of natural monthly streamflow of rivers where hydroelectric plants are located and monthly electricity generation data of hydropower. These data were obtained mainly from government regulatory bodies and power generating companies.

All monthly data of natural streamflow were normalized to zero mean and standard deviation equal to one and subsequently a standard year for each hydroelectric plant was shaped based on the monthly average of the normalized data.

The standard years of all hydroelectric plants that belong to the same country were plotted and grouped according to their hydrological patterns. In doing so, hydroelectric plants that exhibit similar behavior throughout the year could be clustered to create a hotspot.

The standard year of hotpots were designed by summing streamflow data of hydroelectric power plants previously

[3] EIt is important to highlight that the years were reordered. The period 2016-2020 represents the period 2010-2014 in order to make the strong 2010 El Niño coincide with the similar strong 2016 El Niño. And 2020-2030 represent the period 2000-2009.

[4] The total area available for wind power discarded water bodies, urban regions, protected areas; for solar power, open land was available, such as agricultural, barren or grassland.

[5] The power coefficient refers to the power that could be extracted of the wind energy, its maximum value is 0.593, been known as Betz coefficient.

[6] The percentage difference between the generation in the hour h and h-1

grouped as mentioned above. Next, this sum was normalized and a monthly average calculated, yielding a standard year that represents the typical hydrological behavior of a basin or a group of basins in a specific country.

In the case of binational hydroelectric plants, in each nation the value of the flow was reduced by half to avoid double counting, as in the case of Itaipu (Brazil and Paraguay), Yacyretá (Argentina and Paraguay) and Salto Grande (Argentina and Uruguay).

For countries in which only electricity generation was available and no additional information was found, the same procedure of normalization, aggregation and establishment of a standard year was done. However, a supplementary investigation was held with the purpose of removing impoundment plants data. This analysis was accomplished by plotting the standard year of hydroelectric power plants. Those that showed a pattern of homogeneous generation over the months were considered impoundment plants and thus withdrawn from the database.

This step is necessary due to impoundment of hydroelectric plants that can generate energy in drier periods, which may distort the analysis of the natural hydrological pattern of the region where the plant is located and consequently misrepresent the typical year of the hotspot.

For Guyana, Mexico, Panama, Suriname and Venezuela neither streamflow nor electricity generation data were found. For this reason, these countries were not included in the hydro complementarity analysis. For Argentina, Chile and Ecuador mean streamflow data was found for some rivers but without their gauge locations. Thus, in the absence of more accurate data, this study considered that these data represent the streamflow where the hydroelectric plants are located.

In Brazil, hydroelectric plants were grouped by basins. The data used was the natural monthly inflow of the hydroelectric plants in the period between 1931 and 2014 provided by the Operador Nacional do Sistema Elétrico [ONSa]. In the case of cascade hydroelectric plants, this study considered only the plant located downstream. Thereafter, the flow of the plants downstream was added to the flow of plants located in other rivers of the same basin. The standard year basins which achieved the same seasonality in the typical year curve were grouped at the same hotspot, so there were three hotspots. The Brazil 1 hotspot consists of the South Atlantic and Uruguay basins, while Brazil 2 is formed by the East and Southeast Atlantic. Finally, Brazil 3 is composed of the Parnaíba, São Francisco, Tocantins, Amazonas, Paraguay and Parana basins. Brazil 1 has an upward trend from May to October. On the other hand, Brazil 2 has an increase in flow from October until the end of the year. Brazil 3 has higher flow rates between the months of October and March [ONSb].

Brazil was the most complex case, because it has more hydroelectric plants and a bigger territory than other Latin American countries.

There is no data for many months of the six plants in French Guiana which are addressed in this study. The French Guiana hotspot was attained by natural flow data of the hydroelectric power plants between the period 2010 and 2016, which were provided by the Système d'Information du Développement Durable et de l'Environnement (SIDE). The flow rates of French Guiana have similar behavior throughout the year so they were allocated in the same hotspot.

Data gathered for Paraguay was the inflow to its two major binational hydroelectric power plants: Itaipu and Yacyretá. The natural flow data from Yacyretá was attained at the official website of the hydroelectric plant Entidad Binacional Yacyretá [EBY] while the Itaipu information was obtained at Operador Nacional do Sistema Elétrico [ONS]. As these plants show similar trajectories, they were located at the same hotspot.

In Uruguay, the typical year was based on monthly electricity generation data provided by the Administración del Mercado Eléctrico [ADME]. from 2012 to 2016. After normalization, it was observed that the Uruguayan hydroelectric power plants had a similar trend during the year and for this reason this country has only one hotspot.

In Argentina, the standard year was obtained from streamflow data between 1994 and 2016 from the Compañía Administradora del Mercado Mayorista Eléctrico [CAMMESA]. In this study seven hydroelectric plants were analyzed and properly allocated in two hotspots. One formed by six plants and the other by the Yacyretá plant, because they have different hydrological behaviors. In the first one, the flow rates start low and increase until the middle of the year, in Argentina 2 the opposite happens, with the flow failing up to September [CAMMESA].

In the same direction, Chile was also divided into two hotspots. To create the standard year, the streamflow data between 2000 and 2016 was used by the Sistema Nacional de Información del Agua (SNIA). Chile 1 comprised the Biobío and Maule regions, while the Metropolitan and O'Higgins regions were part of hotspot Chile 2. Chile 1 has an upward flow trend from January to July and falls between this month and December. On the other hand, Chile 2 shows a fall from January to July and then there is an increase in the flow from that time, lasting until the end of the year [SNIA].

In the Bolivia analysis, the data provided by the Comité Nacional de Despacho de Carga (CNDC) was the natural monthly inflow, in the period between 2008 and 2016. The Corani and Chojlla are the largest hydropower plants and the others are very small. The principal hydroelectric plants are together in just one hotspot. All of them showed an increase in flow up to March and then a decline until September, when their flows increase again at the beginning of the rainy season [CNDC].

In Ecuador, the standard year was obtained from streamflow data between 1990 and 2013. In this country, two distinct hydrological patterns were identified. The Ocaña, Marcel Laniado and Manduriacu hydropower plants formed the first hotspot which had a higher flow rate between January and June. The second hotspot was defined based on data from the Paute and Mazar hydropower plants that had higher flow rates between May and September [INAHMI].

Colombia's typical year was obtained through natural streamflow data between the period 2000 and 2014, published by the Interconexión Eléctrica S.A (ISA). This country has two hotspots. Colombia 1 includes the regions of Antioquia, Caribbean and East, while Colombia 2 is composed by Valle and Central areas. The first one has an increased flow from January to July and then drops to the end of the year. However, the second region shows a really different trajectory, with flow increasing until May, then falling sharply until September and growing again from this month until December [ISA].

In Costa Rica, the standard year represents monthly electricity generation data provided by the Instituto Costarricense de Eletricidad (ICE) from 2011 to 2015 [ICE]. These data were separated into three distinct patterns that underpinned the three hotspots analyzed in this report. The first hotspot shows a pattern of higher electricity generation between the months of January and July, represented by the Dengo, Arenal and Sandillal hydroelectrics. The second hotspot is represented by Garita 1 and 2, Garita 3 and 4, Pirris and Poas I and II hydropower plants, which have higher electricity generation between the months of September and December. The third hotspot was represented by Peñas Blancas, Cariblanco, Tapezco, Platanar, Zuerkata and Don Pedro hydropower plants that have a high generation in July, November and December.

The El Salvador hotspot was attained by natural flow data between the period 2005 to 2014 of Guajoyo, Cerrón Grande hydropower plants on 5th November and 15th September, which were provided by the Superintendencia General de Electricidad y Telecomunicación (SIGET). The standard year obtained shows higher flow rates between the months of July to November [SIGET].

The standard year of Guatemala was also underpinned by monthly electric generation data between the years of 2006 and 2012 attained from the Comissión Nacional de Energía Electrica (CNEE) website. The standard year built was derived from Aguacapa, Candelaria, El Canada, Los Esclavos, Las Vacas, Matanzas, Pasa Bien, Poza Verde and Renace hydropower plants, which presented a pattern of high generation from June to November [CNEE].

In Honduras the data gathered was for monthly electricity generation between the years 2006 and 2014 by the Empresa Nacional de Energía Electrica (ENEE), the standard year was set from data of hydropower plants El Nispero and Nacaome, resulting in a pattern of high generation in the periods between May and October [ENEE].

In Nicaragua, the data available by the Instituto Nicaraguense de Energía (INE) is the natural monthly inflow of Apanas, Asturias and La Virgen hydropower plants in the period between 2006 and 2015. The standard year established had higher contributions in the volume of water in the months from June to November [NE].

The standard year of Peru is built upon natural streamflow data between the period of 1992 and 2015 published by the Comité de Operaciones del Sistema Interconectado Nacional (COES). The streamflow data employed for the calculation was from the Mantaro river, Santa Eulalia, Tamboraque, Santa, Chancay, Charcani V, Aricota I and II, and San Gaban. The period of higher flow rates is from January to May [COES SINAC].

04.

Results

This section presents the most relevant results, as well as being a tutorial to understand all the products obtained throughout the study.

4.1. Energy Complementarities – Temporal analysis

Figure 5 and Figure 6 show the potential generation and possible complementarity between two areas that are strongly correlated on an hourly basis (WIND_BR_A06 and SOLAR_CL_A03). The figures show that the Brazilian site has intense wind activity in the early hours of the day and the solar resources of the other area could complement its reduction during the day. It also shows the availability of resources throughout typical summer and winter weeks exhibiting seasonal impacts. Because the installable solar capacity is so much greater in Chile than in Brazil the potential generation that would promote complementarity was normalized, utilizing the P50[6] criteria for the firm wind capacity. It means that this analysis assumes that the solar capacity is equal to the median of the wind generation time series in the Brazilian site.

[7] Original criteria indicated by the Brazilian Ministry of Mines and Energy (Ministério de Minas e Energia) to calculate the amount of energy expected to be produced by a wind power plant as a way to mitigate the economic risk associated with inter-annual resource variability. It means that there is a 50% likelihood that the farm's output will be greater than the firm energy determined by this criteria.

Figure 5. Variability of two areas with strong hourly correlations during a summer week.

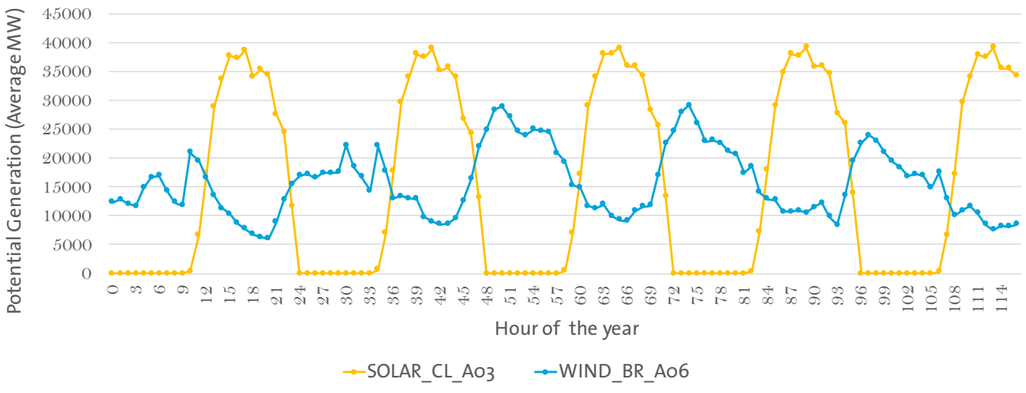

Figure 6: Variability of two areas with strong hourly correlations during a winter week.

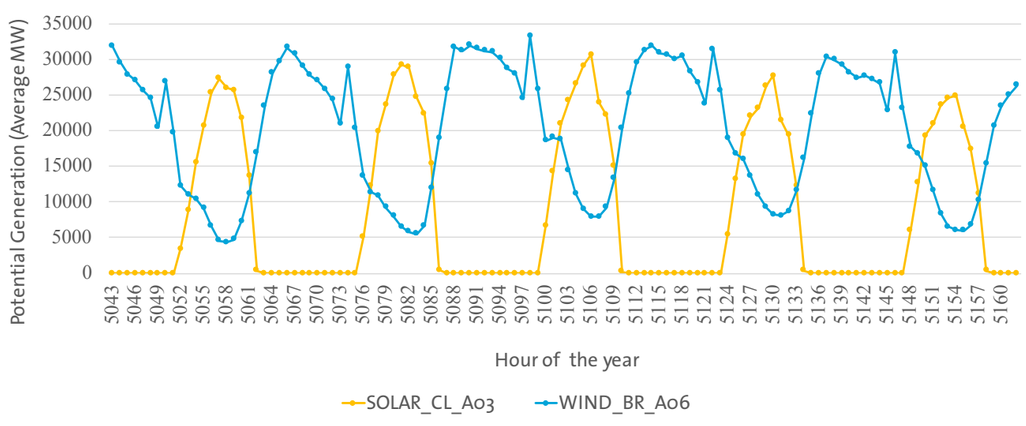

The twenty pairs with the strongest hourly correlation are listed in Table 3. It is clear that all those strongest correlations are between the area WIND_BR_06 and other solar resource hotspots spread over the region. This occurs due to the fact that the area in Brazil has greater wind speeds during the night and can be complemented by solar generation during the day.

Figure 7 and Figure 8 show the seasonal complementarity between the areas of Wind_PE_A01 & Wind_PA_A01 and Wind_BR_A01 & Wind_BR_A03 respectively. These areas have a high (absolute) value of correlation coefficient on a monthly potential energy generation basis. Once again, the monthly totals were adjusted so that the amounts of energy generation could complement each other resources despite the different potential between those areas. The twenty pairs with strongest monthly correlation are list in Table 4.

Table 3. Twenty pairs with the highest hourly correlation factors

Pair		Correlation factor
SOLAR_PE_A01	WIND_BR_A06	-0,451
SOLAR_ES_A01	WIND_BR_A06	-0,444
SOLAR_CL_A03	WIND_BR_A06	-0,442
SOLAR_VE_A01	WIND_BR_A06	-0,442
SOLAR_VE_A03	WIND_BR_A06	-0,442
SOLAR_CO_A02	WIND_BR_A06	-0,441
SOLAR_CO_A01	WIND_BR_A06	-0,441
SSOLAR_CL_A01	WIND_BR_A06	-0,439
SOLAR_EC_A01	WIND_BR_A06	-0,436
SOLAR_CL_A02	WIND_BR_A06	-0,432
SOLAR_PE_A02	WIND_BR_A06	-0,431
SOLAR_BR_A01	WIND_BR_A06	-0,423
SOLAR_AR_A01	WIND_BR_A06	-0,422
SOLAR_PA_A01	WIND_BR_A06	-0,417
SOLAR_MX_A06	WIND_BR_A06	-0,414
SOLAR_MX_A08	WIND_BR_A06	-0,414
SOLAR_VE_A02	WIND_BR_A06	-0,412
SOLAR_AR_A02	WIND_BR_A06	-0,411
SOLAR_MX_A05	WIND_BR_A06	-0,408
SOLAR_MX_A07	WIND_BR_A06	-0,407

Table 4. Twenty pairs with the strongest monthly correlation factors

Pair		Correlation factor
EÓLICA_VE_A04	WIND_BR_A03	-0,907
EÓLICA_VE_A03	WIND_BR_A04	-0,889
EÓLICA_VE_A03	WIND_BR_A05	-0,888
EÓLICA_VE_A03	WIND_BR_A03	-0,875
EÓLICA_VE_A04	WIND_BR_A04	-0,86
EÓLICA_SU_A01	WIND_BR_A03	-0,851
EÓLICA_BR_A05	WIND_BR_A01	-0,850
SOLAR_MX_A01	WIND_CL_A01	-0,849
EÓLICA_SU_A01	WIND_BR_A04	-0,844
EÓLICA_VE_A02	WIND_BR_A03	-0,837
SOLAR_BR_A03	WIND_BR_A01	-0,835
SOLAR_ES_A01	WIND_AR_A01	-0,832
SOLAR_BR_A03	WIND_VE_A03	-0,830
SOLAR_VE_A03	WIND_EC_A01	-0,825
SOLAR_PA_A01	WIND_AR_A01	-0,822
EÓLICA_VE_A02	WIND_BR_A04	-0,816
EÓLICA_PE_A01	WIND_BR_A01	-0,809
SOLAR_EC_A01	WIND_VE_A03	-0,809
EÓLICA_BR_A01	WIND_AR_A01	-0,802
EÓLICA_PE_A01	WIND_CO_A02	-0,801

Figure 7. Seasonal complementarity between areas with a high monthly correlation factor: WIND_PE_A01 and WIND_PA_A01

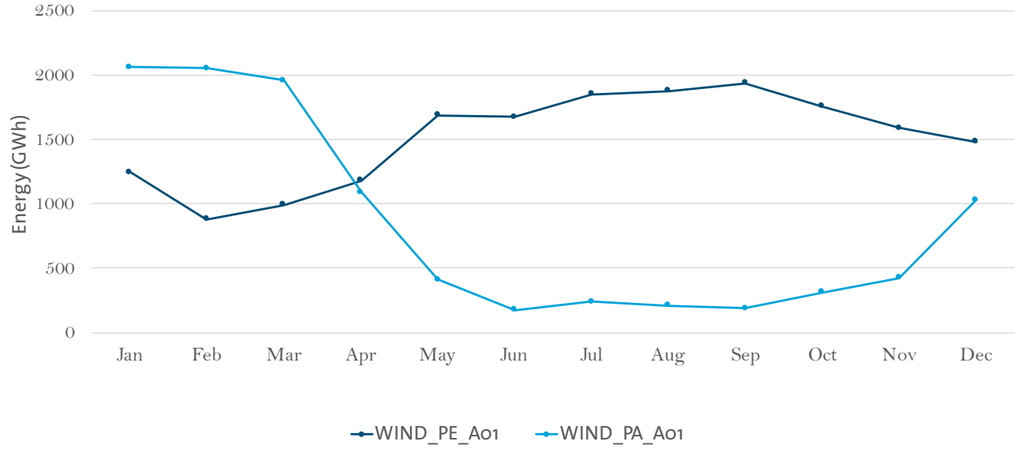

Figure 8. Seasonal complementarity between areas with a high monthly correlation factor: WIND_BR_A01 and WIND_BR_A03

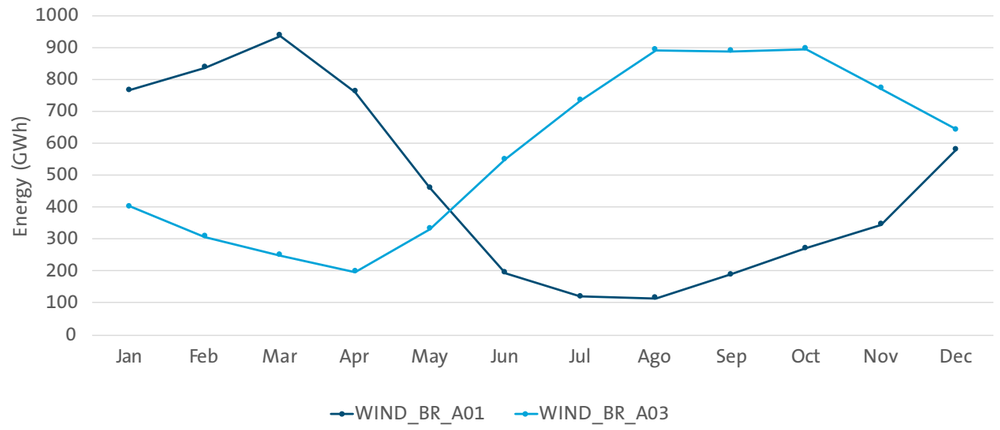

4.2. Energy Complementarities – Geographic analysis based on an hourly scale data

Maps[8] were implemented to specify the regions with good evidence of complementarity of wind and solar resources in Latin America, using the hourly data resources. These maps were developed using the decision criteria[9], frequency and intensity of correlations, enabling the visualization of areas with good potential for complementarity between energy resources.

It is worth noting that the assessed areas consider just the potential power resources integration. The physical capacity through electric interconnections was not evaluated in order to integrate these areas. This would require a different type of analysis, including the different modes of physical and economic integration between regions in Latin America.

Figure 9 shows the correlation of WIND_BR_A06 hotspot with SOLAR_PE_A01, SOLAR_ES_A01, SOLAR_CL_A03, SOLAR_VE_A01, SOLAR_VE_A03, SOLAR_CO_A02, SOLAR_CO_A01, SOLAR_CL_A01, SOLAR_EC_A01, SOLAR_CL_A02, SOLAR_PE_A02, SOLAR_BR_A01, SOLAR_AR_A01, SOLAR_PA_A01, SOLAR_MX_A06, SOLAR_MX_A08, SOLAR_VE_A02, SOLAR_AR_A02, SOLAR_MX_A05, SOLAR_MX_A07, SOLAR_MX_A04 and SOLAR_AR_A03 hotspots. All correlations are higher than -0.40, indicating a good complementarity between regions. That is, the wind regime between these regions is reverse during the day. A reason to WIND_BR_A06 hotspot to be correlated with all these solar sites is the typical wind that blows in this area during the night. This negative correlation can be used to minimize the total variability of the resources.

Figure 10 shows the correlation of WIND_BR_A03 hotspot with WIND_VE_A03 hotspots. The correlation is -0.40, indicating a good complementarity between regions.

[8] These maps were drawn based on arrays of hourly data correlations of wind and solar resources. Only 23 regions with the best indications of complementarity are mapped in the main text.

[9] The frequency of negative correlations and intensity of these correlations were used as decision criteria. The results presented in Figure 9 and Figure 10 show negative correlation over the 15 years of the time series. Thus, the major decision criteria become the value of the correlation intensity between the areas and resources.

Figure 9. Region WIND_BR_A06 and its related region with good evidence of hourly complementarity

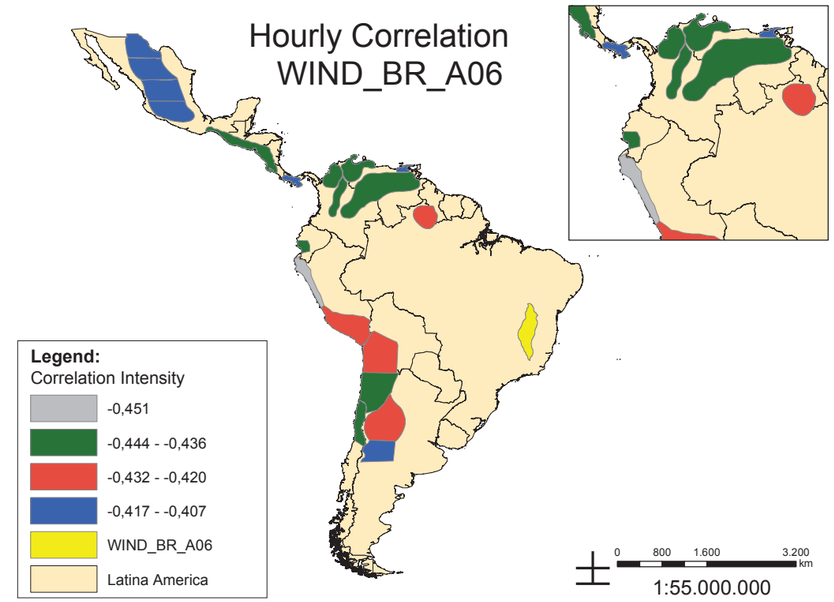

Figure 10. : Region WIND_BR_A03 and its related regions with good evidence of hourly complementarity

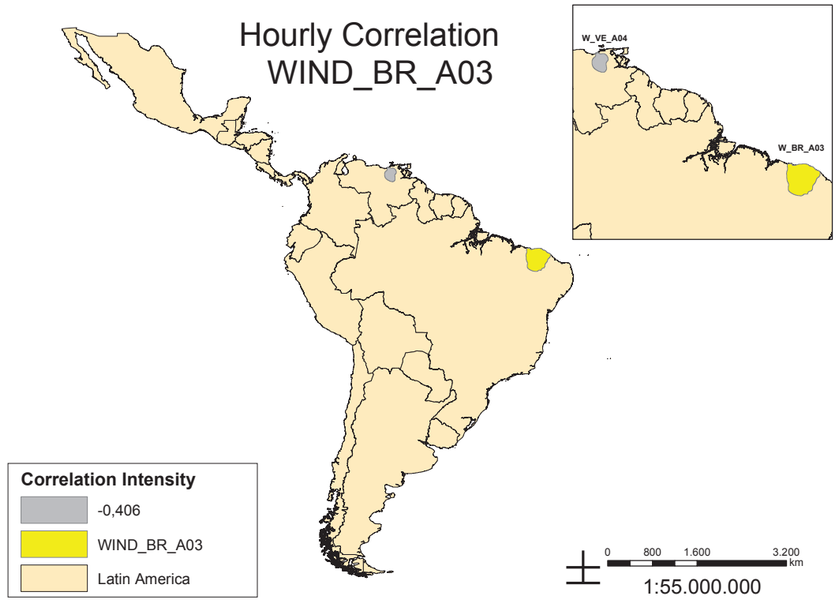

4.3. Energy Complementarities – Geographic analysis based on an seasonally approach

Maps[10] were implemented to specify regions with good evidence of complementarity of wind and solar resources in Latin America, using the average monthly availability of resources. These maps were developed using the decision criteria[11], frequency and intensity of correlations, enabling the visualization of areas with good potential for complementarity between energy resources.

Figure 11 shows the correlation of WIND_BR_A03 hotspot with WIND_VE_A04, WIND_VE_A03, WIND_VE_A02, WIND_SU_A01 hotspots. All correlations are greater than -0.81, which indicates a very good complementarity between regions. That is, the wind regime between these regions is reversed during the year. This negative correlation can be used to minimize the total variability of the resources.

Figure 12 shows the correlation of WIND_BR_A04 hotspot with WIND_VE_A04, WIND_VE_A03, WIND_VE_A02, WIND_SU_A01 hotspots. All correlations are greater than 0.81, which indicates a very good complementarity between regions. That is, the wind regime between these regions is reversed during the year. This negative correlation can be used to minimize the total variability of the resources.

Figure 13 shows the correlation of WIND_BR_A05 hotspot with WIND_VE_A03 hotspots. The correlation is -0.88, which indicates a very good complementarity between regions.

Figure 14 shows the correlation of WIND_BR_A01 hotspot with WIND_BR_A05, SOLAR_BR_A03, WIND_PE_A01 hotspots. All correlations are greater than -0.80, which indicates again a very good complementarity between regions.

Figure 15 shows the correlation of WIND_AR_A01 hotspot with SOLAR_ES_A01, SOLAR_PA_A01, WIND_BR_A01 hotspots. All correlations are greater than -0.80, which indicates a very good complementarity between regions.

Figure 16 shows the correlation of WIND_EC_A01 hotspot with SOLAR_VE_A03 hotspots. The correlation is -0.82, which indicates a very good complementarity between regions.

Figure 17 shows the correlation of WIND_CL_A01 hotspot with SOLAR_MX_A01 hotspots. The correlation is -0.84, which indicates a very good complementarity between regions.

Figure 18 shows the correlation of WIND_VE_A03 hotspot with SOLAR_BR_A03, SOLAR_EC_A01 hotspots. All correlations are greater than -0.80, which indicates a very good complementarity between regions.

Figure 19 shows the correlation of WIND_CO_A02 hotspot with WIND_PE_A01 hotspots. The correlation is -0.80, which indicates a very good complementarity between regions.

[10] These maps were drawn based on arrays of monthly averages of the correlations of time series of wind and solar resources. Only 20 regions with best indicative of complementary are mapped in the main text.

[11] The frequency of negative correlations and intensity of these correlations were used as decision criteria. The results presented in the maps of this section show negative correlation over the 15 years of the time series. Thus, the discussion focuses on the value of the correlation intensity between the areas and resources in the text.

Figure 11. Region WIND_BR_A03 and its related regions with good evidence of monthly complementarity

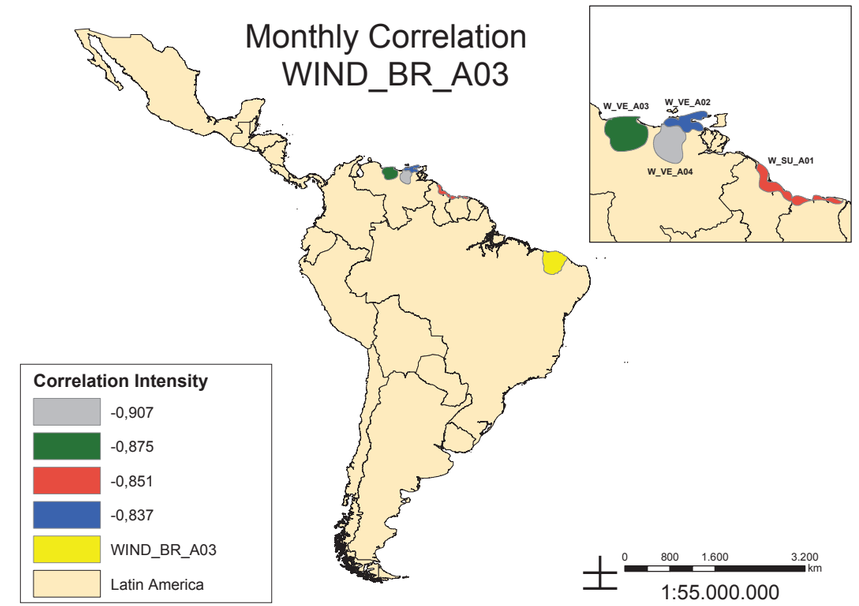

Figure 12. Region WIND_BR_A04 and its related regions with good evidence of monthly complementarity

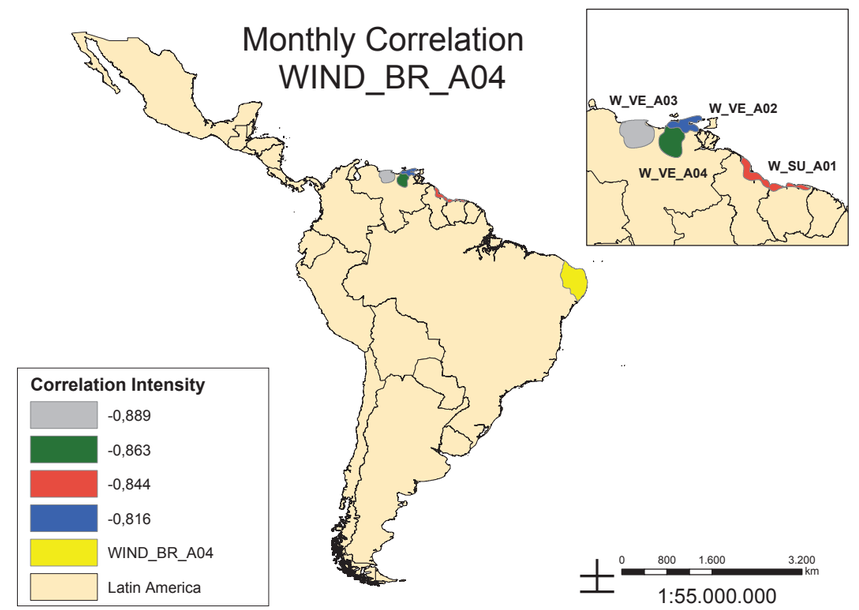

Figure 13. Region WIND_BR_A05 and its related regions with good evidence of monthly complementarity

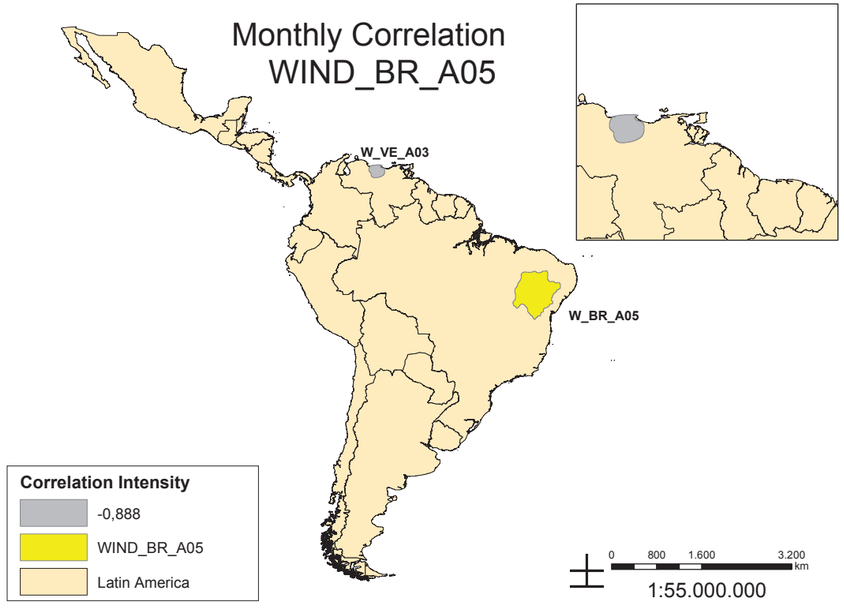

Figure 14. Region WIND_BR_A01 and its related regions with good evidence of monthly complementarity

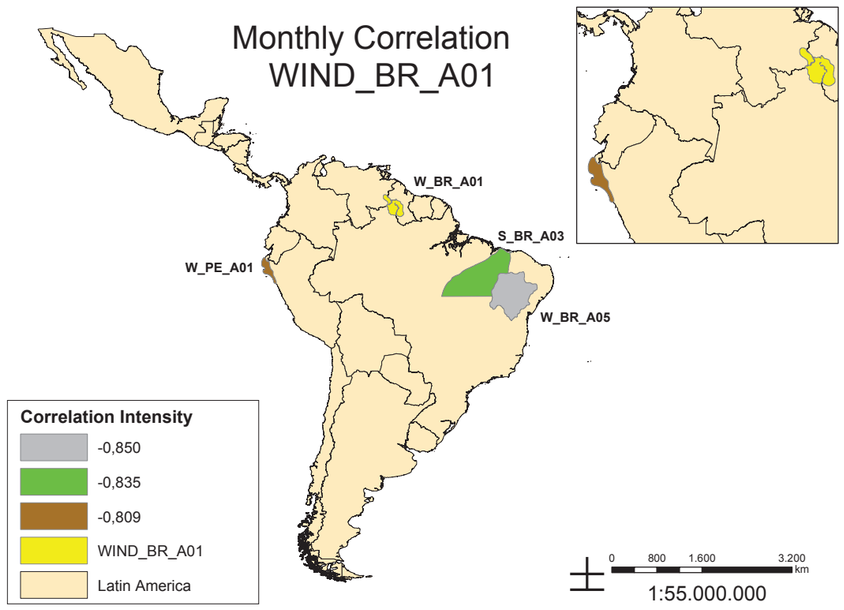

Figure 15. Region WIND_AR_A01 and its related regions with good evidence of monthly complementarity

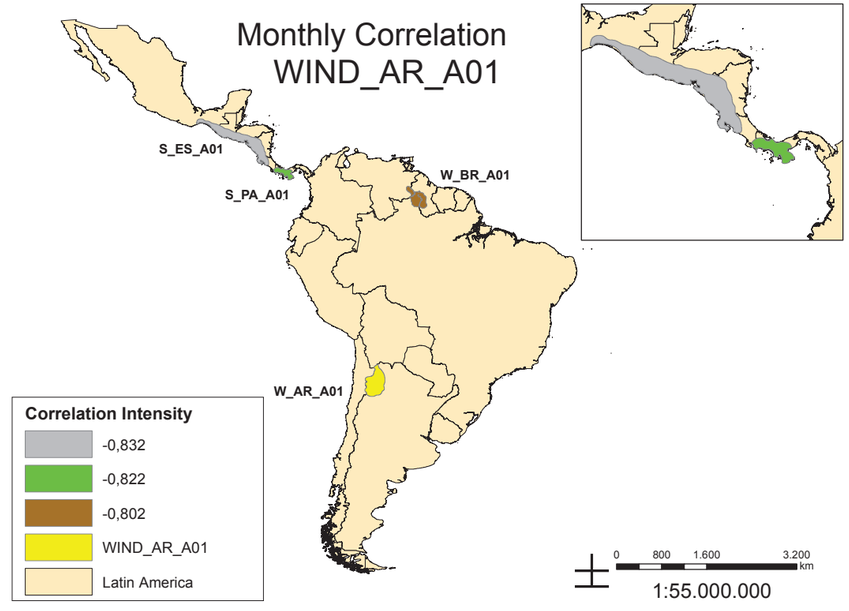

Figure 16. ZAP EÓLICA_CL_A01 y sus regiones relacionadas con buenas evidencias de complementariedad

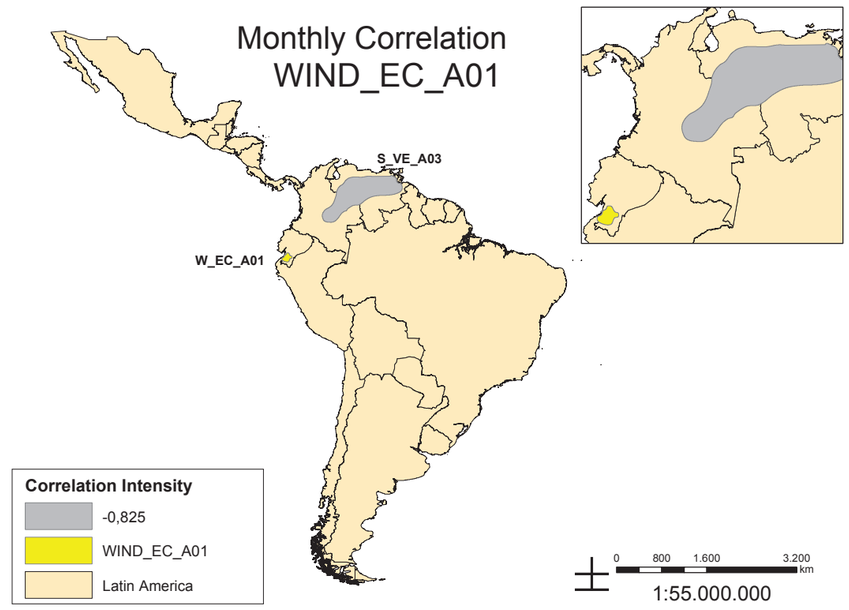

Figure 17. Region WIND_CL_A01 and its related regions with good evidence of complementarity

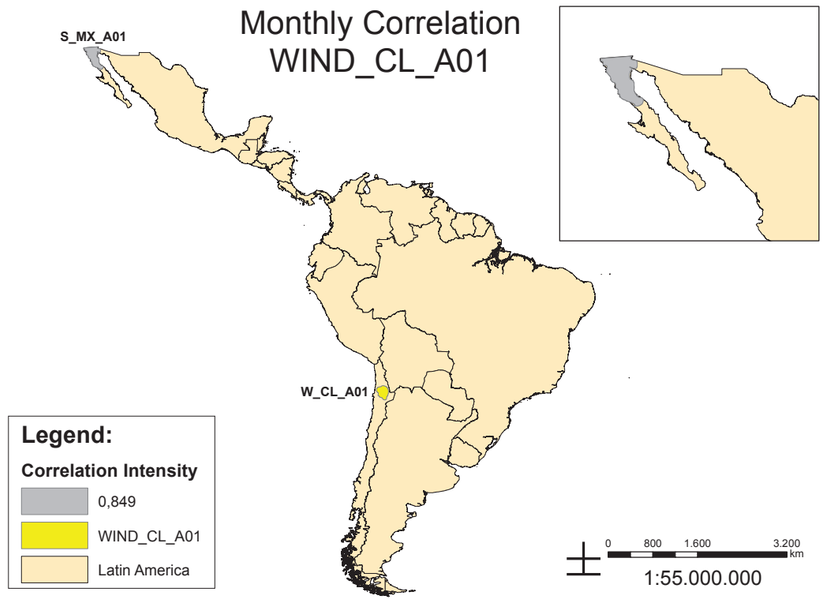

Figure 18. Region WIND_VE_A03 and its related regions with good evidence of complementarity

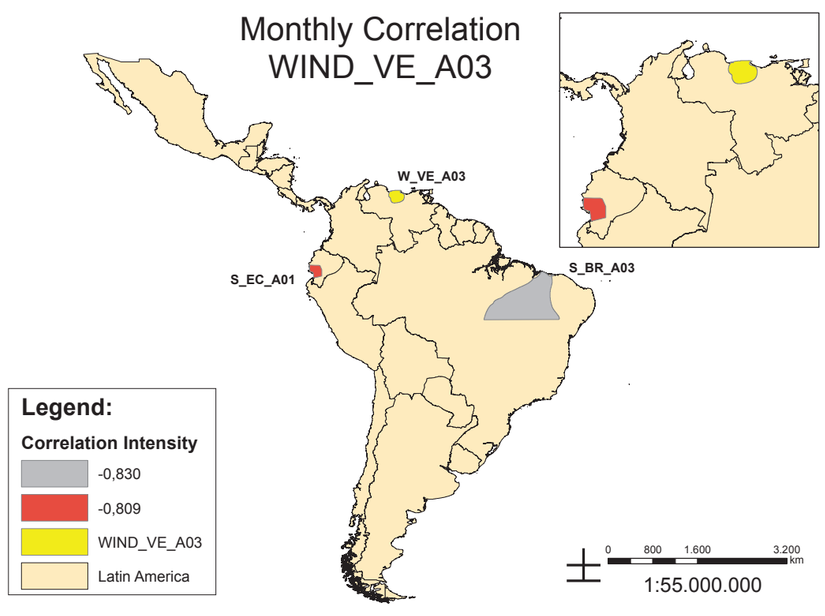

Figure 19. Region WIND_CL_A01 and its related regions with good evidence of complementarity

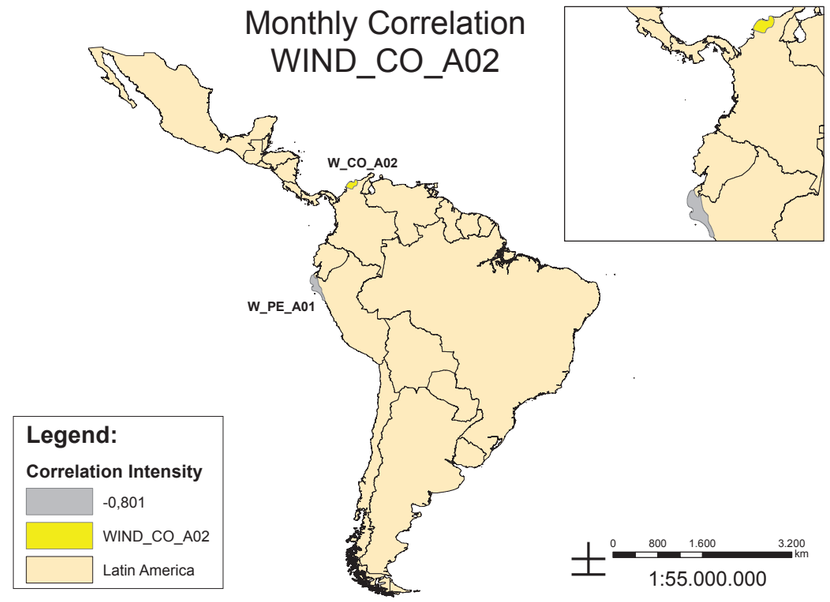

4.4. Energy Complementarities – Geographic analysis based on a seasonal approach with hotspots for hydro power generation

Maps[12] were implemented to specify the regions with good evidence of complementarity of wind, solar and hydro resources in Latin America, using the average annual profile of the resources to estimate the correlation. These maps were developed using just the intensity decision criteria, as the frequency criteria is not available for this analysis. All years were clustered into an average standard year. The intensity of correlations enables the visualization of areas with good potential for complementarity between those energy resources.

Figure 20 shows the correlation of Hydro_Brazil3 hotspot with Hydro_Argentina1, Hydro_Chile1, Hydro_Guatemala, Wind_AR_A03, Wind_BR_A03, Wind_BR_A04, Wind_BR_A10 and Wind_PE_A01. All correlations are more negative than -0.9, which indicates an excellent complementarity between regions. That is, the hydro and wind regimes between these regions are reversed during the year. This negative correlation can be used to minimize the total variability of the resources.

Figure 21 shows the correlation of Hydro_Paraguay hotspot with Wind_AR_A01, Wind_BO_A01, Wind_BR_A05, Wind_BR_A10, Wind_PE_A01, Wind_PE_A02 and Wind_PE_A03. All correlations are greater than -0.9, which indicates an excellent complementarity between regions.

Figure 22 shows the correlation of Hydro_Chile1 with Hydro_Brazil3, Hydro_Peru, Solar_PA_A01, Wind_BR_A01, Wind_CO_A02, Wind_SU_A01 and Wind_VE_A03. The correlation is -0.9, which indicates an excellent complementarity between regions.

[12] These maps were drawn based on arrays of average annual profile of the correlations of time series of wind, solar and hydro resources. It was necessary to build a typical year to handle the problem of different lengths of time series between resources and regions. Only 10 regions with the best complementarity values are mentioned in the main text.

Figure 20. Region Hydro_Brazil3 and its related regions with good evidence of complementarity

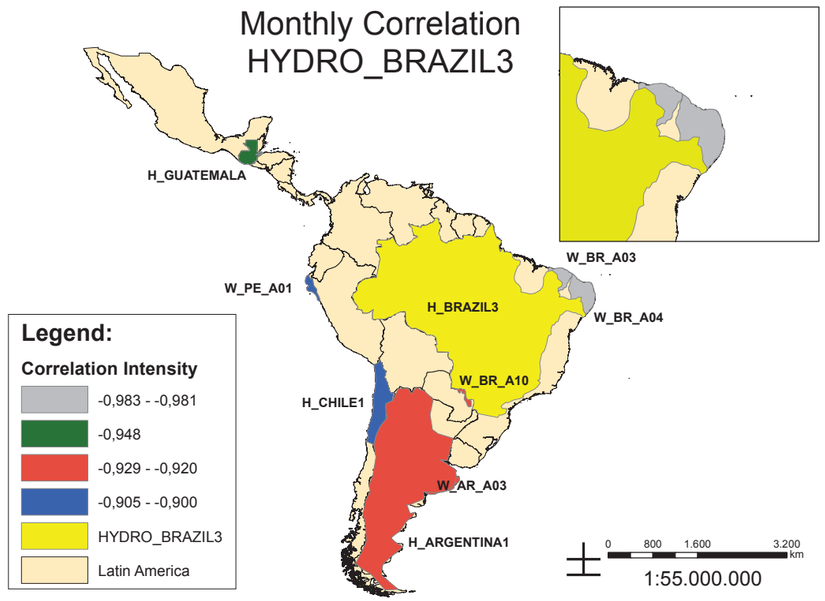

Figure 21. Region Hydro_Paraguay and its related regions with good evidence of complementarity

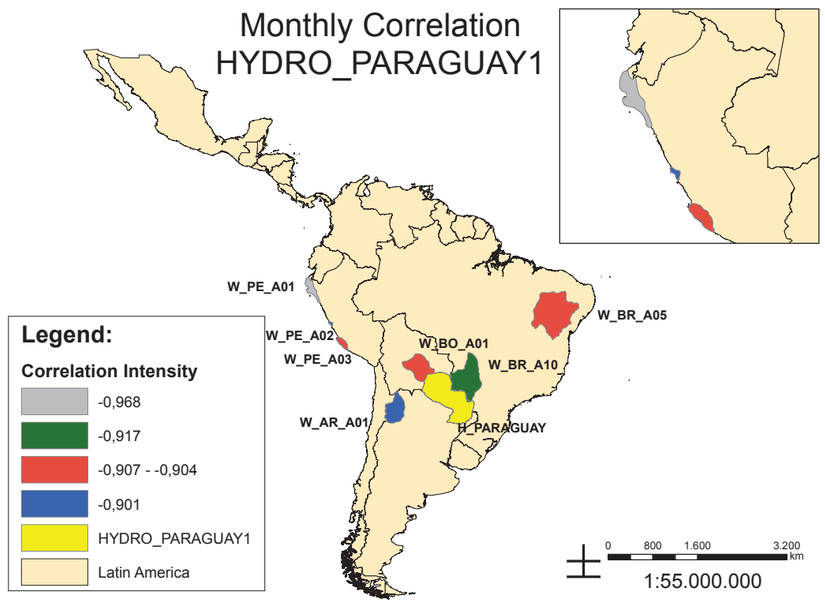

Figure 22. Region Hydro_Chile1 and its related regions with good evidence of complementarity

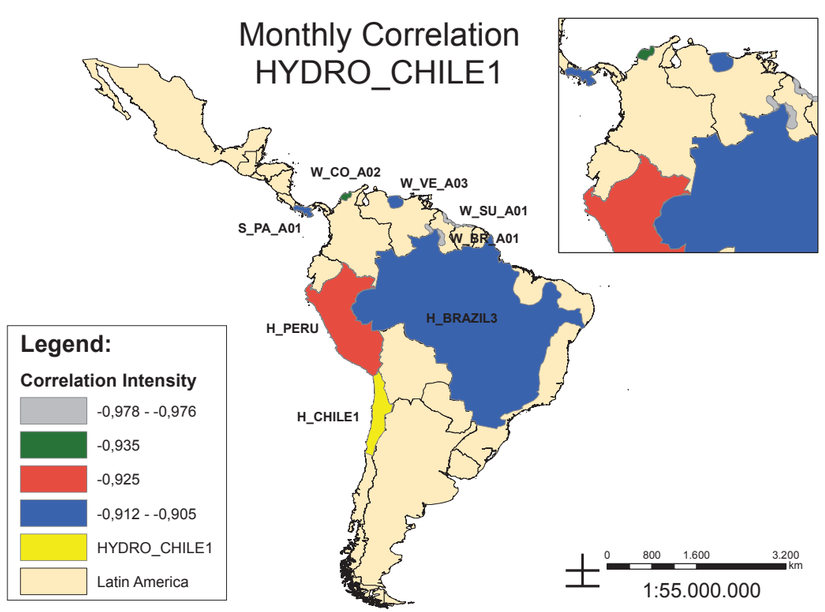

4.5. Summary of Results

The available data were treated to provide variability indices and correlations between the assessed hotspot regions. This report focuses on the major results. Figure 25 and Figure 26 show the IAV intensity for each wind and solar hotspot, respectively.

Figure 25. IAV intensity for wind hotspots

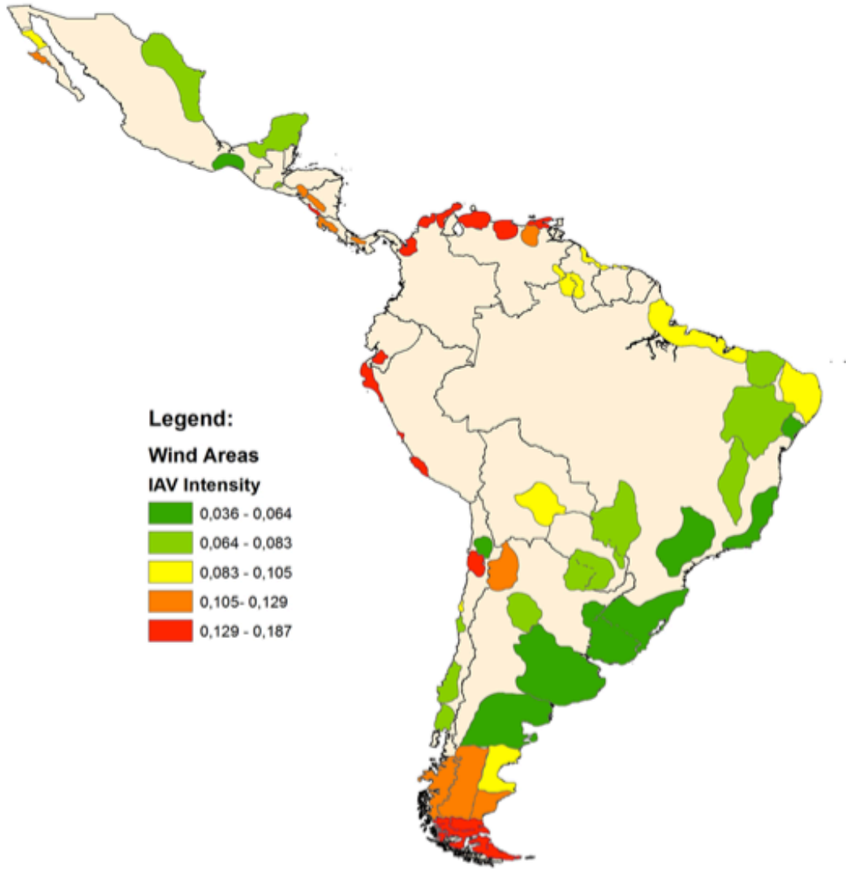

Figure 26. IAV intensity for solar hotspots

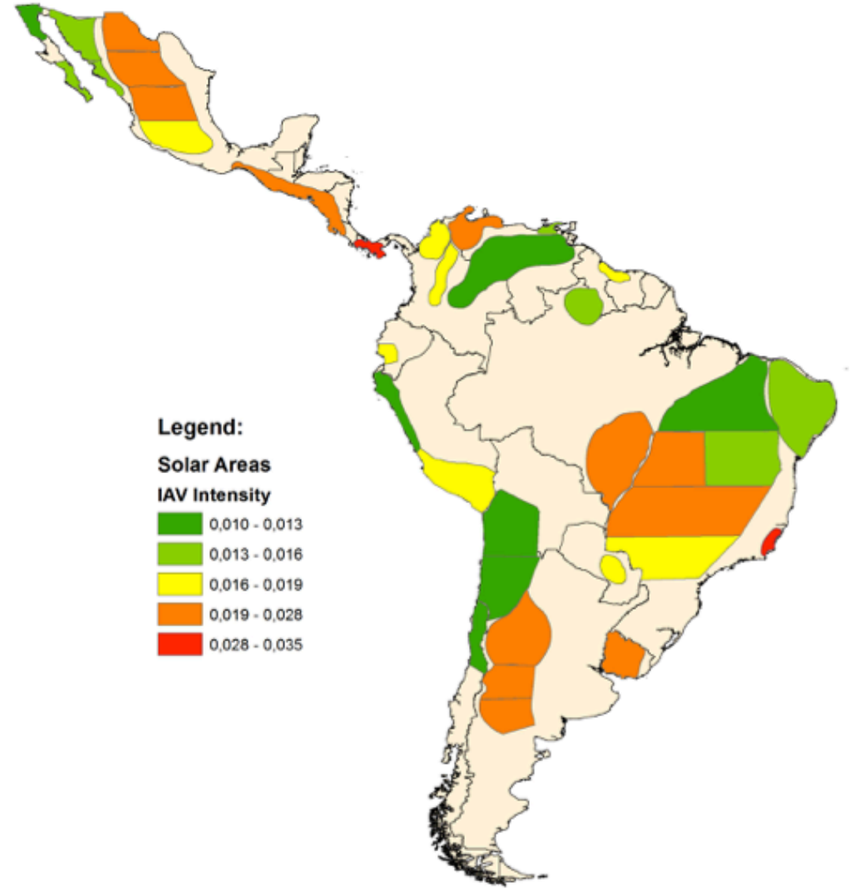

05. Discussion

The present report aimed to analyze the variability and complementarity between renewable energy resources in Latin America. The resources addressed in this analysis are wind, solar and hydropower. The main result of this work is the information generated through the statistical analysis of the wind, solar and hydro databases in Latin America. The analysis focuses on understanding the seasonality of the resources, their variability and possible complementarity.

To reach this objective, several steps were taken. A review of the state of the art for variability indices and studies addressing complementarities between renewable sources was performed. At the same time, the hourly resource data of solar irradiation and wind speed were transformed into electrical energy. With this approach it was possible to evaluate the data in the expected level of this research: energy integration.

Natural cycles in the context of solar energy have three dimensions: seasonal variation, daily variations (from dawn to dusk) and short-term fluctuations due to weather conditions. Wind power, on the other hand, can fluctuate at various time scales: it is subject to seasonal variations of peak electricity production in winter or summer depending on the region, as well as diurnal and hourly changes. There are also very short-term fluctuations in the intra-minute and inter-minute timeframe, that according to IEA (2005) are small relative to installed capacity, compared to hourly or daily variations. Furthermore, wind patterns can also be affected by orography since it plays an important role in the screening, deflection and acceleration of the wind and can create turbulence. This study calculated variability indices using a database with an hourly scale. The calculated indices showed a larger variability for wind power than for solar power generation. This can be explained as in solar power (different to the wind power case) the major variations occur in an intra-minute and inter-minute timeframe and by the larger sensitiveness of wind power to its natural resource (wind speed). Indeed, the wind generation relates to the wind speed through a cubic function, while solar generation presents an almost linear relationship with solar irradiance. An important fact to remark is how strong the region WIND_BR_06 is correlated with other areas: the ten strongest correlations found were from this cited area, this is because this hotspot presents trends of high wind speeds at night: therefore, it is well correlated with many solar areas.

In addition, when the monthly correlation was analysed, for correlations for all data series (done for wind and solar power) and for the correlation of typical years (including hydropower in the correlation analysis), Brazil plays an important role regarding renewable energy integration in LA, since it presents the strongest capacity to complement and being complemented by several LA countries. Besides Brazil, Venezuela also presents strong correlations with countries like Paraguay, Brazil and Ecuador, mainly under a seasonal pattern.

By evaluating the potential availability of resources and complementarity in hotspots in Latin America, it is possible to conclude that energy integration in Latin American countries is a suitable strategy to deal with variable renewable sources electricity generation. Therefore, policymakers and energy planners should work to find ways to dismantle some of the barriers - such as regulatory and interconnection issues - for developing this potential.

06.

References

- ADME. Informe Mensual. Available at: http://www.adme.com.uy/mmee/infmensual.php.
- Anemos, Anemos Gesellschaft für Umweltmeteorologie mbH. Available at: http://www.anemos.de/en/index.php.
- Anjos, P. S., Silva, A. S. A., Stošić, B. & Stošić, T., 2015. Long-term correlations and cross-correlations in wind speed and solar radiation temporal series from Fernando de Noronha Island, Brazil. Physica, A 424, pp. 90–96.
- Arias-Castro, E., Kleissl, J. & Lave, M., 2014. A Poisson model for anisotropic solar ramp rate correlations. Solar Energy, 101, pp. 192–202.
- Badosa, J., Haeffelin, M., Chepfer, H., 2013. Scales of spatial and temporal variation of solar irradiance on reunion Tropical Island. Energy, 88, pp. 42–56.
- Bard, J., Faulstich, S. & Lyding, P., 2011. The German wind turbine reliability database. In Wind Power R&D Seminar--Deep Sea Offshore Wind Power.
- Beluco, A., Souza, P. K. & Krenzinger, A., 2012. A method to evaluate the effect of complementarity in time between hydro and solar energy on the performance of hybrid hydro PV generating plants. Renewable Energy, 45, pp. 24-30.
- Betreiber- Datenbasis, 2011. Windindex der Betreiber-Datenbasis Betreiber - BDB Index. Available at: www.BtrDB.de.

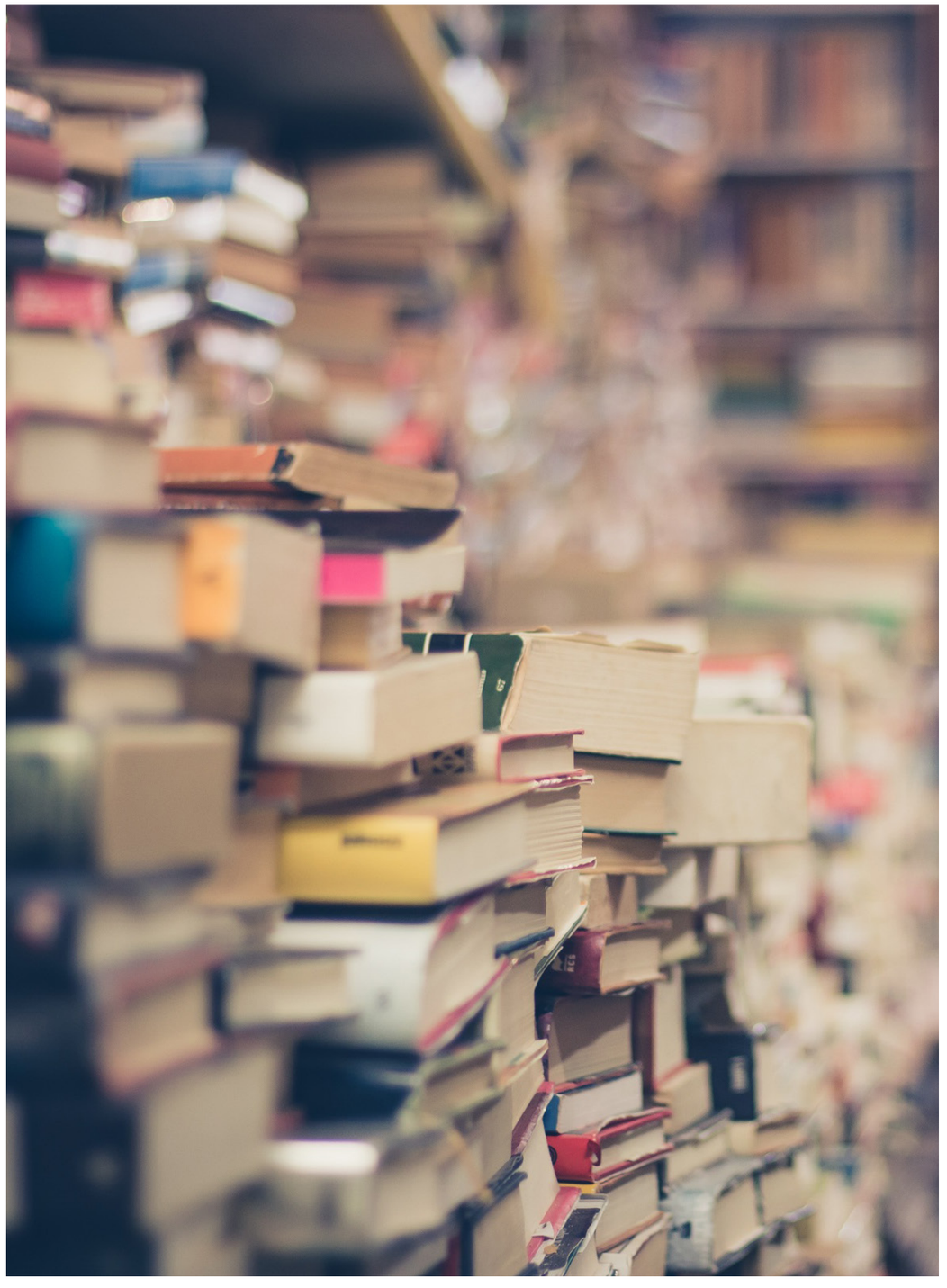

- Bianchi, F. D., De Batista, H., Mantz, R. J., 2007. Wind Turbine Control Systems Principles, Modeling and Gain Scheduling Design. SPRINGER. Available in http://www.springer.com/cda/content/document/cda_downloaddocument/9781846284922-c1.pdf?SGWID=0-0-45-436805-p172423327. Accessed October 2016.

- Branner, K. & Ghadirian, A., 2014. Database about blade faults. Techreport, DTU Wind Energy.

- Buttler, A., Dinkel, F., Franz, S. & Spliethoff, H., 2016. Variability of wind and solar power e an assessment of the current situation in the European Union based on the year 2014. Energy, 106, pp. 147-161.

- CAMMESA. Datos hidráulicos. Available at: http://portalweb.cammesa.com/memnet1/Pages/descargas.aspx.

- CNDC. Evolución de lós Embalses: Caudales de Aporte. Available at: http://www.cndc.bo/media/archivos/boletindiario/caudales.php?id=071016

- Darez, P., Baudry, J. & Darr, C., 2014. Assessment of the inter-annual variability of the global horizontal irradiance in the atacama desert of Chile. In European Photovoltaic Solar Energy Conference and Exhibition (EU PVSEC). Chile.

- EuroWind Index, Making Renewables Predictable. Available at: http://www.eurowind.info/en/.

- EBY. Estadísticas desde la puesta em marcha de la central hidroeléctrica em 1994. Available at: http://www.eby.org.ar/pdf/generacion/2016/YacyretaCaudalesDesdeInicioOperacion.pdf

- Gagné, A., Turcotte, D., Goswamy, N. & Poissant, Y., 2016. High resolution characterisation of solar variability for two sites in Eastern Canada. Solar Energy, 137, pp. 46–54.

- Hamal, C. & Sharma, A., 2006. Adopting a Ramp Charge to Improve Performance of the Ontario Market. Tech. rep. LECG.

- Hammer, A. et al., 2003. Solar energy assessment using remote sensing technologies. Remote Sensing of Environment, 86(3), pp.423–432.

- Häuser, Keiler: Windindices für Deutsch- land. Ingenieur-Werkstatt Energietechnik, Rade.

- Hodge, B., Shedd, S. & Florita, A., 2012. Examining the variability of wind power output in the regulation time frame. In Proc. of 11 th International Workshop on Large-scale Integration of Wind Power into Power Systems. pp. 13–15.

- IEA – International Energy Agency, 2005. Variability of wind power and other renewables – Management options and strategies. Available at: http://www.uwig.org/iea_report_on_variability.pdf, [Accessed January, 2017].

- INAHMI. Anuários Hidrológicos. Available at: http://www.serviciometeorologico.gob.ec/biblioteca/.

- ISET -Wind- Index, Frauenhofer IWES. Kassel: Assessnent of the Annual Available Wind Energy.

- ISA. Información inteligente: Hidrología. Available at: http://informacioninteligente10.xm.com.co/hidrologia/Paginas/HistoricoHidrologia.aspx?RootFolder=%2Fhidrologia%2FHidrologia%2FAportes&FolderCTID=0x0120005447CB19B02C274BB11AE8243E0B8B23&View=%7b41F81D50-FAF7-4E2A-A669-3DB4DD1F7869%7d. Accessed in: August 2016.

- IWR, I.W.R.E., IWR-Windertragsindex Küstengebiex. West deutsches Binnenland, Münster.

- ICE. Información Técnica - Informes Anuales. Disponível em: <http://appcenter.grupoice.com/CenceWeb/CenceDescargaArchivos.jsf?init=true&categoria=3&codigoTipoArchivo=3008>.

- Johnson, G.L., 2006. Wind energy systems, Manhattan, KS: Electronic Edition. Prentice-Hall Inc.

- Kang, B.O., Tam, K.S., 2013. A new characterization and classification method for daily sky conditions based on ground-based solar irradiance measurement data. Sol. Energy, 94, pp. 102–118.

- Kiviluoma, J. et al., 2014. Index for wind power variability. In 13th International Workshop on Large-Scale Integration of Wind Power into Power Systems as well as on Transmission Networks for Offshore Wind Power (WIW 2014).

- Kiviluoma, J. et al., 2012. Short-term energy balancing with increasing levels of wind energy. IEEE Transactions on Sustainable Energy, 3(4), pp.769–776.

- Kougias, I., Szabó, S., Monforti-Ferrario, F., Huld, T. & Katalin Bódis, 2016. A methodology for optimization of the complementarity between small-hydropower plants and solar PV systems. Renewable Energy, 87, pp. 1023-1030.

- Lauret, P., Perez, R., Aguiar, L. M., Tapache`s, E., Diagne, H. M. & David, M., 2016. Characterization of the intraday variability regime of solar irradiation of climatically distinct locations. Solar Energy, 125, pp. 99–110.

- Lave, M., Reno, M.J., Broderick, R.J., 2015. Characterizing local high-frequency solar variability and its impact to distribution studies. Solar Energy, 118, pp. 327–337.

- MA, X. Y.; SUN, Y. Z.; FANG, H. L. Scenario generation of wind power based on statistical uncertainty and variability. IEEE Transactions on Sustainable Energy, v. 4, n. 4, p. 894–904, 2013.

- Marcos, J., Marroyo, L., Lorenzo, E., Alvira, D., Izco, E., 2011. Power output fluctuations in large scale PV plants: one year observations with one second resolution and a derived analytic model. Prog. Photovolt. Res. Appl. 19, pp. 218–227.

- Mazumdar, B. M., Saquib, M. & Das, A. K., 2014. An empirical model for ramp analysis of utility-scale solar PV power. Solar Energy, 107, pp. 44–49.

- Mills, A. & Wiser, R. 2010. Implications of Wide-Area Geographic Diversity for Short-Term Variability of Solar Power. LBNL Report No. 3884E.

- Mills, A., Ahlstrom, M., Brower, M., Ellis, A., George, R., Hoff, T., Kroposki, B., Lenox, C., Nicholas, M., Stein, J., Wan, Y.W., 2010. Understanding Variability and Uncertainty of Photovoltaics for Integration with the Electric Power System. Lawrence Berkeley Natl. Lab.

- Moarefdoost, M. M., Lamadrid, A. J. & Zuluagaa, L. F., 2016. A robust model for the ramp-constrained economic dispatch problem with uncertain renewable energy. Energy Economics, 56, pp. 310–325.

- NASA, N.A. and S.A., MERRA: MODERN ERA-RETROSPECTIVE ANALYSIS FOR RESEARCH AND APPLICATIONS. Global Modelling and Assimilation Office. Available at: https://gmao.gsfc.nasa.gov/research/merra/intro.php [Accessed September 21, 2016].

- NREL, 2011. The importance of flexible electricity supply.

- ONSa. Diagrama Esquemático das Usinas Hidrelétricas do SIN. Available at: http://www.ons.org.br/download/biblioteca_virtual/publicacoes/dados_relevantes_2011/02-Diagrama-Esquematico-das-Usinas-Hidreletricas-do-SIN.html?expanddiv=02

- ONSb. Séries Históricas de Vazões. Available at: http://www.ons.org.br/operacao/vazoes_naturais.aspx.

- Perez, M. J. R. & Fthenakis, V. M., 2015. On the spatial decorrelation of stochastic solar resource variability at long timescales. Solar Energy, 117, pp. 46–58.

- Perez, R., David, M., Hoff, T., Kivalov, S., Kleissl, J., Lauret, P., Perez, M., 2015. Spatial and temporal variability of solar energy. Foundations and Trends in Renewable Energy (forthcoming).

- Perpinán, O., Marcos, J., Lorenzo, E., 2013. Electrical power fluctuations in a network of DC/AC inverters in a large PV plant: relationship between correlation, distance and time scale. Sol. Energy 88, pp. 227–241.

- Ramírez C, J., 2015. MERRA-based study of the wind/solar resource and their complementarity to the hydro resource for power generation in Colombia. Carl von Ossietzky Universitat Oldenburg.

- Rimpl, D. & Westerhellweg, A., 2013. Development of a Wind Index Concept for Brazil. Deutsche Gesellschaft fur Internationale Zusammenarbeit (GIZ) GmbH. Energy Program, GIZ Brazil.

- Ritter, M. et al., 2014. Designing an Index for Assessing Wind Energy Potential Designing an Index for Assessing Wind Energy Potential. In SFB 649 Discussion Paper Series 2014. Berlin: Collaborative Research Center 649: Economic Risk.

- SIDE. Bulletin de la situation hydrologique en Guyane. Available at: http://www.side.developpement-durable.gouv.fr/EXPLOITATION/DRGUYA/

- Silva, A. R., Pimenta, F. M., Assireu, A. T. & Spyrides, M. H. C., 2016. Complementarity of Brazil's hydro and offshore windpower. Renewable and Sustainable Energy Reviews, 56, pp. 413–427.

- Skartveit, A., Olseth, J.A. & Tuft, M.E., 2016. An Hourly Diffuse Fraction Model with Correction for Variability and Surface Albedo. Solar Energy, 63(July), pp.173–183.

- SNIA. Información Oficial Hidrometeorológica y de Calidad de Aguas en Línea. Available at: http://snia.dga.cl/BNAConsultas/reportes

- Stein, J.S., Hansen, C.W., Reno, M.J., 2012. The Variability Index: A New and Novel Metric for Quantifying Irradiance and PV Output Variability. Report SAND2012- 288C2. Sandia National Laboratories.

- The Crown State, 2014. UK MERRA Validation With Offshore Meteorological Data.

- UK Met Office, 2010. National Meteorological Library and Archive Fact sheet 17 — Weather observations over land. United Kingdom.

- Van Haaren, R., Morjaria, M., Fthenakis, V., 2014. Empirical assessment of short-term variability from utility-scale solar PV plants. Prog. Photovol. Res. Appl., 22, pp. 548–559.

- Vindel, J. M. & Polo, J., 2014. Intermittency and variability of daily solar irradiation. Atmospheric Research, 143, pp. 313–327.

- Widén, J., Carpman, N., Castellucci, V., Lingfors, D., Olauson, J., Remouit, F., Bergkvist, M., Grabbe, M. & Waters, R., 2015. Variability assessment and forecasting of renewables: A review for solar, wind, wave and tidal resources. Renewable and Sustainable Energy Reviews, 44, pp. 356–375.

- Winkler, W., Strack, M. & Westerhellweg, A., 2003. Scaling and evaluation of wind data and wind farm energy yields. DEWI Magazine, 23, pp.76–84.

- MA, X. Y.; SUN, Y. Z.; FANG, H. L. Scenario generation of wind power based on statistical uncertainty and variability. IEEE Transactions on Sustainable Energy, v. 4, n. 4, p. 894–904, 2013.

SECTION II

Assessment of **Climate Change Impacts on Solar and Wind Energy Resources** in Latin America

01. Introduction

Scientific evidence of possible changes in climate has been raising interest in the public and the scientific community [IPCC, 2013]. According to the Fifth Assessment Report of the Intergovernmental Panel on Climate Change (AR5), CO_2 emissions have increased by 40% since the pre-industrial period, mainly due to fossil fuel emissions followed by changes in land use [IPCC, 2013]. According to that report, the future climate will begin to behave less like past climates in the coming decades. A modification on climate would affect society and the economic system through multiple sectors, such as altering agricultural yields, influencing coastal areas or changing energy production and consumption. The energy system may be one of the parts of the economy most affected by climate change [Ciscar et al., 2014]. Considering the fact that energy is indispensable to many other sectors, all the climate impacts in the energy sector would be reflected extensively throughout the rest of the economy.

Climate change may affect renewable sources more intensively than the fossil ones since renewable energy endowments are related to a flux of energy, which is intimately related to climate conditions. Fossil fuels can be stocked, so climate change would impact only the access to these resources [Schaeffer et al., 2012, Burnett et al., 2014].

However, implications of possible changes in the potential of renewable resources, such as wind and solar, must be properly understood for future planning purposes. Wind speed and cloudiness (variable that affects solar resource) are strongly influenced by local temperature gradients [Fant et al., 2016].

To plan and operate energy systems, it is very common to use a variety of models, in order to evaluate the effects of climate on operation and planning. However, conventional energy analysis assumes that climate variables are constant, with no modification in time, but this premise may actually increase uncertainty in decisions in a climate change framework [Schaeffer et al., 2012]. So, for the development of policies that aim to cope with climate change, estimating the susceptibility of energy systems and incorporating them into long-term energy planning and operation is imperative in order to improve the reliability of the projects.

In this way, experts from different economic sectors use climate projections as a basis for determining possible impacts and developing mitigation and adaptation actions. Modeled projections of changes in the long-term future state are attractive for national energy investments that are considering large penetration of renewable energy generation in their portfolios [Fant et al., 2016].

This study aims to determine the possible impacts on future long-term wind and solar energy resource complementarity due to climate change for selected regions in Latin America (LA). To do this, results from General Circulations Models (GCM) and a Representative Concentration Pathway (RCP) of the IPCC's fifth Assessment Report (AR5) will be used. A downscale exercise will be performed in order to obtain data at the geographical resolution of the selected regions. The variables obtained from the GCMs will be linked to the wind and solar resources of the data base supplied by the Inter-American Development Bank (IDB) to assess the impact of climate change in the complementarity evaluation carried out in Secction I.

02.

Background

Climate change impact assessments are commonly made with the use of General Circulation Models (GCM). These models are three dimensional representations of the atmosphere and its interactions with land surface and oceans [IPCC,2013]. They are used to project future climate under different forcings, including those related to concentrations of GHG. Therefore, they project climate based on different trajectories for GHG emissions and, as a result, radiative forcings. Such trajectories are represented by a range of scenarios, among which the Representative Concentration Pathways (RCP) [Moss et al, 2010] are the most recent ones. The sections below describe the choice of RCP and GCM used in this study to project the impacts of climate change on the complementarity of renewable energy sources in Latin America.

2.1. Review of the Global Circulation Models (GCMs)

General Circulation Models are the primary tools available for investigating the response of the climate system to various forcings, for making climate predictions on seasonal to decadal time scales and for making projections of future climate over the coming century and beyond [Flato, 2013]. This section draws on GCM features and specifically on the Hadley Centre Global Environment Model (HadGEM2) and the Model for Interdisciplinary Research on Climate (MIROC5), as these constitute a set of coordinated and thus consistent and increasingly well-documented climate model experiments.

A GCM is composed of many grid cells that represent horizontal and vertical areas on the Earth's surface (Figure 1) In each one of the cells, GCMs compute the following: water vapor and cloud atmospheric interactions, direct and indirect effects of aerosols on radiation and precipitation, changes in snow cover and sea ice, the storage of heat in soils and oceans, surface fluxes of heat and moisture, and large-scale transport of heat and water by the atmosphere and oceans [Wilby et al., 2009].

The spatial resolution of GCMs is generally quite coarse, with a grid size of about 100–500 kilometers. Each modeled grid cell is homogenous, (i.e., within the cell there is one value for a given variable). Moreover, they are usually dependable at timescales of monthly averages and longer. In summary, GCMs provide quantitative estimates of future climate change that are valid at the global and continental scale and over long periods [ARCC, 2014].

Atmosphere–Ocean General Circulation Models (AOGCMs) were the "standard" climate models assessed in the AR4 and AR5. Their primary function is to understand the dynamics of the physical components of the climate system (atmosphere, ocean, land and sea ice), and to make projections based on future greenhouse gas (GHG) and aerosol forcing. These models continue to be extensively used, and in particular are run (sometimes at higher resolution) for seasonal to decadal climate prediction applications in which biogeochemical feedbacks are not critical. In addition, high-resolution or variable-resolution AOGCMs are often used in process studies or applications with a focus on a particular region [ARCC, 2014]. An overview of the AOGCMs can be found in Table 1.

Figure 1. Conceptual structure of a GCM model.

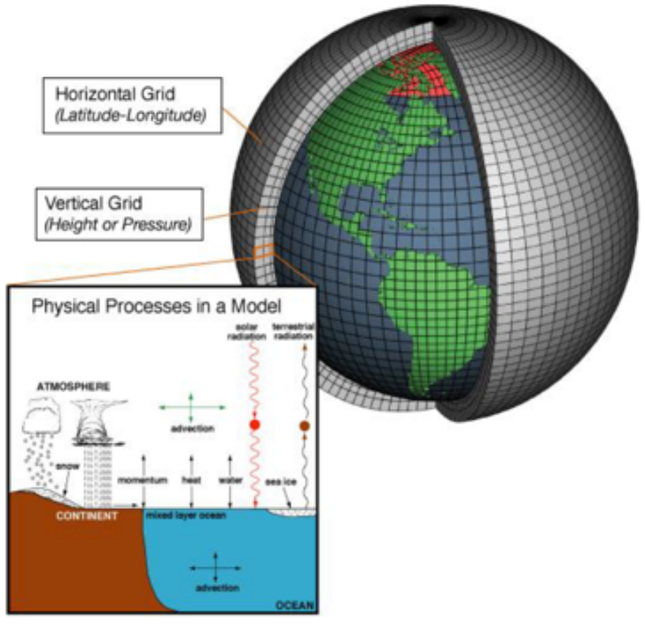

Source: [ARCC, 2014]

Table 1. Main features of the Atmosphere–Ocean General Circulation Models (AOGCMs) and Earth System Models (ESMs) participating in Coupled Model Intercomparison Project Phase 5 (CMIP5), and a comparison with Coupled Model Intercomparison Project Phase 3 (CMIP3), including components and resolution of the atmosphere and the ocean models.

	Model name		AOGCM Atmos	AOGCM Land Surface	AOGCM Ocean	AOGCM Sea-Ice	FC	ESM Aerosol	ESM Atmos Chem	ESM Land Carbon	ESM Ocean BGC
CMIP5	ACCESS1.0, ACCESS1.3	Australia									
	BCC-CSM1.1, BCC-CSM1.1(m)	China									
	BNU-ESM	China									
	CanCM4	Canada									
	CanESM2										
	CCSM4	USA									
	CESM1 (BGC)										
	CESM1 (WACCM)		HT								
	CESM1 (FASTCHEM)										
	CESM1 (CAM5)										
	CESM1 (CAM5.1-FV2)	USA									
	CMCC-CM, CMCC-CMS	Italy	HT								
	CMCC-CESM		HT								
	CNRM-CM5	France									
	CSIRO-Mk3.6.0	Australia									
	EC-EARTH	Europe									
	FGOALS-g2	China									
	FGOALS-s2										
	FIO-ESM v1.0	China									
	GFDL-ESM2M, GFDL-ESM2G	USA									
	GFDL-CM2.1										
	GFDL-CM3		HT								
	GISS-E2-R, GISS-E2-H	USA	HT					p2,p3*	p2, p3*		
	GISS-E2-R-CC, GISS-E2-H-CC		HT					p2,p3*	p2, p3*		
	HadGEM2-ES	UK									
	HadGEM2-CC		HT								
	HadCM3										
	HadGEM2-AO	Korea									
	INM-CM4	Russia									
	IPSL-CM5A-LR / -CM5A-MR / -CM5B-LR	France	HT								
	MIROC4h, MIROC5	Japan	HT								
	MIROC-ESM		HT								
	MIROC-ESM-CHEM		HT								
	MPI-ESM-LR / -ESM-MR / -ESM-P	Germany	HT								
	MRI-ESM1	Japan	HT								
	MRI-CGCM3		HT								
	NCEP-CFSv2	USA									
	NorESM1-M	Norway									
	NorESM1-ME										
AMIP	GFDL-HIRAM C180 / -HIRAM C360	USA									
	MRI-AGCM3.2S / -AGCM3.2H	Japan									
CMIP3	BCC-CM1	China					FC				
	BCCR-BCM2.0	Norway									
	CCSM3	USA									
	CGCM3.1(T47)	Canada					FC				
	CGCM3.1(T63)						FC				
	CNRM-CM3	France									
	CSIRO-MK3.0, CSIRO-MK3.5	Australia									
	ECHAM5/MPI-OM	Germany									
	ECHO-G	D/Korea					FC				
	FGOALS-g1.0	China									
	GFDL-CM2.0	USA									
	GFDL-CM2.1										
	GISS-AOM	USA									
	GISS-EH										
	GISS-ER										
	INGV-ECHAM4	Italy									
	INM-CM3.0	Russia					FC				
	IPSL-CM4	France									
	MIROC3.2(hires)	Japan	HT								
	MIROC3.2(medres)										
	MRI-CGCM2.3.2	Japan					FC				
	NCAR-PCM	USA									
	UKMO-HadCM3	UK									
	UKMO-HadGEM1										

Increasing complexity

Increasing resolution Atmosphere / Ocean
(total number of horizonal grid points)
8000 30000 52000
12000 50000 110000

Source: [IPCC, 2014]

Earth System Models (ESMs) are the current state-of-the-art models, and they expand on AOGCMs to include representation of various biogeochemical cycles such as those involved in the carbon cycle, the sulfur cycle, or ozone [Flato, 2013]. These models provide the most comprehensive tools available for simulating past and future response of the climate system to external forcing, in which biogeochemical feedbacks play an important role. An overview of the ESMs can be found in Table 1.

It is crucial therefore to evaluate the performance of these models, both individually and collectively. In particular, the IPCC (2014) draws heavily on model results collected as part of the Coupled Model Intercomparison Projects (CMIP3 and CMIP5) [Meehl et al., 2007; Taylor et al., 2012].

In Table 2 official CMIP model names are used. HT stands for High-Top atmosphere, which has a fully resolved stratosphere with a model top above the stratopause. AMIP stands for models with atmosphere and land surface only, using observed sea surface temperature and sea ice extent. A component is colored when it includes at least a physically based prognostic equation and at least a two-way coupling with another component, allowing climate feedbacks. For aerosols, lighter shading means 'semi-interactive' and darker shading means 'fully interactive'. The resolution of the land surface usually follows that of the atmosphere, and the resolution of the sea ice follows that of the ocean. In moving from CMIP3 to CMIP5, note the increased complexity and resolution as well as the absence of artificial flux correction (FC) used in some CMIP3

2.1.1. HadGEM2

The HadGEM2 family of Met Office Unified Model climate configurations stands for the Hadley Center Global Environment Model version 2. HadGEM2 is a configuration of the Met Office Unified Model (UM) developed from UM version 6.6. HadGEM2-ES was the first Met Office Hadley Centre model to include Earth System components as standard (Martin et al., 2011). The Unified Model is used by a number of institutions around the world both for operational weather forecasting and for climate research (ENES,2015).

It is important to highlight the model main characteristics: the HadGEM2-ES climate model comprises an atmospheric GCM at N96 and L38 horizontal and vertical resolution, and an ocean GCM with a 1-degree horizontal resolution (increasing to 1/3 degree at the equator) and 40 vertical levels. Earth system components included are the terrestrial and ocean carbon cycle and tropospheric chemistry. Terrestrial vegetation and carbon are represented by the dynamic global vegetation model, TRIFFID, which simulates the coverage and carbon balance of 5 vegetation types (broadleaf tree, needleleaf tree, C3 grass, C4 grass and shrub). Ocean biology and carbonate chemistry are represented by diat-HadOCC which includes limitation of plankton growth by macro- and micro-nutrients, and also simulates emissions of DMS to the atmosphere (ENES, 2015). Most of this information can also be found from HadGEM2´s homepage (Metoffice, 2016).

According to Collins et al. (2011), HadGEM2-ES has been designed for the specific purpose of simulating and understanding the centennial scale evolution of climate including biogeochemical feedbacks.

2.1.2. MIROC5

MIROC5 is a Japanese cooperatively developed model known as Model for Interdisciplinary Research on Climate (MIROC), version 5 [WATANABE et al., 2010]. It is spectral in the atmospheric component with resolution T85, which is approximately 150 km in the horizontal, and has 40 vertical atmospheric levels. It is coupled to COCO 4.5 ocean model [HASUMI, 2007] with 50 levels in depth and 1° of horizontal resolution. The radiative fluxes are calculated by a k-distribution scheme [SEKIGUCHI and NAKAJIM, 2008]. The aerosol model, the SPRINTARS, is coupled to cloud microphysics scheme together with the radiation scheme, it uses the MATSIRO land surface scheme [TAKATA, EMORI and WATANABE, 2003] with 6 soil layers. Each grid box is formed by three tiles of potential vegetation, cropland, and lake. The scheme also contains river routing and the effects of snow on albedo. Sea ice thermodynamics and dynamics are represented.

2.2. The Representative Concentration Pathways (RCP)

Climate change generates effects or influences certain processes and natural phenomena. As the characteristics of each environment are constantly changing over time, the assessment of an impact must presuppose an analysis of these conditions at a future time. For this, climatic models are applied using the information of future scenarios assumptions [van Vuuren et al., 2011a].

Scenarios are used to explore the consequences of different adaptation and mitigation strategies under uncertainty [van Vuuren et al., 2011a]. There are several key challenges involved in developing scenarios. One of these challenges is that the relevant factors for mitigation and adaptation often act at different spatial and temporal scales. Consequently, scenarios should be able to bridge these scales, by providing enough information on global trends and processes (e.g. international economic factors, international institutional factors and demographic trends) [Toth, 2003].

In the assessment of future environmental conditions, studies on the climate change impacts acquire significant levels of uncertainty. This is partly because there are a very large number of factors that determine the future system vulnerability, such as social capital, institutions and governance, technological capabilities and level of economic development [Brooks et al., 2005]. These factors are highly dependent on context and scale of analysis [Adger, 2003]. The extensive uncertainties in future radiative forcing and in the possible responses to climate change forces the use of different scenarios to explore potential socioeconomic and environmental impacts [Moss et al., 2010]. These uncertainties are influenced by the magnitude of the exposed system, the sensitivity of the exposed system, and its adaptive capacity. Climate vulnerability is therefore a function of an interaction between social and biophysical vulnerabilities, interpreted in quantitative and qualitative ways [van Vuuren et al., 2012].

The projections and estimations made by different studies would hardly point exactly to the same future scenario. Considering that the description of these future scenarios serves as a basis for applying climate change models and assessing impacts, the studies would present differences regardless of the application of climate models [van Vuuren et al., 2011a]. As a manner to have a pattern of the initial parameters and allowing a valid comparison of the various existing works, in addition to simplify the process of creating the starting scenarios of the model, climate change studies started to adopt common scenarios pre-established by the scientific community [van Vuuren et al., 2011a]. In the past, several sets of scenarios have performed such a role, including the IS92 scenarios and, more recently, the scenarios from the Special Report on Emission Scenarios (SRES). Such scenarios would allow evaluating the "costs" and "benefits" of long-term climate goals [van Vuuren et al., 2011].

The need for new scenarios induced the Intergovernmental Panel on Climate Change (IPCC) to request the scientific community to develop a new group of scenarios to simplify future assessment of climate change [IPCC 2007]. The community subsequently designed a process of three phases [Moss et al. 2010]: 1) Development of a scenario set containing emission, concentration and land-use trajectories—referred to as "representative concentration pathways" (RCPs); 2) A parallel development phase with climate model runs and development of new socioeconomic scenarios; 3) A final integration and dissemination phase.

The RCPs are intended to form a key element of the new process. They were selected to span the range for those factors that determine future climate change [van Vuuren et al., 2012]. In total, four RCPs were developed: RCP2.6, RCP4.5, RCP6 and RCP8.5, with the associated numbers indicating the radiative forcing reached (in W/m2) at the end of the 21st century compared to the preindustrial state [Wild et al., 2015]. Each of the RCPs covers the 1850–2100 period, and extensions have been formulated for the period thereafter (up to 2300) [van Vuuren et al., 2011]. Central to the concept of the RCPs is that any single radiative forcing pathway can result from a diverse range of socioeconomic, technological and policy development scenarios [Wild et al., 2015].

As part of this process and based on discussions within the context of the IPCC, several design criteria were established [Moss et al. 2008]. These criteria stem from their intended use to facilitate climate research and assessment: 1) The RCPs should be based on scenarios published in the existing literature, developed independently by different modeling groups and be representative of the entire literature, in terms of emissions and concentrations; 2) The RCPs should provide information on all components of radiative forcing that are needed as input for climate modeling and atmospheric chemistry modeling; 3) The RCPs should have harmonized base year assumptions for emissions and land use and allow for a smooth transition between analyses of historical and future periods without sudden transitions; 4) The RCPs should cover the time period up to 2100, but information also needs to be made available for the centuries thereafter

Table 2 shows the overview of RCPs: the authors who created it, the models used to design it, information on emissions, concentrations and accompanying land use and land cover

The four selected RCPs were considered to be representative of the literature, and included one mitigation scenario leading to a very low forcing level (RCP2.6), a medium baseline or a high mitigation case (RCP6), an intermediate mitigation scenario (RCP4.5) and one very high baseline emission scenario (RCP8.5) [van Vuuren et al., 2011].

Table 3 shows the main characteristics of each RCP.

The scenarios selected from the literature were published during the 2006–2007 period. As new historical data become available and modeling methods are improved, each team is encouraged to update their original scenario and expand their result, without changing the basic assumptions behind them [van Vuuren et al., 2011].

Table 2. Overview of representative concentration pathways (RCPs)

	Description[a]	Publication - Model
RCP 8.5	Rising radiative forcing pathway leading to 8.5 W/m² (~1370 ppm CO2e) by 2100	Riahi et al. 2007 - MESSAGE
RCP 6	Stabilization without overshoot pathway to 6 W/m² (~850 ppm CO2e) at stabilization after 2100	Fujino et al. 2006; Hijioka et al. 2008 - AIM
RCP 4.5	Stabilization without overshoot pathway to 4.5 W/m² (~650 ppm CO2e) at stabilization after 2100	Clarke et al. 2007; Smith and Wigley 2006; Wise et al. 2009 - GCAM
RCP 2.6	Peak in radiative forcing at ~3 W/m² (~490 ppm CO2e) before 2100 and then decline (the selected pathway declines to 2.6 W/m² by 2100)	Van Vuuren et al. 2007a; Van Vuuren et al. 2006 - IMAGE

a Approximate radiative forcing levels were defined as +/- 5% of the stated level in W/m2 relative to pre-industrial levels. Radiative forcing values include the net effect of all anthropogenic GHGs and other forcing agents.

Source: [van Vuuren et al., 2011]

Table 3. Main characteristics of each RCP

Scenario Component	RCP 2.6	RCP 4.5	RCP 6	RCP 8.5
Green House Gas Emissions	Very low	Medium-low mitigation and very low baseline	Medium baseline and high mitigation	High baseline
Agricultural area	Medium for cropland and pasture	Very low for both cropland and pasture	Medium for cropland but very low for pasture (total low)	Medium for both cropland and pasture
Air pollution	Medium-low	Medium	Medium	Medium-high

Source: van Vuuren et al., 2011

The elaborate development process to create a RCP is necessary so that the RCPs may provide a consistent analytical thread that runs across communities involved in climate research. RCPs are reasonable with their design criteria. Given their comprehensiveness in terms of sources covered, as well as in spatial detail, they provide a unique basis for detailed climate model runs. The assessment of vulnerability, impacts and adaptation requires not only a description of expected climate change, but also associated a description of socioeconomic conditions [van Vuuren et al., 2012]. The RCPs represent an important step in the development of new scenarios for climate research and provide a good basis for exploring the range of climate outcomes by the climate modeling community [van Vuuren et al., 2011].

2.3. Impacts of Global Climate Change on Renewable Resources in LA

Several energy sector studies are based on climate models (General Circulation Models – GCMs) in order to establish how these possible weather variations may have a direct or indirect impact on energy supply and demand. According to Lucena [2010], the impacts of climate change on several sectors have been studied since the 1980s, however, literature on the effects on the energy sector, particularly electricity is relatively new and limited. In this section, a scientific literature review is done on climate change impacts, taking into consideration more renewable sources; especially it focuses more on wind.

In Central and South America, temperatures have risen between 0.7°C and 1°C since the mid-1970s, except for coastal Chile, where they have fallen by 1°C, and annual precipitations have risen in the southeastern part of South America and fallen in Central America and the southern and central parts of Chile. The region has experienced changes in climate variability and significant impacts from extreme climate events, although many of these extreme phenomena are not necessarily attributable to climate change [Magrin et al., 2014; IPCC, 2014].

The Latin American and Caribbean region is also affected by various climate phenomena including the Intertropical Convergence Zone, the North and South American monsoon system, El Niño Southern Oscillation, Atlantic Ocean oscillations and tropical cyclones, [IPCC, 2014]. These phenomena affect the subregional climate and changes in their patterns have major implications for climate projections. The El Niño Southern Oscillation will continue to be (at a high confidence interval) the dominant form of interannual variability in the tropical Pacific, and rising humidity levels will likely intensify El Niño precipitation variability [IPCC, 2014].

2.3.1. Impacts of Global Climate Change on Wind Resource

Renewable generation capacity in Latin America and the Caribbean, at the end of 2015, amounted to 212.4 GW. According to IRENA [2016] wind energy accounted for 7% share of the regional total, with an installed capacity of 15.5 GW. Renewable energy generation capacity increased by 13.1 GW during 2015, the largest annual increase since the beginning of the time series (year 2000). Wind capacity increased by 4.6 GW [IRENA, 2016].

Expansion of wind energy installed capacity is poised to play a key role in climate change mitigation. However, wind energy is also susceptible to global climate change. Some changes associated with climate evolution will likely benefit the wind energy industry while other changes may negatively impact wind energy developments, those "gains and losses" are dependent of the region under consideration. Herein we review possible mechanisms by which global climate variability and change may influence the wind energy resource and operating conditions [Pryor y Barthelmie, 2013].

Wind energy, like many of the renewable technologies, is susceptible to climate change because the 'fuel' is related to the global energy balance and resulting atmospheric motion (Hubbert, 2009). Hence here we seek to 'close the loop' by asking the question; 'what impact might global climate change have on the wind energy industry?'

Atmospheric conditions enter into the design and operation of wind turbines and wind farms largely under the rubric of 'external conditions'. The wind climate governs the energy density in the wind and hence the power that can potentially be harnessed:

$$E = 1/2\ \rho\ U^3 \qquad \text{(Eq. 1)}$$

In this equation, E represents the energy density (Wm $^{-2}$), ρ is the air density (Kg m $^{-3}$) and U the wind speed at hub-height (m s^{-1}).

Given the energy in the wind is the cube of wind speed (Eq. (1)), a small change in the wind climate can have substantial consequences for the wind energy resource. For a change in wind speed at turbine hub-height of 0.5 m s-1, from 5 to 5.5 m s-1 (i.e. a 10% change), the energy density increases by over 30%. It is also clear that the wind resource is largely dictated by the upper percentiles of the wind speed distribution, a factor that is further amplified by the non-linear relationship between incident wind speed and power production from a wind turbine [Pryor and Barthelmie, 2013].

The wind climate also governs aspects of the wind turbine design, via its governing role in wind turbine loading through, for example, turbulence intensity, wind shear across the turbine blades, and transient wind conditions such as the occurrence of extreme wind speeds and directional changes [DNV/RISØ, 2002]. Other atmospheric conditions that are of importance to the design, operation or power production from wind turbines include operational temperatures, air density, icing and corrosion and abrasion due to airborne particles [DNV/RISØ, 2002].

The principal and most direct mechanism by which global climate change may impact the wind energy industry is by changing the geographic distribution and/or the inter- and intraannual variability of the wind resource. Research undertaken to quantify this effect generally relies on application of downscaling methodologies designed to extract higher resolution projections of climate parameters of interest from coupled Atmosphere-Ocean General Circulation Models [Pryor and Barthelmie, 2013].

The inter- (and intra-) annual variability of wind speeds, wind indices and energy density are naturally a function of the regional climate, and frequency and intensity of transient storm systems, and the spatial scale of aggregation. At short time scales this variability leads to variable output of electricity production [European Wind Energy Association, 2009] and the need for short-term prediction [Pryor and Barthelmie, 2006]. At longer time scales (seasonal and beyond) it has relevance for coupling of production to demand, reliability of electricity production and project economics. Given the high capital costs of most renewable energy systems relative to operation and maintenance and discounting of future revenues [Blanco, 2009], inter-annual variability can play a key role in dictating economic feasibility, hence 'The importance

of a good wind year to start on when building a wind farm' [Frandsen and Petersen, 1993].

Little research has been conducted to indicate if the inter-annual and inter-decadal variability of wind speeds and energy density will increase or decrease under climate change scenarios. In light of evidence of changing storm tracks [Christensen et al., 2007] it seems probable that at least in some locations a change in inter- and intra-annual variability of the wind resource is likely.

Climate change may also alter not only the wind resource, but also the environmental context, operation and maintenance and/or design of wind developments. A major issue in design of wind turbines and wind farms is to characterize wind turbine loads which affect the performance and lifetime of the turbines [Hau, 2006]. Loads relating to external conditions can be divided into extreme loads which arise mainly from extreme (i.e. inherently rare) events with return periods of 1–50 years and fatigue loads [Dekker and Pierik, 1999] which are primarily determined by the mean wind speed and the standard deviation of wind speed fluctuations that are strongly related to site turbulence levels [Frandsen, 2007]. Because of the complexity of interactions between wind turbines and turbine components with external conditions, structural dynamic models are used to assess loads based on a number of frequently updated design load cases [Hau, 2006].

We are not aware of any study that has sought to quantify possible changes in the parameters used in the design load cases in the context of climate evolution. However, changes in extreme loads which frequently arise from high-wind speeds [Moriaty, 2008] may well evolve as a result of changing storm intensity and tracking. Wind turbines are designed for different conditions [IEC, 2005] based on hub-height values of the mean annual wind speed, the reference (extreme) wind speed (highest mean 10-min average wind speed value to be expected in a 50-year period) and the characteristic turbulence intensity to be expected at 15m/s [Hau, 2006]. Average turbulence levels are most strongly related to site characteristics such as topography and surface type (DNV/RISØ, 2002) and as such are likely to be only moderately impacted by changes in climate. Potential changes in mean wind speeds were discussed above and therefore we limit our discussion below to extreme wind speeds and some of the other principal climatological parameters of interest.

Wind power is a new source in Latin America and Caribbean, which explains the limited literature on the impacts temperature rises may have on it. Although more research is needed in this field, it is expected that new findings may lead to a changes in perception and valuation of energy technology alternatives (in particular renewable energy systems highly dependent on climate conditions such as wind energy technologies) [Contreras-Lisperguer and Cuba, 2008]. If this change in appraisal or valuation is effected, it may alter energy policies and decision making processes, including plans of action and development of appropriate strategies for energy sector development in the Caribbean and South America region. The paragraphs that follow describe the changes in climate observed in the Caribbean and the wider region of the Americas [Contreras-Lisperguer and Cuba, 2008].

The Caribbean region is a unique climatic and geological area in the world, where climate variability is influenced by many physical and atmospheric interactions such as the convergence zone of trade winds, El Niño-Southern Oscillation (ENSO), and variations in Sea Surface Temperatures (SST) caused by surface and deep water currents among many other atmospheric teleconnection patterns. All these occurrences are the perfect ingredients for the incidence of extreme weather events. If we add to this the effects of human induced climate change, the results obtained by atmospheric-oceanic numerical models are alarming. Over the last decades, wind storms, floods and droughts have been the most significant and frequent natural disasters occurring in the Caribbean [Contreras-Lisperguer and Cuba, 2008].

Wind energy is not affected by changing water supplies as opposed to fossil-fuel based power systems or other alternative energy systems that need cooling. Nevertheless, projected climate change impacts are likely to have significant positive or negative impacts on wind energy generation given that the latter depends strongly on climatic and environmental conditions at a particular site. Wind is caused by the uneven heating of the earth's surface by the sun. Since the earth's surface is made of very different types of land cover and water, it absorbs the sun's heat at different rates; this generates temperature gradients and is the reason why wind flows. Therefore, if temperature gradients change it can be argued that wind patterns may also change [Contreras-Lisperguer and Cuba, 2008].

For Contreras-Lisperguer and Cuba [2008] in order to ensure the sustainability of future wind energy projects, the identification of locations where deep changes in global atmospheric circulation are expected is critical. It is in such locations that radical changes in wind patterns will occur, thus leading to changes in wind space, time dynamics and scale that may influence and/or determine the wind energy potential in locations that may currently be under consideration as suitable sites. It is important to enhance meteorological services in the region in order to better assess the present and future potential of RE resources.

Overall, when considering the potential impact of climate change on wind energy potential, investing in wind energy systems presents significant challenges to local governments and investors. It is recommended that climate change projection modeling and economic assessment studies be performed in order to understand the extent to which climate change may affect a wind energy project and also determine what the long term financial viability may be [Contreras-Lisperguer and Cuba, 2008]. To the best of the author's knowledge, no quantitative study of the possible impacts of climate change in the Caribbean was found in the scientific literature.

Garreaud and Falvey [2008] developed a work which documented the wind changes between present-day conditions and those projected for the end of the 21st century under two Intergovernmental Panel on Climate Change (IPCC) scenarios (A2[13] and B2[14]). They first estimate and interpret the changes of the wind field over the southeast Pacific from 15 coupled atmosphere–ocean Global Circulation Models (AOGCMs). Very consistent among the GCMs is the strengthening of the southerlies along the subtropical coast as a result of a marked increase in surface pressure farther south. Garreaud and Falvey (2008) then examine the coastal wind changes in more detail using the Providing Regional Climate for Impact Studies (PRECIS) regional climate model (RCM) with 25 km horizontal resolution nested in the Hadley Centre Atmospheric global Model (HadAM3). PRECIS results indicate that the largest southerly wind increase occurs between 37–41 °S during spring and summer, expanding the upwelling-favorable regime in that region, at the same time that coastal jets at subtropical latitudes will become more frequent and last longer than current events. This study showed a large increase in wind near the surface, up to 15 per cent in average speed for the A2 scenarios. In the B2 scenario, results show seasonal wind patterns similar to the A2 scenario, but with up to 25 per cent increase.

However, it must be remembered that changes in vegetation pattern may have significant impacts on wind speeds, as they are affected by friction with the soil surface. Wind regression at different heights is very much influenced by irregularities and characteristics of land biomes. Projections made by the Instituto Nacional de Pesquisas Espaciais - INPE for the 2070-2099 period, using global climate models, show more humid biomes (such as tropical forest) being replace by biomes adapted to less availability of water like the desert and semiarid [INPE, 2007]. Such alterations could also influence wind potential in climate change scenarios.

Goubanova et al [2010] used a statistical downscaling method to assess the regional impact of climate change on the sea-surface wind over the Peru–Chile upwelling region as simulated by the global coupled general circulation model IPSL-CM4. Taking advantage of the high-resolution QuikSCAT wind product and of the NCEP reanalysis data, a statistical model based on multiple linear regressions is built for the daily mean meridional and zonal wind at 10 m for the period 2000–2008. The large-scale 10 m wind components and sea level pressure are used as regional circulation predictors. The skill of the downscaling method is assessed by comparing with the surface wind derived from the ERS satellite measurements, with in situ wind observations collected by the International Comprehensive Ocean-Atmosphere Data - ICOADS and through cross validation. It is then applied to the outputs of the IPSL-CM4 model over stabilized periods of the pre-industrial, IPCC CO2 doubling (2 x CO2) and quadrupling (4 x CO2) climate scenarios relative to the pre-industrial simulations. The results indicate that surface along-shore winds off central Chile (off central Peru) experience a significant intensification (weakening) during Austral winter (summer) in warmer climates. This is associated with a general decrease in intra-seasonal variability.

In relation to Brazil, more studies were found. LUCENA et al. [2010] used the 'delta method' to assess climate change impacts on wind generation potential in Brazil. The results of this study show that the wind potential will probably not suffer any negative impacts. On the contrary, for scenarios A2 and B2 results showed an increase in Brazil's wind potential as time goes by. The Brazilian Northeast, as well as the coast of the North and Northeast regions are areas that have shown to be particularly attractive for wind power exploration. These scenarios (A2 and B2) were dynamically downscaled in regional climate projections for Brazil by an expert team on Brazilian weather from CPTEC/INPE, who used the PRECIS (Providing Regional Climates for Impacts Studies) model [United Nations, 2016]. This is a regional climate model developed by the Hadley Centre, which downscales the results from the general circulation model (GCM) HadCM3. Future predictions for Brazilian wind

[13] The A2 storyline and scenario family describes a very heterogeneous world. The underlying theme is self-reliance and preservation of local identities. Fertility patterns across regions converge very slowly, which results in continuously increasing global population. Economic development is primarily regionally oriented and per capita economic growth and technological change are more fragmented and slower than in other storylines.

[14] The B2 storyline and scenario family describes a world in which the emphasis is on local solutions to economic, social, and environmental sustainability. It is a world with continuously increasing global population at a rate lower than A2. The scenario is also oriented toward environmental protection and social equity, it focuses on local and regional levels.

potential were based on wind's average annual speed in 50km by 50km squares, for the time intervals considered by PRECIS.

LUCENA et al. [2010] indicate that the wind average speeds would increase considerably in coastal regions in general, particularly in the country's North and Northeast regions. This study points to a greater frequency of wind with speeds over 8.5 m/s at the coast, which raises the possibility of including different turbine designs that may generate more power at higher speeds in future analyses. Results based on climate projections show that wind power generation could increase threefold in Brazil in scenario B2 and fourfold in scenario A2, when compared with the 2010 reference situation. However, these results are not determinant due to climate projection uncertainties and assumptions made in the study. In sum, this study indicates that wind power generation in Brazil will not be hindered by climate change.

Lucena, Szklo, and Schaeffer [2009] provided a theoretical analysis on issues relevant to climate change impacts on wind power generation, such as the downscaling in speed distribution frequency, transposition of wind speed measuring height and possible alterations in vegetable cover. In addition, Pryor and Barthelmie [2010] conducted a review of studies focused on climate change impacts (Global Climate Change) in wind power generation. They analyzed the mechanism through which climate change may influence wind resources and its operational conditions, as well as the tools that have been employed to quantify these effects and uncertainties related to them.

In Pereira et al. [2013], climate change impacts on wind power are assessed by simulating future scenarios on the Brazil's gross potential, taking into account climate scenarios of the IPCC SRES A1B emissions. The analysis was done for Brazil's South and Northeast regions. Ground stations' data trends were studied like wind forecasts based on the global circulation model HadCM3. The Eta model was used to downscale a 40 Km by 40 Km resolution and 38 vertical layers. The Eta model was updated every 6 hours with the boundary conditions of the HadCM3 outputs.

This study, Pereira et al. [2013], employed observational data time series between 1960 – 2007 from selected national weather stations to seek for trends in wind speed; however, the search did not produce conclusive results. On the other hand, the Eta model predictions – HadCM3 for A1B scenario indicates an average growth trend from 15 to 30 per cent for onshore wind power density for most of Brazil's Northeast region. Indeed, some regions showed an over 100 per cent increase, particularly the Northeast. In addition, with the exception of the country's North and Northeast regions, the study pointed to a fall in future offshore wind power density, particularly off the coast of the state of Bahia.

Nevertheless, the same study pointed to a small increase in wind power density in Brazil's South region, when compared with results for the Northeast. This means an average increase of 10 per cent, reaching over 20 per cent in some areas. The central region of the Rio Grande do Sul state, which extends to the south of Uruguay, showed a small decreasing trend in wind power. This region also showed the highest seasonal variability, with a global minimum in the austral summer (December-February) and an increase in the rest of year, in relation to the baseline period. Therefore, according to PEREIRA et al. [2013], it is possible to expect that the impact of global climate change on wind power in Brazil's Northeast and South may be favorable to existing and future projects in both regions. Table 4 summaries the studies cited above.

2.3.2. Impacts of Global Climate Change on Solar Resource

Massive solar power plants are likely to make a significant contribution to electricity generation in a possible low-carbon future. The calculation of electricity generation potential by PV technology is a basic step in analyzing scenarios for future energy supply. However, this future will also experience significant climate change caused by past and ongoing emissions of greenhouse gases and aerosols [Crook et al., 2011]. Therefore, it is important not only to quantify the present solar resource but also to anticipate how the solar resource will change along with any climate change in the future [Burnett et al., 2014]; this information will assist site choice, critical long-term energy output and financial calculations for future solar power plants [Crook et al., 2011]. The implications of possible changes in usable wind and solar potential must be well understood for future planning purposes [Hegerl et al., 2007].

It is ironic that much of the motivation to use renewable sources of energy generation comes from the desire to mitigate climate change, and climate change directly affects renewable energy resources [Burnett et al., 2014]. Climate change can affect solar energy resources by changing atmospheric water vapor content, cloudiness and cloud characteristics, which affects atmospheric transmissivity [Cutforth et al., 2007]. Cloudiness is strongly influenced by local temperature gradients as well as large-scale climate oscillations. Land surface changes can also affect local cloudiness and could be amplified in urban areas [Denman et al., 2007], but making connections between climate change and changes in solar irradiation is a complicated matter [Hegerl et al., 2007]. In the case of solar energy, cloud cover is the most important property of the climate to consider. The increase in atmospheric particles (aerosols) can, in turn, increase cloud cover by providing greater numbers of cloud condensation nuclei. Global solar irradiance levels depend on the cloud cover characteristics, and therefore will change due to climate change [Burnett et al., 2014].

Table 4. Summary of studies assessing the impacts of climate change on wind resources

Energy Sector Studies	Scope of analysis	Related impacts on wind resources
PRYOR y BARTHELMIE (2010)	Global climate change impact on the wind energy industry	Change in design and operation of wind turbines and wind farms
LUCENA et al. (2010)	Climate change impacts on wind generation potential in Brazil	Results of this study show that the wind potential will probably not suffer any negative impacts
LUCENA, SZKLO y SCHAEFFER (2009)	Theoretical analysis on issues relevant to climate change impacts on wind power generation	Speed distribution frequency, transposition of wind speed measuring height and possible alterations in vegetable cover
PEREIRA et al. (2013)	Impacts on wind power at Brazil's South and Northeast regions	Results indicate an average growth trend from 15 to 30 per cent for onshore wind power density for most of Brazil's Northeast region
GARREAUD y FALVEY (2009	Wind changes over the Southeast Pacific between present-day conditions and those projected for the end of the 21st century under two Intergovernmental Panel on Climate Change (IPCC) scenarios (A2 and B2)	Results indicate that the largest southerly wind increase occurs between 37–41 °S during spring and summer, expanding the upwelling-favorable regime in that region, at the same time that coastal jets at subtropical latitudes will become more frequent and last longer than current events
CONTRERAS-LISPERGUER y CUBA (2008)	Changes climate observed in the Caribbean	Radical changes in wind patterns will occur, thus leading to changes in wind space, time dynamics and scale that may influence and/or determine the wind energy potential in locations that may currently be under consideration as suitable sites
GOUBANOVA et al. (2010)	Impact of climate change on the sea-surface wind over the Peru–Chile upwelling region	Results indicate that surface along-shore winds off central Chile (off central Peru) experience a significant intensification (weakening) during Austral winter (summer) in warmer climates

These modifications can have effects on electricity generation from photovoltaic and concentrated solar power (CSP) arrays [Schaeffer et al., 2012]. Changes in PV output and its fractional contributions from temperature and insolation are all very location dependent. The ambient temperature affects the electrical efficiency of a solar photovoltaic cell. While climate data on cloudiness from climate models may be difficult to obtain, the relationship between temperature and photovoltaic efficiency is well documented. For most PV cell materials, PV output has a near linear response to cell temperature with a negative gradient, and an approximately proportional response to total irradiance except under low levels [Crook et al., 2011]. A 2% reduction in global solar radiation will reduce solar PV cell output by 6%, these projections significantly impact solar energy generation and cost-effectiveness [Contreras-Lisperguer et al.,2008].

The efficiency of concentrated solar power (CSP) can also be impacted by climate change, as it consists of a thermal machine and, as such, its efficiency is altered by ambient temperature variations. CSP output has an approximately linear response to ambient temperature with a positive gradient. Furthermore, CSP based on solar electric generation systems (SEGS) operate a Rankine cycle and, therefore, is exposed to the increased water use and lower efficiency [Schaeffer et al., 2012]. Not only temperature variations, but also changes in direct insolation affect CSP output, with an approximately proportional response to direct irradiance [Crook et al., 2011]. CSP does not utilize diffuse irradiance whereas non-concentrating PV utilizes both direct and diffuse irradiance. Irradiance

is largely a function of cloud cover and cloud properties. Climate change will impact regional patterns of temperature and irradiance, and therefore affect regional PV and CSP output [Crook et al., 2011].

Other climatic variables have a notable impact on PV output. The wind influences the output of PV because forced convection removes heat from the cell and therefore reduces the cell temperature, increasing its efficiency. Dust settling on PV panels and solar collectors is a significant problem in more arid regions, while rainfall cleans the panels by removing dust [Crook et al., 2011], so the change in these climatic variables would also modify PV output.

There has been some previous work all over the world trying to measure the effects of climate change on solar energy. Fant et al. [2016] showed a method that introduces uncertainty from emission scenarios, climate sensitivity, and regional climate outcomes. A statistical model was used to expand upon a hybrid approach to include solar parameter estimations, efficiently producing a portfolio of possible outcomes. They found a wide range to the distributional as well as regional results. These differences were a result of model-response disparity as well as the choice of emission scenario. Nevertheless, the results of this study indicated that, the long-term mean solar resource potential would most likely keep unchanged by 2050 [Fant et al., 2016].

The study conducted by Gunderson et al. [2014] evaluated the current and future solar energy potential through the use of grid-connected PV power plants near the Black Sea region. Incident solar radiation flux from re-analyses, spatial interpolation, and the application of the Delta change method were used to assess the current and future solar resource potential. They simulated data to determine potential change in climate and land-use according to two different development scenarios. The results of Gunderson et al. [2014] showed that the solar resource is sufficient for solar PV power installations in the Black Sea Region and the results also suggested that the solar resource is not expected to vary greatly over the next century over the Black Sea Region, some uncertainties remain. However, it is possible to conclude that land-use changes will have a significant impact on suitable sites for PV power generation [Gunderson et al., 2014].

According to Schaeffer et al. [2012], impacts on climatic variables may have different trends around the world and the same applies to solar energy resources, having positive impacts in terms of increase in solar radiation in some situations (e.g., a reported increase in solar radiation of 5.8% in southeastern Europe [Bartók, 2010]) and negative impacts in solar radiation in other situations (e.g., a decrease trend in incoming solar radiation in Canada [Cutforth et al., 2007]).

In Burnett et al [2014], they characterized the UK solar resource for both the present and future climates providing a detailed assessment. The present solar irradiation level was assessed through the conversion of 30 years of observed historical monthly average sunshine duration data. After combining this with the UKCP09 probabilistic climate change projections, they examined the effect of climate change to give estimates of the future UK solar resource. They found that climate change would increase the average resource in the south of the UK, while marginally decreasing it in the Northwest. The overall effect was a mean increase of the UK solar resource: however, it would have greater seasonal variability and discrepancies between geographical regions [Burnett et al., 2014].

Crook et al. [2011] calculated how climate change was likely to alter the output of photovoltaic and concentrated solar power plants over the next 80 years, taking a global perspective. Established computer models indicated that changes in solar power plant output would show considerable regional differences. For example, PV generation was likely to increase significantly in Europe and China, but decrease in many parts of the world such as western America and the Middle East. This is caused by either a change in temperature or insolation, with considerable regional differences. CSP output is likely to increase by more than 10% in Europe, increase by several percent in China and a few percent in Algeria and Australia, and decrease by a few percent in western USA and Saudi Arabia. This demonstrates that CSP is usually more sensitive to climate change than PV, although there are strong regional differences [Crook et al., 2011]. Figure 2 to Figure 4 present a series of maps showing the absolute change in temperature and insolation (total and direct), all over a 10-year mean centered on 2080. The data presented is from the HadGEM1 model.

It is important to note that there is a lack of data regarding impacts of climate changes on solar resources in Latin America and the Caribbean. The use of solar energy in the Caribbean is widely known and disseminated, but only on a local scale or for domestic uses [Contreras-Lisperguer et al.,2008]. As the quantity of solar plants in Caribbean and South America is still incipient, the interest in this kind of study is still growing for the region.

In many studies about climate change impacts the authors mention the uncertainties related to these works [Gunderson et al., 2014, Crook et al., 2011, Fant et al., 2016]. Some of them assert that these uncertainties are due to the use of GCMs [Fant et al., 2016] and some authors suggest, for future studies, developing a similar

Figure 2. Change in surface temperature. Source: (Crook et al., 2011).

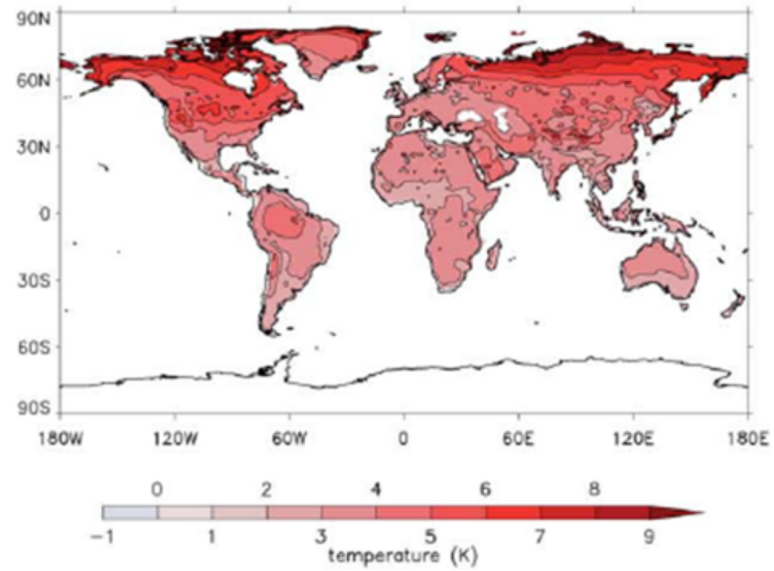

Source: [Crook et al., 2011].

Figure 3. Change in total insolation. Source: (Crook et al., 2011).

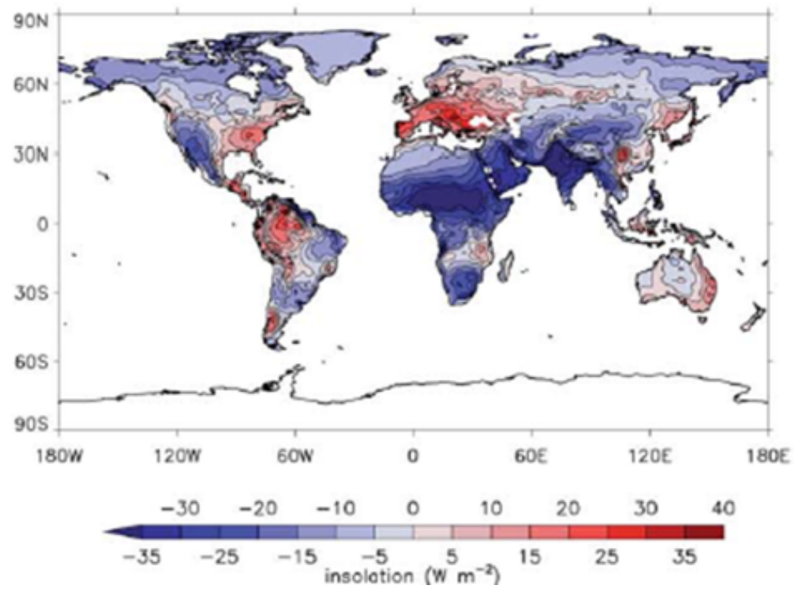

Source: [Crook et al., 2011].

Figure 4. Change in direct insolation. Source: (Crook et al., 2011).

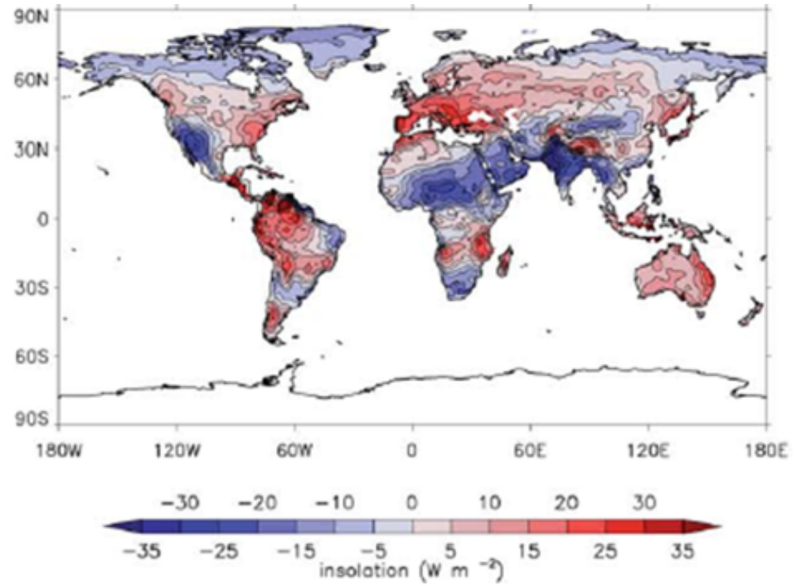

Source: [Crook et al., 2011].

analysis using different climate models in order to reach a better understanding of the uncertainty in energy output caused by uncertainty in projected insolation change [Crook et al., 2011].

The effects of climate changes in the energy sector are quite diverse and tied to particular seasons, regions and energy generation resources [Fant et al., 2016]. Climate change will have a notable impact on plants energy output, in some regions more than the others, so planners, policy makers, and investors of solar energy must include climate change in their longer-term projections when selecting locations and technology for the new large-scale interconnected plants [Crook et al., 2011]. The installed capacity of PV power is increasing at a fast rate [Gunderson et al., 2014] so integrating solar activity variations to solar energy project development may benefit from further analysis, and their impacts on solar energy production [Contreras-Lisperguer et al.,2008]. The Table 5 presents a general overview of several impacts of the above mentioned studies.

2.3.3. Impacts of Global Climate Change on Hydropower

Due to growing concern about climate change, fossil energy sources are increasingly being encouraged to be traded for clean energy, including hydroelectricity. However, changes in climatology, by reason of climate change, are often not considered in alternative energy projects. Variation in both rainfall and temperature can affect energy production [Mukheibir, 2013].

Among the consequences of climate change, one can expect a drop in water quality in general, as well as risks to the quality of drinking water, despite conventional treatment, due to interconnected factors like: temperature increase; increase in sediments, nutrients and pollutant loads from strong rainfall; increase in pollutant concentration during droughts; and interruption of treatment facilities during floods [IPCC, 2014]. According to the IPCC, there is strong evidence that climate change will reduce surface and underground hydro resources in most dry subtropical areas, during the 21st century. This problem can cause competition for water between the economic sectors, like agriculture and industry.

Flow variation in rivers and levels of lakes caused by global climate change can impact the generation of electricity

Table 5. Summary of studies assessing the climate change impacts on the solar resource

Energy Sector Studies	Climate Variables	Related impacts
Fant et al. (2016)	Global horizontal irradiance (GHI) and global mean temperature	The long-term mean solar resource potential would most likely keep unchanged by 2050 in southern Africa
Gunderson et al. (2014)	Daily downward solar radiation and total cloud cover	The solar resource is not expected to vary greatly over the next century over the Black Sea Region
Burnett et al. (2014)	Sunshine duration and global horizontal irradiance (GHI)	Climate change would increase the average solar resource in the south of the UK, while marginally decreasing it in the Northwest. However, it would have greater seasonal variability and discrepancies between geographical regions
Crook et al. (2011)	Surface temperature, total insolation and direct insolation	The change in solar power plant output would show considerable regional differences.

athwart hydraulic power [Chiew, 2016]. Is also depends on alterations in volume, intensity and rainfall time, that is occasioned by evapotranspiration, which is function of temperature, insolation, wind speed and atmospheric humidity. The answer to changes in climate variation is different among the distinct river basins, depending on their hydrological and physical characteristics, as also of the amount of water stored on the surface and underground [Kundzewicz et al.,2008]. Climate change will affect the function and operation of flood control, drainage and irrigation systems, and change water resource management. There is another preoccupation, because we cannot simply use past hydrological experience to predict future conditions [Lucena, 2010].

The concern with changes in weather conditions started in the 1960s. However, the first studies on the hydrological impacts of climate change began in 1980 [Nemec; Schaake, 1982]. This is one of the areas that the international scientific literature has paid more attention to. The importance of the hydrological cycle came to light in the Generation Circulation Model (GCM) results. GCM is the baseline for most studies on climate change impacts on water resources, which relates chemical alterations in the atmosphere with great climate variation.

The limitations of models that study the impact of global climate change on hydrological systems are mainly the spatial scale, but also the representation of extreme weather events on larger scales, vegetable cover and absence of mention of extreme events such as droughts and floods [Lucena, 2010]. Another problem is the small number of studies with analysis of climate change impacts on underground water, including the uncertainty in the relationship between surface and underground rivers [Alley, 2001; Kundzewicz, 2007]. There are few papers on the theme of climate change on water resources that focus on Latin America. When they approach this region, most of these cases are reported from Brazil.

In Salatti et al. [2010], the HadRM3P model calculated the Brazilian water balance between 2011 and 2100 for scenarios A2 and B2, compared with the period 1961-1990, designated as the reference. The results are really worrisome, with a dramatically drop in flows by 2100 in the East Atlantic and Eastern Northeast basins, coming close to zero.

The same model was integrated by Marengo et al. [2010] to obtain the climatology model for the present time (1961-1990) and then, to future projections (2071-2100) for scenarios A2 and B2. This study concludes that the Amazon and the Northeast are the most vulnerable areas in Brazil. Average warming may reach 5 °C in 2100 in scenario A2 and 3 °C in B2, although gradual temperature increase in the Amazon could reach 7-8 °C or 4-6°C in 2100, respectively. For the whole country, the tendency is an increase in temperature and extreme heat, as well as a reduction in the frequency of frost, due to a rise in the minimum temperature, particularly in the south, southeast and mid-west states. However, in all of the scientific literature on climate change impacts on water resourc-

es, there is a trend in the Brazil regions: an increasing frequency and intensity of extreme events, higher water stress in the Northeast, large falls in rainfall in the Amazon region and small flow increases in the south's basins.

According to Soito and Freitas [2011], vulnerability and adaptation of water resources is related to average trends and also variability alterations in hydrological systems or extreme events, when global climate change is present. The study points out that in the projections made so far, results for South America have not agreed with respect to flow predictions. First of all, because of rainfall prediction differences and, secondly, as a consequence of differing expected evaporation values. In the same way, in countries exposed to water stress, a negative effect on the flow of rivers, and the refilling of underground water reservoirs and aquifers is expected from climate change.

The impacts of climate change on hydropower generation come from alterations in flow variation or in the seasonality regime. The vulnerability of a hydropower plant depends on the water storage capacity of reservoirs [Schaeffer et al., 2012]. Lucena et al. [2009] affirmed that the impacts on electricity generation are not proportionate impacts on flow, because of the water storage capacity of reservoirs in Brazilian plants.

Central America is one of the most vulnerable regions to climate change. The region is strongly affected by extreme temperature and precipitation events due to its geographic location. This often leads to droughts and floods, which tends to increase further in the coming years, according to models that study climate change. Due to the high dependence of hydropower dams for electricity generation in the region, more than 50% in 2015, it is very important to identify the possible impacts of climate change on the flow of rivers that allow the production of energy in these hydropower plants [IDB, 2016].

In the IDB study [2016], seven Central American countries were studied: Belize, Costa Rica, El Salvador, Guatemala, Honduras, Nicaragua and Panama. In future projections in this region, electricity production will fall 39.5% in 2090 and an increase of 3,8 °C in the average temperature, between 2060 and 2099. In this scenario the droughts will be more frequent and the maximum flows will fall during the XXI century.

A key region in Central America that is vulnerable to impacts of climate change is the Rio Lempa basin, the largest river system in Central America, which includes El Salvador, Honduras and Guatemala. Maurer et al. [2009] analysed hydrologic impacts of projected climate changes on Rio Lempa Basin and the inflow variation of two major hydropower reservoirs, due to changes in temperature and precipitation from 16 climate models using two emissions IPCC scenarios (B1 and A2) during 2040-2069 and 2070-2099. The results indicated a decrease of 5% (B1) and 10.4% (A2) in project average precipitation and 13% (B1) and 24% (A2) of reduction in reservoir inflow in 2070-2099. Moreover, the frequency of low flow years will increase which will impact the hydropower capacity of 33% to 53% for the same period.

CEPAL (2012) investigated the effects of climate change on hydroelectricity generation from two hydropower plants: Cerrón Grande in Rio Lempa basin (El Salvador) and Chixoy in Chixoy basin (Guatemala). They used the following GCM: HADCM3, GFDL R30 y ECHAM4 for scenario B2 and HADGEM1, GFDL CM2.0 y ECHAM4 for scenario A2. The variation of temperature and precipitation was projected for the years 2020, 2030, 2050, 2070 and 2100, and changes in streamflow was simulated in software Water and Power Potential (WAPPO).

The projected results for A2 scenario found a reduction in Chixoy´s power generation of approximately 25% in 2020, 37% in 2030, 47% in 2050, 70% in 2070 and 83% in 2100 in comparison of average power generation from 1979 to 2008. Regarding the Cerrón Grande hydropower plant the projected decrease in electricity generation is 22% in 2030, 34% in 2030, 41% in 2050, 57% in 2070 and 71% in 2100, compared to average generation between 1984 to 2009. In B2 scenario an increase of 4% and 6% in electricity generation was expected for 2020 in Chixoy and Cerrón Grande, respectively. However, in the following years the results again indicate a decrease in energy production that will reach 26% in Chixoy and 17% in Cerron Grande in 2100.

Despite the negative impacts mentioned above, the study carried out by Popescu et al. [2014] has resulted in an increase in potential hydropower as a result of climate change in La Plata Basin, Located in five countries: Argentina, Brazil, Bolivia, Paraguay, Uruguay. Popescu et al. [2014] studied the impact of hydrological changes on hydropower production in La Plata Basin based on PROMES-UCLM and RCA-SMHI climate change scenarios. The study used projected climate parameters from two regional climate models as an input of a hydrological rainfall – runoff model for the time slots of 2031-2050 and 2079-2098. Results showed an increase of the hydropower energy potential for both periods.

[15] The general circulation models used are BCCR-BCM2.0, CGCM3.1 (T47), CNRM-CM3, CSIRO-Mk3.0, GFDL-CM2.0, GFDL-CM2.1, GISS-ER, INM-CM3.0, IPSL-CM4, MIROC3.2, ECHO-G, ECHAM5/MPI-OM, MRI-CGCM2.3.2 , PCM, CCSM3, UKMO-HadCM3

Hydropower generation in Amazonia will be more vulnerable in the dry season, challenging future energy security across the region that has many hydropower projects without reservoirs like Belo Monte in Brazilian Amazonia [Lucena et al., 2013].

In Brazil, the main projected impact was a drop in the system's reliability and extreme hydropower generation effects in the North and Northeast regions [Lucena et al., 2009]. In this study, the South and Southeast basins have a positive variation in firm energy. So, the aggregate average energy keeps regular. But in Paranaíba and East Atlantic basins, water surplus fall in 80 per cent in some points of the projections, with a dramatically drop in energy production.

According to IPCC [2014], in many regions, changes in rainfall or the melting of snow and ice are altering hydrological systems and affecting water resources in terms of quantity and quality. Glaciers are shrinking almost all over the world and permafrost is melting in high altitude and latitude regions due to climate change, affecting the flow of available water resources. In South America, hydropower is the main source of renewable energy and has an important role in the electric sector. Therefore, if climate change affects hydraulic plants, this will concern all of the electric energy system [Zwaan et al., 2016]. Table 6 summaries the studies cited above.

Table 6. Summary of studies assessing the impacts of climate change on hydropower resource

Energy Sector Studies	Related impacts on hydropower resource
Chiew (2016)	Change in flow rivers and level of lakes impacting hydropower generation
Salatti et al. (2010)	Climate impacts on water balance at Brazil's basins projected for the 21st century considering two IPCC scenarios (A2 and B2). The results indicate a drastic fall in flows by 2100 in the East Atlantic and Eastern Northeast basins
Marengo et al. (2010)	Changes in temperature and precipitation at Brazil's regions projected for the 21st century considering two IPCC scenarios (A2 and B2). Increase in temperature and in the frequency of droughts, especially in Amazon and Northeast regions
IDB (2016)	Impacts on hydropower generation in Central America. Results indicate 39,5% of fall in electricity production (more than 50% generated by hydroelectricity generation), between 2060 and 2099
CEPAL (2012)	Effects of climate change on Cerrón Grande in Rio Lempa basin and Chixoy in Chixoy basin, under two Intergovernmental Panel on Climate Change (IPCC) scenarios (A2 and B2). Results indicate a reduction in Chixoy's power generation of approximately 83% in 2100 and a fall of 71% in Cerrón Grande hydropower in the same period.
Lucena et al. (2009)	Impact of climate change in the Brazilian region. The main impact is a drop in the system's reliability and extreme hydropower generation effects in the North and Northeast regions. In Parnaíba and East Atlantic basins, water surplus fall in 80 per cent in some points of the projections, with a dramatically drop in energy productions.

03. Methodology

This study aims to determine the possible impacts on the future long-term wind and solar energy resource complementarity caused by climate change in selected regions of the LAC. This study focuses on the annual seasonality of the wind and solar energy resources. Based on the climate projections for the IDB database, the energy complementarity was re-evaluated between the areas that showed complementarity in the first report of this study.

The flowchart below shows the steps taken to achieve the goal of the study. The assumptions and procedures of each step are described hereafter

Figure 5. Flowchart of the steps taken to achieve the goal of the study

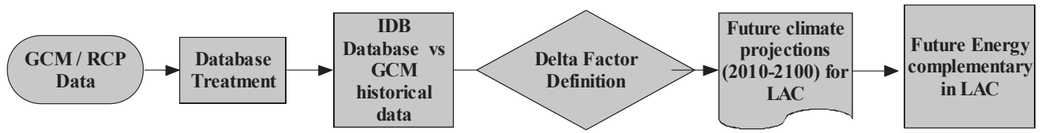

a) GCM/RCP Data

To develop the climate projections, MIROC-ESM-CHEM and HadGEM2-ES General Circulation Models (GCMs) were considered. The choice of the GCMs was based on studies performed in Brazil by CHOU et al. [2014a, 2004b], who used these models to research downscaling of the results obtained from the GCMs for South America.

The GCM results were obtained from the Inter-Sectoral Impact Model Integration and Intercomparison Project (ISI-MIP2 Phase a)[16] database version 20160708, which were processed by HEMPLE et al. [2013]. The variables used are the short wave downwelling radiation – rsds (Wm^{-2}) and the near-surface wind magnitude – wind speed (ms^{-1}).

For each GCM, two Representative Concentration Pathways were chosen: ii) the RCP 4.5 scenario, that represent a stabilization scenario in which total radiative forcing is stabilized before 2100 and ii) the RCP 8.5 scenario that represents increasing greenhouse gas emissions over time, this scenario can be the most pessimistic scenario for wind and solar resources [Riahi et al., 2011].

The RCP4.5 is an intermediate emission/radiative forcing, which integrates lower energy intensity, strong reforestation programs, dietary changes and stringent climate policies. The RCP8.5 is a high emissions/radiative forcing scenario, which combines assumptions about high population and relatively slow income growth with modest rates of technological change and energy intensity improvements, leading in the long term to high energy demand and GHG emissions in the absence of climate change policies [Riahi et al., 2011].

b) Database Treatment

The IDB database comprises 36 areas with high potential solar PV resources and 50 high potential wind energy resources (hotspots). The results of the Report IPart I indicate the areas that presented a seasonal complementarity. Thus, these pairs of hotspots are the focus of this second report and of Part II and are shown in Table 7 .

The GCMs typically have a horizontal resolution of 250 to 600 km. The outputs of the GCMs were transformed to a regional-scale for each representative region. In this way, a representative point for each wind and solar potential generation area was chosen (Figure 6).

Table 7. Seasonal complementarities obtained in Report I.

WIND_EC_A01	SOLAR_VE_A03
WIND_CO_A02	WIND_PE_A01
WIND_CL_A01	SOLAR_MX_A01
WIND_BR_A05	WIND_VE_A03
WIND_VE_A03	SOLAR_BR_A03
	SOLAR_EC_A01
	WIND_BR_A05
WIND_BR_A01	SOLAR_BR_A03
	WIND_PE_A01
WIND_AR_A01	SOLAR_ES_A01
	SOLAR_PA_A01
	WIND_BR_A01
WIND_BR_A04	WIND_VE_A03
	WIND_VE_A04
	WIND_SU_A01
	WIND_VE_A02
WIND_BR_A03	WIND_VE_A04
	WIND_VE_A03
	WIND_SU_A01
	WIND_VE_A02

[16] ISIMIP is a community-driven climate-impacts modelling initiative aimed at contributing to a quantitative and cross-sectoral synthesis of the differential impacts of climate change, including the associated uncertainties. ISIMIP offers a consistent framework for cross-sectoral, cross-scale modelling of the impacts of climate change (ISIMIP, nd).

The GCMs results for the wind speed (near-surface wind magnitude – wind (m.s-1)) were extrapolated to estimate the wind speed at a standard wind turbine height (100m) The extrapolation was made using the Power Law [Kubik et al., 2011], which is an empirical equation expressed in (Eq. 2).

$$u_2 = u_1 \left(z_2 / z_1 \right)^a \qquad \text{(Eq. 2)}$$

Where a is the wind shear coefficient, for neutral stability conditions this coefficient is approximately 1/7, u_1 is the know wind velocity at the reference height z_1 and u_2 is the extrapolated speed at the height z_2.

Once the wind speed data is extrapolated, the monthly value (median) for each resource (wind speed and solar irradiation) is calculated, both for IDB database and for GCM simulations. The GCM simulation results are composed by the historical simulated data (model runs for the 1961-2004 period) and the future climate projections (2005-2099). The climate projections were clustered in 3 groups: i) 2010-2040, ii) 2041-2070, iii) 2071-2100.

c) IDB Database versus GCM Historical Data

As mentioned, two GCMs were consider, the HADGEM2-ES and MIROC-ESM-CHEM. With the aim of selecting the GCM that best represent the IDB database, a comparison between the two GCM historical data (1961-2004) and the IDB data was made. This comparison was made between "equivalent" years.

An "equivalent" year was created for the IDB data as well as for each of the GCMs historical data. It was obtained through (Eq. 3).

$$EY_m = median\left(Data_{m,i} \right) \ \forall\, i < T \qquad \text{(Eq. 3)}$$

Where EY is the equivalent year, m is the month, Data is the resource value, i is the year and T is the period of analysis.

This study defined two decision criteria to determine which GCM simulation historical data best represent the historical IDB database: i) the determination coefficient

Figure 6. Reference point for the historical and future climate data of each area that presented complementarity without climate change impact

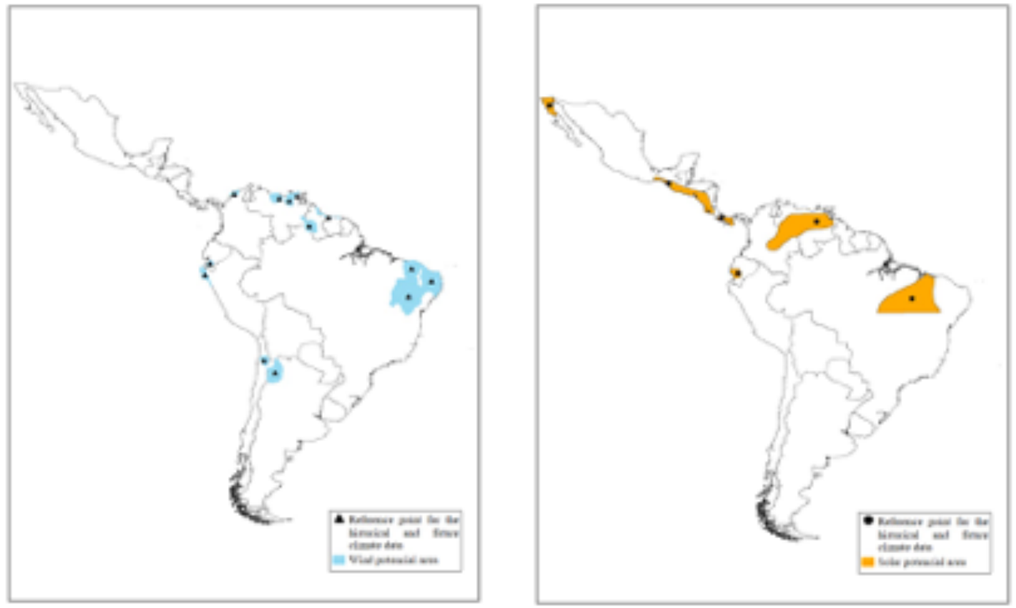

[Nagelkerke, 1991] that provides a measure of how well a model replicates the "observed" data and ii) the correlation coefficient [Kougias et al., 2016] that, in this case, measures the strength and direction of the linear relationship between the IDB database and the GCM historical data.

d) Delta Factor Definition

As mentioned, the climate projections were clustered in 3 groups: i) 2010-2040, ii) 2041-2070, iii) 2071-2100. An "equivalent" year for each one of these groups was created using (Eq. 3). The delta factors were defined for each GCM climate projections (RCP 4.5 and RCP 8.5).

A monthly delta factor will be applied to these "equivalent" years. The delta factor to be applied is defined by (Eq. 4).

$$delta_{m,p}=(\overset{GCM}{EY}_{m,p}-\overset{GCM\text{-}H}{EY}_{m})\ /(\overset{GCM\text{-}H}{EY}_{m})$$

$$such\ that\quad p=\{p_1,p_2,p_3\},\quad m=\{1,2,\ldots,12\} \qquad \text{(Eq. 4)}$$

Where p_1 represents the 2010-2040 cluster, p_2 represents the 2041-2070 cluster, p_3 represents the 2071-2100 cluster, m is the month analyzed, $\overset{GCM\text{-}H}{EY}_{m}$ is the equivalent year of the GCM historical data and $\overset{GCM}{EY}_{m,p}$ is the equivalent year of the GCM climate projections.

e) Future Climate Projections (2010-2100) for Latin America

As it was pointed in section 2.2, climate scenarios make implicit or explicit assumptions about the extrapolation of climate model biases from current to future time periods. Such assumptions are inevitable because of the lack of future observations and, being subjected to different sources of uncertainty [Kerkhoff et al, 2014]. Therefore, a sensitivity analysis was made between each monthly value of the cluster projection period with the monthly historical value for the chosen GCM. The result of this variation is called, in this study, the "delta factor".

The monthly delta factor is applied to the equivalent year obtained from the IDB database, (Eq. 5). In this way, the variability in the gridded observations is preserved and the comparison between future scenarios and historical modeled is straightforward and easily interpreted.

$$NP_p = delta_{m,p} * \overset{IDB}{EY}_{m} \qquad \text{(Eq. 5)}$$

It is important to highlight that for a coherent use of the delta factor, it is necessary that the historical database simulations are aligned with the seasonal pattern of the resource i.e. the resource data of historical GCM and IDB must have good seasonal consistency.

f) Future Energy Complementary in LAC

The renewable energy resources complementarity in LAC, obtained in the report I, is reviewed in order to identify possible impacts as a consequence of climate change. The potential complementarity between resources is evaluated by the linear correlation method, Pearson method.

04.

Results

The historical simulation data of HadGEM2-ES and MI-ROC-ESM-CHEM with scenarios of RCP 4.5 and RCP 8.5 were considered for this Report. A statistical analysis was made to check the seasonal consistence between the simulated historical GCM versus the IDB database. The seasonal patterns were built using the monthly medians of each database available.

The comparison between IDB database and the GCMs data was based on the correlation factor, to determine the strength and direction of the linear relationship between the IDB database and the GCM historical data, and the ordinary least square (OLS) method in order to assess the goodness of fit measured by the coefficient of determination R^2. The analysis using the correlation factor was inconclusive since for each area that was considered, the correlation factor presented a similar value for both GCM models. The results using OLS were more enlightening.

Appendix 7.1 shows the equivalent - year monthly pattern of the historical databases and their R2 coefficient and correlation values, for the areas that presented energy complementary in the first report of this study. This process indicated that most of the area analyzed had a good seasonal consistency, except for two areas: (i) SOLAR_ES_A01 had different seasonality between the months of fall and spring; (ii) WIND_CL_A01 did not show the same seasonality for the all period analyzed. It is not possible to assess future impacts on the complementarity when the historical GCM simulation is not adjusted to the original data resource. Therefore, the correlation of WIND_CL_A01 & SOLAR_MX_A01 was not considered for the analysis.

Additionally, the OLS analysis was done over the whole set of data, the statistical parameters are exposed in Table 8. This study chooses to work with the HadGEM2-ES as it presented a better fit for the IDB database.

4.1 Trend Analysis in the Solar Radiation and Wind Speed Resources for the selected cases of Latin America

The use of the delta factor helps to analyzed possible future projection of the renewable energy resources i.e. solar radiation and wind speed resources. In this section the delta factor impact of the two scenarios (RCP4.5 and RCP8.5) in the renewable energy resource will be analyzed. In other words, the main findings of the possible trend of the resources are described. The analysis was based on HadGEM2-ES model. The delta factor for each hotspot is presented in the appendix 7.3 and the trend of the resources of the selected areas is shown in appendix 7.5.

Tabla 8. Bondad de ajuste entre datos históricos

GCM	R^2	p-value
HadGEM2-ES	0,8404	< $2,2e^{-16}$
MIROC-ESM-CHEM	0,8308	< $2,2e^{-16}$

For both scenarios, RCP 4.5 and RCP 8.5, the solar resource of the hotspots did not show a significant variation in the average irradiation during the period of analysis on a yearly basis. These results are coherent with the discussion made in the section 2.3.2. The exceptions were for Solar_EC_A01, that from the year 2040 and for both scenarios, the radiation in that area show increasing trend. The SOLAR_PA_A01 area presented a small decrease in the solar radiation for the whole period of analysis, especially in the RCP8.5 scenario.

Additionally, in a seasonal analysis, for the RCP 4.5 scenario, the solar radiation shows an increase during the winter (Jun- Aug) in the following areas: SOLAR_EC_A01 (2010-2100) and SOLAR_VE_A03 (2040-2100). The SOLAR_BR_A03 area presents a decrease for the summer (Dec- Feb) for the period of 2010 - 2100. In the case of RCP8.5 the results for SOLAR_BR_A03 show a decrease, when compared to historical data, during the summer and an increase during the winter, it occurs for the whole analyzed period. For SOLAR_MX_A01, the solar irradiation presents a decrease for the winter and an increased during the summer for the period of 2041-2100.

On the other hand, in the RCP4.5 scenario the wind speed resource shows variation in the annual seasonality. For instance, the seasonal analysis using the delta factors shows a decrease in the monthly average wind speed of WIND_BR_A04 and WIND_BR_A05, especially in the period of 2010-2070. On the other hand, the wind hotspots in Ecuador and Venezuela show a trend of increasing wind speed during the whole period of analysis.

In the case of scenario RCP8.5, during the period 2010-2040, the average wind speed of the areas WIND_CO_A02, WIND_BR_A01, WIND_EC_A01, WIND_PE_A01 and WIND_BR_A05 shows a decrease when compared to the historical model on a yearly basis. However, 66% of the wind hotspot showed a strong tendency to have higher wind speeds after 2040. In all of the cases the increase in wind speed is stronger during the RCP 8.5 scenario. WIND_BR_A01 and WIND_BR_03 are the areas that present the most intensive delta.

4.2 Climate Change Impact on Energy Complementarities – Analysis based on an Seasonal Approach

To assess the impact of global climate change on wind and solar complementarity, it was necessary, based on the climate projection of the HadGEM2-ES (RCP4.5 and RCP8.5), to create scenarios that would show the future behavior of the wind and solar resources in LA. These scenarios were built using the delta factors defined by (Eq. 4) and presented in Appendix 7.2.

Based on the climate projections for the IDB database, the energy complementarity was re-evaluated between the areas that showed a complementarity in the first report of this study.

As the Table 9 and Table 10 will show, the behavior of the climate projection complementarities for the period of 2010 -2040 based on the RCP4.5 are quite similar to the ones based on the RCP 8.5. The exception were WIND_PE_A01 & WIND_CO_A02, whose complementarity remained unchanged during the RCP 4.5 scenario but decreased for the RCP 8.5 scenario and WIND_PE_A01 & WIND_BR_A01 whose complementarity increased in the RCP 8.5 but decreased in the RCP 4.5. For the periods of 2041-2070 and 2071-2100 the complementarities between scenarios differ greatly.

Appendix 7.2 presents the behavior of each one of the areas that presented complementarity for each period of time (2010-2040, 2041-2070, 2071-2100) for the scenarios RCP 4.5 and 8.5. The main findings are presented in the next two sections.

4.2.1 Climate Change Impact on Energy Complementarities – RCP 4.5

In this section the main findings for the energy complementarities based on HadGEM2-ES model and RCP4.5 are presented.

- In this scenario, for the period of 2010-2040, 47.3% of the selected cases had no significant variations regarding the historical complementarity and 36.8% improved. For the period of 2041-2070 the numbers were are 47.3% and 31.5% respectively and for the period of 2071-2100 the numbers were 47.3% and 26.3%

- Even though during the whole period of analysis (2010-2100) the great majority of the energy complementarities remain unchanged or even increased, the number of areas that show a reduction in their correlation factor, as the years get closer to 2100, increased. For the period of 2010-2040, 16% of the selected cases show a decrease in their complementarity, 21% for 2041-2071 and 26% for 2071-2100. This means that the complementarity of fourteen pairs of hotspots remained around or higher than the historical value for the whole period analyzed (projection for 2010 until 2100)

- Five pairs of hotspots the complementarities were lower than the historical value in the last period of the analysis: WIND_VE_A03 & WIND_BR_A05, SOLAR_BR_A03 & WIND_BR_A01, SOLAR_ES_A01 & WIND_AR_A01, SOLAR_VE_A03 & WIND_EC_A01, WIND_SU_A01 & WIND_BR_A04.

- There were no cases in which the polarity of the correlation factor changed to a positive correlation

Table 9 summarizes the impact of climate change, based on HadGEM2-ES model and RCP4.5 scenario, in the renewable energy complementarity between the hotspot analyzed, categorizing the increments with no significant variations and decrements.

Table 9. Climate Change Impact on Energy Complementarities based on HadGEM2-ES model and RCP4.5 scenario

4.2.2 Climate Change Impact on Energy Complementarities – RCP 8.5

In this section the main findings for the energy complementarities based on HadGEM2-ES model and RCP8.5 are presented.

- In 84% of the selected cases, the complementarity, for the time period of 2010-2040, improved or had no significant variations regarding the historical complementarity; the figure was 63% for the period of 2041-2070. Moreover, for three pairs of hotspots (WIND_VE_A03 & WIND_BR_A04, WIND_SU_A01 & WIND_BR_A03 and SOLAR_PA_A01 & WIND_AR_A01) the complementarity remained around or higher than the historical value for the whole period analyzed (projection for 2010 until 2100). For the long term planning this result could encourage the expansion of solar and wind projects since no strong variation in the generation profile is expected.

- SOLAR_BR_A03 & WIND_BR_A01 and WIND_PE_A01 & WIND_CO_A02 are special cases in which the polarity of the correlation factor changed to a positive correlation, the first one in the period of 2071-2100 and the second one in the period of 2010-2040.

- The 2071-2100 period stands out by the strong decrease tendency (68% of the cases) in the energy complementarities.

Table 9. Climate Change Impact on Energy Complementarities based on HadGEM2-ES model and RCP4.5

	2010-2040	2041-2070	2071-2100
Increment (the correlation factor became more negative by 5%)	WIND_VE_A04 & WIND_BR_A04 WIND_BR_A05 & WIND_BR_A01 WIND_SU_A01 & WIND_BR_A04 WIND_VE_A02 & WIND_BR_A03 SOLAR_BR_A03 & WIND_VE_A03 SOLAR_PA_A01 & WIND_AR_A01 WIND_VE_A02 & WIND_BR_A04 SOLAR_EC_A01 & WIND_VE_A03 WIND_BR_A01 & WIND_AR_A01	WIND_VE_A04 & WIND_BR_A04 WIND_BR_A05 & WIND_BR_A01 WIND_SU_A01 & WIND_BR_A04 WIND_VE_A02 & WIND_BR_A03 SOLAR_BR_A03 & WIND_VE_A03 SOLAR_PA_A01 & WIND_AR_A01 SOLAR_EC_A01 & WIND_VE_A03 WIND_BR_A01 & WIND_AR_A01 WIND_PE_A01 & WIND_CO_A02	WIND_VE_A04 & WIND_BR_A03 WIND_VE_A03 & WIND_BR_A04 WIND_VE_A04 & WIND_BR_A04 WIND_SU_A01 & WIND_BR_A03 WIND_VE_A02 & WIND_BR_A03 SOLAR_BR_A03 & WIND_VE_A03 SOLAR_PA_A01 & WIND_AR_A01 WIND_BR_A01 & WIND_AR_A01 WIND_PE_A01 & WIND_CO_A02
No significant variation (less than 5%)	WIND_VE_A04 & WIND_BR_A03 WIND_VE_A03 & WIND_BR_A04 WIND_VE_A03 & WIND_BR_A05 WIND_VE_A03 & WIND_BR_A03 WIND_SU_A01 & WIND_BR_A03 SOLAR_VE_A03 & WIND_EC_A01 WIND_PE_A01 & WIND_CO_A02	WIND_VE_A04 & WIND_BR_A03 WIND_VE_A03 & WIND_BR_A04 WIND_VE_A03 & WIND_BR_A05 WIND_VE_A03 & WIND_BR_A03 WIND_SU_A01 & WIND_BR_A03 WIND_VE_A02 & WIND_BR_A04	WIND_VE_A03 & WIND_BR_A03 WIND_BR_A05 & WIND_BR_A01 WIND_SU_A01 & WIND_BR_A04 WIND_VE_A02 & WIND_BR_A04 SOLAR_EC_A01 & WIND_VE_A03
Decrement (the correlation factor became more positive by 5%)	SOLAR_BR_A03 & WIND_BR_A01 SOLAR_ES_A01 & WIND_AR_A01 WIND_PE_A01 & WIND_BR_A01	SOLAR_BR_A03 & WIND_BR_A01 SOLAR_ES_A01 & WIND_AR_A01 SOLAR_VE_A03 & WIND_EC_A01 WIND_PE_A01 & WIND_BR_A01	WIND_VE_A03 & WIND_BR_A05 SOLAR_BR_A03 & WIND_BR_A01 SOLAR_ES_A01 & WIND_AR_A01 SOLAR_VE_A03 & WIND_EC_A01 WIND_PE_A01 & WIND_BR_A01

Table 10 summaries the impact of climate change, based on HadGEM2-ES model and RCP8.5 scenario, in the renewable energy complementarity between the hotspot analyzed, categorizing the increments, no significant variations and decrements.

Tabla 10. Impacto del cambio climático en las complementariedades energéticas en base al modelo HadGEM2-ES y el escenario RCP8.5

	2010-2040	[2041-2070]	[2071-2100]
Increment (the correlation factor became more negative than 5%)	WIND_VE_A04 & WIND_BR_A04 WIND_BR_A05 & WIND_BR_A01 WIND_SU_A01 & WIND_BR_A04 WIND_VE_A02 & WIND_BR_A03 SOLAR_BR_A03 & WIND_VE_A03 SOLAR_PA_A01 & WIND_AR_A01 WIND_VE_A02 & WIND_BR_A04 WIND_PE_A01 & WIND_BR_A01 SOLAR_EC_A01 & WIND_VE_A03 WIND_BR_A01 & WIND_AR_A01	EWIND_VE_A03 & WIND_BR_A04 WIND_SU_A01 & WIND_BR_A03 SOLAR_BR_A03 & WIND_VE_A03 SOLAR_PA_A01 & WIND_AR_A01 WIND_VE_A04 & WIND_BR_A03	SOLAR_PA_A01 & WIND_AR_A01
No significant variation (less than 5%)	WIND_VE_A04 & WIND_BR_A03 WIND_VE_A03 & WIND_BR_A04 WIND_VE_A03 & WIND_BR_A05 WIND_VE_A03 & WIND_BR_A03 WIND_SU_A01 & WIND_BR_A03 SOLAR_VE_A03 & WIND_EC_A01	WIND_VE_A03 & WIND_BR_A03 WIND_VE_A04 & WIND_BR_A04 WIND_BR_A05 & WIND_BR_A01 WIND_SU_A01 & WIND_BR_A04 WIND_VE_A02 & WIND_BR_A03 SOLAR_EC_A01 & WIND_VE_A03 WIND_BR_A01 & WIND_AR_A01 WIND_PE_A01 & WIND_CO_A02	WIND_VE_A03 & WIND_BR_A04 WIND_SU_A01 & WIND_BR_A03

	2010-2040	[2041-2070]	[2071-2100]
Decrement (the correlation factor became more positive than 5%)	SOLAR_BR_A03 & WIND_BR_A01 SOLAR_ES_A01 & WIND_AR_A01 WIND_PE_A01 & WIND_CO_A02	WIND_VE_A03 & WIND_BR_A05 SOLAR_BR_A03 & WIND_BR_A01 SOLAR_ES_A01 & WIND_AR_A01 SOLAR_VE_A03 & WIND_EC_A01 WIND_VE_A02 & WIND_BR_A04 WIND_PE_A01 & WIND_BR_A01	WIND_VE_A04 & WIND_BR_A03 WIND_VE_A03 & WIND_BR_A05 WIND_VE_A03 & WIND_BR_A03 WIND_VE_A04 & WIND_BR_A04 WIND_BR_A05 & WIND_BR_A01 WIND_SU_A01 & WIND_BR_A04 WIND_VE_A02 & WIND_BR_A03 SOLAR_BR_A03 & WIND_BR_A01 SOLAR_ES_A01 & WIND_AR_A01 SOLAR_BR_A03 & WIND_VE_A03 SOLAR_VE_A03 & WIND_EC_A01 WIND_VE_A02 & WIND_BR_A04 WIND_PE_A01 & WIND_BR_A01 SOLAR_EC_A01 & WIND_VE_A03 WIND_BR_A01 & WIND_AR_A01 WIND_PE_A01 & WIND_CO_A02

05. Discussion

Climate variables such as solar radiation and wind speed are important factors that influence renewable energy availability; thus, changes in these variables would impact the power generation and the complementarity between the hotspots analysed.

In the behavior analysis of the wind and solar resources under the RCP4.5 and RCP8.5 scenarios, the impact of global climate change is more prominent in wind resources; this impact is greater in the RCP 8.5 scenario than the RCP 4.5 scenario. The data show a tendency for higher wind speeds in LA from 2040, especially in the Caribbean Region: WIND_VE_A03, WIND_SU_A01, WIND_CO_A02 and WIND_BR_A01. In some areas, like WIND_CO_A02 and WIND_VE_A03, the moving average in the final period (2071-2100) reaches values up to 44.03% and 42.80% higher than the historical mean. For both scenarios, RCP 4.5 and RCP 8.5, the solar resource of the hotspots did not show a significant variation in the average irradiation during the period of analysis.

As mentioned in this study, the RCP 4.5 is a scenario of intermediate mitigation, with a lower concentration of greenhouse gases in the atmosphere than the RCP 8.5 scenario. The RCP8.5 is the most pessimistic scenario, with more radiative forcing per square meter. Therefore, a lower impact was expected on the historical complementarity values of the analysed regions, due to climate change, in the RCP 4.5 scenario, and as presumed, for the whole period of analysis, the RCP4.5 scenario presents favourable results for the complementarities of the most pairs of regions. For the period of 2010 – 2040, 84% of the cases show no change or even improve their complementarity. For 2041 – 2070 and 2071-2100 the numbers were 78% and 73%, respectively. This means that for the last period of the projection only five pairs of hotspots had their complementarities negatively impacted (WIND_VE_A03 & WIND_BR_A05, SOLAR_BR_A03 & WIND_BR_A01, SOLAR_ES_A01 & WIND_AR_A01, SOLAR_VE_A03 & WIND_EC_A01, WIND_SU_A01 & WIND_BR_A04).

In this study the RCP8.5 scenario shows high impacts on the historical complementarities in the last period of the projection (2041-2010), 85% of the cases analysed show a decrease in the seasonal complementarities. For the period of 2040-2070, the decrease was in 37% of cases and 16% in the period of 2010-2040. Additionally, in the RCP8.5 scenario there were two special cases whose complementarities change to a positive correlation (SOLAR_BR_A03 & WIND_BR_A01 and WIND_PE_A01 & WIND_CO_A02) the first one in the period of 2071-2100 and the second one in the period of 2010-2040. It happens because the intra-annual behaviour of the resources for WIND_BR_A01 and WIND_CO_A02 undergo a strong variation.

The results of this study show strong negative impacts on the complementarities in the projection of the last analysed period. However, it is possible to see the results of both scenarios as an incentive for renewable energy investment in LA since, as far as this study can indicate, global climate change should not have a severe impact in the complementarity of most of the current potential areas to be integrated, until 2070.

Therefore, investors and energy planners should carefully evaluate the expansion of wind and solar power in those hotspots, especially if these areas are expected to benefit from the current complementarity by planning a future integration. Despite these cases, the study shows that climate change does not seem to be a barrier to the present and future development and integration of renewable energy sources in Latin America's energy matrix.

06.

References

- Adger, W. N., 2003. Social capital, collective action, and adaptation to climate change. Economic Geography 79 (4), 387–404.
- ALLEY, W. M., 2001. Ground water and climate. Grounwater, v. 39, n.2, p.161.
- ARCC – African and Latin American Resilience to Climate Change Project (2014). “A review of downscaling methods for climate change projections”.
- Barthelmie RJ, Murray F, Pryor SC. The economic benefit of short-term forecasting for wind energy in the UK electricity market. Energy Policy 2008;36(5):1687–96.
- Bartók, B. 2010. Changes in solar energy availability for south-eastern Europe with respect to global warming. Physics and Chemistry of the Earth, Parts A/B/C; 35(1-2), 63-69.
- Blanco MI. The economics of wind energy. Renewable and Sustainable Energy Reviews 2009;13:1372–82.
- Brooks, N., Adger, W. N., Kelly, P. M., 2005. The determinants of vulnerability and adaptive capacity at the national level and the implications for adaptation. Global Environmental Change Part A 15 (2), 151–163.
- Burnett, D., Barbour, E., Harrison, G. P. 2014. The UK solar energy resource and the impact of climate change. Renewable Energy 71, 333-343
- CEPAL- Comisión Económica para América Latina y el Caribe. La economía del cambio climático en Centroamérica. Dos casos de impactos potenciales en la generación de hidroelectricidad. , Serie Técnica 2012. [S.l: s.n.], 2012.

- CHIEW, F.H.S., 2006. Estimation of rainfall elasticity of streamflow in Australia. Hydrological Sciences Journal, v.51, n.4, p.613-625.

- Christensen JH, et al. Regional climate projections. In: Solomon S, et al., editors. Climate change 2007: the physical science basis. Contribution of Working Group I to the fourth assessment report of the intergovernmental panel on climate change. Cambridge, United Kingdom and New York, NY, USA: Cambridge University Press; 2007.

- Chou, Sin Chan ; Lyra, André ; Mourão, Caroline ; Dereczynski, Claudine ; Pilotto, Isabel ; Gomes, Jorge ; Bustamante, Josiane ; Tavares, Priscila ; Silva, Adan ; Rodrigues, Daniela ; Campos, Diego ; Chagas, Diego ; Sueiro, Gustavo ; Siqueira, Gracielle ; Nobre, Paulo ; Marengo, José . Evaluation of the Eta Simulations Nested in Three Global Climate Models. American Journal of Climate Change, v. 03, p. 438-454, 2014a. http://dx.doi.org/10.4236/ajcc.2014.35039

- Chou, Sin Chan ; Lyra, André ; Mourão, Caroline ; Dereczynski, Claudine ; Pilotto, Isabel ; Gomes, Jorge ; Bustamante, Josiane ; Tavares, Priscila ; Silva, Adan ; Rodrigues, Daniela ; Campos, Diego ; Chagas, Diego ; Sueiro, Gustavo ; Siqueira, Gracielle ; Marengo, José . Assessment of Climate Change over South America under RCP 4.5 and 8.5 Downscaling Scenarios. American Journal of Climate Change, v. 03, p. 512-527, 2014b. http://dx.doi.org/10.4236/ajcc.2014.35043

- Collins, W.J., N. Bellouin, M. Doutriaux-Boucher, N. Gedney, T. Hinton, C. D. Jones, S. Liddicoat, G. Martin, F. O'Connor, J. Rae, C. Senior, I. Totterdell, S. Woodward, T. Reichler, J. Kim, 2011. Development and evaluation of an Earth-System model – HadGEM2. Geosci. Model Dev., 4, 1051–1075.

- Ciscar, J. C., Dowling, P. 2014. Integrated assessment of climate impacts and adaptation in the energy sector. Energy Economics 46, 531–538.

- Contreras-Lisperguer, R., Cuba, K. 2008. THE POTENTIAL IMPACT OF CLIMATE CHANGE ON THE ENERGY SECTOR IN THE CARIBBEAN REGION: An effort to understand how climate change may impact the productivity of existing and future energy production systems in the Caribbean. Department of Sustainable Development, Organization of American States.

- Crook, J. A., Jones, L. A., Forster, P. M., Crook, R. 2011. Climate change impacts on future photovoltaic and concentrated solar power energy output. Energy Environ. Sci. 4, 3101.

- Cutforth, H. W., Judiesch, D. 2007. Long-term changes to incoming solar energy on the Canadian Prairie. Agricultural and Forest Meteorology 145, 167-175

- Dekker JWM, Pierik JTG. European wind turbine standards II, vol. ECN-C-99- 073. Petten: ECN Solar and Wind Energy; 1999.

- Denman KL, Brasseur G, Chidthaisong A, Ciais P, Cox PM, Dickinson RE, Hauglustaine D, Heinze C, Holland E, Jacob D, Lohmann U, Ramachandran S, da Silva Dias PL, Wofsy SC, Zhang X. Couplings between changes in the climate system and biogeochemistry. In: Solomon S, Qin D, Manning M, Chen Z, Marquis M, Averyt KB, Tignor M, Miller HL, 2007. Climate Change 2007: The physical science basis. Contribution of working group I to the fourth assessment report of the intergovernmental panel on climate change. Cambridge University Press, Cambridge, United Kingdom and New York, NY, USA.

- DNV/Risø. Guidelines for the design of wind turbines, 2nd ed., Copenhagen, Denmark: Jydsk cetraltrykkeri; 2002. p. 286.

- European Wind Energy Association. Wind energy. The facts. A guide to the technology, economics and future ofwind power. London: Earthscan; 2009. p. 568.

- ENES – European Network for Earth System modelling. 2016. Available at: https://verc.enes.org/models/earthsystem-models/metoffice-hadley-centre/hadgem2-es. Accessed on: 29 Nov. 2016.

- Fant, C., Schlosser, C. A., Strzepek, K. 2016. The impact of climate change on wind and solar resources in southern Africa. Applied Energy 161, 556–564

- Flato, G., J. Marotzke, B. Abiodun, P. Braconnot, S.C. Chou, W. Collins, P. Cox, F. Driouech, S. Emori, V. Eyring, C. Forest, P. Gleckler, E. Guilyardi, C. Jakob, V. Kattsov, C. Reason and M. Rummukainen, 2013: Evaluation of Climate Models. In: Climate Change 2013: The Physical Science Basis. Contribution of Working Group I to the Fifth Assessment Report of the Intergovernmental Panel on Climate Change [Stocker, T.F., D. Qin, G.-K. Plattner, M. Tignor, S.K. Allen, J. Boschung, A. Nauels, Y. Xia, V. Bex and P.M. Midgley (eds.)]. Cambridge University Press, Cambridge, United Kingdom and New York, NY, USA.

- Frandsen S, Petersen EL. The importance of a good wind year to start on when building a wind farm. In: European wind energy conference 1993; 1993.

- Frandsen S. Turbulence and turbulence-generated fatigue loading in wind turbine clusters; Risø-R-1188(EN)) available from Risoe National Laboratory, Roskilde, Denmark (and online at; http://www.risoe.dk/rispubl/VEA/veapdf/ris-r-1188.pdf) 2007. p. 128.

- Garreaud, R. D. and Falvey, M. (2009). The coastal winds off western subtropical South America in future climate scenarios. International Journal of Climatology, 29(4), 543-554.

- Goubanova, K., Echevin, V., Dewitte, B., Codron, F., Takahashi, K., Terray, P., Vrac, M. Statistical downscaling of sea-surface wind over the Peru-Chile upwelling region: diagnosing the impact of climate change from the IPSL-CM4 model. Springer, 2010.

- GOURDJI, Sharon et al. Sustainable Development Opportunities at the Climate, Land, Energy, and Water Nexus in Nicaragua., n. 33 , 2014.

- Gunderson, I., Goyette, S., Gago-Silva, A., Quiquerez, L., Lehmann, A. 2014. Climate and land-use change impacts on potential solar photovoltaic power generation in the Black Sea region. Environmental Science & Policy (Article in press). ENVSCI-1356; No. of Pages 12

- Hasumi, H. (2007) CCSR Ocean Component Model (COCO), Version 4.0. CCSR Report, Centre for Climate System Research.

- Hau E. Wind turbines: fundamentals, technologies, application, economics. Birkha¨user; 2006.

- Hegerl GC, Zwiers FW, Braconnot P, Gillett NP, Luo Y, Marengo Orsini JA, Nicholls N, Penner JE, Stott PA. Under-standing and Attributing Climate Change. In: Solomon S, Qin D, Manning M, Chen Z, Marquis M, Averyt KB, Tignor M, Miller HL, 2007.Climate Change 2007: The Physical Science Basis. Contribution of Working Group I to the Fourth Assessment Report of the Intergovernmental Panel on Climate Change. Cambridge University Press, Cambridge, United Kingdom and New York, NY, USA.

- Hempel, S., Frieler, K., Warszawski, L., Schewe, J., Piontek, F., 2013. A trend-preserving bias correction – the ISI-MIP approach. ESDD 4: 49–92

- Hubbert MK. Energy resources of the Earth. Scientific American 1971;224:60–70.

- IDB, 2016.Vulnerabilidad al cambio climático de los sistemas de producción hidroeléctrica em Centroamérica y sus opciones de adaptación.

- IEC. International standard, IEC61400. Part 1. Safety requirements, 3rd edition, IEC, FDIS; 2005.

- INPE. (2007). Caracterização do clima atual e definição das alterações climáticas para o território brasileiro ao longo do Século XXI, Relatório No. 6: Mudanças Climáticas e Possíveis Alterações nos Biomas da América do Sul CPTEC. São Paulo, Brazil: INPE; 2007.

- IPCC (2007) Report of the 26th session of the IPCC., 2007. Bangkok. April 30–May. Intergovernmental Panel on Climate Change, Geneva, Switzerland

- IPCC - INTERGOVERNMENTAL PANEL ON CLIMATE CHANGE, 2013, Climate Change 2013: The Physical Science Basis. Contribution of Working Group I to the Fifth

- Assessment Report of the Intergovernmental Panel on Climate Change. Cambridge, Reino Unido e New York, NY, EUA. Cambridge University Press.

- IPCC, 2014: Climate Change 2014: Impacts, Adaptation, and Vulnerability. Summaries, Frequently Asked Questions, and Cross-Chapter Boxes. A Contribution of Working Group II to the Fifth Assessment Report of the Intergovernmental Panel on Climate Change [Field, C.B., V.R. Barros, D.J. Dokken, K.J. Mach, M.D. Mastrandrea, T.E. Bilir, M. Chatterjee, K.L. Ebi, Y.O. Estrada, R.C. Genova, B. Girma, E.S. Kissel, A.N. Levy, S. MacCracken,P.R. Mastrandrea, and L.L. White (eds.)]. World Meteorological Organization, Geneva, Switzerland, 190 pp.

- IPCC, 2014. Climate Change 2014: Impacts, Adaptation and Vulnerability. Summary for Policy Makers. Contributions of the Working Group II to the Fifth Assessment Report.

- IRENA – International Rnewable Energy Agency. Renewables in Latin America and the Caribbean, 2016. Available at: http://www.irena.org/DocumentDownloads/Publications/LAC_stats_highlights_2016.pdf Accessed on December, 2016.

- Kerkhoff, C; Künsch, H; Schär, C. 2014. Assessment of Bias Assumptions for Climate Models. American Meteorological Society. Vol. 27, pp. 6799–6818. DOI: http://dx.doi.org/10.1175/JCLI-D-13-00716.1

- Kougias, I., Szabó, S., Monforti-Ferrario, F., Huld, T. & Katalin Bódis, 2016. A methodology for optimization of the complementarity between small-hydropower plants and solar PV systems. Renewable Energy, 87, pp. 1023-1030.

- Kubik, M. L., Phil J. Coker, and C. Hunt., 2011. Using meteorological wind data to estimate turbine generation output: a sensitivity analysis." World Renewable Energy Congress-Sweden; 8-13 May; 2011; Linköping; Sweden. No. 057. Linköping University Electronic Press.

- KUNDZEWICZ, Z. W. et al., 2007. Freshwater resources and their management, Cambridge, UK, 173-210. Climate Change 2007: Impacts, Adaptation and Vulnerability. Contribution of Working Group II to the Fourth Assessment Report to the Intergovernmental Panel on Climate Change.

- KUNDZEWICZ, Z.W., et al., 2008. The implications of projected climate change for freshwater resources and t heir management. Hydrological Sciences Journal, v.53, n. February, p.3-10.

- Lucena, A.F.P, Szklo, A.S., Schaeffer, R. (2009). Renewable Energy in an Unpredictable and Changing Climate. Modern Energy Review v. 1, p. 22-25.

- Lucena, A.F.P., Szklo, A.S., Schaeffer, R. Souza, R.R., Borba, B.S.M.C., Costa, I.V.L., et al., 2009. The vulnerability of renewable energy to climate change in Brazil, Energy Policy, v.37, pp.879-889.

- LUCENA, A. F. P, SCHAEFFER, R., SOUZA, R. R.; BORBA, B. S. M. C.; COSTA, I. V. L., 2009. The vulnerability of renewable energy to climate change in Brazil, Energy Policy, v37, p. 879-889.

- LUCENA, A. F. P., 2010. Proposta metodológica para avaliação da vulnerabilidade às mudanças climáticas globais no setor hidrelétrico. Universidade Federal do Rio de Janeiro, 208 p.

- LUCENA, A. F. P.; SZKLO, A. S.; SCHAEFFER, R.; SORIA, R.; RODRIGUEZ, M.C., 2013. Amazonia Security Agenda. Strengthening the water, energy, food, and health security nexus in the region and beyond.

- Magrin, Graciela and others (2014), "Chapter 27. Central and South America", Climate Change 2014: Impacts, Adaptation, and Vulnerability. Part B: Regional Aspects. Contribution of Working Group II to the Fifth Assessment Report of the Intergovernmental Panel on Climate Change, V.R. Barros and others (eds.), Cambridge, Cambridge University Press.

- Marengo, J. A., et al., 2010. Cenários futuros sobre o clima no Brasil. Economia da Mudança do Clima no Brasil: Custos e Oportunidades. São Paulo: CPTEC/ INPE.

- Martin G. M., N. Bellouin, W. J. Collins, I. D. Culverwell, P. R. Halloran, S. C. Hardiman, T. J. Hinton, C. D. Jones, R. E. McDonald, A. J. McLaren, F. M. O'Connor, M. J. Roberts, J. M. Rodriguez, S. Woodward, M. J. Best, M. E. Brooks, A. R. Brown, N. Butchart, C. Dearden, H. Derbyshire, I. Dharssi, M. Doutriaux-Boucher, J. M. Edwards, P. D. Falloon, N. Gedney, L. J. Gray, H. T. Hewitt, M. Hobson, M. R. Huddleston, J. Hughes, S. Ineson, W. J. Ingram, P. M. James, T. C. Johns, C. E. Johnson, A. Jones, C. P. Jones, M. M. Joshi, A. B. Keen, S. Liddicoat, A. P. Lock,

A. V. Maidens, J. C. Manners, S. F. Milton, J. G. L. Rae, J. K. Ridley, A. Sellar, C. A. Senior, I. J. Totterdell, A. Verhoef, P. L. Vidale and A. Wiltshire. 2011. The HadGEM2 family of Met Office Unified Model climate configurations. Geosci. Model Dev., 4, 723–757.

- MAURER, E. P.; ADAM, J. C.; WOOD, A. W. Climate model based consensus on the hydrologic impacts of climate change to the Rio Lempa basin of Central America. Hydrology and Earth System Sciences v. 13, n. 2, p. 183–194 , 18 fev. 2009.

- Meehl, G. A., et al., 2007: The WCRP CMIP3 multimodel dataset —A new era in climate change research. Bull. Am. Meteorol. Soc., 88, 1383–1394.

- MET OFFICE – Climate prediction model: HadGEM2. Available at: http://www.metoffice.gov.uk/research/modelling-systems/unified-model/climate-models/hadgem2. Accessed on November, 2016.

- Moriarty P. Safety-factor calibration for wind turbine extreme loads. Wind Energy 2008; 11:601–12.

- Moss R., Babiker M., Brinkman S., Calvo E., Carter T., Edmonds J., Elgizouli I., Emori S., Erda L., Hibbard K. A., 2008. Towards new scenarios for analysis of emissions, climate change, impacts, and response strategies. IPCC Expert Meeting Report on New Scenarios. Intergovernmental Panel on Climate Change, Noordwijkerhout

- Moss, R. H., Edmonds, J. A., Hibbard, K. A., Manning, M. R., Rose, S. K., van Vuuren, D. P., Carter, T. R., Emori, S., Kainuma, M., Kram, T., 2010. The next generation of scenarios for climate change research and assessment. Nature 463, 747–756.

- MUKHEIBIR, Pierre. Potential consequences of projected climate change impacts on hydroelectricity generation. Climatic Change v. 121, n. 1, p. 67–78 , 3 nov. 2013.

- Nagelkerke, Nico JD. "A note on a general definition of the coefficient of determination." Biometrika 78.3 (1991): 691-692.

- NEMEC, J., & SCHAAKE, J., 1982. Sensitivity of water resource systems to climate variation. Hydrological Sciences Journal, 27(3), 327-343.

- Olsina F, Roscher M, Larisson C, Garces F. Short-term optimal wind power generation capacity in liberalized electricity markets. Energy Policy 2007;35(2):1257–73.

- Pereira, E. B., Martins, F. R., Pes, M. P., da Cruz Segundo, E. I. & Lyra, A. D. A. (2013). The impacts of global climate changes on the wind power density in Brazil. Renewable energy, 49, 107-110.

- POPESCU, I.; BRANDIMARTE, L.; PEVIANI, M. Effects of climate change over energy production in La Plata Basin. International Journal of River Basin Management v. 12, n. 4, p. 319–327 , 2 out. 2014.

- Pryor, S. C., Barthelmie, R. J. (2010). Climate change impacts on wind energy: A review. Renewable and sustainable energy reviews, 14(1), 430-437.

Reichler, T., and J. Kim, 2008: How Well Do Coupled Models Simulate Today's Climate? Bull. Amer. Meteor. Soc., 89, 303-311.

- SALATTI, E. et al., 2010. Estimativas da oferta de recursos hídricos no Brasil em cenários futuros de clima (2015-2100). São Paulo: Economia da Mudança do Clima no Brasil: Custos e Oportunidades.

- SCHAEFFER, R.; LUCENA, A. F.P.; BORBA, B. S. M. C.; NOGUEIRA, L. P. P.; FLEMING, F. P.; BOULAHYA, M.S., 2012. Energy sector vulnerability to climate change: a review. Energy Policy, v.38, n.1, p.1-12.

- Sekiguchi, M. and Nakajim, T. (2008) A k-Distribution-Based Radiation Code and Its Computational Optimization for an Atmospheric General Circulation Model. Journal of Quantitative Spectroscopy and Radiative Transfer, 109, 2779-2793. http://dx.doi.org/10.1016/j.jqsrt.2008.07.013

- SOITO, J.; FREITAS, M., 2011. Amazon and the expansion of hydropower in Brazil: Vulnerability, impacts and possibilities for adaptation to global climate change. Renewable and Sustainable Energy Reviews, v.15, n.6, p. 3165-3177.

- Stott, P.A., S. F. B. Tett, G. S. Jones, M. R. Allen, J. F. B. Mitchell, and G. J. Jenkins, 2000: External Control of 20th Century Temperature by Natural and Anthropogenic Forcings. Science, 290, 2133-2137.

- Takata, K., Emori, S. and Watanabe, T. (2003) Development of the Minimal Advanced Treatments of Surface Interaction and Runoff. Global and Planetary Change, 38, 209-222. http://dx.doi.org/10.1016/S0921-8181(03)00030-4

- Taylor, K. E., R. J. Stouffer, and G. A. Meehl, 2012: An overview of CMIP5 and the experiment design. Bull. Am. Meteorol. Soc., 93, 485–498.

- Toth, F. L., 2003. State of the art and future challenges for integrated environmental assessment. Integrated Assessment 4, 250–264.

- Tuller SE, Brett AC. The characteristics of wind velocity that favor the fitting of a Weibull distribution in wind speed analysis. Journal of Climate and Applied Meteorology 1984; 23:124–34.

- UNITED NATION. (2016). Compendium on methods and tools to evaluate impacts of, and vulnerability and adaptation to climate change. Available at: http://unfccc.int/2860.php. Accessed on: 18 Nov. 2016.

- van Vuuren, D. P., Edmonds, J., Kainuma, M., Riahi, K., Thomson, A., Hibbard, K., Hurtt, G. C., Kram, T., Krey, V., Lamarque, J.F., Matsui, T., Meinshausen, M., Nakicenovic, N., Smith, S. J., Rose, S. K., 2011. Representative concentration pathways: an overview. Climatic Change, 109, 5–31

- van Vuuren, D. P., Isaac, M., Kundzewicz, Z. W., Arnell, N., Barker, T., Criqui, P., Berkhout, F., Hilderink, H., Hinkel, J., Hof, A., Kitous, A., Kram, T., Mechler, R., Scrieciu, S., 2011a. The use of scenarios as the basis for combined assessment of climate change mitigation and adaptation. Global Environmental Change, 21, 575–591.

- van Vuuren, D. P., Riahi, K., Moss, R., Edmonds, J., Thomson, A., Nakicenovic, N., Kram, T., Berkhout, F., Swart, R., Janetos, A., Rose, S. K., Arnell, N., 2012. A proposal for a new scenario framework to support research and assessment in different climate research communities Global Environmental Change, 22, 21–35

- Veers PS, Butterfield S. Extreme load estimation for wind turbines: issues and opportunities for improved practice. In: AIAA Aerospace Science Meeting; 2001.

- Watanabe, M., Suzuki, T., O'ishi, R., Komuro, Y., Watanabe, S., Emori, S., et al. (2010) Improved Climate Simulation by MIROC5: Mean States, Variability, and Climate Sensitivity. Journal of Climate, 23, 6312-6335. http://dx.doi.org/10.1175/2010JCLI3679.1

- Wilby, R. L., Troni, J., Biot, Y., Tedd, L., Hewitson, B. C., Smith, D. M., & Sutton, R. T. (2009). "A review of climate risk information for adaptation and development planning." International Journal of Climatology 29(9), 1193-1215.

- Wild, M., Folini, D., Henschel, F., Fischer, N., Müller, B. 2015. Projections of long-term changes in solar radiation based on CMIP5 climate models and their influence on energy yields of photovoltaic systems. Solar Energy, 116, 12–24

- ZWAAN, et al., 2016. Energy technology roll- out for climate change mitigation: A multi-model study for Latin America. Energy Economics,v.56, p. 526-542.

07.

Appendices

7.1. Comparison between IDB database and GCMs simulation historical databases

This appendix presents the comparison between the equivalent year (seasonal pattern) of the IDB database and the equivalent year (seasonal pattern) of the GCMs historical simulation data for the areas that presented complementarity in the first report of this study.

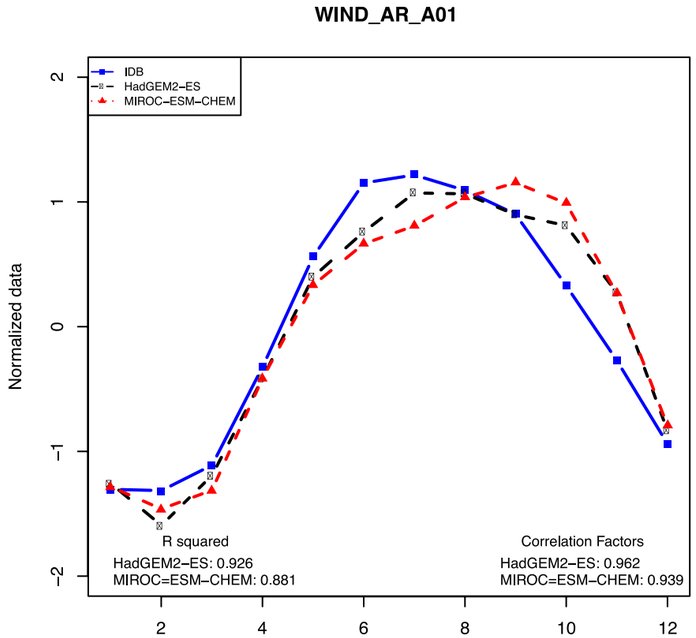
WIND_AR_A01
IDB
HadGEM2–ES
MIROC–ESM–CHEM
Normalized data
Month
R squared
HadGEM2–ES: 0.926
MIROC=ESM–CHEM: 0.881
Correlation Factors
HadGEM2–ES: 0.962
MIROC=ESM–CHEM: 0.939

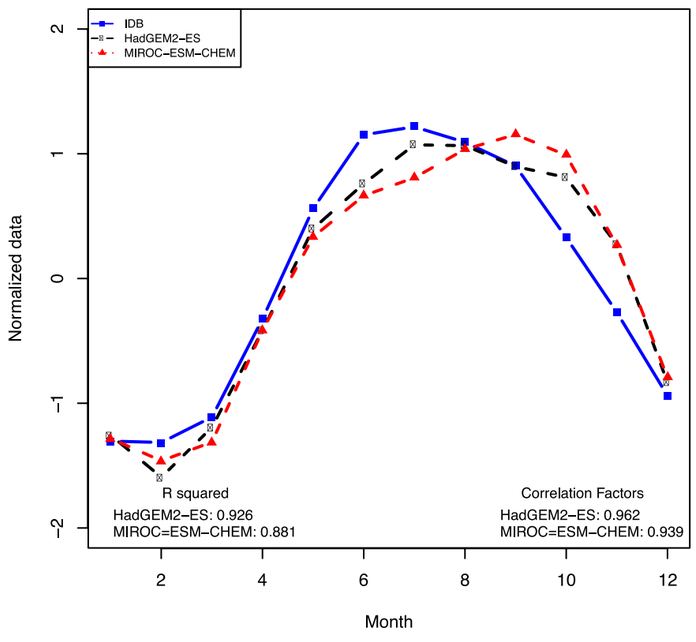
WIND_AR_A01
IDB
HadGEM2–ES
MIROC–ESM–CHEM
Normalized data
Month
R squared
HadGEM2–ES: 0.926
MIROC=ESM–CHEM: 0.881
Correlation Factors
HadGEM2–ES: 0.962
MIROC=ESM–CHEM: 0.939

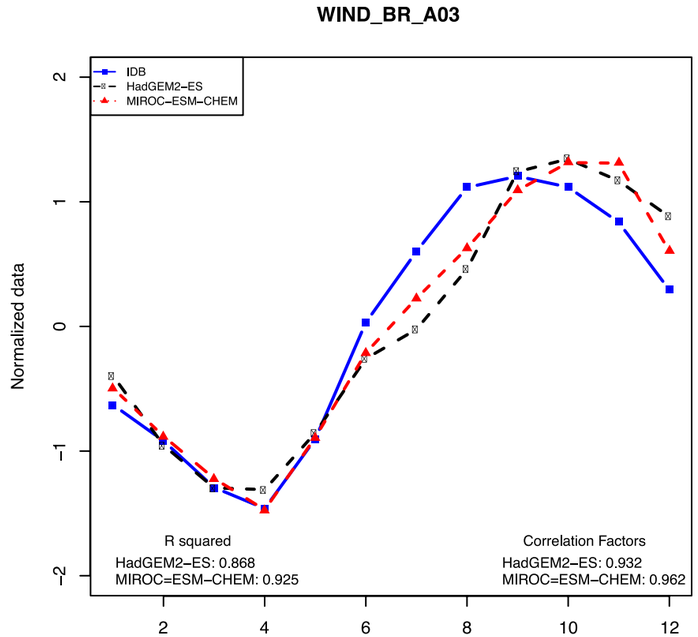
WIND_BR_A03
IDB
HadGEM2–ES
MIROC–ESM–CHEM
Normalized data
Month
R squared
HadGEM2–ES: 0.868
MIROC=ESM–CHEM: 0.925
Correlation Factors
HadGEM2–ES: 0.932
MIROC=ESM–CHEM: 0.962

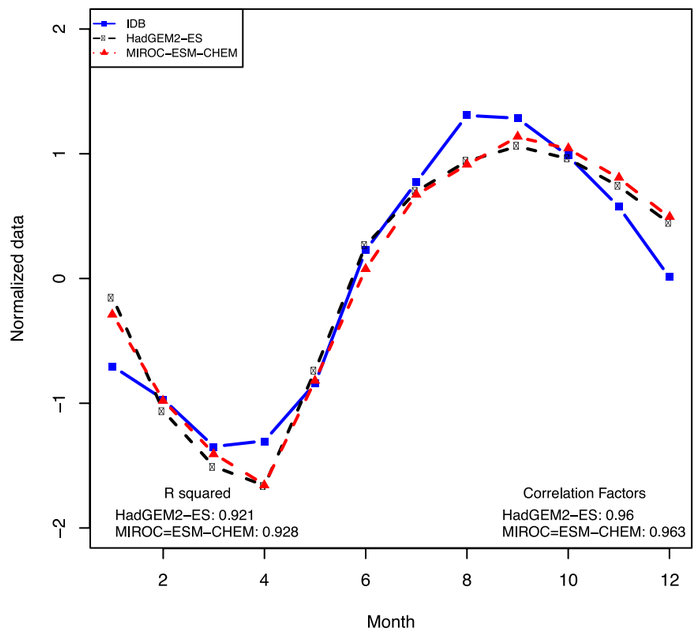
WIND_BR_A04
IDB
HadGEM2–ES
MIROC–ESM–CHEM
Normalized data
Month
R squared
HadGEM2–ES: 0.921
MIROC=ESM–CHEM: 0.928
Correlation Factors
HadGEM2–ES: 0.96
MIROC=ESM–CHEM: 0.963

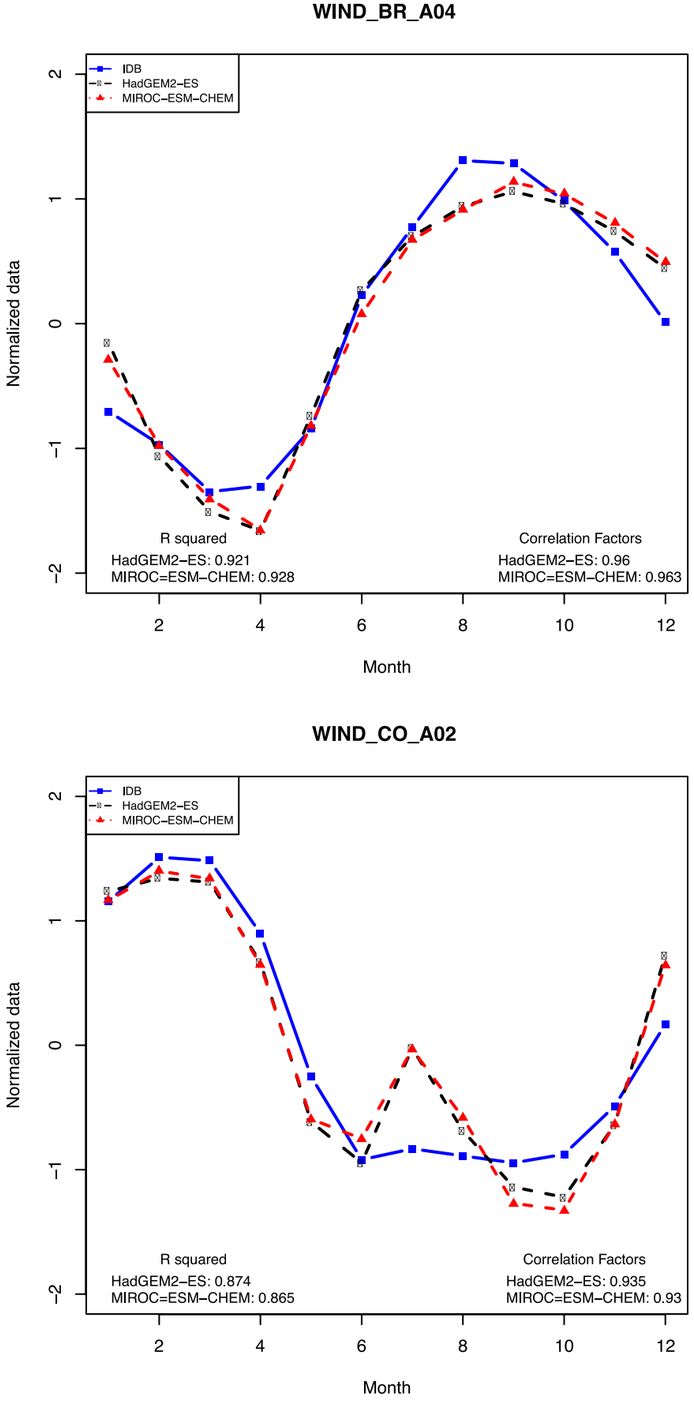
WIND_BR_A04
IDB
HadGEM2–ES
MIROC–ESM–CHEM
Normalized data
Month
R squared
HadGEM2–ES: 0.921
MIROC=ESM–CHEM: 0.928
Correlation Factors
HadGEM2–ES: 0.96
MIROC=ESM–CHEM: 0.963

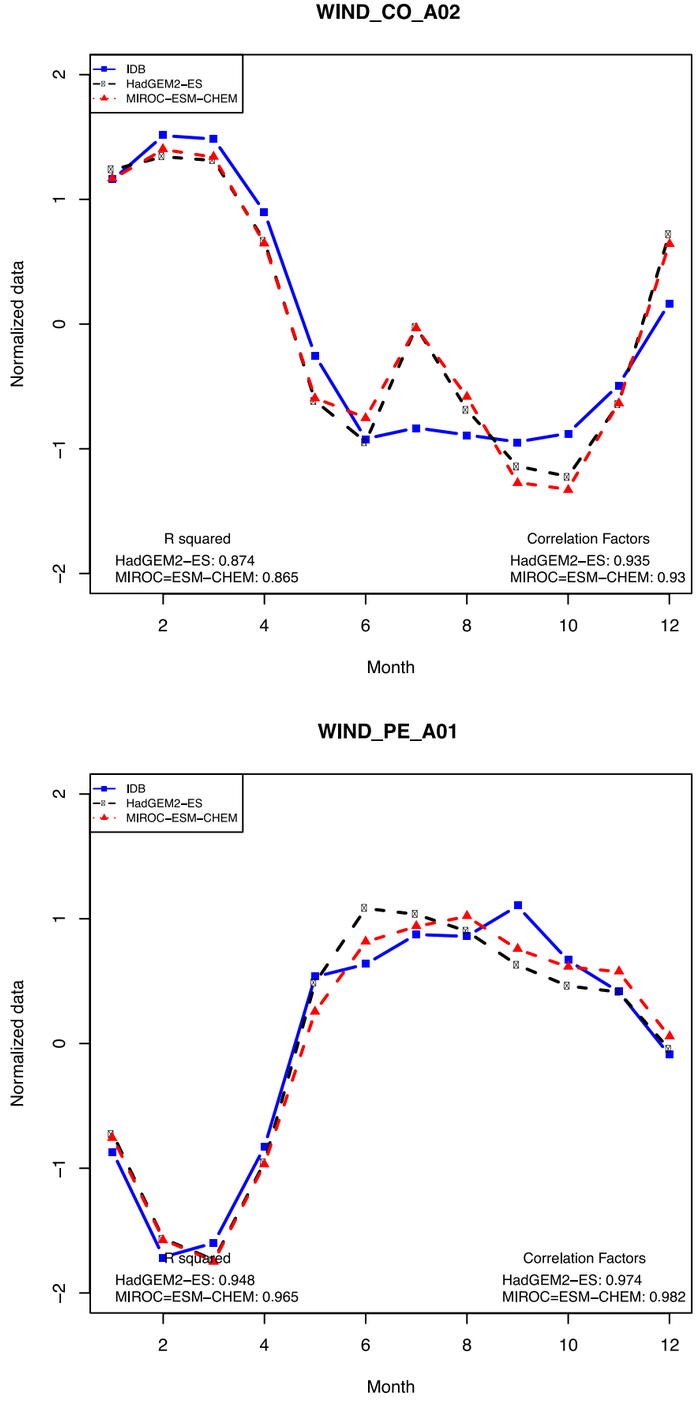
WIND_CO_A02
IDB
HadGEM2–ES
MIROC–ESM–CHEM
Normalized data
Month
R squared
HadGEM2–ES: 0.874
MIROC=ESM–CHEM: 0.865
Correlation Factors
HadGEM2–ES: 0.935
MIROC=ESM–CHEM: 0.93

WIND_CO_A02
IDB
HadGEM2–ES
MIROC–ESM–CHEM
Normalized data
Month
R squared
HadGEM2–ES: 0.874
MIROC=ESM–CHEM: 0.865
Correlation Factors
HadGEM2–ES: 0.935
MIROC=ESM–CHEM: 0.93

WIND_PE_A01
IDB
HadGEM2–ES
MIROC–ESM–CHEM
Normalized data
Month
R squared
HadGEM2–ES: 0.948
MIROC=ESM–CHEM: 0.965
Correlation Factors
HadGEM2–ES: 0.974
MIROC=ESM–CHEM: 0.982

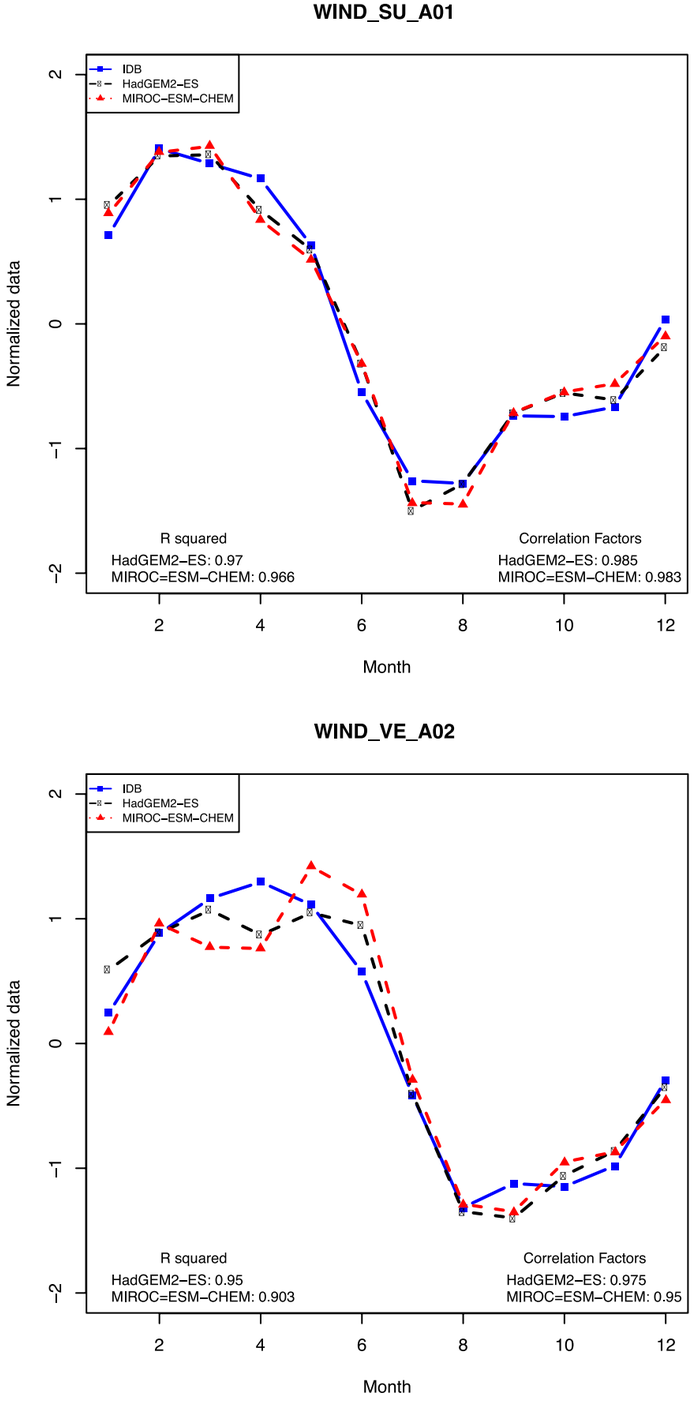
WIND_SU_A01
IDB
HadGEM2–ES
MIROC–ESM–CHEM
Normalized data
Month
R squared
HadGEM2–ES: 0.97
MIROC=ESM–CHEM: 0.966
Correlation Factors
HadGEM2–ES: 0.985
MIROC=ESM–CHEM: 0.983

WIND_VE_A02
IDB
HadGEM2–ES
MIROC–ESM–CHEM
Normalized data
Month
R squared
HadGEM2–ES: 0.95
MIROC=ESM–CHEM: 0.903
Correlation Factors
HadGEM2–ES: 0.975
MIROC=ESM–CHEM: 0.95

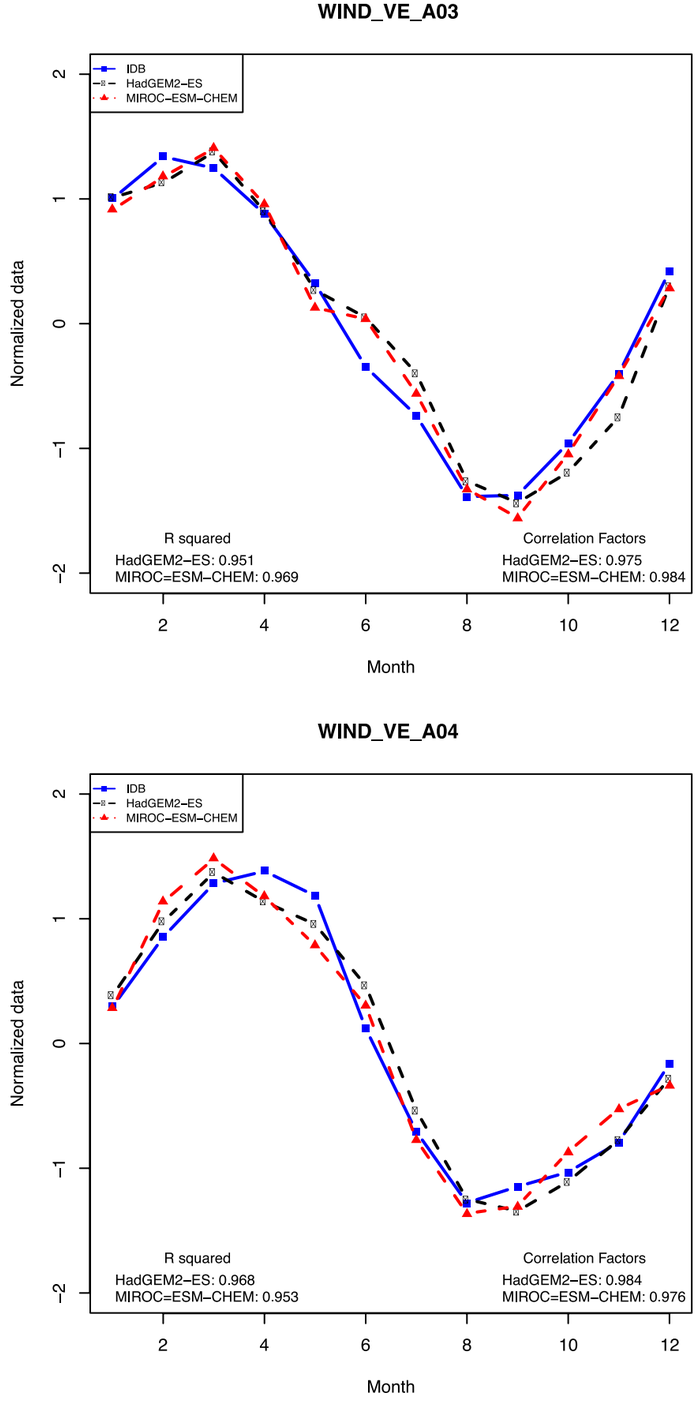
WIND_VE_A03
IDB
HadGEM2–ES
MIROC–ESM–CHEM
Normalized data
Month
R squared
HadGEM2–ES: 0.951
MIROC=ESM–CHEM: 0.969
Correlation Factors
HadGEM2–ES: 0.975
MIROC=ESM–CHEM: 0.984

WIND_VE_A04
IDB
HadGEM2–ES
MIROC–ESM–CHEM
Normalized data
Month
R squared
HadGEM2–ES: 0.968
MIROC=ESM–CHEM: 0.953
Correlation Factors
HadGEM2–ES: 0.984
MIROC=ESM–CHEM: 0.976

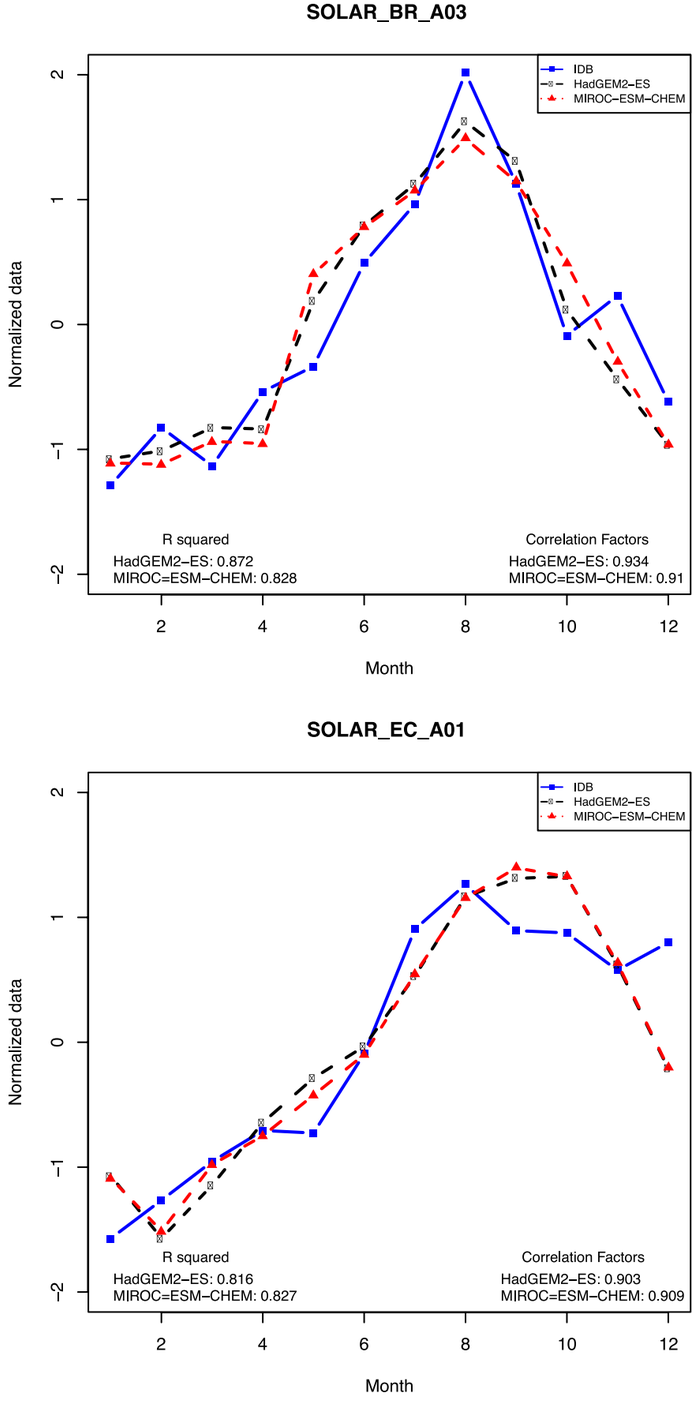
SOLAR_BR_A03
IDB
HadGEM2–ES
MIROC–ESM–CHEM
Normalized data
Month
R squared
HadGEM2–ES: 0.872
MIROC=ESM–CHEM: 0.828
Correlation Factors
HadGEM2–ES: 0.934
MIROC=ESM–CHEM: 0.91

SOLAR_EC_A01
IDB
HadGEM2–ES
MIROC–ESM–CHEM
Normalized data
Month
R squared
HadGEM2–ES: 0.816
MIROC=ESM–CHEM: 0.827
Correlation Factors
HadGEM2–ES: 0.903
MIROC=ESM–CHEM: 0.909

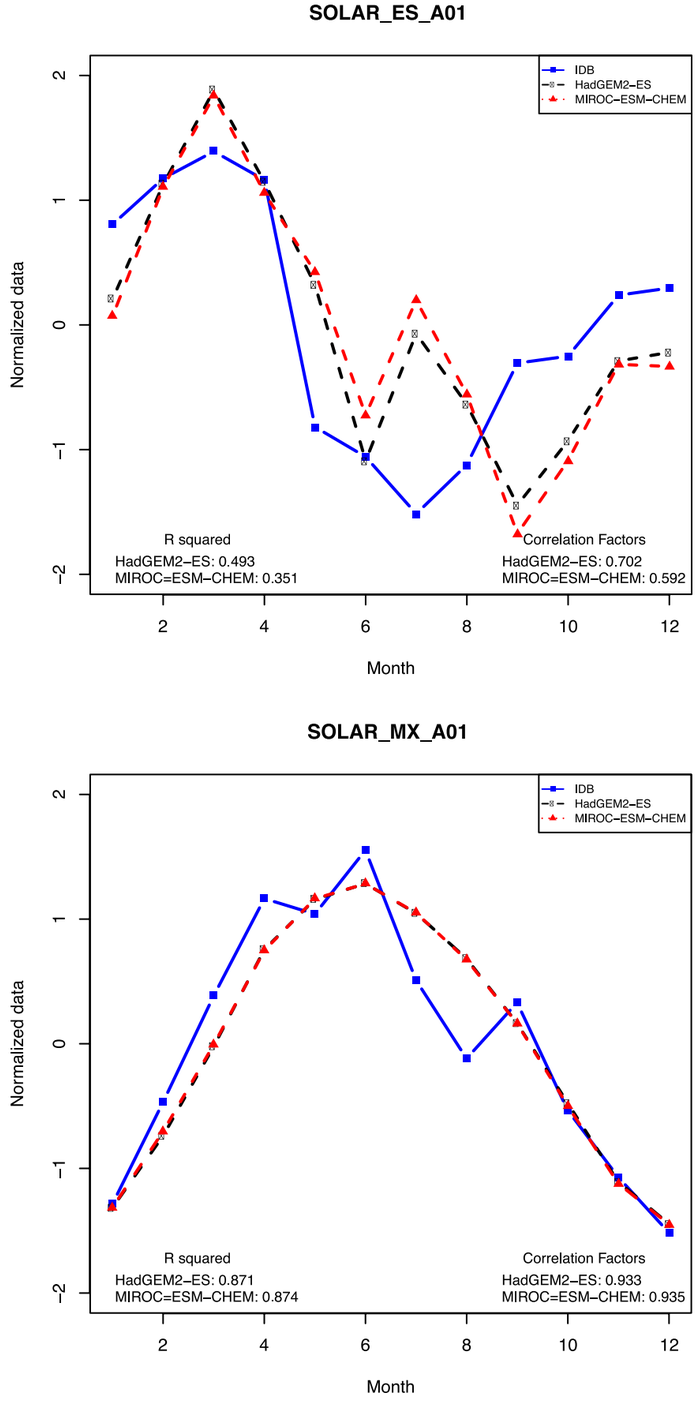
SOLAR_ES_A01
IDB
HadGEM2–ES
MIROC–ESM–CHEM
Normalized data
Month
R squared
HadGEM2–ES: 0.493
MIROC=ESM–CHEM: 0.351
Correlation Factors
HadGEM2–ES: 0.702
MIROC=ESM–CHEM: 0.592

SOLAR_MX_A01
IDB
HadGEM2–ES
MIROC–ESM–CHEM
Normalized data
Month
R squared
HadGEM2–ES: 0.871
MIROC=ESM–CHEM: 0.874
Correlation Factors
HadGEM2–ES: 0.933
MIROC=ESM–CHEM: 0.935

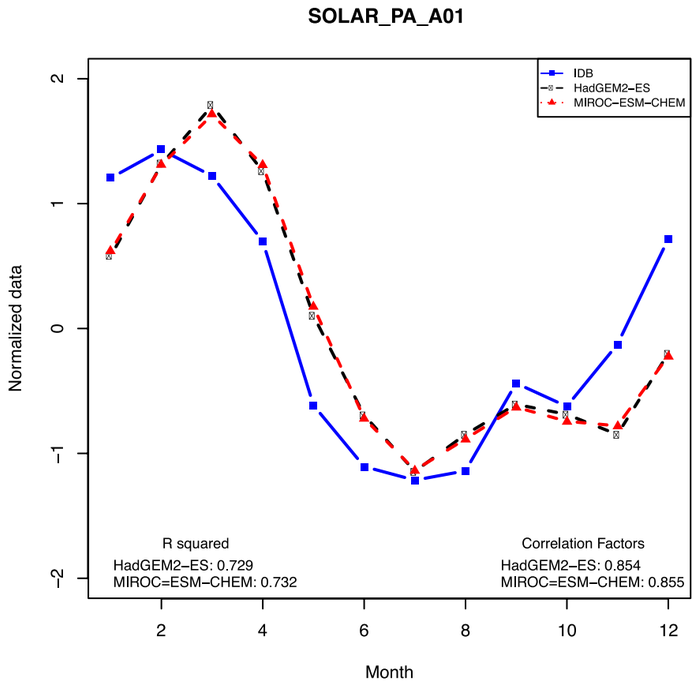

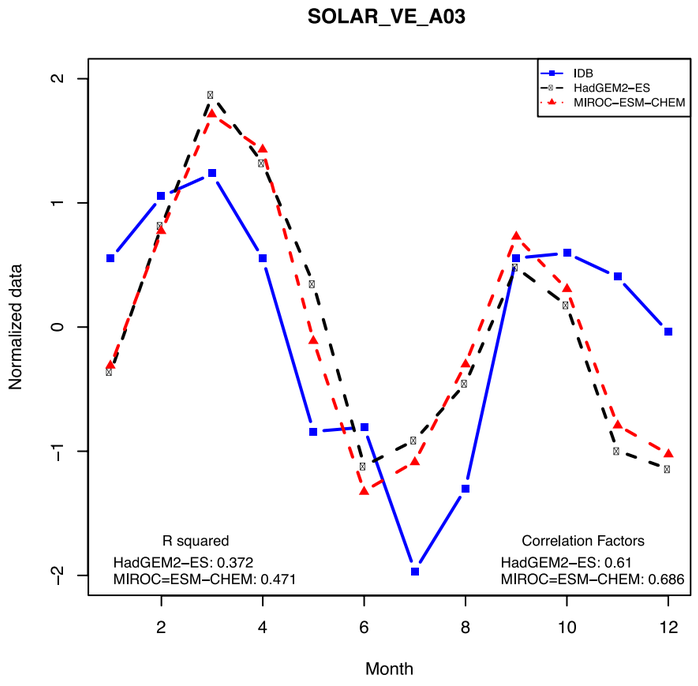

7.2. Climate Change Impact on Energy Complementarities based on HadGEM2-ES model

Based on the climate projections for the IDB database, the energy complementarity was re-evaluated between the areas that had complementary in the first report of this study. This appendix shows the impact of climate change in the renewable energy complementarity between the hotspots analyzed for 3 different periods of time: 2010-2040, 2041-2070, 2071-2100 and for two scenarios: RCP 4.5 and RCP8.5.

Climate Change Impact on Energy Complementarities based on HadGEM2-ES model and RCP 4.5 Scenario

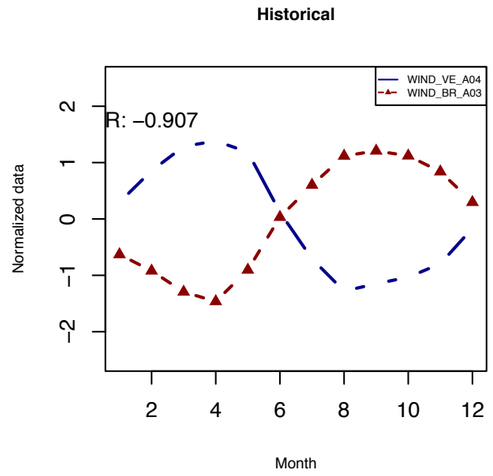

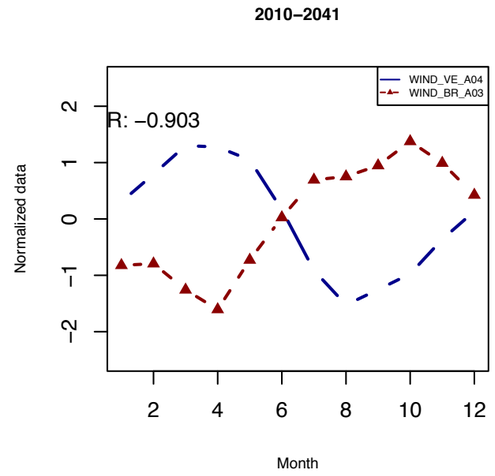

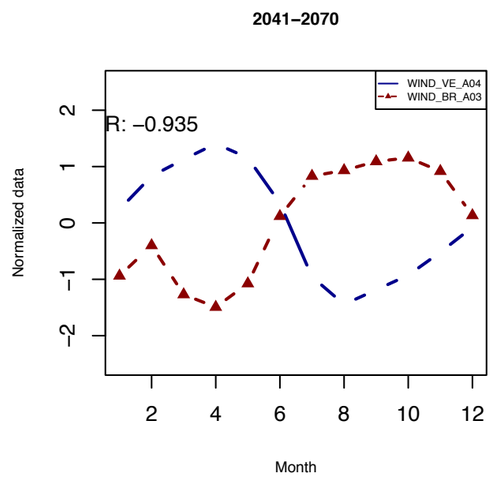

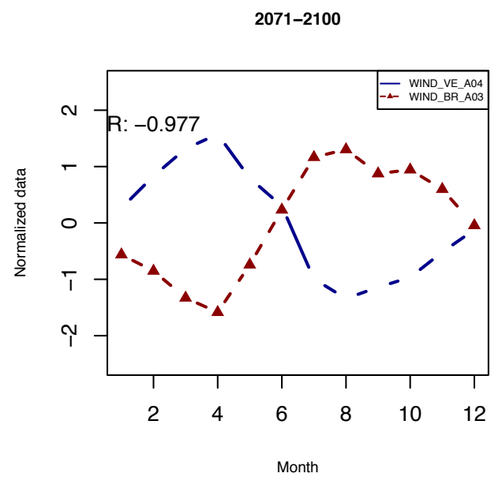

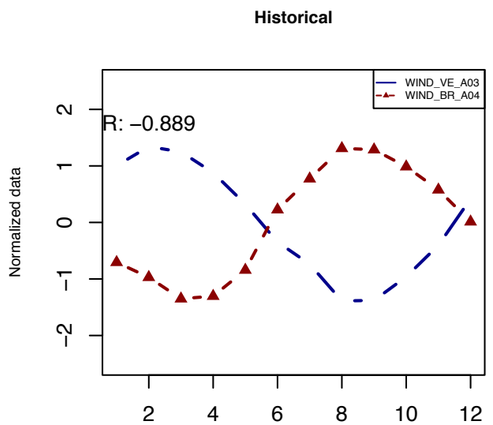
Historical
WIND_VE_A03
WIND_BR_A04
R: −0.889
Normalized data
Month

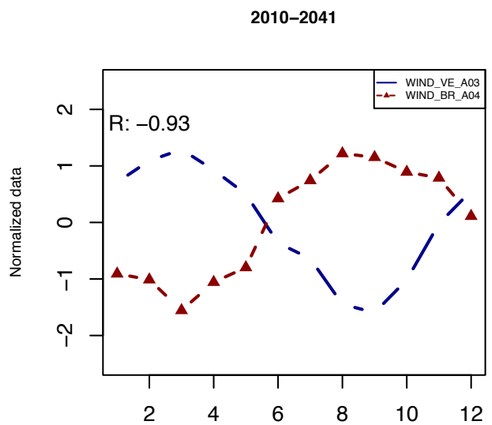
2010–2041
WIND_VE_A03
WIND_BR_A04
R: −0.93
Normalized data
Month

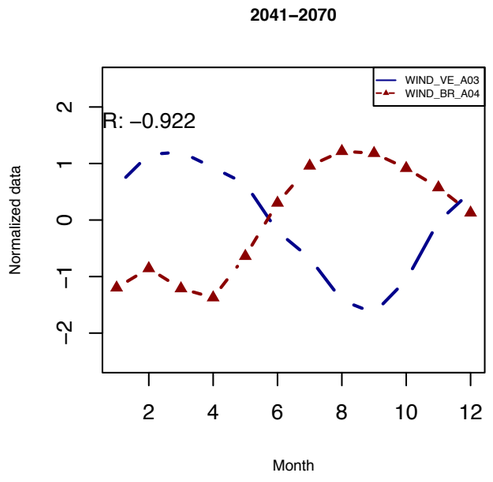
2041–2070
WIND_VE_A03
WIND_BR_A04
R: −0.922
Normalized data
Month

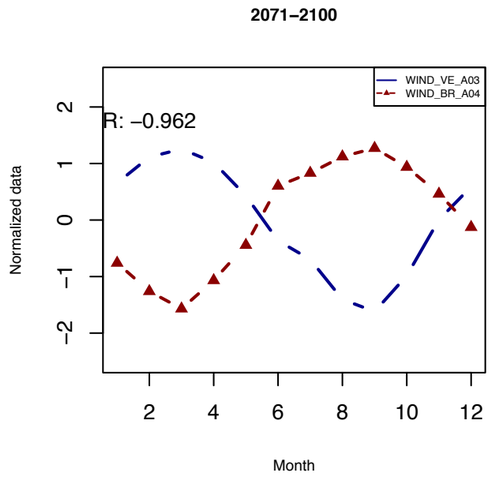
2071–2100
WIND_VE_A03
WIND_BR_A04
R: −0.962
Normalized data
Month

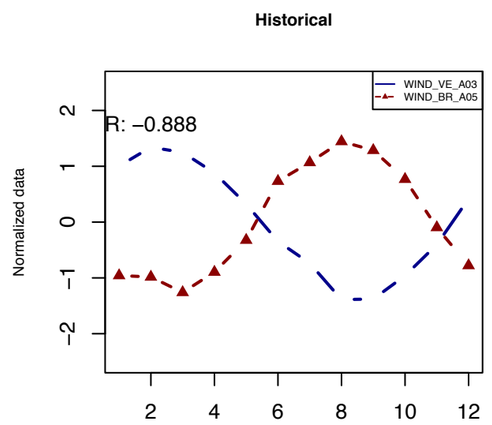
Historical
WIND_VE_A03
WIND_BR_A05
R: −0.888
Normalized data
Month

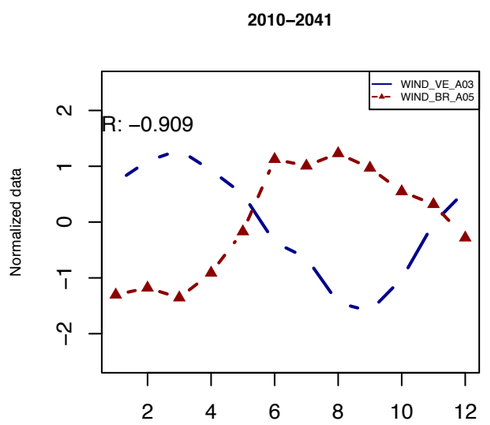
2010–2041
WIND_VE_A03
WIND_BR_A05
R: −0.909
Normalized data
Month

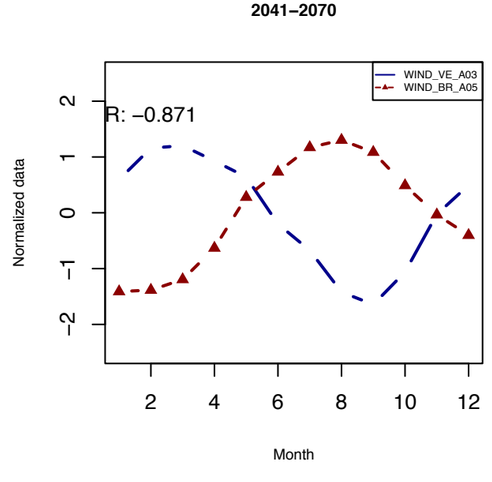
2041–2070
WIND_VE_A03
WIND_BR_A05
R: −0.871
Normalized data
Month

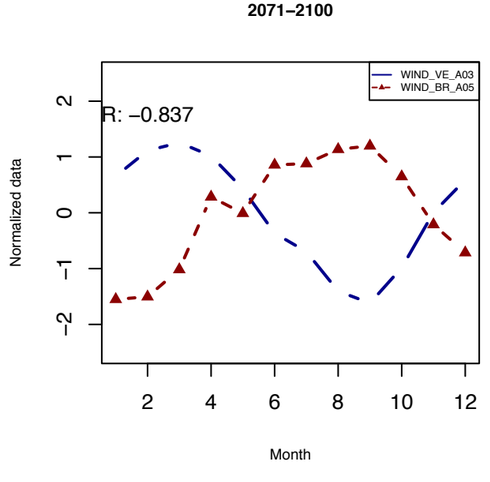
2071–2100
WIND_VE_A03
WIND_BR_A05
R: −0.837
Normalized data
Month

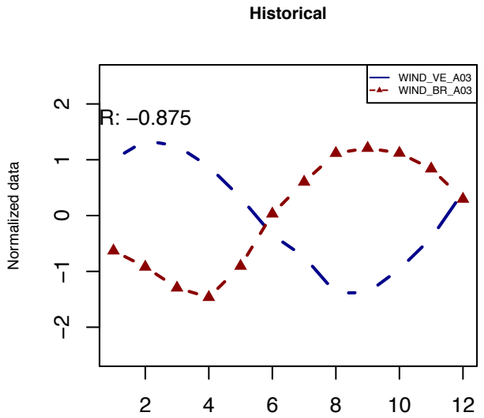
Historical
WIND_VE_A03
WIND_BR_A03
R: −0.875
Normalized data
Month

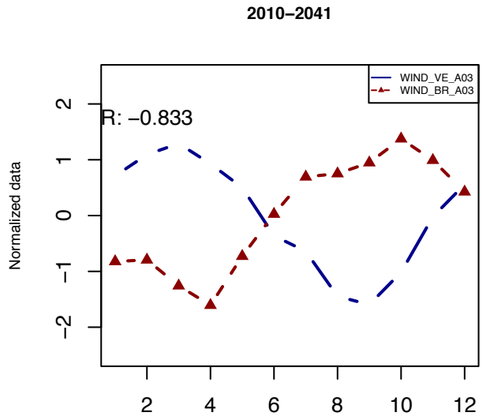
2010–2041
WIND_VE_A03
WIND_BR_A03
R: −0.833
Normalized data
Month

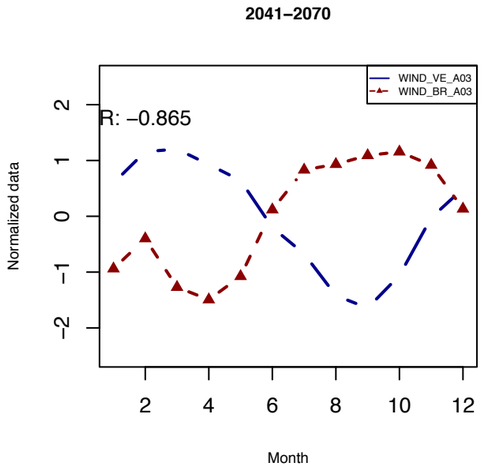
2041–2070
WIND_VE_A03
WIND_BR_A03
R: −0.865
Normalized data
Month

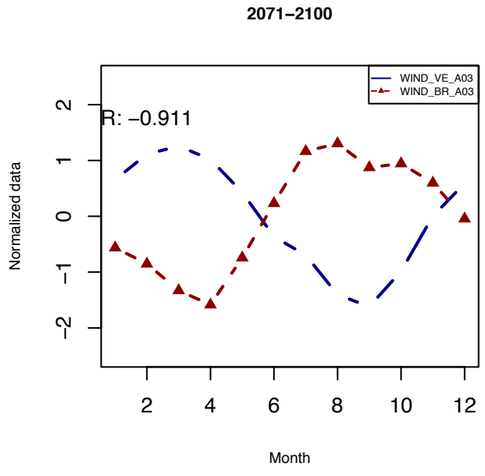
2071–2100
WIND_VE_A03
WIND_BR_A03
R: −0.911
Normalized data
Month

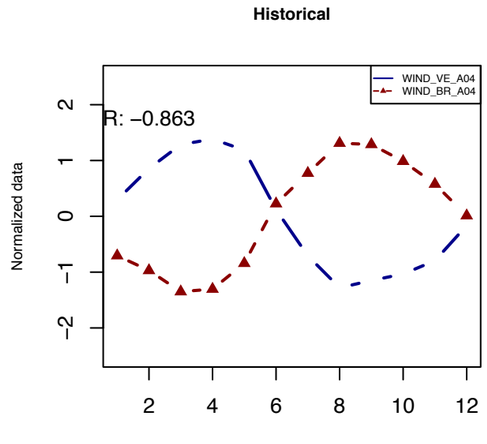
Historical
WIND_VE_A04
WIND_BR_A04
R: −0.863
Normalized data
Month

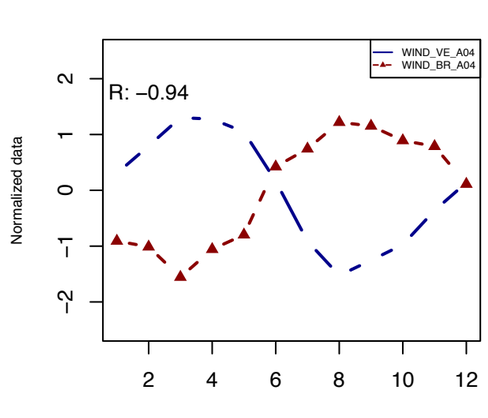
2010–2041
WIND_VE_A04
WIND_BR_A04
R: −0.94
Normalized data
Month

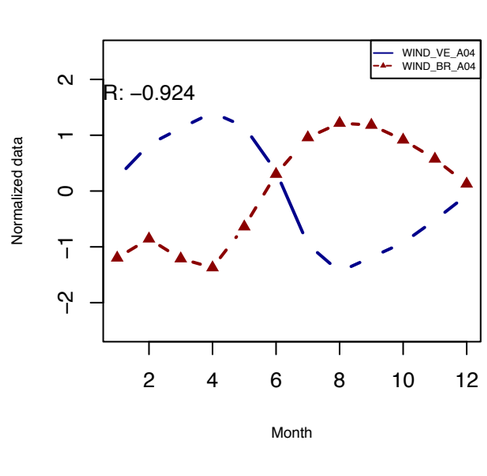
2041–2070
WIND_VE_A04
WIND_BR_A04
R: −0.924
Normalized data
Month

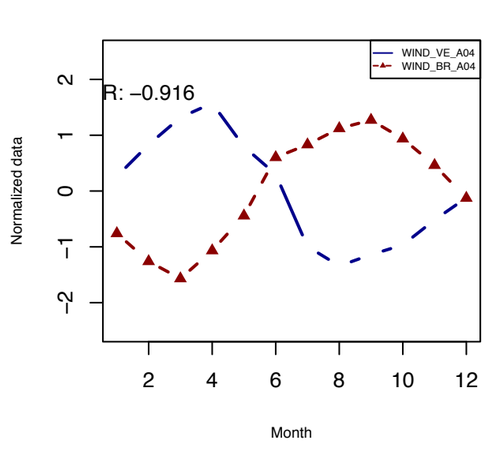
2071–2100
WIND_VE_A04
WIND_BR_A04
R: −0.916
Normalized data
Month

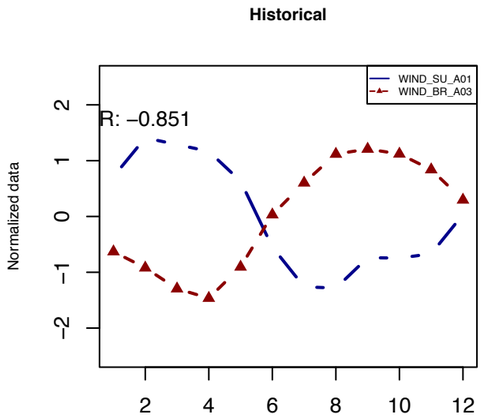
Historical
WIND_SU_A01
WIND_BR_A03
R: −0.851
Normalized data
Month

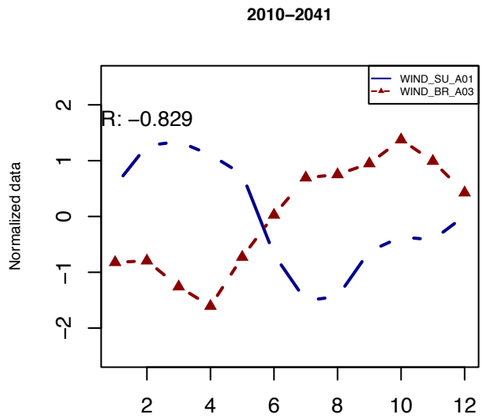
2010–2041
WIND_SU_A01
WIND_BR_A03
R: −0.829
Normalized data
Month

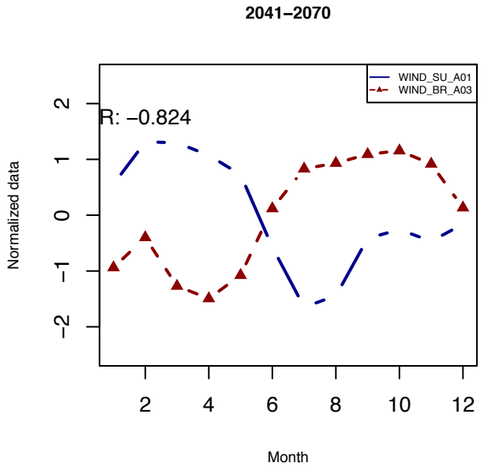
2041–2070
WIND_SU_A01
WIND_BR_A03
R: −0.824
Normalized data
Month

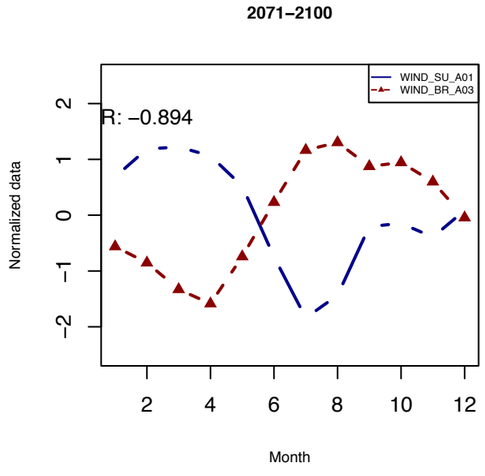
2071–2100
WIND_SU_A01
WIND_BR_A03
R: −0.894
Normalized data
Month

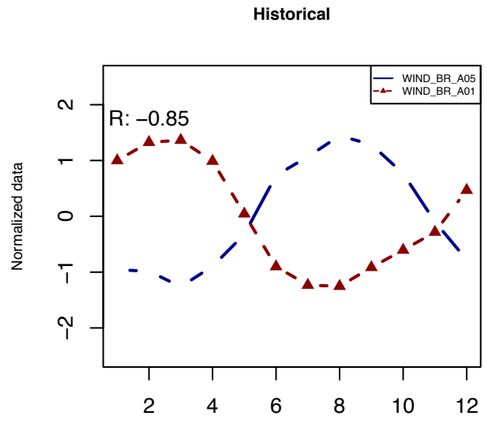
Historical
WIND_BR_A05
WIND_BR_A01
R: −0.85
Normalized data
Month

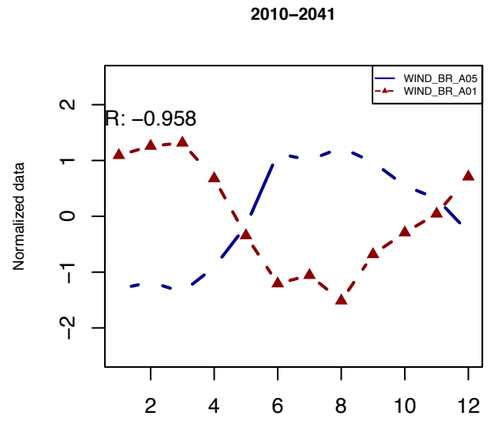
2010–2041
WIND_BR_A05
WIND_BR_A01
R: −0.958
Normalized data
Month

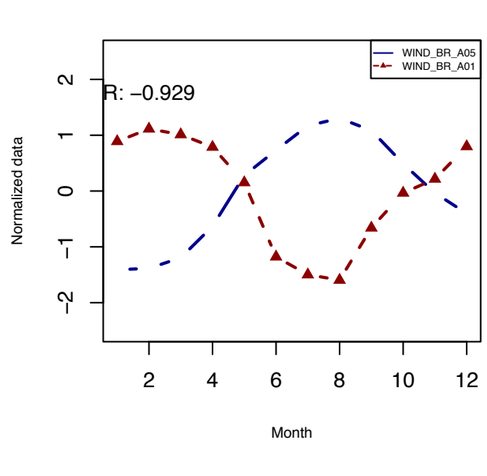
2041–2070
WIND_BR_A05
WIND_BR_A01
R: −0.929
Normalized data
Month

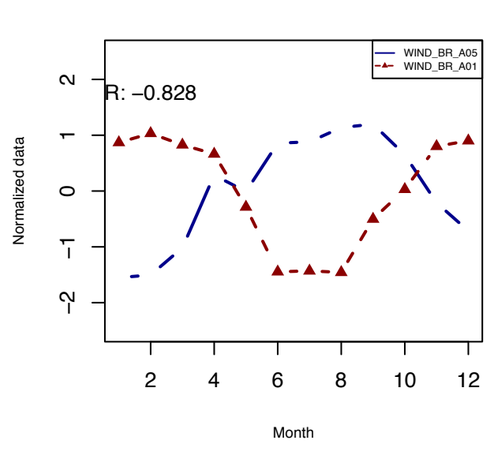
2071–2100
WIND_BR_A05
WIND_BR_A01
R: −0.828
Normalized data
Month

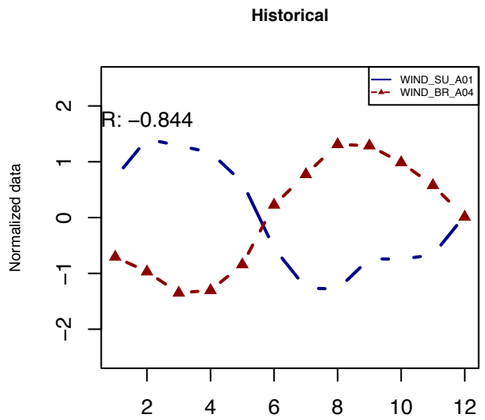
Historical
WIND_SU_A01
WIND_BR_A04
R: −0.844
Normalized data
Month

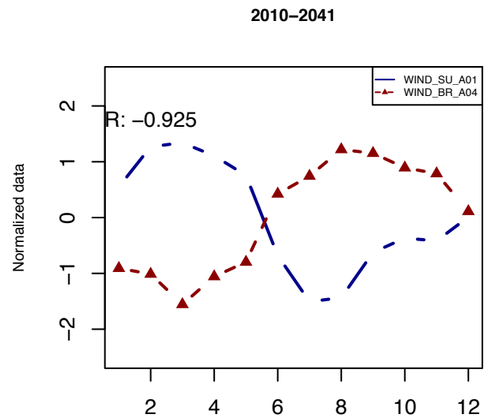
2010−2041
WIND_SU_A01
WIND_BR_A04
R: −0.925
Normalized data
Month

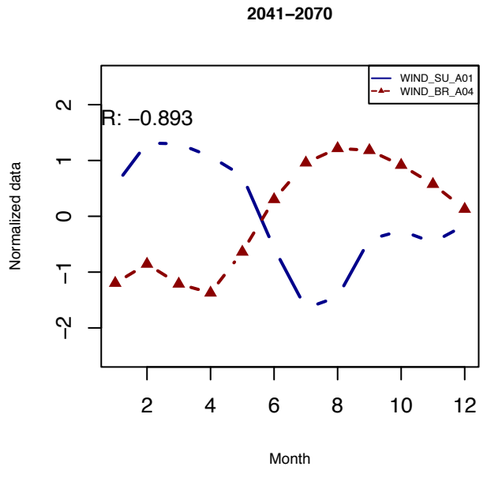
2041−2070
WIND_SU_A01
WIND_BR_A04
R: −0.893
Normalized data
Month

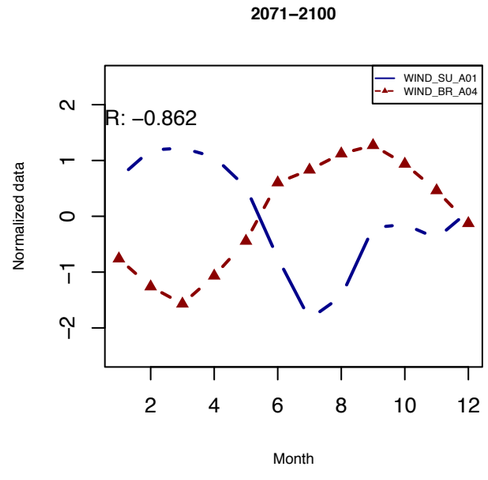
2071−2100
WIND_SU_A01
WIND_BR_A04
R: −0.862
Normalized data
Month

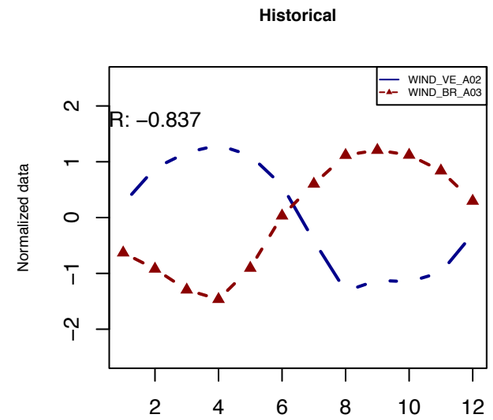
Historical
WIND_VE_A02
WIND_BR_A03
R: −0.837
Normalized data
Month

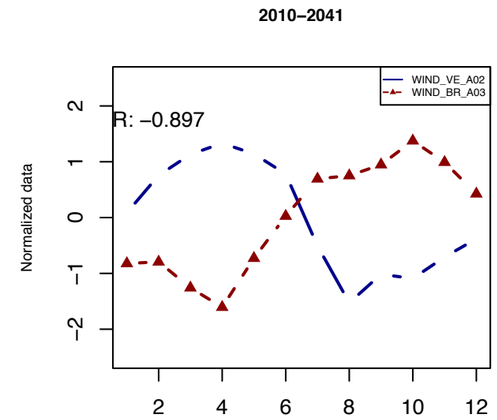
2010−2041
WIND_VE_A02
WIND_BR_A03
R: −0.897
Normalized data
Month

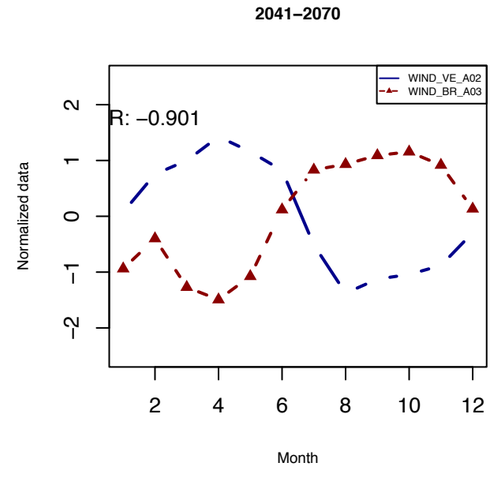
2041−2070
WIND_VE_A02
WIND_BR_A03
R: −0.901
Normalized data
Month

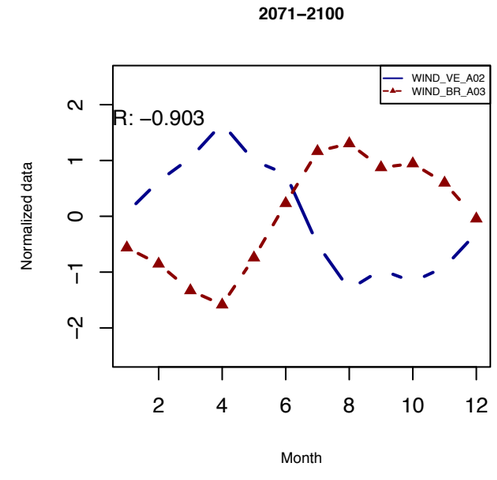
2071−2100
WIND_VE_A02
WIND_BR_A03
R: −0.903
Normalized data
Month

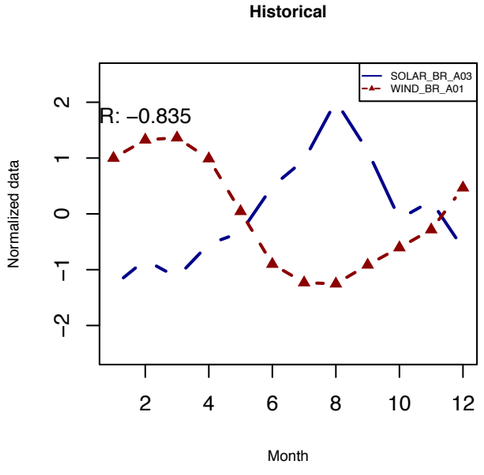
Historical
SOLAR_BR_A03
WIND_BR_A01
R: −0.835
Normalized data
Month

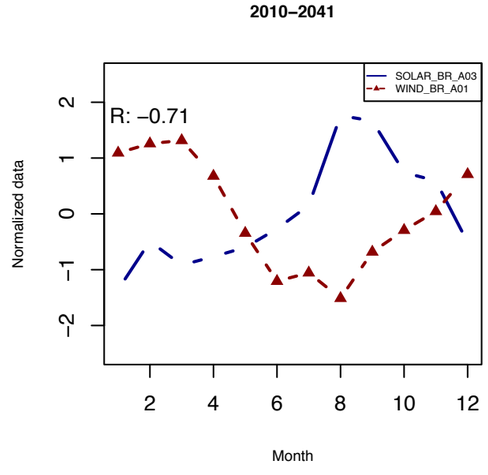
2010–2041
SOLAR_BR_A03
WIND_BR_A01
R: −0.71
Normalized data
Month

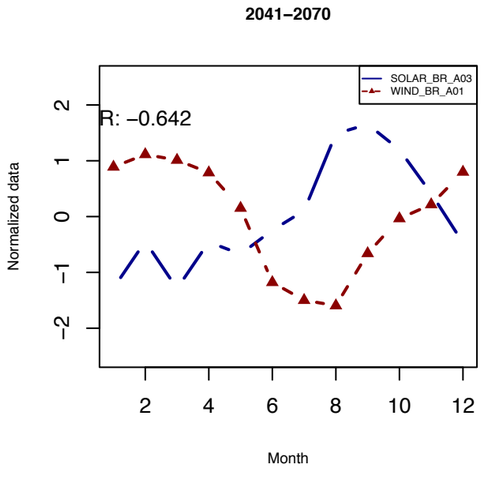
2041–2070
SOLAR_BR_A03
WIND_BR_A01
R: −0.642
Normalized data
Month

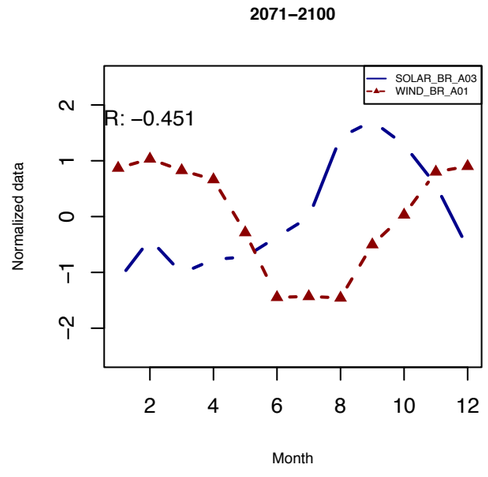
2071–2100
SOLAR_BR_A03
WIND_BR_A01
R: −0.451
Normalized data
Month

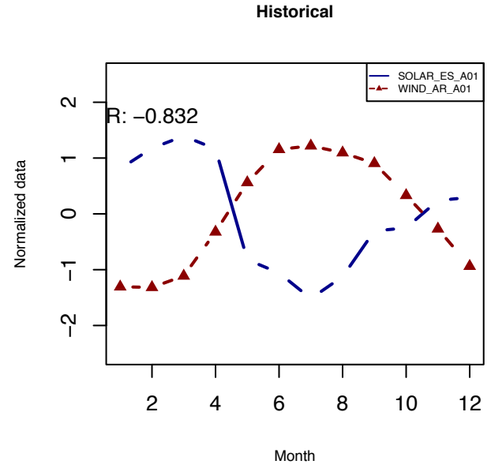
Historical
SOLAR_ES_A01
WIND_AR_A01
R: −0.832
Normalized data
Month

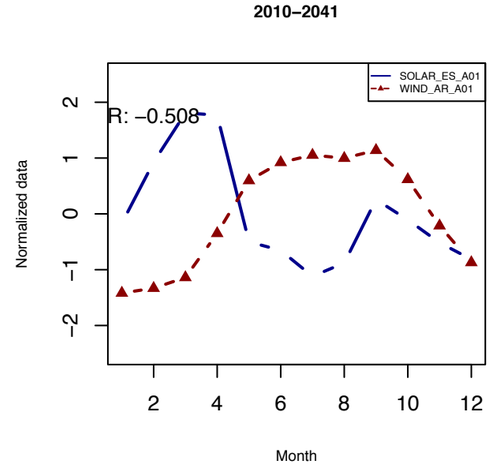
2010–2041
SOLAR_ES_A01
WIND_AR_A01
R: −0.508
Normalized data
Month

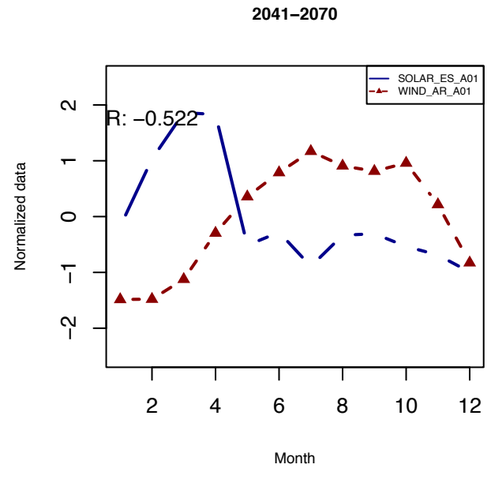
2041–2070
SOLAR_ES_A01
WIND_AR_A01
R: −0.522
Normalized data
Month

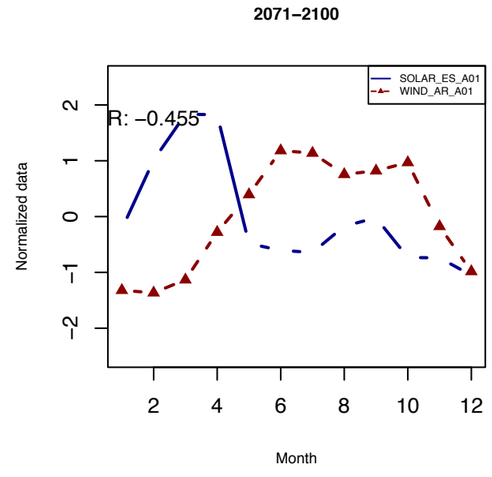
2071–2100
SOLAR_ES_A01
WIND_AR_A01
R: −0.455
Normalized data
Month

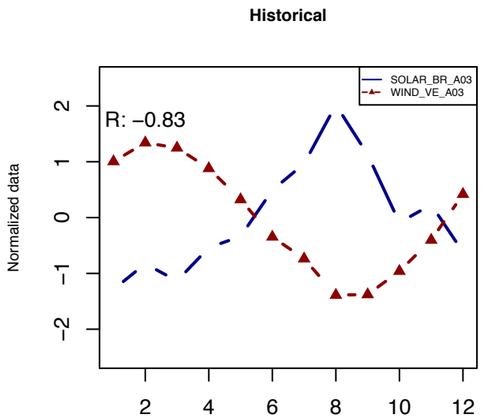
Historical
SOLAR_BR_A03
WIND_VE_A03
R: −0.83
Normalized data
Month

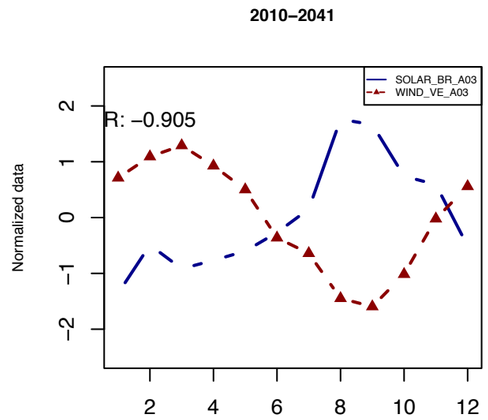
2010−2041
SOLAR_BR_A03
WIND_VE_A03
R: −0.905
Normalized data
Month

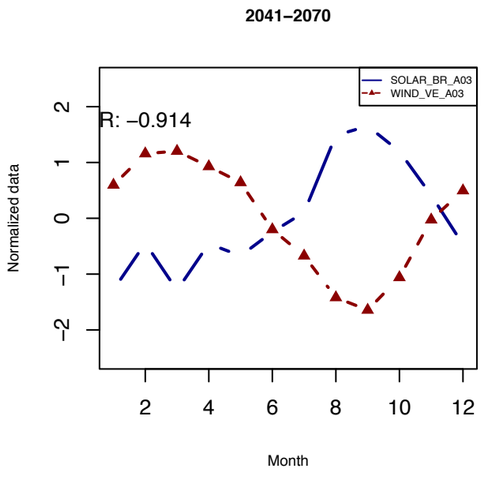
2041−2070
SOLAR_BR_A03
WIND_VE_A03
R: −0.914
Normalized data
Month

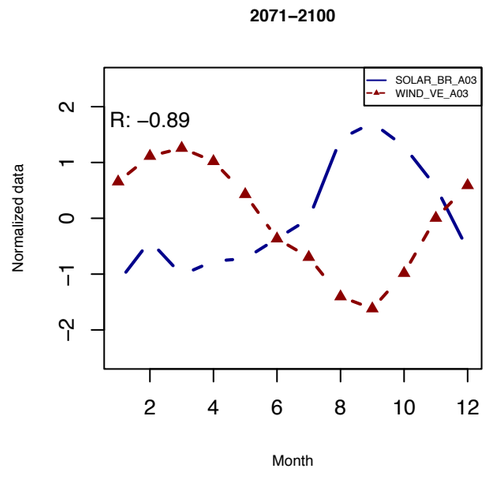
2071−2100
SOLAR_BR_A03
WIND_VE_A03
R: −0.89
Normalized data
Month

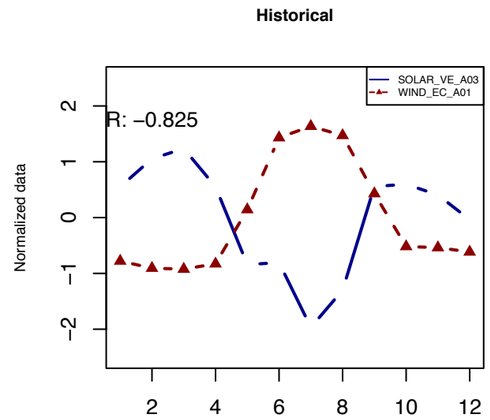
Historical
SOLAR_VE_A03
WIND_EC_A01
R: −0.825
Normalized data
Month

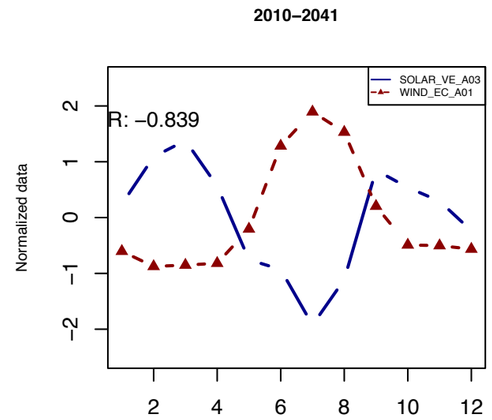
2010−2041
SOLAR_VE_A03
WIND_EC_A01
R: −0.839
Normalized data
Month

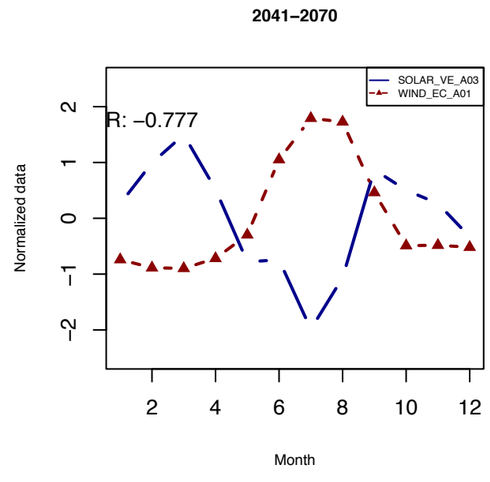
2041−2070
SOLAR_VE_A03
WIND_EC_A01
R: −0.777
Normalized data
Month

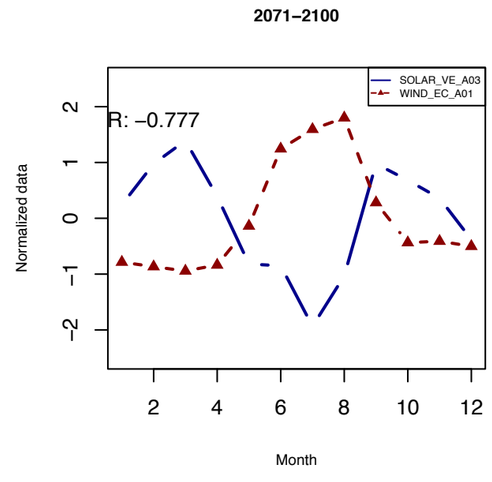
2071−2100
SOLAR_VE_A03
WIND_EC_A01
R: −0.777
Normalized data
Month

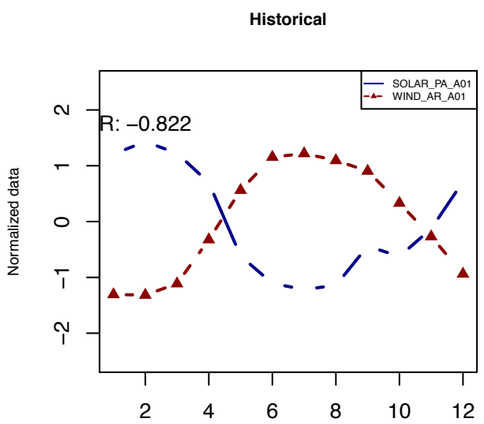
Historical
SOLAR_PA_A01
WIND_AR_A01
R: −0.822
Normalized data
Month

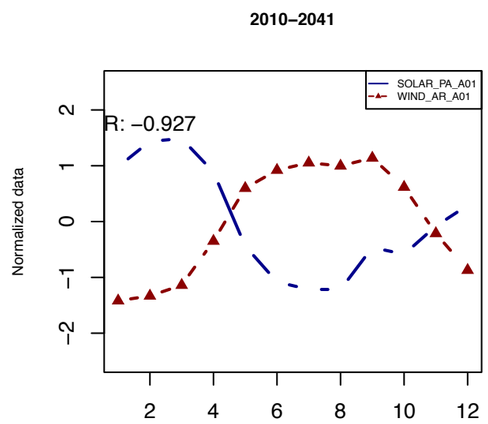
2010–2041
SOLAR_PA_A01
WIND_AR_A01
R: −0.927
Normalized data
Month

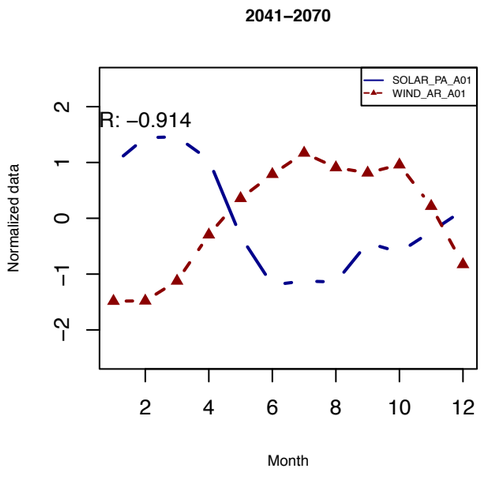
2041–2070
SOLAR_PA_A01
WIND_AR_A01
R: −0.914
Normalized data
Month

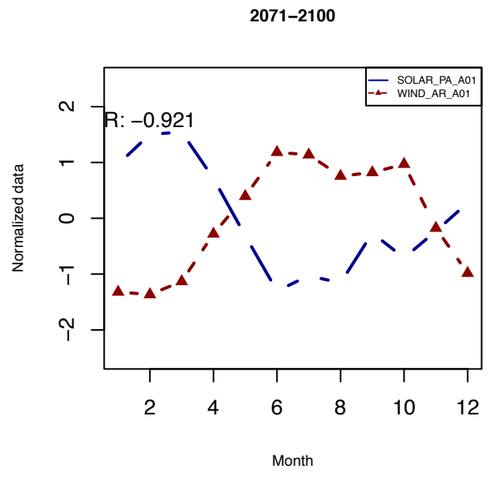
2071–2100
SOLAR_PA_A01
WIND_AR_A01
R: −0.921
Normalized data
Month

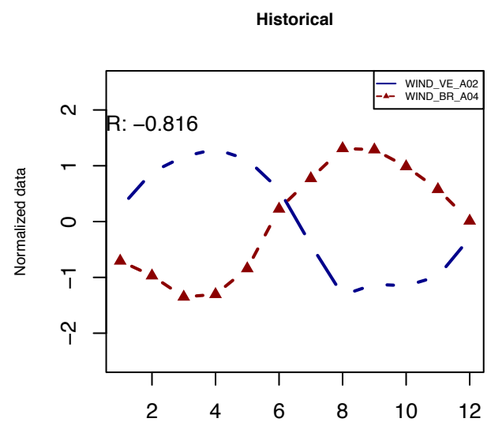
Historical
WIND_VE_A02
WIND_BR_A04
R: −0.816
Normalized data
Month

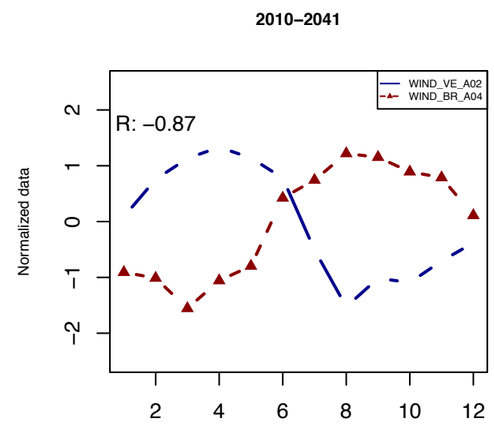
2010–2041
WIND_VE_A02
WIND_BR_A04
R: −0.87
Normalized data
Month

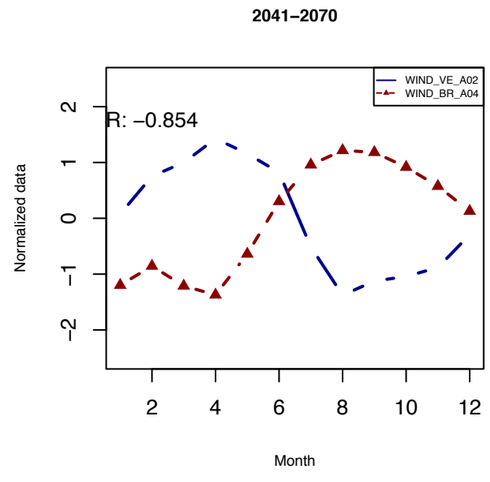
2041–2070
WIND_VE_A02
WIND_BR_A04
R: −0.854
Normalized data
Month

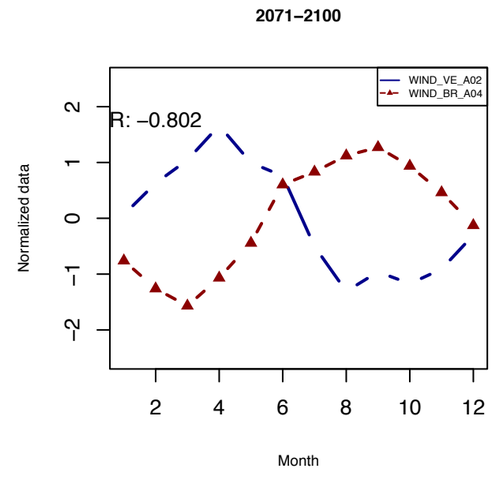
2071–2100
WIND_VE_A02
WIND_BR_A04
R: −0.802
Normalized data
Month

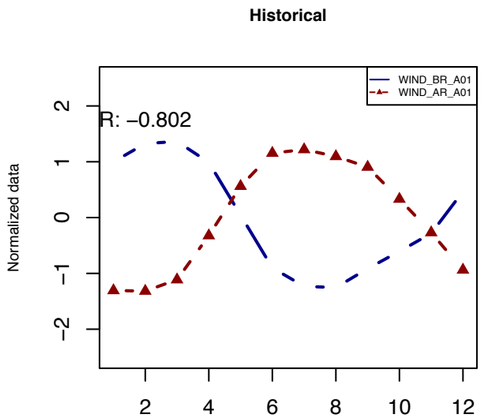
Historical
WIND_BR_A01
WIND_AR_A01
R: −0.802
Normalized data
Month

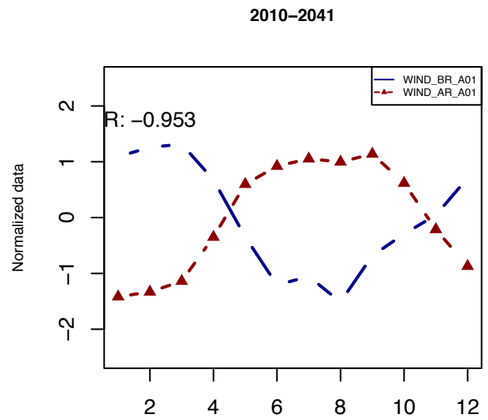
2010−2041
WIND_BR_A01
WIND_AR_A01
R: −0.953
Normalized data
Month

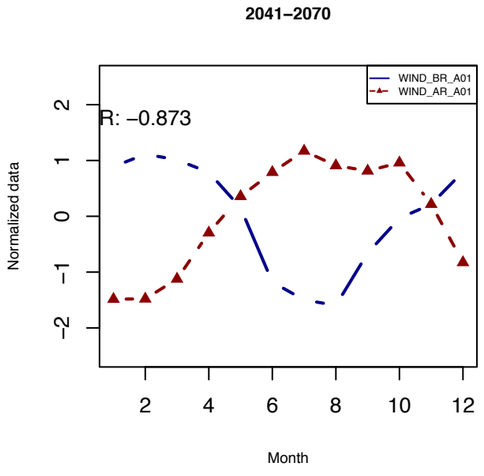
2041−2070
WIND_BR_A01
WIND_AR_A01
R: −0.873
Normalized data
Month

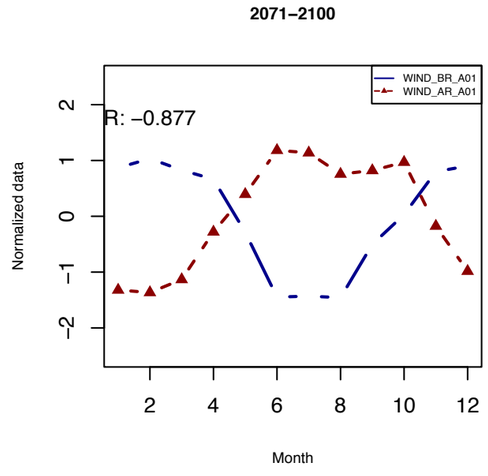
2071−2100
WIND_BR_A01
WIND_AR_A01
R: −0.877
Normalized data
Month

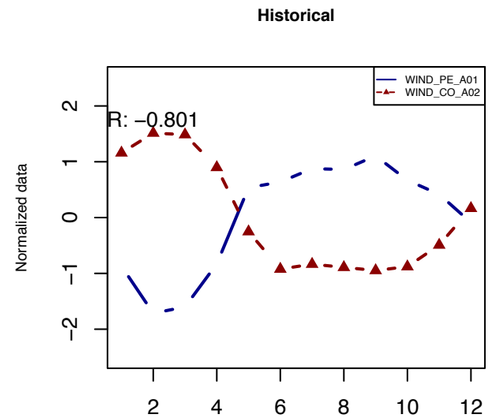
Historical
WIND_PE_A01
WIND_CO_A02
R: −0.801
Normalized data
Month

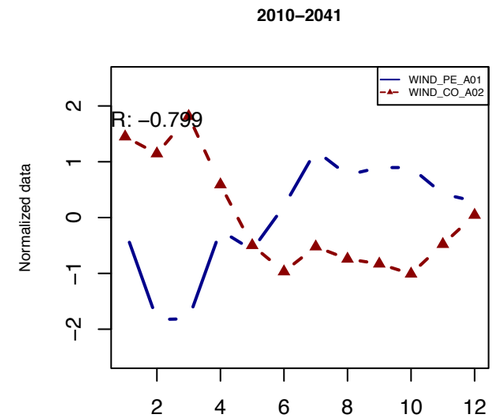
2010−2041
WIND_PE_A01
WIND_CO_A02
R: −0.799
Normalized data
Month

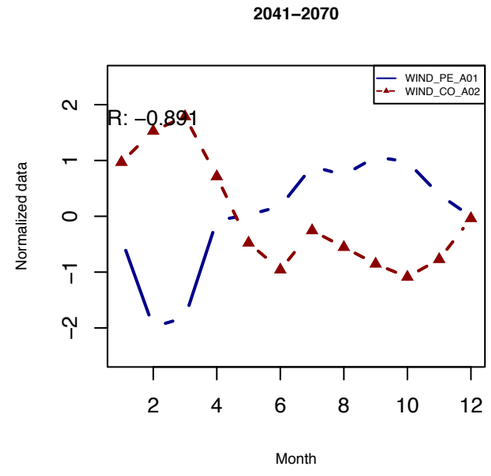
2041−2070
WIND_PE_A01
WIND_CO_A02
R: −0.891
Normalized data
Month

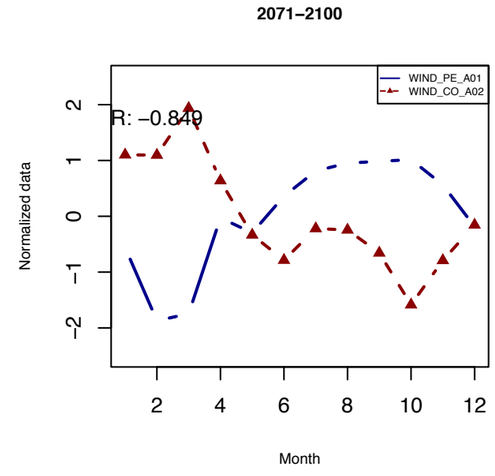
2071−2100
WIND_PE_A01
WIND_CO_A02
R: −0.849
Normalized data
Month

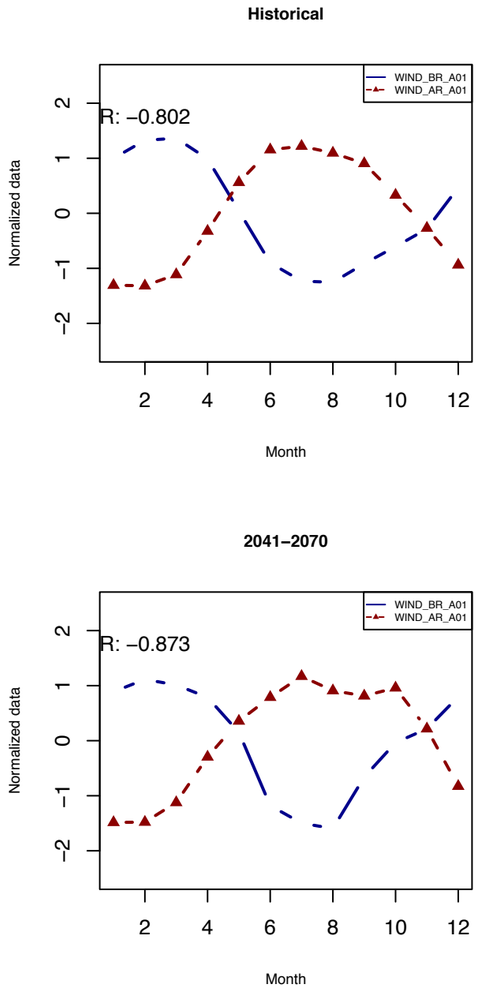
Historical
WIND_BR_A01
WIND_AR_A01
R: −0.802
Normalized data
Month

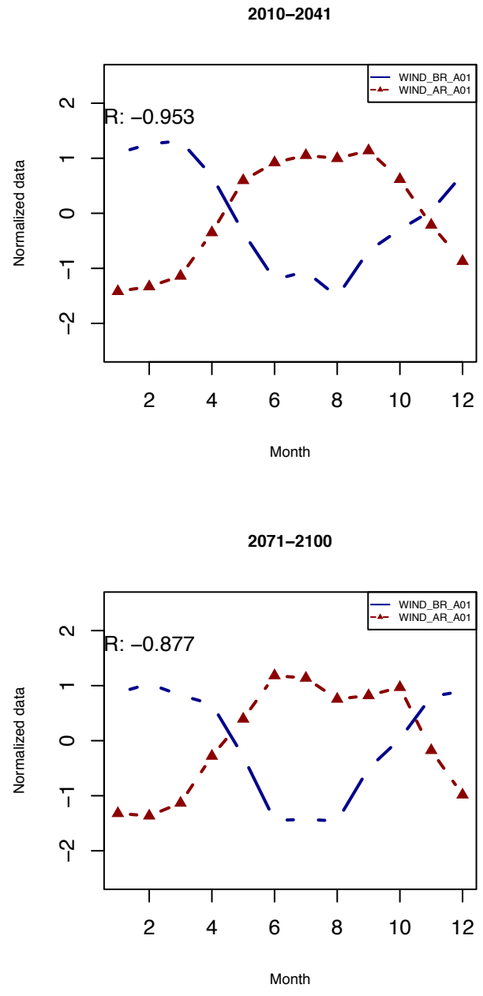
2010–2041
WIND_BR_A01
WIND_AR_A01
R: −0.953
Normalized data
Month

2041–2070
WIND_BR_A01
WIND_AR_A01
R: −0.873
Normalized data
Month

2071–2100
WIND_BR_A01
WIND_AR_A01
R: −0.877
Normalized data
Month

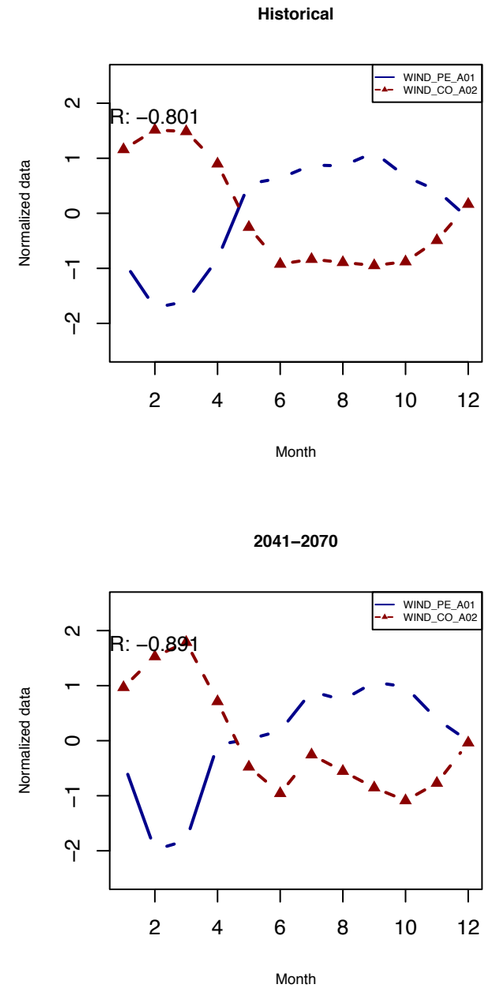
Historical
WIND_PE_A01
WIND_CO_A02
R: −0.801
Normalized data
Month

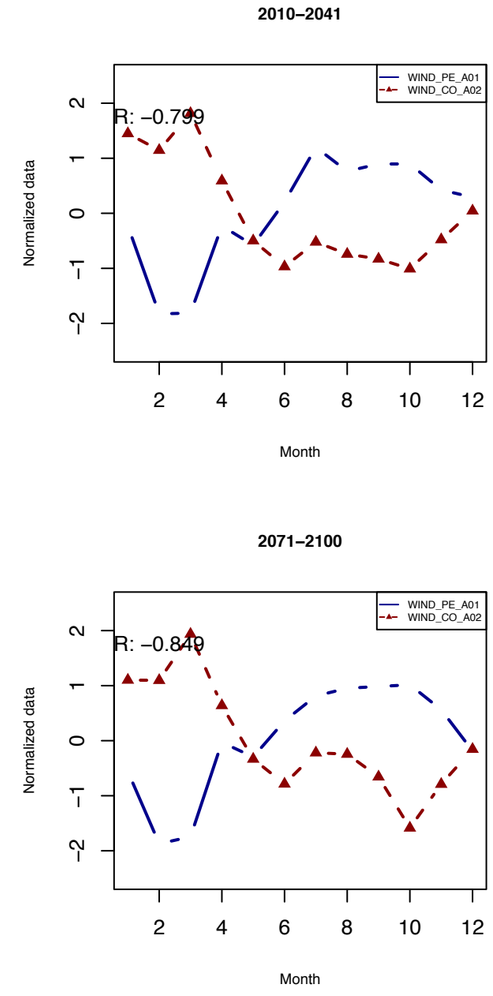
2010–2041
WIND_PE_A01
WIND_CO_A02
R: −0.799
Normalized data
Month

2041–2070
WIND_PE_A01
WIND_CO_A02
R: −0.891
Normalized data
Month

2071–2100
WIND_PE_A01
WIND_CO_A02
R: −0.849
Normalized data
Month

Climate Change Impact on Energy Complementarities based on HadGEM2-ES model and RCP 8.5 Scenario

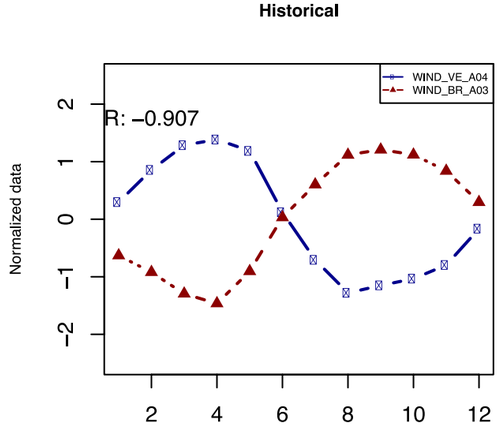

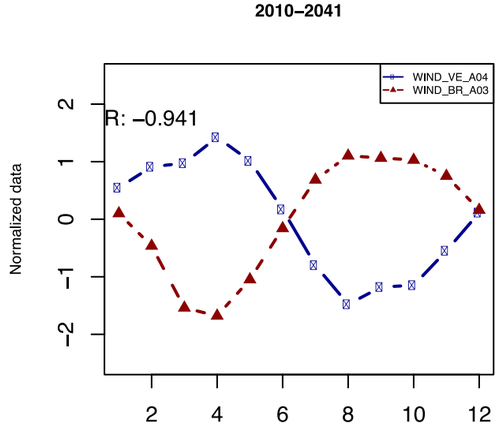

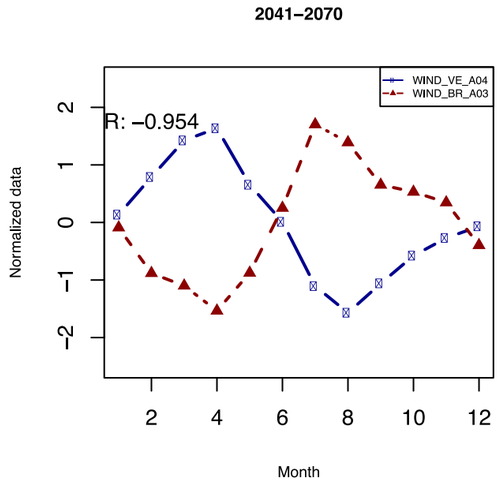

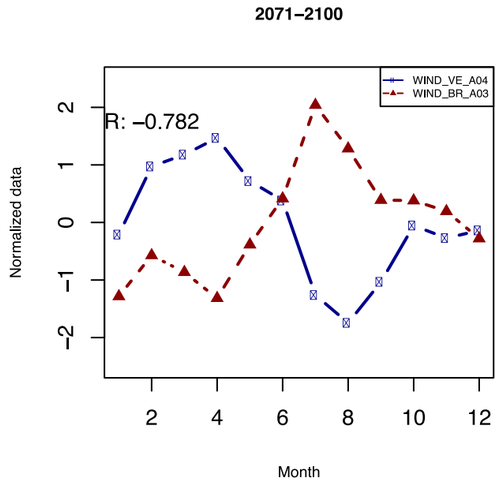

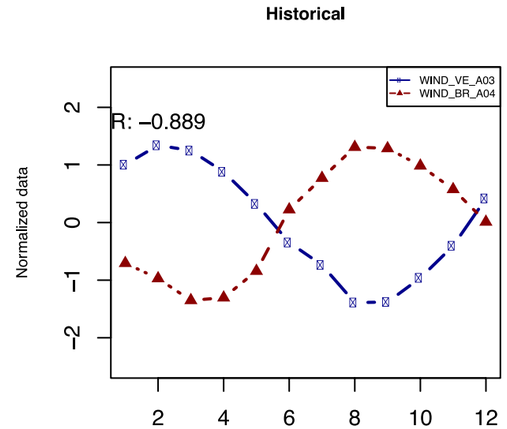

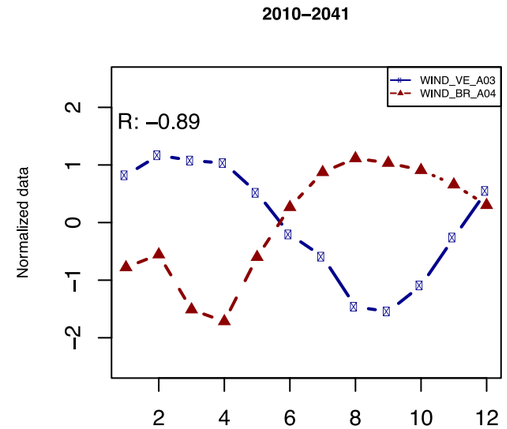

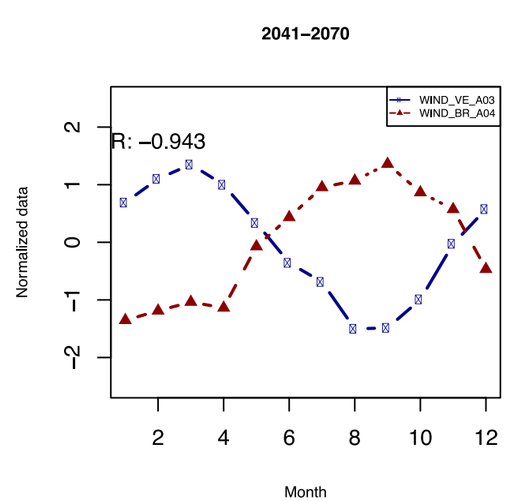

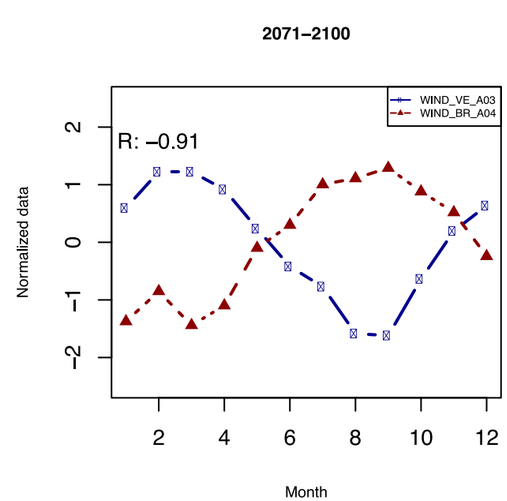

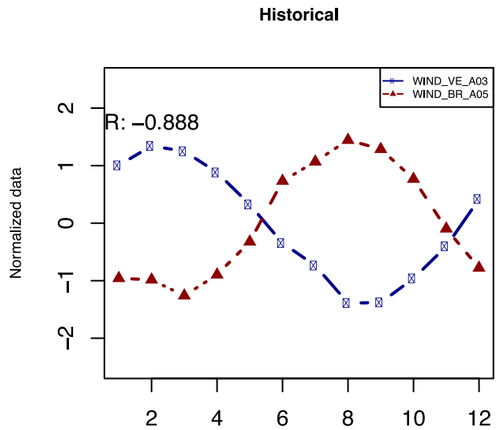
Historical
WIND_VE_A03
WIND_BR_A05
R: –0.888
Normalized data
Month

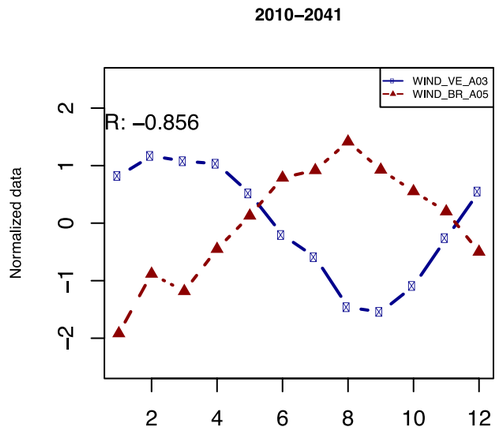
2010–2041
WIND_VE_A03
WIND_BR_A05
R: –0.856
Normalized data
Month

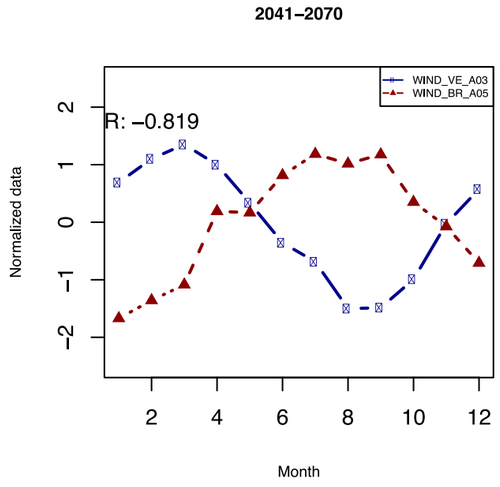
2041–2070
WIND_VE_A03
WIND_BR_A05
R: –0.819
Normalized data
Month

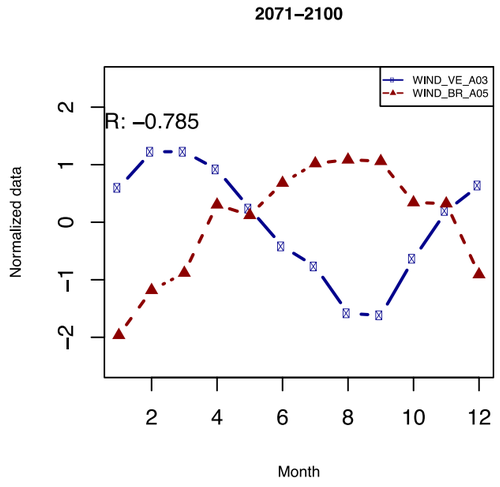
2071–2100
WIND_VE_A03
WIND_BR_A05
R: –0.785
Normalized data
Month

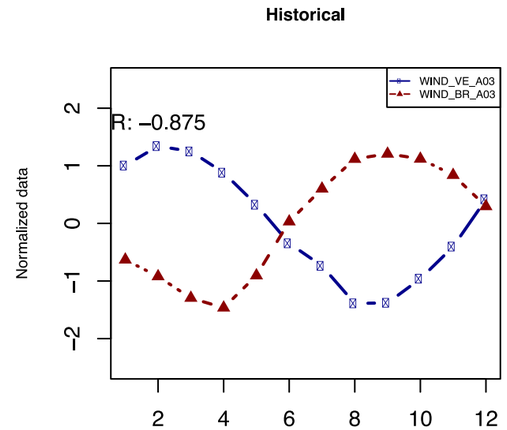
Historical
WIND_VE_A03
WIND_BR_A03
R: –0.875
Normalized data
Month

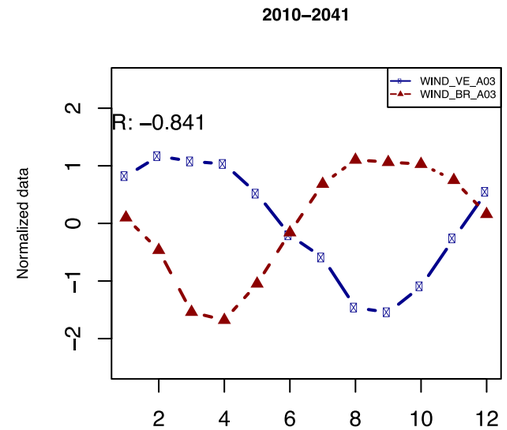
2010–2041
WIND_VE_A03
WIND_BR_A03
R: –0.841
Normalized data
Month

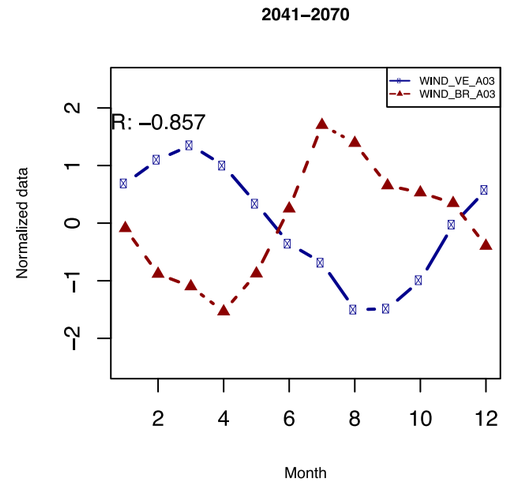
2041–2070
WIND_VE_A03
WIND_BR_A03
R: –0.857
Normalized data
Month

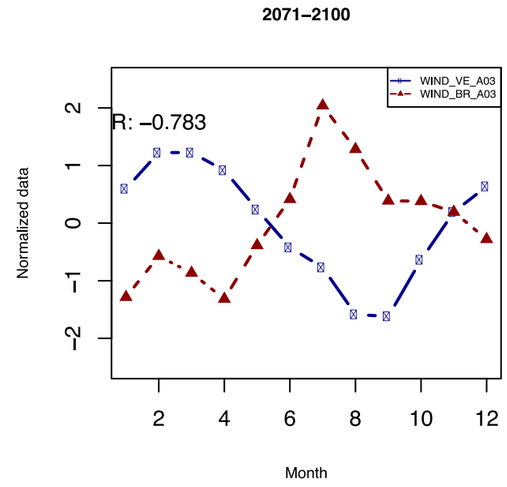
2071–2100
WIND_VE_A03
WIND_BR_A03
R: –0.783
Normalized data
Month

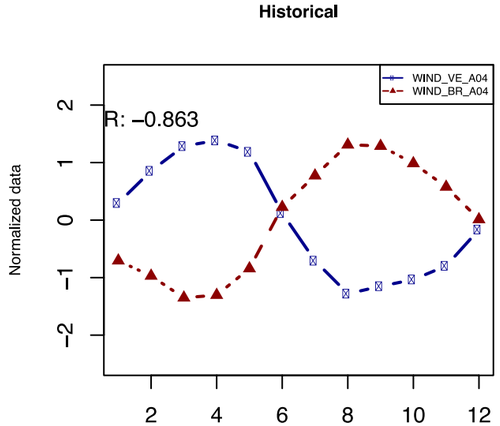
Historical
WIND_VE_A04
WIND_BR_A04
R: –0.863
Normalized data
Month

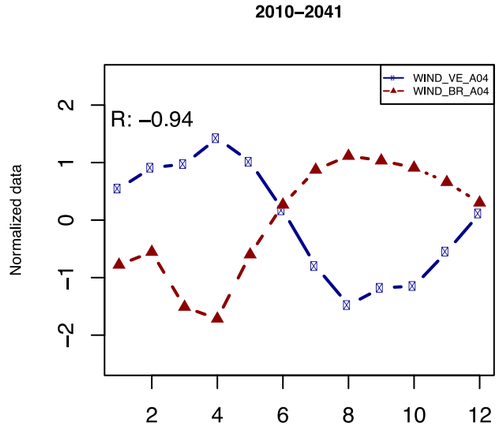
2010–2041
WIND_VE_A04
WIND_BR_A04
R: –0.94
Normalized data
Month

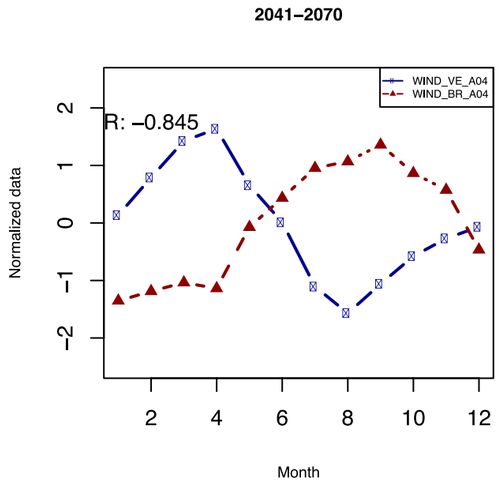
2041–2070
WIND_VE_A04
WIND_BR_A04
R: –0.845
Normalized data
Month

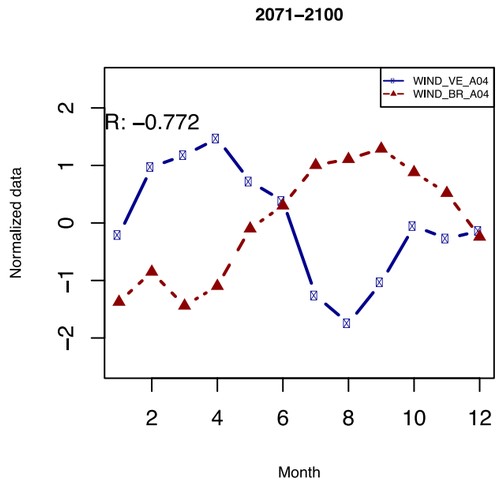
2071–2100
WIND_VE_A04
WIND_BR_A04
R: –0.772
Normalized data
Month

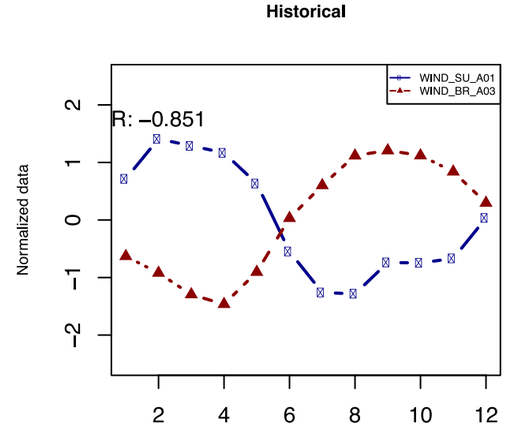
Historical
WIND_SU_A01
WIND_BR_A03
R: –0.851
Normalized data
Month

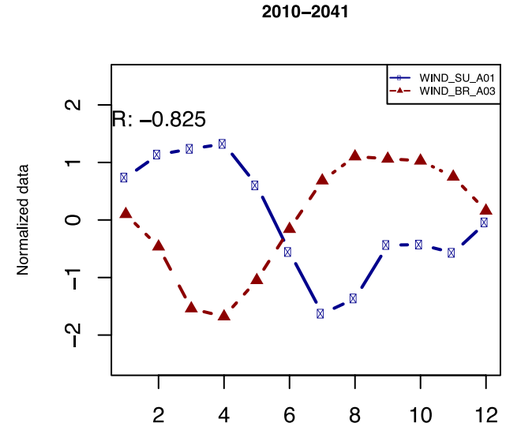
2010–2041
WIND_SU_A01
WIND_BR_A03
R: –0.825
Normalized data
Month

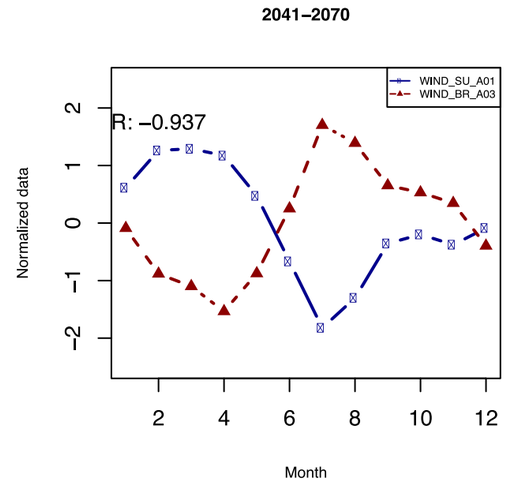
2041–2070
WIND_SU_A01
WIND_BR_A03
R: –0.937
Normalized data
Month

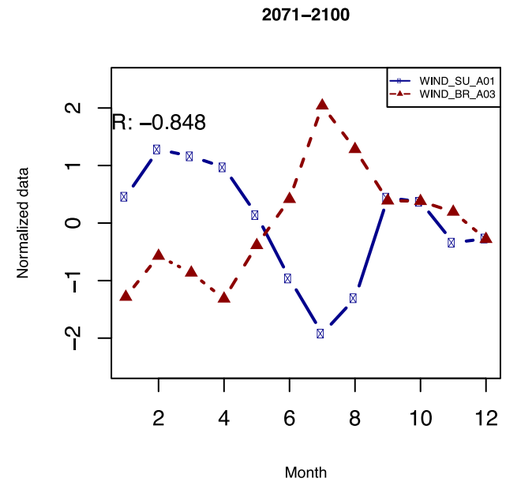
2071–2100
WIND_SU_A01
WIND_BR_A03
R: –0.848
Normalized data
Month

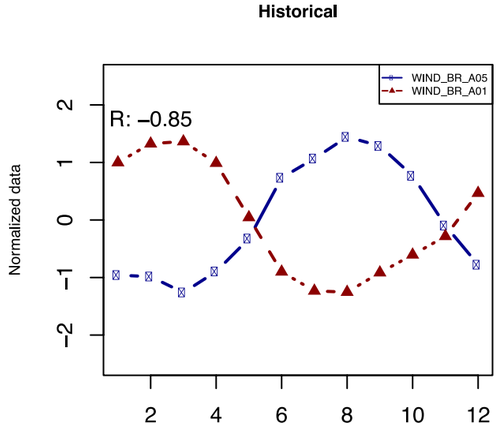
Historical
WIND_BR_A05
WIND_BR_A01
R: –0.85
Normalized data
Month

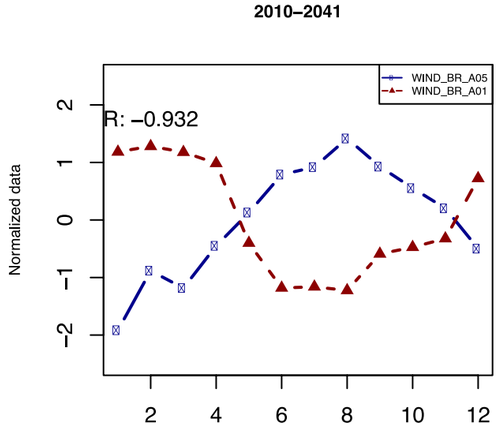
2010–2041
WIND_BR_A05
WIND_BR_A01
R: –0.932
Normalized data
Month

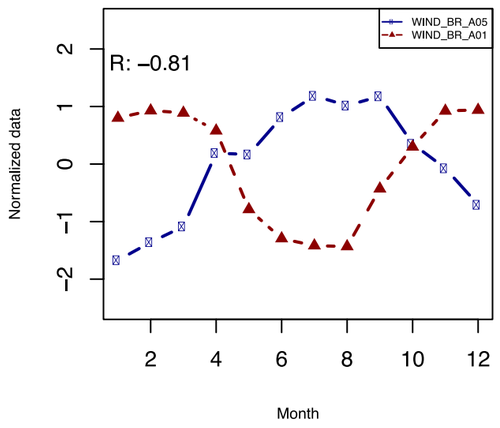
2041–2070
WIND_BR_A05
WIND_BR_A01
R: –0.81
Normalized data
Month

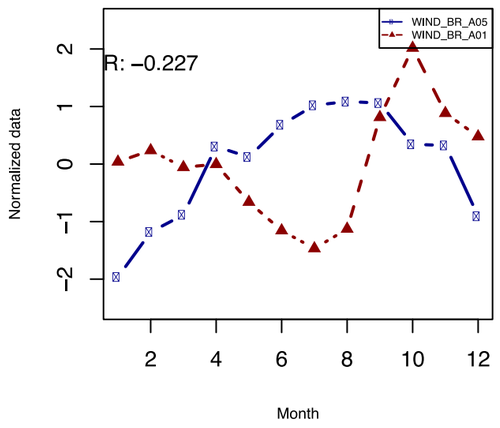
2071–2100
WIND_BR_A05
WIND_BR_A01
R: –0.227
Normalized data
Month

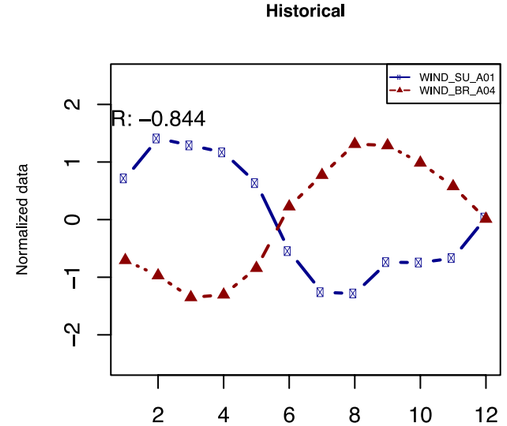
Historical
WIND_SU_A01
WIND_BR_A04
R: –0.844
Normalized data
Month

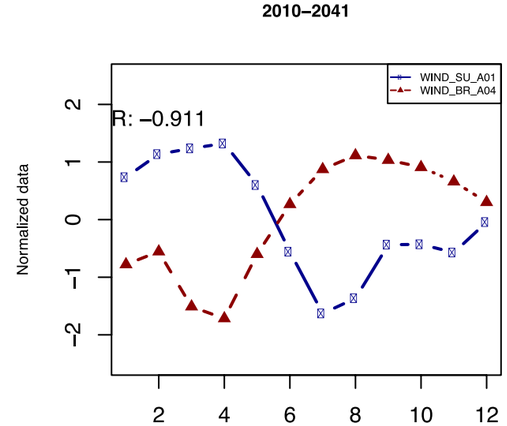
2010–2041
WIND_SU_A01
WIND_BR_A04
R: –0.911
Normalized data
Month

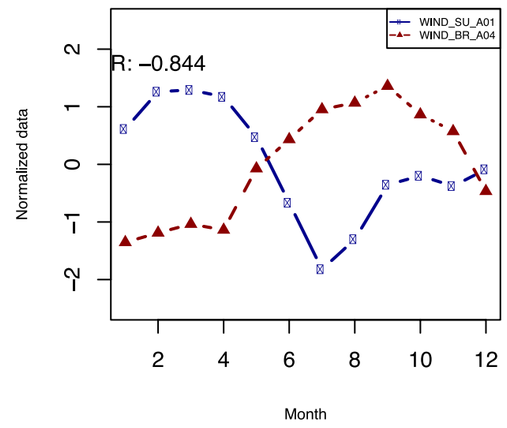
2041–2070
WIND_SU_A01
WIND_BR_A04
R: –0.844
Normalized data
Month

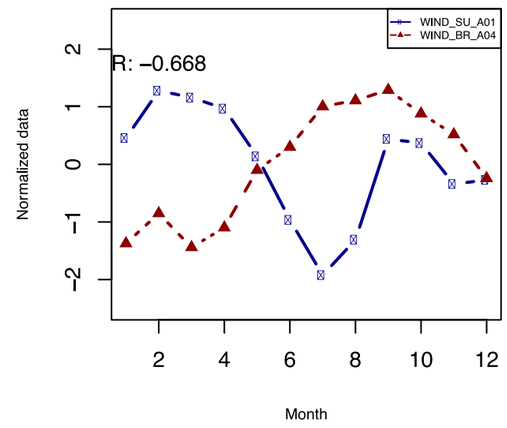
2071–2100
WIND_SU_A01
WIND_BR_A04
R: –0.668
Normalized data
Month

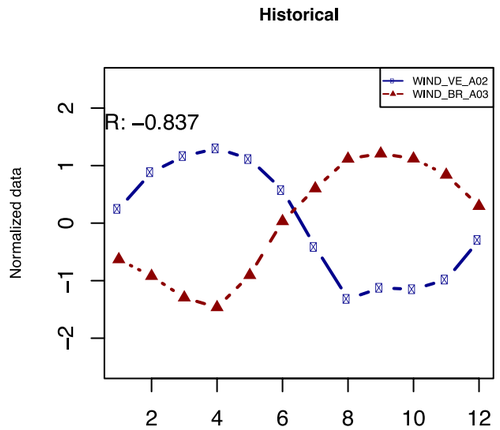
Historical
WIND_VE_A02
WIND_BR_A03
R: –0.837
Normalized data
Month

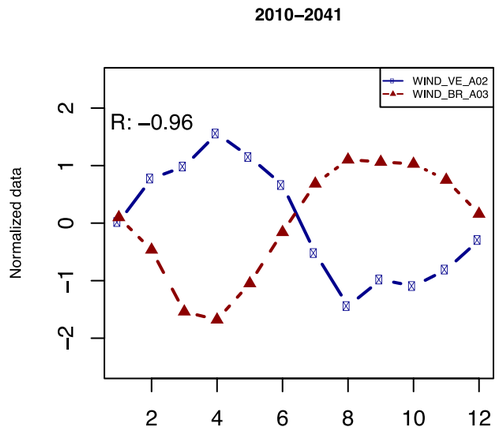
2010–2041
WIND_VE_A02
WIND_BR_A03
R: –0.96
Normalized data
Month

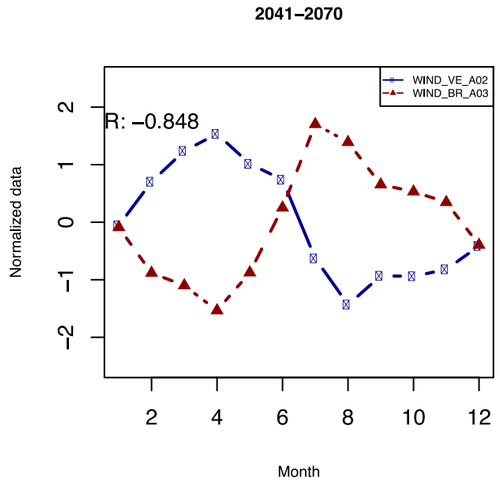
2041–2070
WIND_VE_A02
WIND_BR_A03
R: –0.848
Normalized data
Month

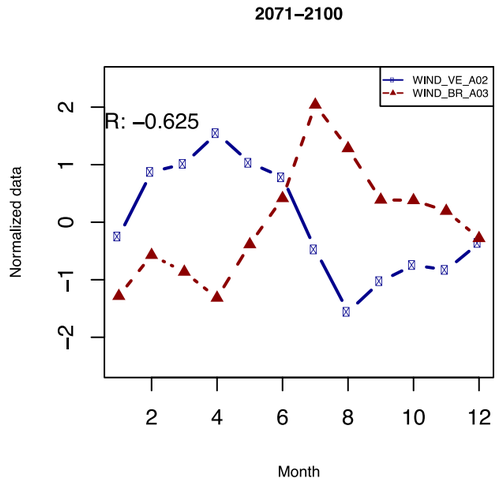
2071–2100
WIND_VE_A02
WIND_BR_A03
R: –0.625
Normalized data
Month

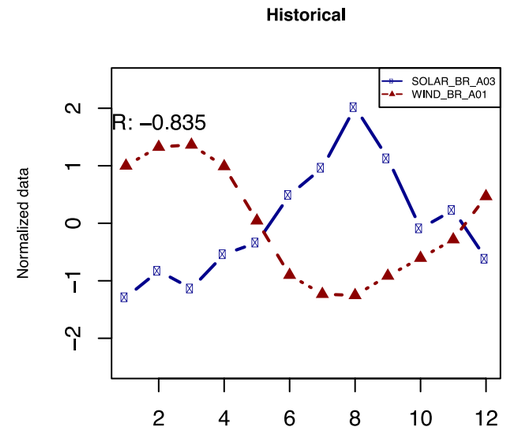
Historical
SOLAR_BR_A03
WIND_BR_A01
R: –0.835
Normalized data
Month

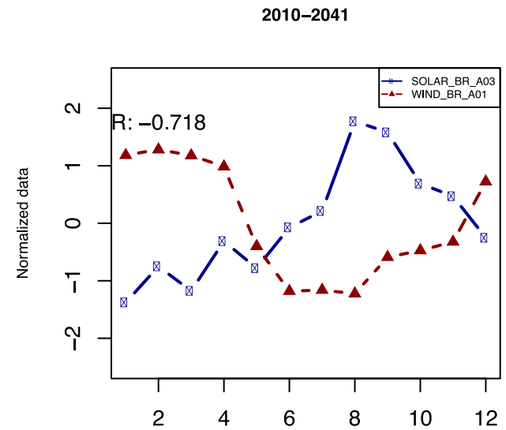
2010–2041
SOLAR_BR_A03
WIND_BR_A01
R: –0.718
Normalized data
Month

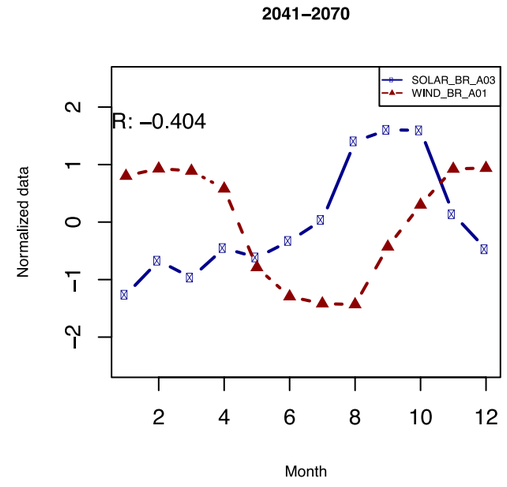
2041–2070
SOLAR_BR_A03
WIND_BR_A01
R: –0.404
Normalized data
Month

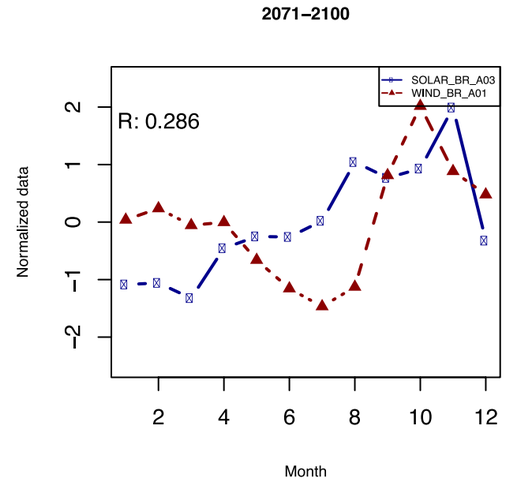
2071–2100
SOLAR_BR_A03
WIND_BR_A01
R: 0.286
Normalized data
Month

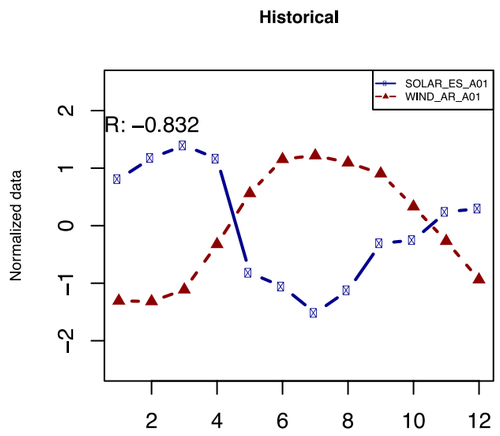
Historical
SOLAR_ES_A01
WIND_AR_A01
R: −0.832
Normalized data
Month

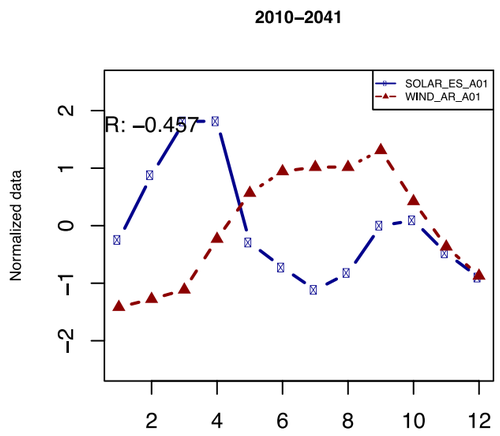
2010–2041
SOLAR_ES_A01
WIND_AR_A01
R: −0.457
Normalized data
Month

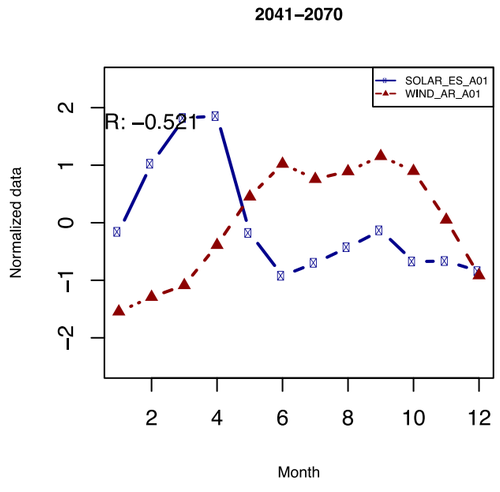
2041–2070
SOLAR_ES_A01
WIND_AR_A01
R: −0.521
Normalized data
Month

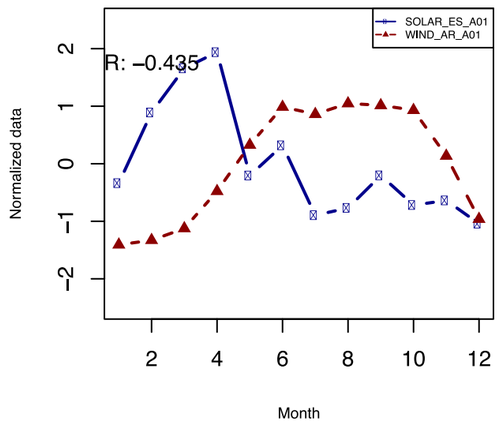
2071–2100
SOLAR_ES_A01
WIND_AR_A01
R: −0.435
Normalized data
Month

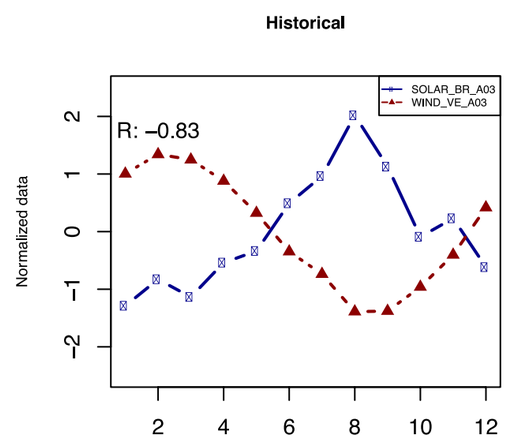
Historical
SOLAR_BR_A03
WIND_VE_A03
R: −0.83
Normalized data
Month

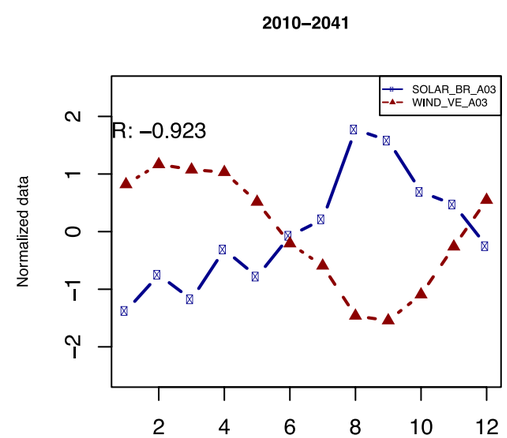
2010–2041
SOLAR_BR_A03
WIND_VE_A03
R: −0.923
Normalized data
Month

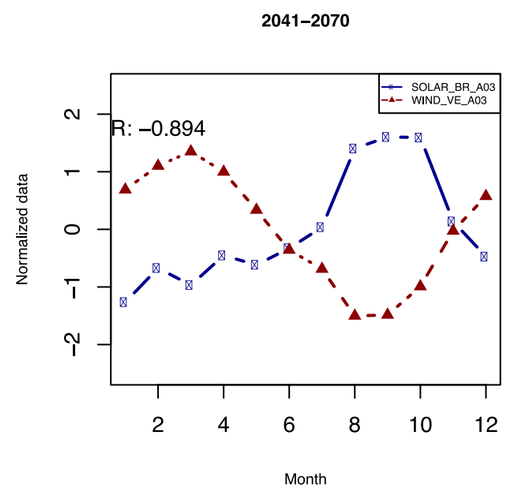
2041–2070
SOLAR_BR_A03
WIND_VE_A03
R: −0.894
Normalized data
Month

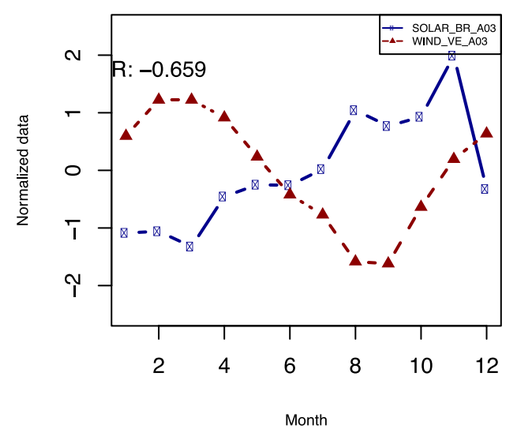
2071–2100
SOLAR_BR_A03
WIND_VE_A03
R: −0.659
Normalized data
Month

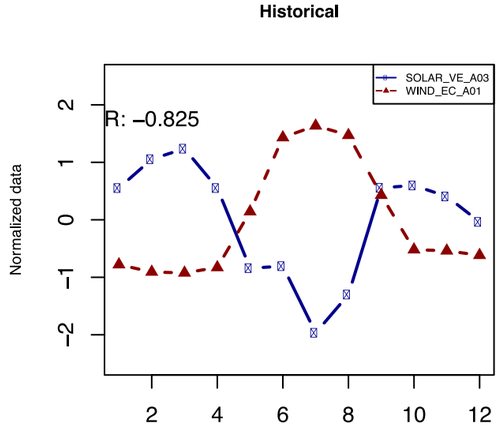
Historical
SOLAR_VE_A03
WIND_EC_A01
R: –0.825
Normalized data
Month

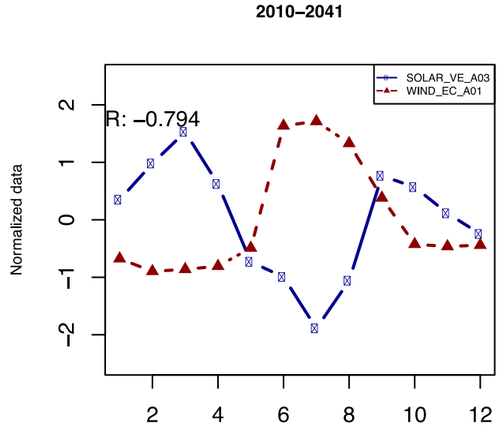
2010–2041
SOLAR_VE_A03
WIND_EC_A01
R: –0.794
Normalized data
Month

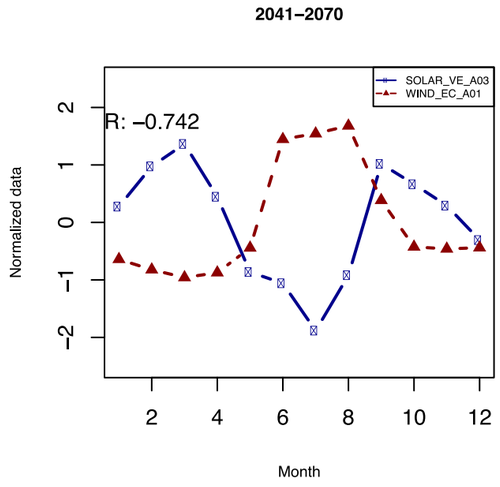
2041–2070
SOLAR_VE_A03
WIND_EC_A01
R: –0.742
Normalized data
Month

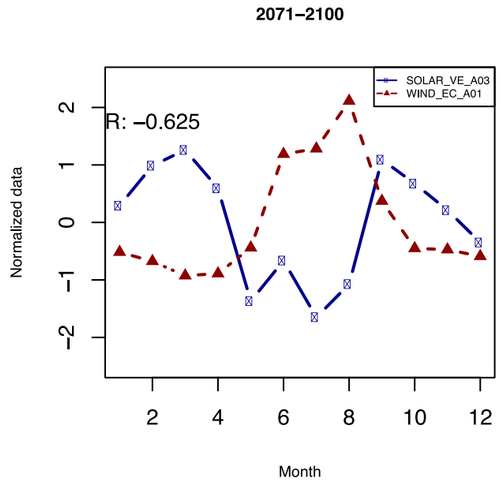
2071–2100
SOLAR_VE_A03
WIND_EC_A01
R: –0.625
Normalized data
Month

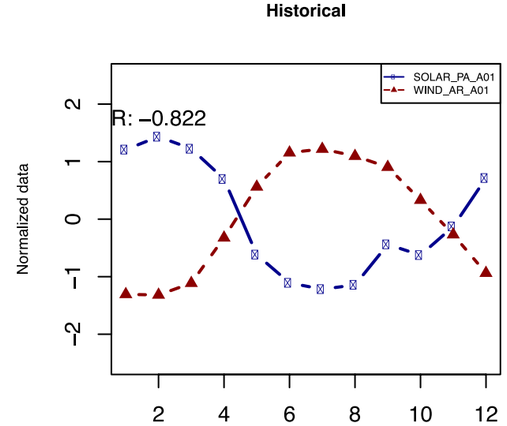
Historical
SOLAR_PA_A01
WIND_AR_A01
R: –0.822
Normalized data
Month

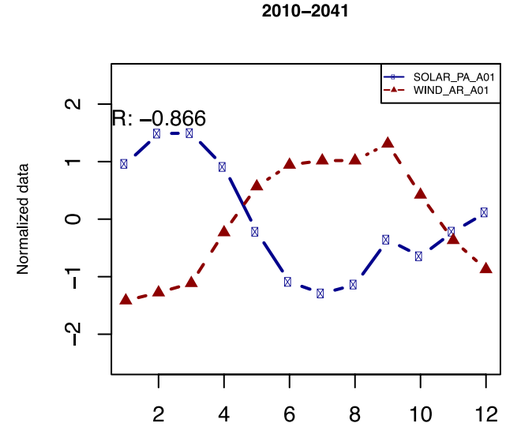
2010–2041
SOLAR_PA_A01
WIND_AR_A01
R: –0.866
Normalized data
Month

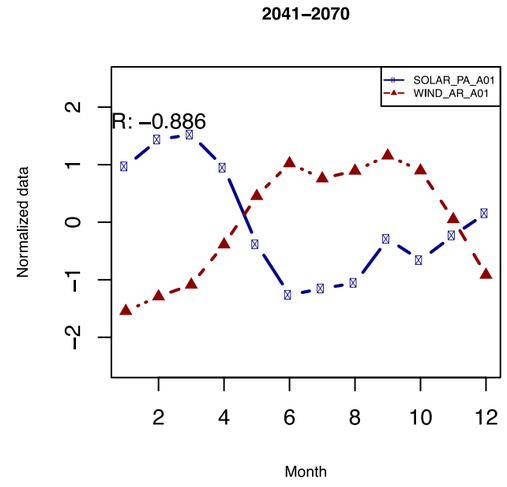
2041–2070
SOLAR_PA_A01
WIND_AR_A01
R: –0.886
Normalized data
Month

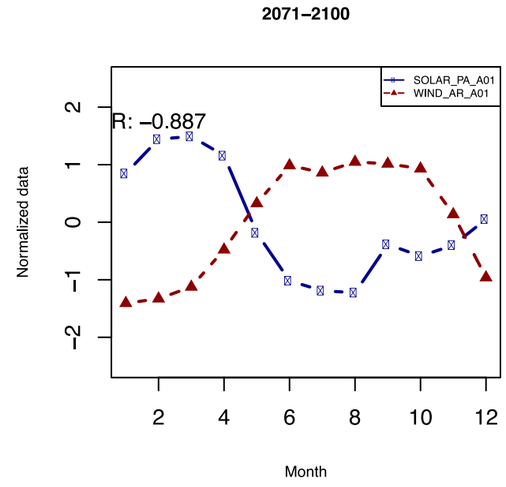
2071–2100
SOLAR_PA_A01
WIND_AR_A01
R: –0.887
Normalized data
Month

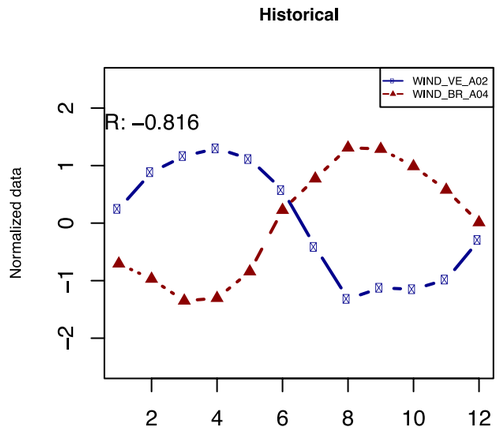
Historical
WIND_VE_A02
WIND_BR_A04
R: –0.816
Normalized data
Month

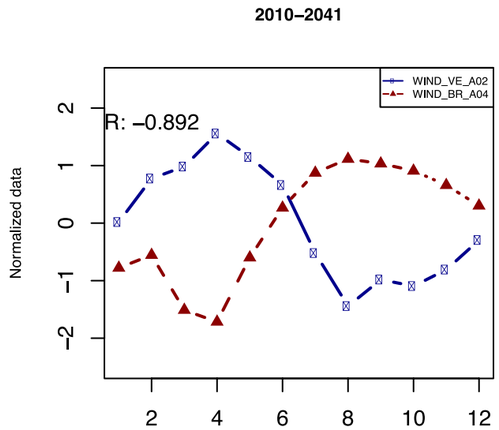
2010–2041
WIND_VE_A02
WIND_BR_A04
R: –0.892
Normalized data
Month

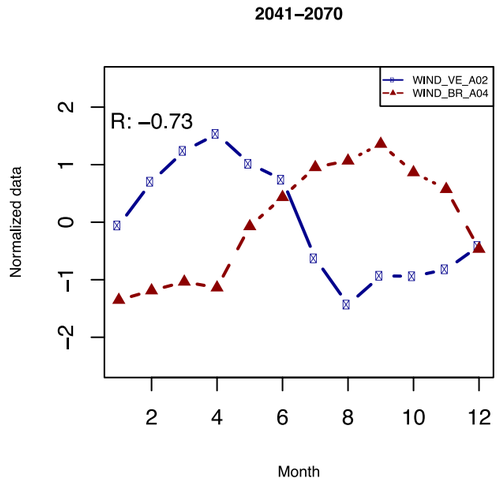
2041–2070
WIND_VE_A02
WIND_BR_A04
R: –0.73
Normalized data
Month

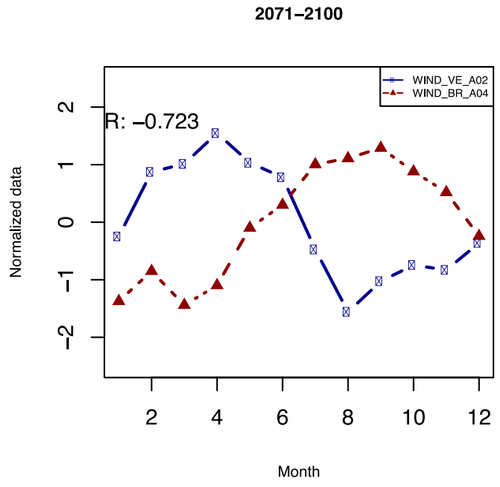
2071–2100
WIND_VE_A02
WIND_BR_A04
R: –0.723
Normalized data
Month

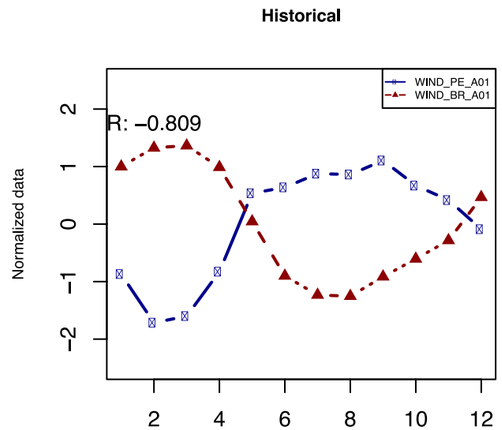
Historical
WIND_PE_A01
WIND_BR_A01
R: –0.809
Normalized data
Month

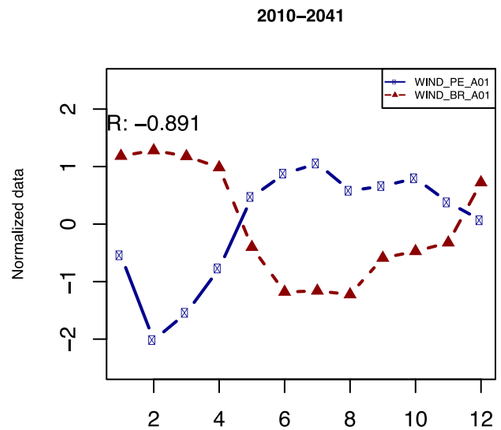
2010–2041
WIND_PE_A01
WIND_BR_A01
R: –0.891
Normalized data
Month

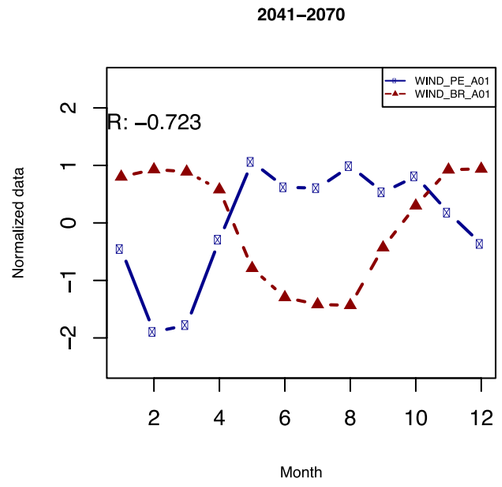
2041–2070
WIND_PE_A01
WIND_BR_A01
R: –0.723
Normalized data
Month

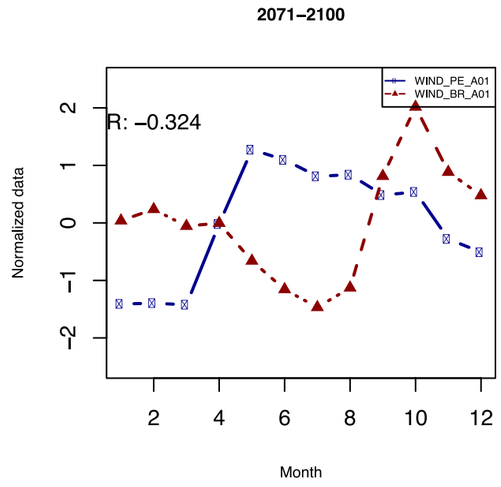
2071–2100
WIND_PE_A01
WIND_BR_A01
R: –0.324
Normalized data
Month

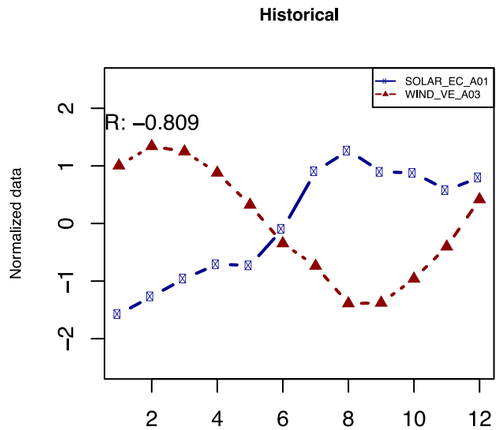
Historical
SOLAR_EC_A01
WIND_VE_A03
R: –0.809
Normalized data
Month

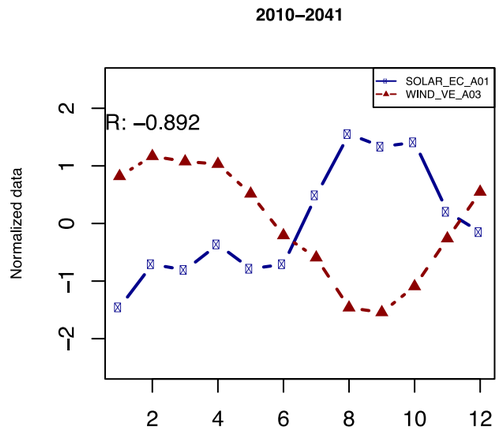
2010–2041
SOLAR_EC_A01
WIND_VE_A03
R: –0.892
Normalized data
Month

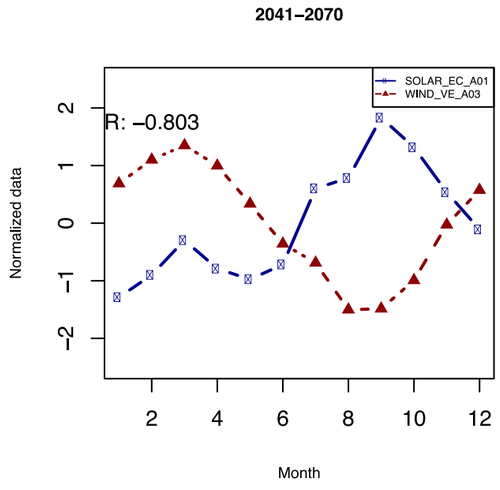
2041–2070
SOLAR_EC_A01
WIND_VE_A03
R: –0.803
Normalized data
Month

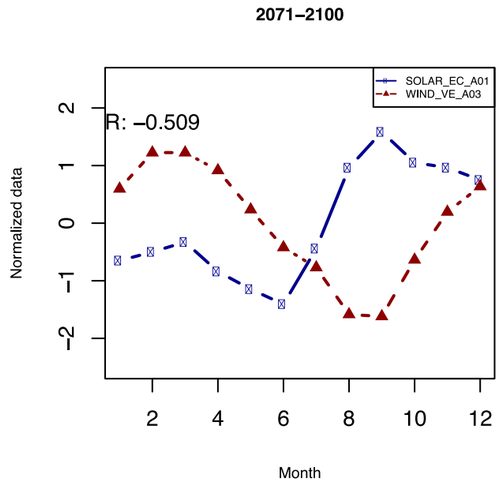
2071–2100
SOLAR_EC_A01
WIND_VE_A03
R: –0.509
Normalized data
Month

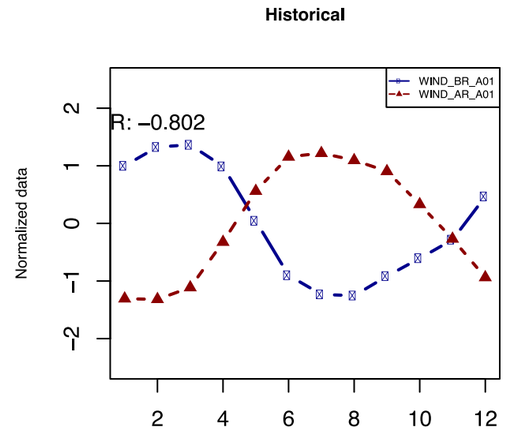
Historical
WIND_BR_A01
WIND_AR_A01
R: –0.802
Normalized data
Month

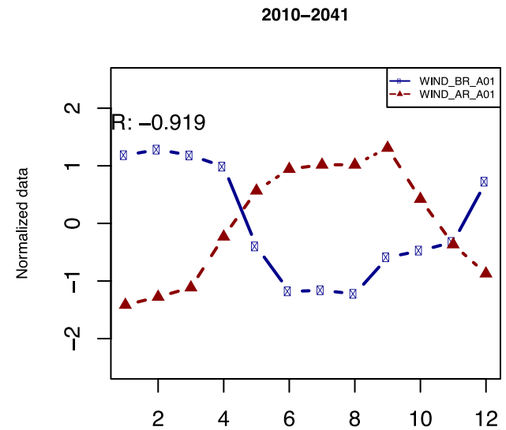
2010–2041
WIND_BR_A01
WIND_AR_A01
R: –0.919
Normalized data
Month

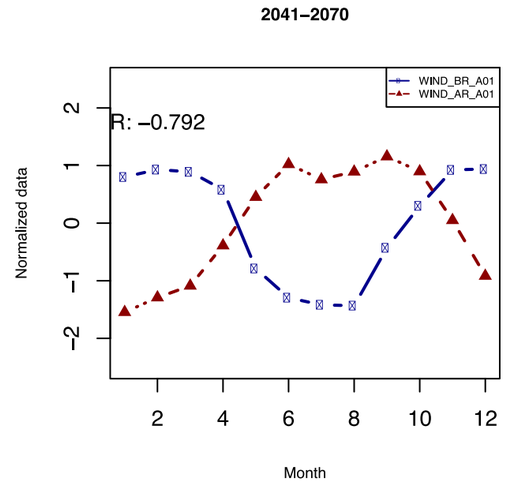
2041–2070
WIND_BR_A01
WIND_AR_A01
R: –0.792
Normalized data
Month

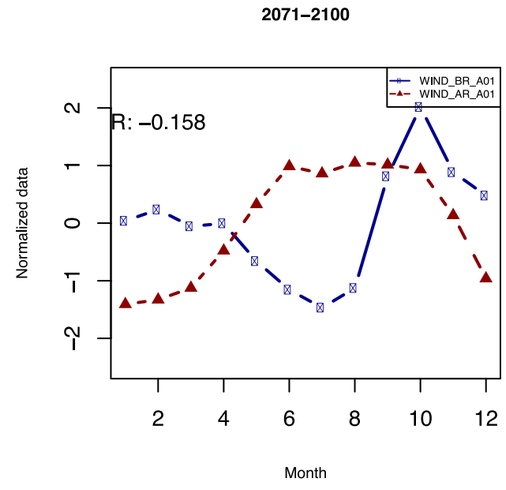
2071–2100
WIND_BR_A01
WIND_AR_A01
R: –0.158
Normalized data
Month

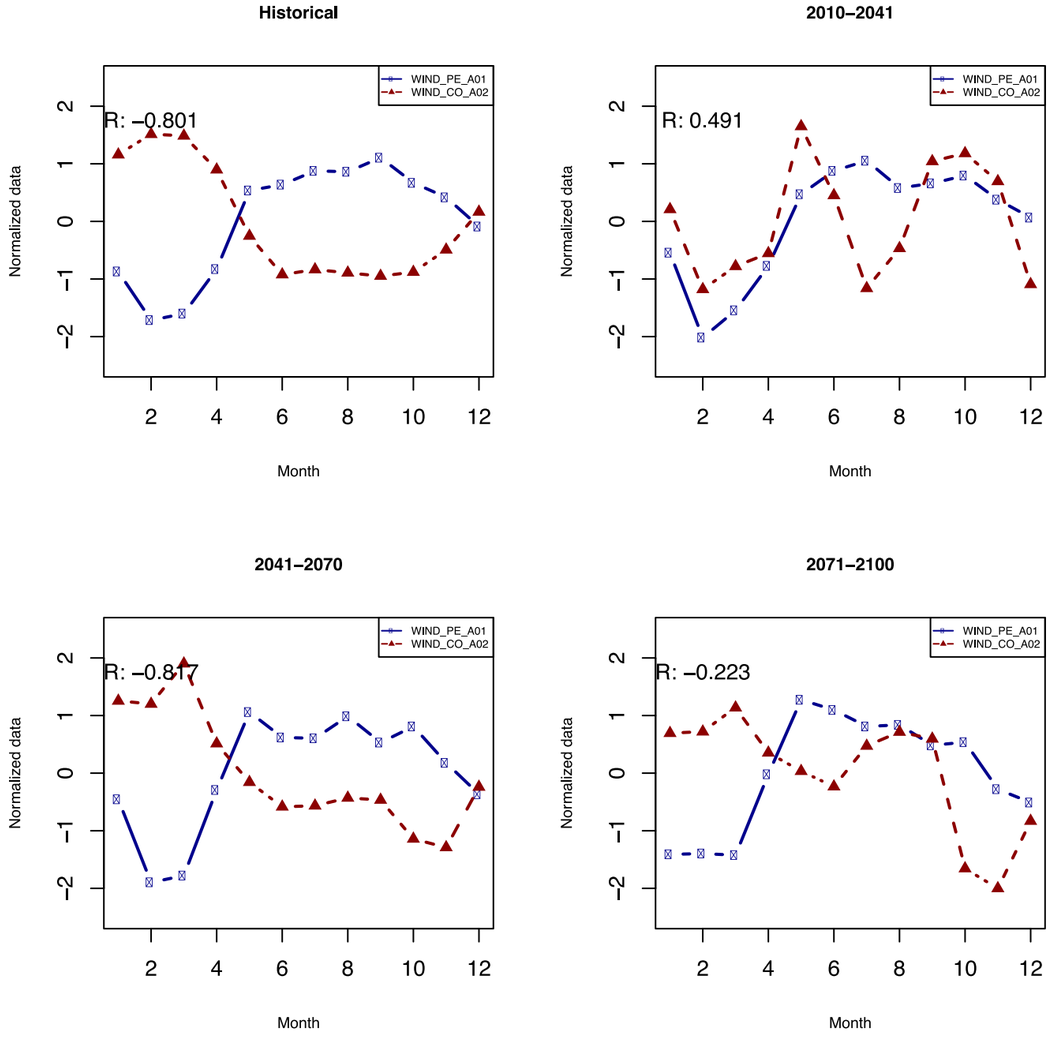

7.3. Trend of the Climate Projection for Wind and Solar Resources based on HadGEM2-ES Model

This appendix presents the trend of the climate projection for wind and solar resources, of the selected cases, based on HadGEM2-ES Model simulation results for the RCP 4.5 and RCP 8.4 scenarios.

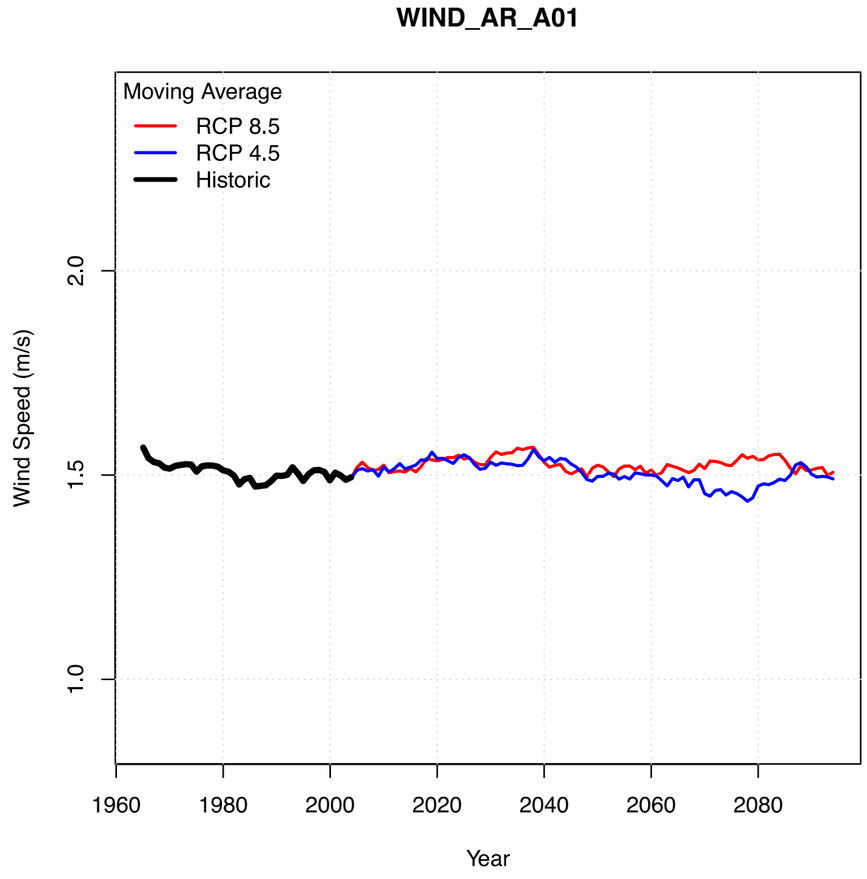

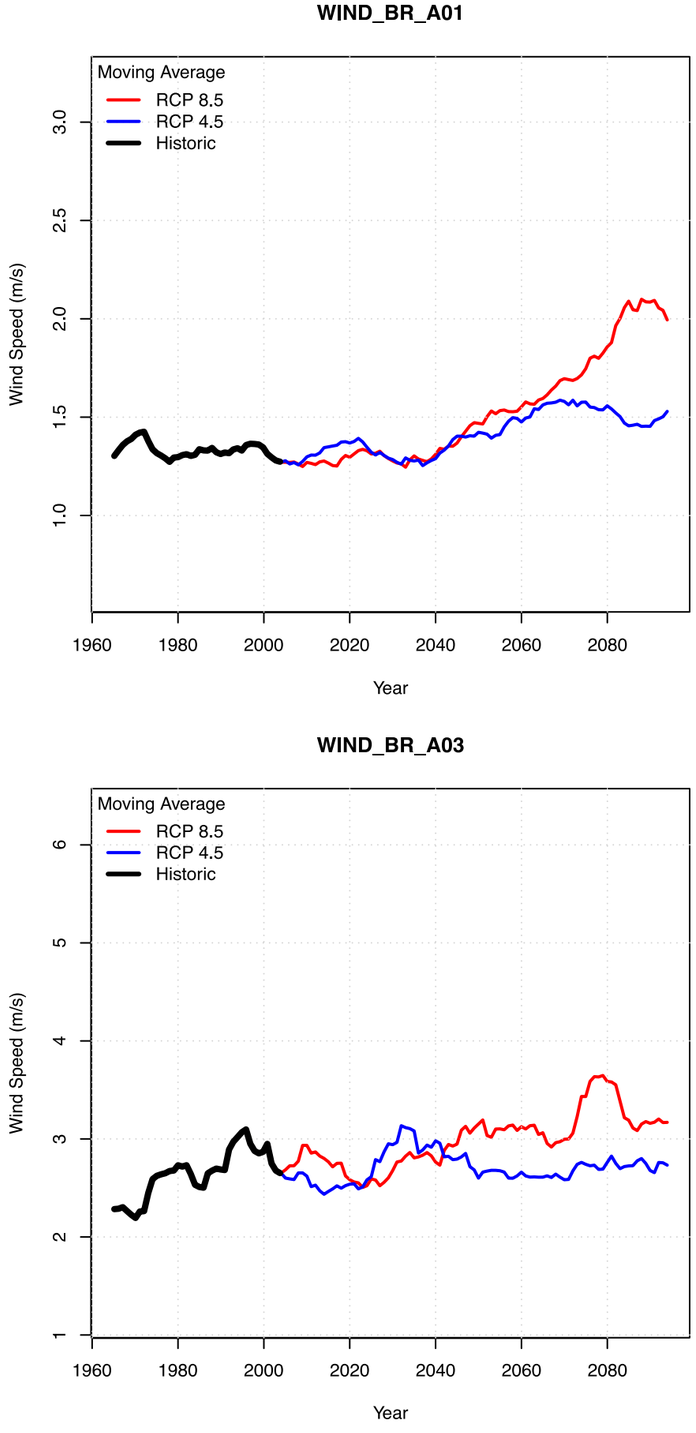
WIND_BR_A01
Moving Average
RCP 8.5
RCP 4.5
Historic
Wind Speed (m/s)
1.0
1.5
2.0
2.5
3.0
1960
1980
2000
2020
2040
2060
2080
Year

WIND_BR_A03
Moving Average
RCP 8.5
RCP 4.5
Historic
Wind Speed (m/s)
1
2
3
4
5
6
1960
1980
2000
2020
2040
2060
2080
Year

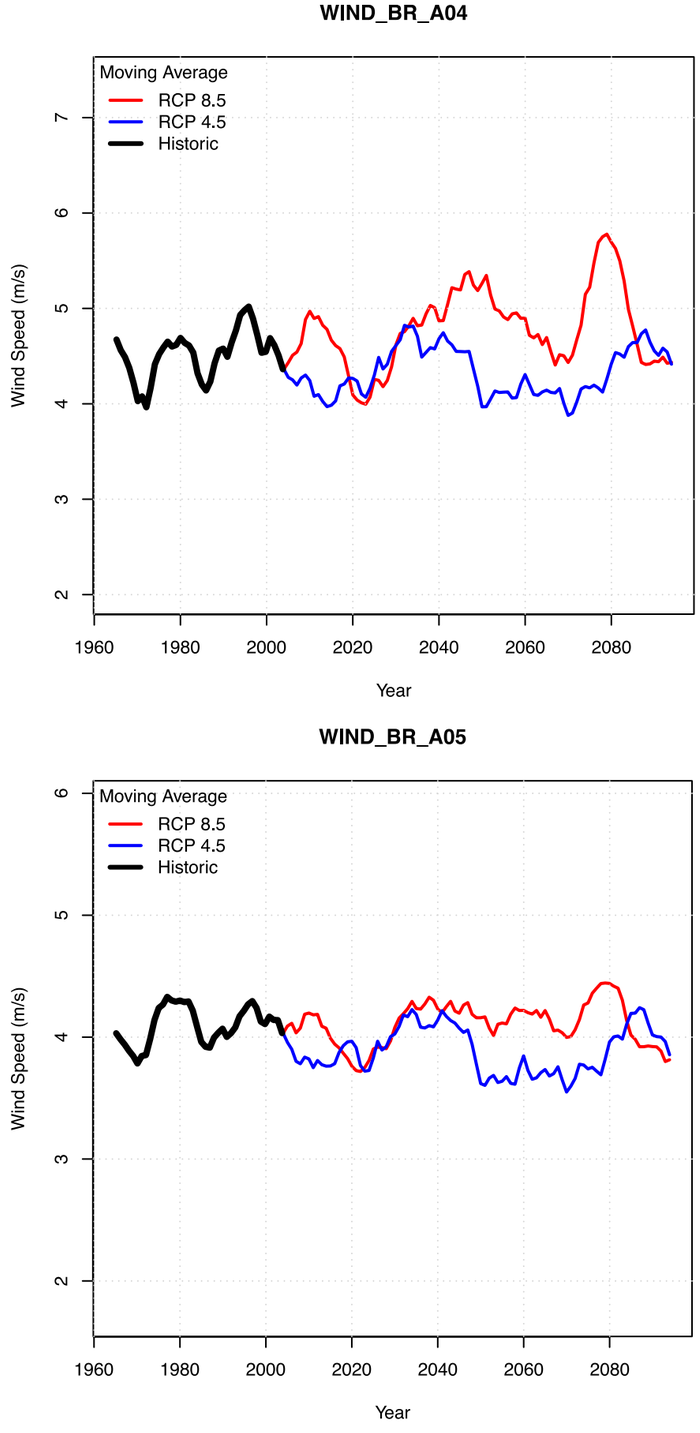
WIND_BR_A04
Moving Average
RCP 8.5
RCP 4.5
Historic
Wind Speed (m/s)
2
3
4
5
6
7
1960
1980
2000
2020
2040
2060
2080
Year

WIND_BR_A05
Moving Average
RCP 8.5
RCP 4.5
Historic
Wind Speed (m/s)
2
3
4
5
6
1960
1980
2000
2020
2040
2060
2080
Year

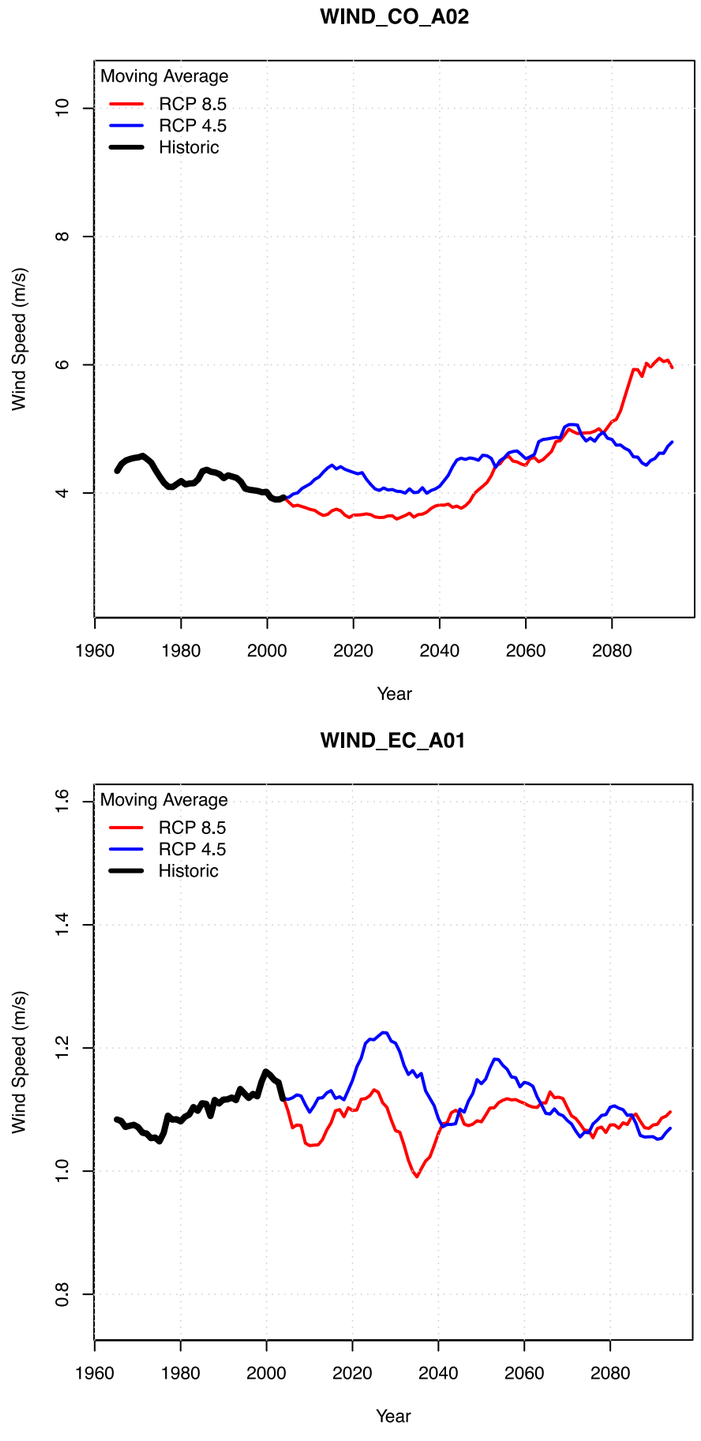
WIND_CO_A02
Moving Average
RCP 8.5
RCP 4.5
Historic
Wind Speed (m/s)
4
6
8
10
1960
1980
2000
2020
2040
2060
2080
Year

WIND_EC_A01
Moving Average
RCP 8.5
RCP 4.5
Historic
Wind Speed (m/s)
0.8
1.0
1.2
1.4
1.6
1960
1980
2000
2020
2040
2060
2080
Year

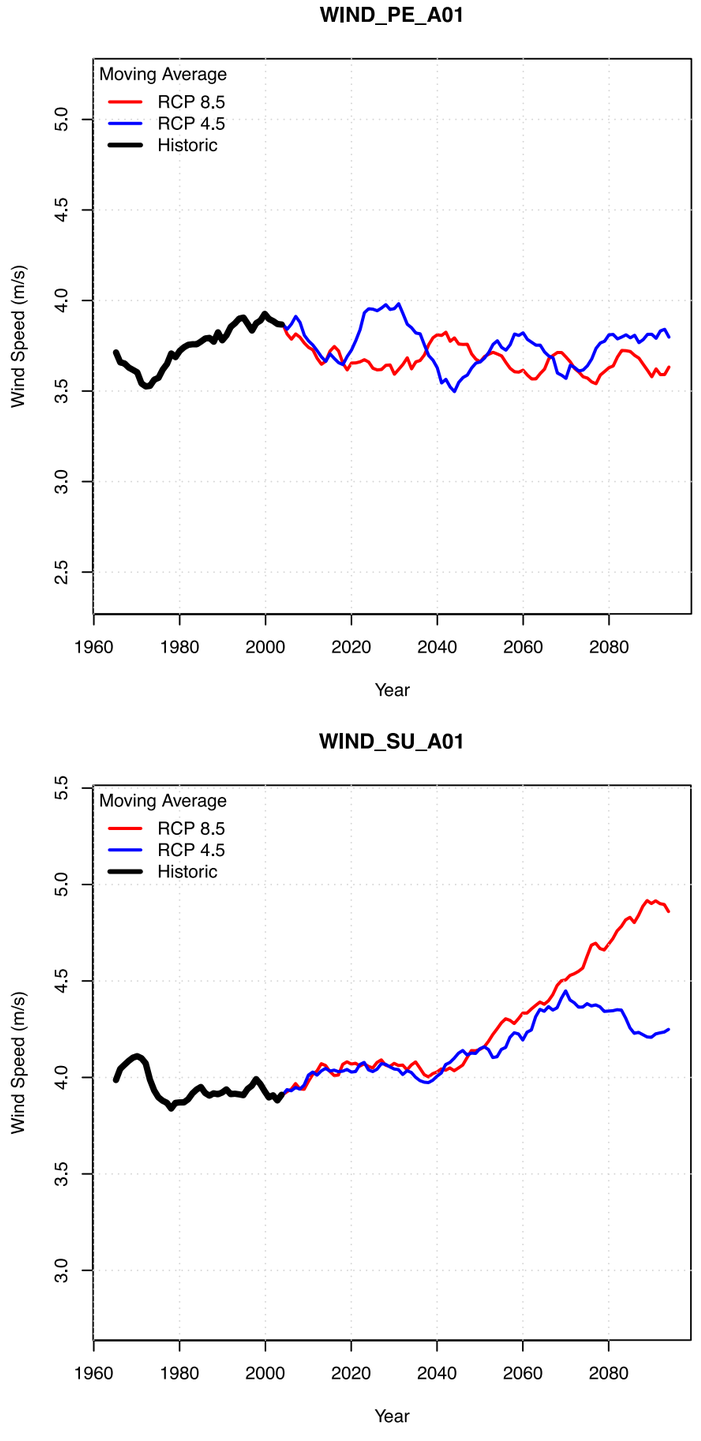
WIND_PE_A01
Moving Average
RCP 8.5
RCP 4.5
Historic
Wind Speed (m/s)
2.5
3.0
3.5
4.0
4.5
5.0
1960
1980
2000
2020
2040
2060
2080
Year

WIND_SU_A01
Moving Average
RCP 8.5
RCP 4.5
Historic
Wind Speed (m/s)
3.0
3.5
4.0
4.5
5.0
5.5
1960
1980
2000
2020
2040
2060
2080
Year

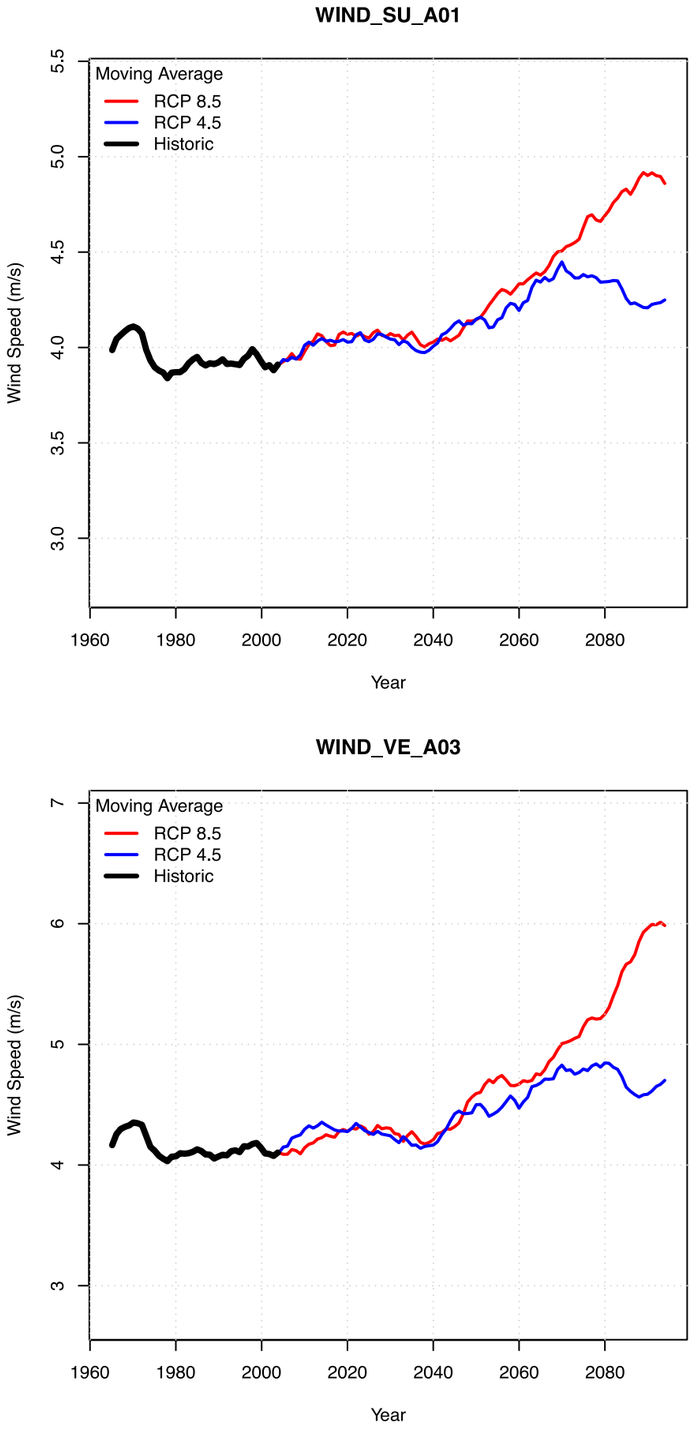
WIND_SU_A01
Moving Average
RCP 8.5
RCP 4.5
Historic
Wind Speed (m/s)
3.0
3.5
4.0
4.5
5.0
5.5
1960
1980
2000
2020
2040
2060
2080
Year

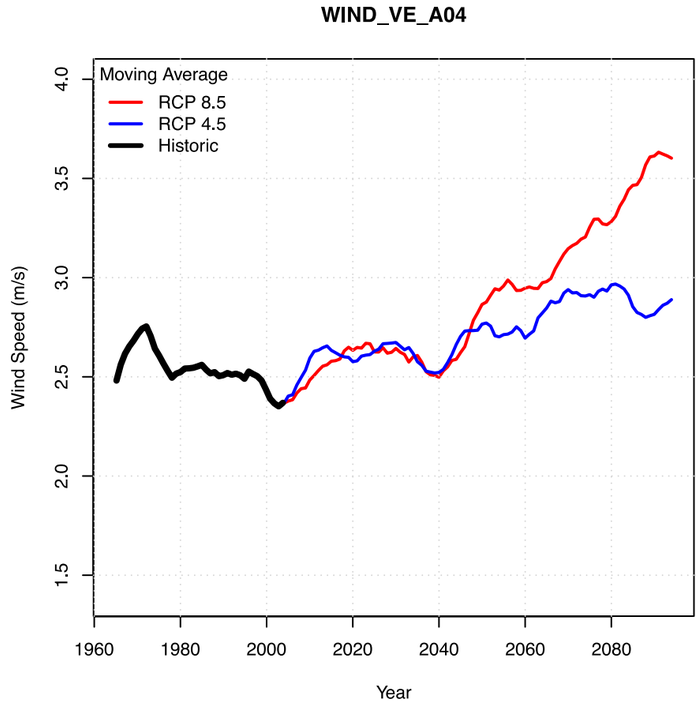
WIND_VE_A04
Moving Average
RCP 8.5
RCP 4.5
Historic
Wind Speed (m/s)
1.5
2.0
2.5
3.0
3.5
4.0
1960
1980
2000
2020
2040
2060
2080
Year

WIND_VE_A03
Moving Average
RCP 8.5
RCP 4.5
Historic
Wind Speed (m/s)
3
4
5
6
7
1960
1980
2000
2020
2040
2060
2080
Year

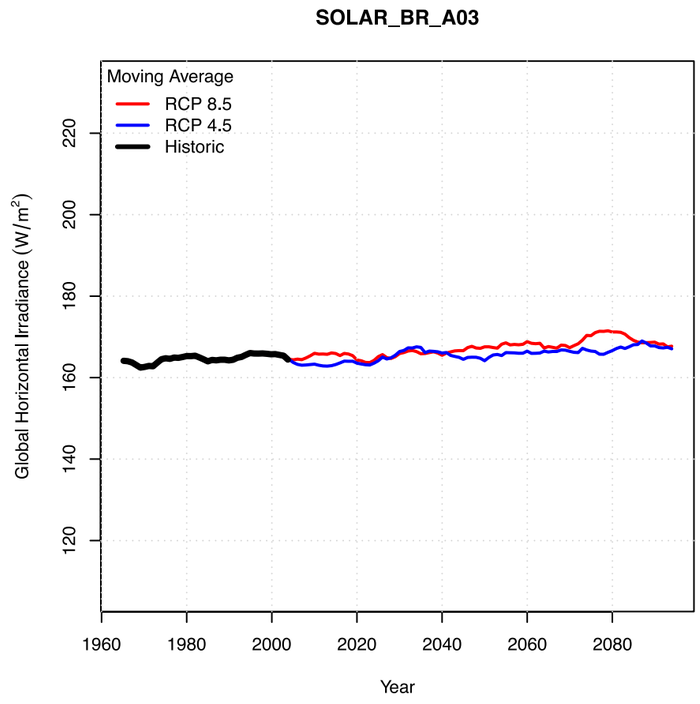
SOLAR_BR_A03
Moving Average
RCP 8.5
RCP 4.5
Historic
Global Horizontal Irradiance (W/m2)
120
140
160
180
200
220
1960
1980
2000
2020
2040
2060
2080
Year

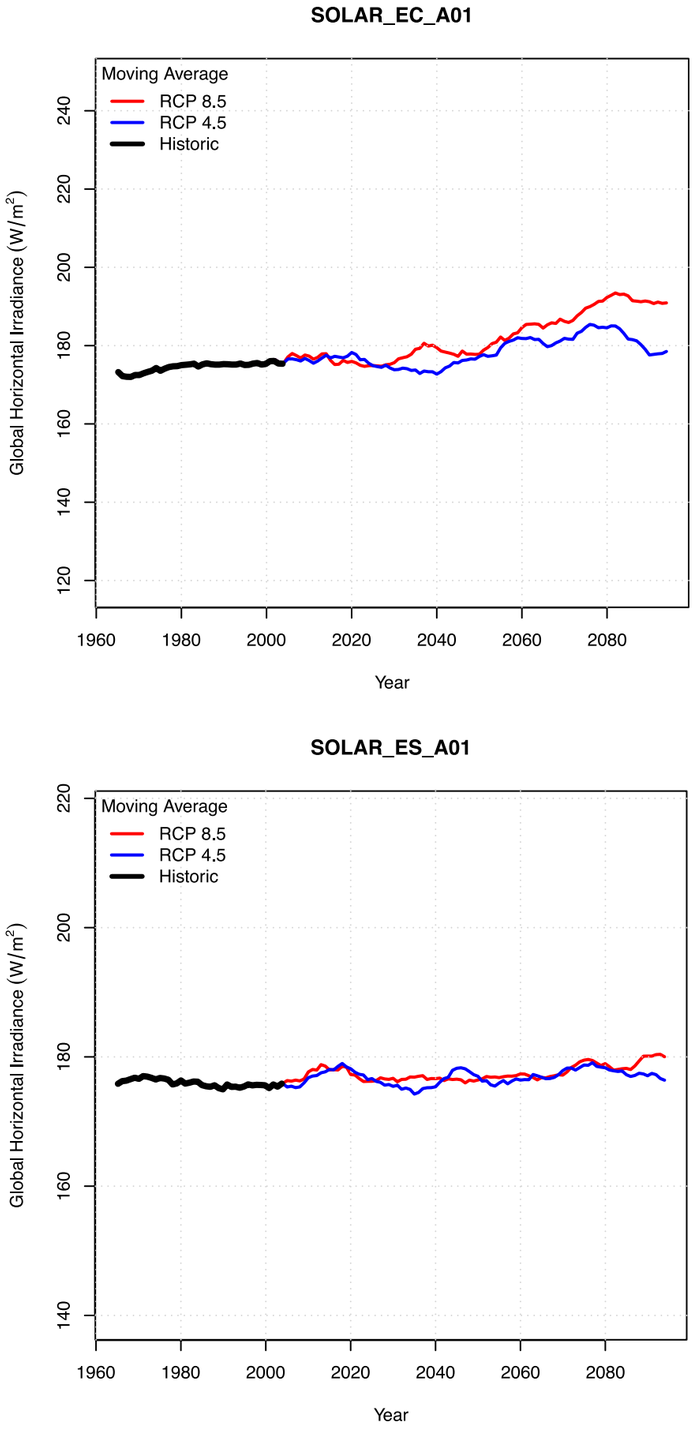
SOLAR_EC_A01
Moving Average
RCP 8.5
RCP 4.5
Historic
Global Horizontal Irradiance (W/m2)
120
140
160
180
200
220
240
1960
1980
2000
2020
2040
2060
2080
Year

SOLAR_ES_A01
Moving Average
RCP 8.5
RCP 4.5
Historic
Global Horizontal Irradiance (W/m2)
140
160
180
200
220
1960
1980
2000
2020
2040
2060
2080
Year

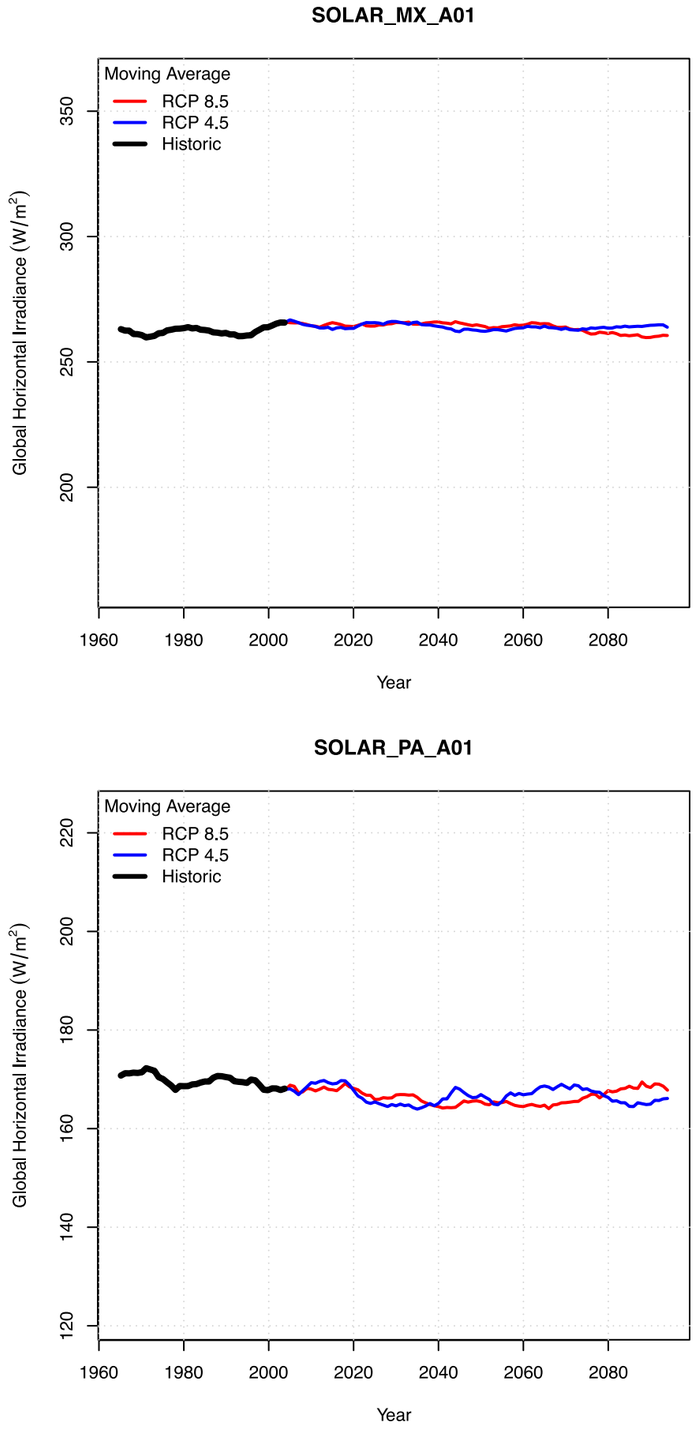
SOLAR_MX_A01
Moving Average
RCP 8.5
RCP 4.5
Historic
Global Horizontal Irradiance (W/m2)
200
250
300
350
1960
1980
2000
2020
2040
2060
2080
Year

SOLAR_PA_A01
Moving Average
RCP 8.5
RCP 4.5
Historic
Global Horizontal Irradiance (W/m2)
120
140
160
180
200
220
1960
1980
2000
2020
2040
2060
2080
Year

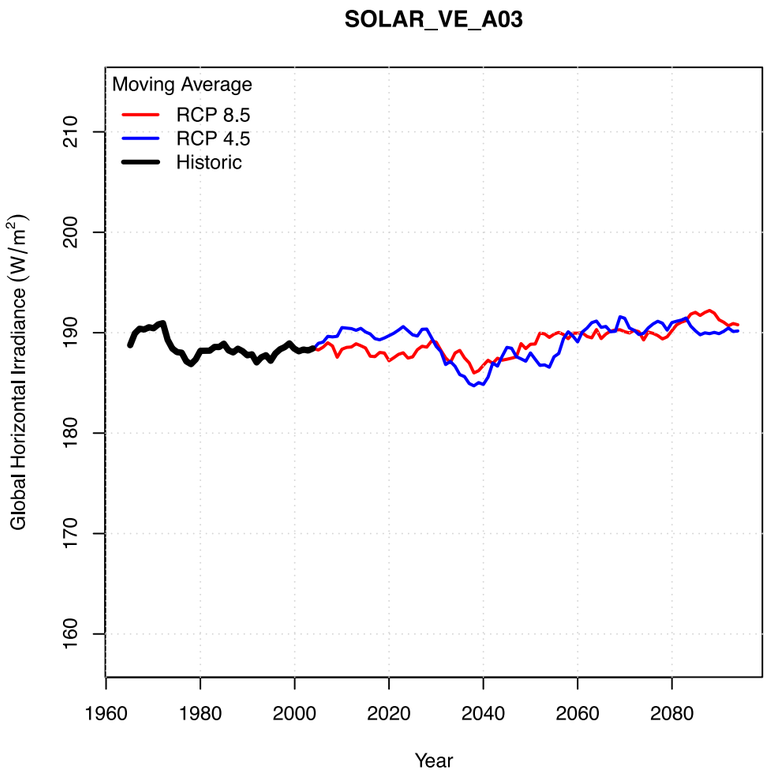
SOLAR_VE_A03
Moving Average
RCP 8.5
RCP 4.5
Historic
Global Horizontal Irradiance (W/m2)
160
170
180
190
200
210
1960
1980
2000
2020
2040
2060
2080
Year